DISSERTATION

ASSESSMENT OF ANOPHELES VECTORIAL CAPACITY METRICS AND MALARIA TRANSMISSION FACTORS WITHIN THE RIMDAMAL II STUDY

Submitted by

Lyndsey Irene Gray

Department of Microbiology, Immunology, and Pathology

In partial fulfillment of the requirements

Fort the Degree of Doctor of Philosophy

Colorado State University

Fort Collins, Colorado

Fall 2021

Doctoral Committee:

Advisor: Brian Foy

Rebekah Kading
Rachel Mueller
Mark Stenglein

ABSTRACT

ASSESSMENT OF ANOPHELES VECTORIAL CAPACITY METRICS AND MALARIA TRANSMISSION FACTORS WITHIN THE RIMDAMAL II STUDY

Malaria is a mosquito-borne disease that results when *Plasmodium* parasites infect a human through the bite of an infectious female *Anopheles* mosquito. It is a major cause of morbidity and mortality in the world, resulting in over 200 million cases and hundreds of thousands of deaths each year. Currently, more than 90% of the malaria disease burden is found within the World Health Organization (WHO) African Region. Burkina Faso, a country located in West Africa along the Sahel geographic belt, has some of the highest malaria transmission intensities in the world. Although ongoing mosquito vector control and disease prevention efforts have resulted in notable reductions in malaria mortality and morbidity, the level of recorded malaria endemicity in Burkina Faso has not yet significantly decreased. This phenomenon may be facilitated by weak integration of global health programs targeting both mosquito vectors and *Plasmodium* parasites. Additionally, the efficacy of current malaria control efforts is severely threatened by widespread insecticide and antiparasitic drug resistance. As such, we investigated whether ivermectin, a novel malaria control tool that can target both *Plasmodium* and *Anopheles*, could significantly reduce childhood malaria disease incidence through mass drug administrations (MDAs) in a cluster randomized, double blind, clinical trial known as the Repeat Ivermectin Mass Drug Administrations for control of Malaria (RIMDAMAL II). In this thesis, I use entomological data derived from this study to both elucidate and measure changes in

mosquito host factors that contribute to *Anopheles* spp. vector competence and vectorial capacity for malaria.

An anopheline mosquito's ability to effectively transmit *Plasmodium* parasites from one human to another is dependent upon several behavioral, physiological, and ecological considerations. Vector competence, the ability of a mosquito to support each *Plasmodium* developmental stages, transmit sporozoites, and produce new human infections, is one of the key physiological parameters that govern successful transmission of *Plasmodium*. Vector competence is biologically complex, varying considerably between different *Anopheles* and *Plasmodium* species due to factors such as mosquito internal tissue physiology, immune responses, and mosquito-parasite genotype interactions. Although vector competence is usually quantitatively measured in laboratory settings, it can be qualitatively observed in field settings by noting the relationship between specific *Anopheles* and *Plasmodium* species over time. Additional parameters that shape a mosquito's ability to successfully transmit malaria parasites between infectious and susceptible humans define its vectorial capacity, which can be quantified from field settings. These include mosquito density, host biting rate, daily and lifetime survival probability, and malaria's extrinsic incubation period (EIP). Subsequent chapters of this thesis will explore novel and comparative means of assessing the most significant components of vectorial capacity, mosquito survivorship, as well as enumerate potential, observed indicators of vector competence for *Anopheles* mosquitoes and *Plasmodium* species within the context of RIMDAMAL II.

Because mosquito age is one of the most significant determinants of mosquito vectorial capacity, researchers have long sought an age grading technique that can be easily translated into measurements of epidemiological importance. The Detinova parity technique, which estimates

age from the mosquito ovary and tracheole skein morphology, has been most often used for mosquito age grading despite significant limitations, including being based solely on the physiology of ovarian development. In this thesis, we have developed a modernized version of the original mosquito aging method that estimates mosquito chronological age from wing wear and wing scale loss. We conducted laboratory experiments using adult *An. gambiae* held in insectary cages or mesocosms, the latter of which also featured ivermectin bloodmeal treatments. Sampled mosquitoes were age graded by parity assessments and both human- and computational-based wing evaluations. Although the Detinova technique was not able to detect differences in age population structure between treated compared to control mesocosms, significant differences were apparent using the wing scale technique. Furthermore, analysis of wing images using averaged left and right wing pixel intensity scores predicted mosquito age at high accuracy. Overall, our results suggest that this technique could be an accurate and practical tool for future mosquito age grading endeavors, which we later tested in the first study year of RIMDAMAL II.

The difficulties of field work and the biological complexities of wild mosquitoes have made age grading challenging, and therefore hindered entomologists' capability to quickly, accurately, and precisely quantify the survivorship variables needed for monitoring the vectorial capacity of a given anopheline population. Presently, two age grading methods are frequently used in mosquito surveillance efforts due to their speed, accessibility, and/or reliability: the Detinova parity technique and near-infrared spectroscopy (NIRS). Our RIMDAMAL II trial provided an opportunity to compare these methods alongside wing scale counting in a true field environment hyperendemic for malaria. Analyzing data generated from female *Anopheles gambiae* s.l sampled during the 2019 field season only, we conducted a comparative analysis of

the accuracy, feasibility, and field viability of these two techniques alongside wing wear-based age grading. Our data show that parity assessment, while inexpensive, is highly subjective and also technically demanding for the large sample sizes typical in a field trial. Age grading with wing scales can be relatively fast and thus can be performed on large datasets, done inexpensively, and analyzed without complex modeling. In comparison, NIRS is also rapid and capable of processing of large datasets, though the initial costs of the field spectroscopy machine are high and the need for mathematical and modeling expertise is a downside. Overall, we show that wing scale and NIRS age grading have similar median age prediction trends across sampled village and time points, but their distributions of predicted ages were noticeably different.

In addition to mosquito age, other mosquito physiological characteristics and *Anopheles-Plasmodium* interaction dynamics impact malaria transmission. These factors fall within the domain of vector competence. We conducted an observational analysis of the entomological data derived from both study years of RIMDAMAL II, using field data and follow-up qPCR analyses to determine changes in *Plasmodium* and *Anopheles* species dynamics and sporozoite infection rates over time. Expectedly, we identified *An. gambiae* s.s as the primary transmitter of any *Plasmodium* spp. in the area. However, we noted a surprising role for *An. funestus*, which were more *Plasmodium*-positive than expected and compared to what is reported in the literature specific to Burkina Faso. Likewise, although *P. falciparum* continues to be the dominant malaria parasite in the region, an atypically high prevalence for *P. ovale* was detected. Lastly, our analyses indicated that standard entomological measurements of malaria were insufficient for representing disease transmission risks, and should be paired with other, age-based metrics to be more robust. Overall, our findings present the first signs that malaria transmission dynamics may

be shifting within our study region in Burkina Faso, which might have significant implications for future vector and disease control efforts.

ACKNOWLEDGEMENTS

> "It's like the great stories, Mr. Frodo, the ones that really mattered. Full of darkness and danger they were. And sometimes you didn't want to know the end, because how could the end be happy? How could the world go back to the way it was when so much bad has happened? But in the end, it's only a passing thing, this shadow. Even darkness must pass. A new day will come. And when the sun shines, it'll shine out the clearer. I know now folks in those stories had lots of chances of turning back, only they didn't. They kept going because they were holding on to something. […] That there's some good in this world, Mr. Frodo, and it's worth fighting for."[1]

I knew that pursuing a PhD was going to be a hard and arduous journey, but I don't think I realized the extent to which it would test my personal and mental fortitude. These past four and a half years have been full of unexpected challenges – shifting security and geopolitical concerns that upheaved my field work plans, a pandemic that shattered many of my support systems, global supply chain disruptions that hamstringed my lab work, to name a few – as well as longstanding, personal battles that I've had to continuously fight. I have had my fair share of people tell me that I or my science wasn't enough. There were so many moments of doubt where I seriously considered walking away from this degree. Finding the will to hold on, the clarity to set and meet my own standards of success, and mustering the strength to pick myself up after every fall has been a monumental undertaking. And yet, despite all the effort it took to keep going, I never doubted that I could one day make it to this point. I couldn't be prouder of who I am, or the work that I've achieved and enclosed in this thesis. In many ways, it represents the best of me and other scientists like me – the endeavor to do something meaningful with your life and to try to make the world just a little bit better in the process. Even though every PhD journey is an individual one, no person is truly an island. Much of what I have accomplished and all the ways that I have grown is thanks to thousands of acts of kindness and support from others. To those people, I am truly grateful.

First and foremost, my work simply would not have been possible without the dedication, resiliency, and guidance from a tribe of collaborators. Emmanuel Sougué, in particular, was the backbone of my RIMDAMAL research. Without him, none of our field work in Burkina Faso would have been possible. The rest of the IRSS team, notably Dr. Roch Dabiré and Dr. Fabrice Somé, as well as my primary collaborators at Yale University – Dr. Sunil Parikh, McKenzie Colt, and Dr. Hanna Ehrlich – were instrumental in guiding and advising my research. Likewise, I couldn't be more appreciative of Ruth McCabe and Dr. Tom Churcher, our colleagues at Imperial College London, who gave me so much of their time, creativity, and support as we tackled the computational heavy lifting enclosed within this thesis. And of course, I will forever be in debt to Dr. Bryce Asay and Blue Kroma. I am still amazed that a single, nerdy conversation with two near strangers in a windowless TA office eventually turned into a full working partnership, a new avenue of research, and, most importantly, friendship. Bryce and Blue have come through and supported me in so many ways that go above and beyond the call of duty, and I will never forget it.

I am incredibly lucky that I have had a dream team committee. Before coming to CSU, I had a list of professors that I hoped I'd have the privilege to learn from and one day work alongside. The fact that every single one of them agreed to serve on my committee still astounds me. I could not have asked for a better outside committee member than Dr. Rachel Mueller. I always knew I could count on Dr. Mueller to keep me grounded and steady throughout my PhD. She constantly supported me when I needed it most (including taking my panic-laden phone calls in the middle of a pandemic) and never stopped believing I'd find my way to the finish line. Dr. Mark Stenglein has challenged me in all the ways I needed. He made my science better by ensuring that I always asked the right questions, thereby improving my decision making, my

experiments, and my science in the process. I am a more discerning and prepared scientist thanks to him. I simply could not have finished my PhD without Dr. Rebekah Kading. Trying to summarize all the ways she has been there for me these past four and a half years in just a handful of sentences is an impossible undertaking. Suffice it to say that her unconditional support and encouragement has been a lifeline. I would be remiss not to mention the guidance and wisdom I received from Dr. Bill Black. Dr. Black's work was one of the cornerstones of my master's research at Emory, and one of the reasons why I applied to CSU. I feel incredibly honored that I had the chance to learn from him and include him in my PhD journey. And naturally, none of this would have been possible without Dr. Brian Foy. I will always be grateful for the time, creativity, and guidance he gave me these past years. Looking back over my time at CSU, all of my favorite moments were thanks to him – being a pseudo-cartographer in Burkina Faso, all the hours spent excitedly discussing results in his office, meeting collaborators from across the globe, gaining the confidence to present my findings and know that they mattered. I wouldn't be the scientist or leader that I am if it were not for him.

My friendships have sustained me throughout graduate school, and they are what I regard as one of my highest successes. I entered this PhD program with an amazing cohort of incredible people. I am fortunate to know that they are all friends, not just colleagues. I thank Jaz Donkoh, Amy Fox, Laura St. Claire, and Bekah McMinn for all their support. I will always wish them nothing but the best and know they'll make it across the PhD finish line too. The incredible women of Graduate Women in Science and my peers in the National Science Policy Network have been my bedrocks. They have provided me with community, opportunity, and support when I needed it most. Dr. Amal El-Ghazaly has been an everlasting friend. I've always seen her as one step ahead of me, and she's used that perspective to remind me to be patient, to endure, and

to be encouraged by what comes next. I am lucky to have a peer mentor and an eternal friend in her. Dr. Claire Strebinger has been my go-to partner in crime since high school. Sustaining that friendship in the decades since has been the adventure of a lifetime. Meeting and extending that friendship to her partner, Patrick Nuessly, was a gift and I am so grateful to have him as a friend. I thank both of them for being my Colorado family, for all the times they kicked me out of lab and threw me into the wilderness, and for reminding me how beautiful the world around me is. Ramya Maddali-Chew has been a forever friend to me. I have shared so many moments, both big and small, with her that I truly can't envision who I would be without her friendship. In the moments when I've lost my way, when I've been at my lowest, when I've forgotten what I stand for, she has been there to remind me and make me believe in myself again. I have stayed hopeful and joyful because of her. Jason Maddali-Chew's steady friendship has sustained me, inspired me to ask the questions that matter in life, and challenged me to use my talents in ways that are truly meaningful. I look forward to the day when I embrace my inner Bertha Mason and live in Ramya and Jason's attic.

This PhD is dedicated to and would not be possible without my parents, Janet and Dr. David Gray. Even when I am far away, even when I am in the middle of a challenge that seems impossible, even when facing a task that only I can complete, I have never felt alone thanks to them. For as long as I can remember, they have believed not only that my dreams are possible, but also that those dreams are bigger than I could imagine. They've been right every single time. My mom and dad are my biggest cheerleaders; they've encouraged me to keep going, have helped guide me through every decision, and celebrated alongside me every step of the way. Their unwavering support, love, and encouragement is the reason I am the person I am today. Knowing that I make them proud is the only success I will ever truly need.

I adopted Chaplin to keep me stable in graduate school, and he has been an unconditional source of love in my life. Loki, who I adopted a year later, has reminded me how gentle and kind life can be even in the darkest of moments. My "scale babies," Tesla and Lysander, were and have been constant sources of joy and laughter these past years. Taking care of all of them has taught me how to care for myself.

Thank you all for reminding me that I have indeed succeeded, for being the good in the world that I hold onto, and for proving that all of this was indeed worth fighting for.

Onward and upward.

TABLE OF CONTENTS

CHAPTER 1: OVERVIEW OF THE LITERATURE

1.1 Malaria and *Plasmodium*

Although malaria is an ancient infectious disease that has affected humans for millennia, it continues to be one of the world's most devastating diseases, resulting in anywhere between 200-500 million cases each year.[2,3] In 2018 alone, over 400,000 deaths and an estimated 228 million cases of malaria occurred globally, 93% of which occurred in the World Health Organization (WHO) African Region.[4,5] Over 50% of all cases globally were accounted for by Nigeria (25%), followed by the Democratic Republic of the Congo (12%), Uganda (5%), and Côte d'Ivoire, Mozambique and Niger (4% each).[4] Malaria also most severely impacts society's most vulnerable, disproportionately affecting those in poverty; 58% of malaria cases occur in the poorest 20% of the world's population.[6] With malaria-affiliated global health costs tallying over $12 billion each year, malaria is also a driver of further global economic inequality.[7] Similarly, malaria more severely affects women and children. Due to their high work burden, women can have greater exposure to malaria-carrying mosquitoes and have limited ability and decision-making power to seek treatment when either they or their family fall ill.[8] Pregnant women are also disproportionately at risk; those infected with malaria experience higher risk of maternal death and more severe disease outcomes, as well as higher risk of miscarriage, intrauterine demise, premature delivery, low-birth-weight neonates, and neonatal death.[9] In high transmission areas, their children, too, are at high risk since they have not yet acquired immunity and are thus more susceptible to severe malaria.[10,11] In 2019, 272, 000 (67%) malaria deaths were estimated to be in children aged under 5 years.[4]

The WHO's Global Technical Strategy for Malaria aimed for a reduction of 40% of malaria from the 2015 baseline by 2020.[12] To meet that goal, four key strategies were recommended to reduce disease transmission: (1) rapid malaria diagnosis in humans and treatment with artemisinin-based combination therapy (ACT) to ensure the rapid and full elimination of *Plasmodium* parasites from a patient's bloodstream; (2) chemopreventive drug administration for vulnerable populations, like pregnant women and children, at designated time points during the period of greatest malarial risk; (3) distributing long-lasting insecticide-treated nets (LLINs) and insecticide-treated bed nets (ITNs) in order to reduce exposure to biting, disease-carrying mosquitoes; (4) conducting indoor residual spraying (IRS) to kill malaria-transmitting mosquitoes. Despite these recommendations and consistent malarial control efforts globally, the milestones set out by the WHO's Global Technical Strategy for Malaria remain as yet unachieved[4] This suggests that the current strategy is insufficient and that complementary, innovative disease prevention tools are needed to not just target malaria-transmitting mosquitoes, but also the parasites themselves.[13]

1.1.1 Plasmodium biology and transmission in humans

Malaria is a mosquito-borne disease caused by unicellular eukaryotes of the genus *Plasmodium*.[14] Although more than 100 *Plasmodium* species exist in nature, just five species are known to infect humans.[15] An obligate parasite of humans and insects, *Plasmodium* species pursue a complex, two-host life cycle in which mosquitoes act as both hosts and carriers.[14]

A new round of the *Plasmodium* life cycle begins after an infectious female mosquito vector salivates during human blood feeding, depositing anywhere from one to several hundred sporozoite forms of the parasite into the dermis.[16–21] Most of these sporozoites find a capillary, which they then use to travel the peripheral blood circulation until they reach the liver blood

vessels (sinusoids).[17,22] After crossing the sinusoidal wall, sporozoites use a form of locomotion called gliding motility to migrate through multiple hepatocytes before arresting and infecting a final hepatocyte.[22–24] When infecting cells, the sporozoite forms a parasitophorous vacuole, inside which they then grow and multiply exponentially (exoerythrocytic schizogony).[25] Between 2-16 days later, the resulting new invasive and motile form (merozoites, which are now thousands of times more abundant than the original invading sporozoites) induce the death and detachment of their host hepatocytes and enter the sinusoid lumen in the form of a parasite-filled vesicle known as a merosome.[26,27] Merozoites are released into the bloodstream and eventually find and invade an erythrocyte (also known as a red blood cell, RBC).[26,28] Once inside the RBC, merozoites develop inside a parasitophorous vacuole formed during RBC invasion, multiply asexually by schizogony, and undergo two stages: a trophic period where the parasite enlarges and forms a "ring form," and a period where the trophozoite enlarges further upon ingesting the host cytoplasm and hemoglobin.[29] The end of this trophic period is accompanied by multiple rounds of nuclear division to produce a schizont, which ultimately ruptures to release thousands of new merozoites into the bloodstream (it should be noted that this stage produces most of the symptoms associated with human malaria disease, discussed further in section 1.1.2).[29,30] This intraerythrocytic propagation cycle is repeated multiple times.[31] Some of the RBC-released merozoites undergo sexual differentiation (gametocytogenesis) to form male and female gametocytes.[32,33]

The second major stage of malaria parasite development occurs after gametocytes are ingested by female mosquito vectors during blood feeding.[34] Within approximately 15 minutes, gametocytes exit the ingested red blood cells and, after being exposed to the internal biochemical and physical conditions in the mosquito midgut, mature into gametes.[35,36] Haploid male gametes

undergo a process known as exflagellation, where they undergo three rounds of DNA replication in a matter of minutes, ultimately forming eight male, haploid microgametes.[37–39] These male microgametes detach from the exflagellation center and fertilize female gametes, subsequently forming a diploid zygote.[34,40]After one round of DNA replication to become tetraploid, zygotes develop into motile ookinetes, which migrate through the blood bolus to ultimately penetrate and traverse the midgut epithelial wall from the apical side, egresses from the basal end, and reach the basal lamina.[37,41] This invasion step is accompanied by a severe reduction in ookinete numbers due to attack by the mosquito immune system and other host protective mechanisms.[37,42]Approximately 18-24 hours after the original ingestion of the infected blood feed, the surviving ookinetes attached to the mosquito midgut basal lamina become immobile and begin to transform into oocysts. Oocysts grow and undergo multiple rounds of DNA synthesis and mitosis for approximately 7-10 days, eventually rupturing to release haploid sporozoites into the haemocoel located within the mosquito body cavity.[2,41] *Plasmodium* parasites then undergo their second bottleneck stage, as sporozoite populations suffer heavy losses.[37,43,44] Sporozoites that do not successfully reach and invade the salivary gland within eight hours are efficiently degraded by rapid immune processes in regions of high hemolymph flow; it is estimated that only 19% of sporozoites invade the salivary glands.[44] These remain alive throughout the life of the mosquito vector and are the only form of *Plasmodium* capable of naturally infecting other humans.[32,34,45]

1.1.2 The human health outcomes of Plasmodium development and replication

Although *Plasmodium* parasites go through a complex life cycle with multiple development stages, only a small number of these forms lead to clinical disease. In fact, most malaria-infected individuals exhibit few symptoms or are asymptomatic.[4,46] Symptoms can only

begin when the first liver schizont ruptures and releases merozoites into peripheral circulation, an event which is silent for most patients who will later become clinically ill.[22,47] As the parasites continue to cycle through their asexual development stages (merozoite reinvasion, trophozoite development, schizont rupture) over repeating intervals of 24-48 hours, the level of parasitemia increases.[34,47] The human immune response also increases to match these levels, causing cyclical bouts of fever, inflammation, myalgia, rigor, headache, and fatigue.[48–50]

More complicated and severe forms of malaria encompass a broad spectrum of syndromes, the development of which may be influenced by an individual's age, exposure and immune status, or the specific parasite species behind the infection.[47,51] It includes complications that affect specific organs such as the brain in cerebral malaria (CM) or the placenta in malaria in pregnancy (MiP), as well as severe anemia, hypoglycemia, metabolic acidosis, acute respiratory distress, renal abnormalities, neurological changes, and coma.[47,52–54] Global trends indicate that overall malaria-induced mortality rates are declining and the relative global frequency of severe malaria remains low.[4] However, the reported case fatality rate for severe malaria patients, especially children with CM, has not substantially changed over the past several decades.[55]

1.1.3 Overview of the five Plasmodium parasite species that cause human disease

Only five *Plasmodium* species are known to infect and cause disease in humans: *Plasmodium falciparum*, *P. vivax*, *P. ovale*, *P. malariae,* and *P. knowlesi*.[15] Anopheline mosquitoes serve as the exclusive host and carrier for all five parasite species.[16]

Unlike the other four malaria species, *P. falciparum*'s life cycle differs in several notable ways. Liver-stage merozoites rupture the hepatocyte at approximately the same time with none remaining in the liver.[22,56] Once in the peripheral blood stream, *P. falciparum* invades RBCs with no preference to erythrocyte age.[15,47] During the latter half of the intra-erythrocytic cycle, mature

falciparum-infected RBCs are not seen in the peripheral blood.[56] Instead, late-stage parasitized erythrocytes use parasite-encoded proteins (predominantly PfEMP1) on the RBC surface to sequester and bind to the luminal surface of vascular endothelial cells, which can compromise blood flow.[49,51,56] *P. falciparum*-infected RBCs can also bind to the placental wall and seize essential placental molecules, resulting in MiP, serious pregnancy complications, and health problems for both the mother and fetus.[47,57] Additionally, they can bind to the brain endothelium and cause complications leading to CM, the most severe complication of any *P. falciparum* infection.[47,58] In highly endemic settings, children under five years old are at the highest risk for CM (mortality of 10-20%), while in low endemic settings all ages are at risk and mortality can be higher in adults.[58] For this reason, *P. falciparum* is the malaria parasite species most commonly associated with severe and complicated disease.[15] In fact, most malaria-associated morbidity and mortality in sub-Saharan Africa is caused by *P. falciparum*.[59]

P. vivax is the second most prevalent cause of malaria worldwide, the leading cause of malaria outside of Africa, and the most widely distributed of all human malaria-causing *Plasmodium* species.[40,56,60] However, most (72%) of *P. vivax* infections occur in the Americas and Southeast Asia, placing approximately 2.5 billion people at risk.[61] Like *P. falciparum,* it can also cause pregnancy complications and congenital malaria.[47] *P. vivax* poses challenges to malaria eradication campaigns due to its unique biology. First, this species of *Plasmodium* continuously produces gametocytes even in its early intraerythrocytic propagation cycles, resulting in high transmission potential.[16,47]Additionally, a portion of the liver stage parasites are able to develop into a dormant form called hypnozoites, which can remain latent up to two years before reactivating to initiate blood-stage infection.[62] The exact mechanism behind hypnozoite triggering is not yet fully understood, though they are the most common origin of blood-stage

infections.[47,61,62] Hypnozoite reactivation combined with *P. vivax*'s relatively short schizont maturation to rupturing period (48 hours) not only causes recurrent malaria, but also increases the risk of severe anemia.[52,56] Additionally, even though it typically exhibits relatively low parasitemia, *P. vivax* is known to trigger greater inflammatory responses and more severe clinical symptoms due to its preference to infect reticulocytes instead of mature RBCs.[62] This is because *P. vivax* merozoite invasion is dependent upon the parasite's Duffy binding protein (PvDBP) interacting with reticulocyte receptors.[63]

P. ovale was first identified by Stevens in 1922, but it wasn't until 2010 that the parasite was further distinguished into two sympatric sibling species, *P. ovale curtisi* and *P. ovale wallikeri.*[64–66] Though genetically distinct, *P. ovale curtisi* and *P. ovale walliker* are morphologically identical.[67] Both are considered endemic in sub-Saharan Africa, but can on rare occasion be found in parts of Oceana and Asia.[56] It is regarded as a slow-growing species that requires 48 hours to complete a given intraerythrocytic propagation cycle.[16,64] Like its close relative *P. vivax,* a proportion of the liver-stage *P. ovale* parasites can form dormant hypnozoites that can reactivate anywhere from several weeks to years after initial infection.[68] Also similar to *P. vivax*, *P. ovale* prefers to invade young RBCs. Parasitemia, therefore, is typically very low in infected humans.[47] However, it seldom produces severe malaria cases.[56]

P. malariae was first described as an infectious human disease in 1886 after observing that malaria parasites in some patients followed a 72 hour-long intraerythrocytic propagation cycle.[69] Although *P. malariae* presence has been reported on all continents, it is most prolific in Africa and the southwest Pacific.[56,70] A common cause of morbidity, it is known to produce the highest incidence of malaria fever among children less than 10 years old.[71] A unique feature of this parasite species is that, like *P. falciparum*, liver tissue merozoites synchronously rupture the

hepatocyte, completely exit into the blood stream, and then preferentially invade older RBCs.[56] Without treatment, blood-stage parasites endure for extremely long periods of time, sometimes for the lifetime of the human host.[71,72] *P. malariae* parasites remain at very low numbers in reticulocytes and kidneys, but can recrudesce years after the period of initial exposure and cause malaria disease.[70] In its most severe form, the most distinguishing symptom of *P. malariae* infection is an irreversible, immune-mediated, nephrotic syndrome that can also present years after the last exposure.[73] Deaths associated with *P. malariae* are usually from end-stage renal disease.[56]

P. knowlesi has the most limited distribution of the five human-infecting malaria species, located predominantly in Southeast Asia.[74] It is most notable for being a zoonotic parasite transmitted between non-human primate hosts (especially long-tailed macaques, pig-tailed macaques, and banded leaf monkeys) by anopheline mosquitoes, causing spill-over infections in humans where the parasite, vector, host and human converge.[75] It is also unique in the fact that it repeats its intraerythrocytic propagation every 24 hours.[16] Rapid spread of *P. knowlesi* is limited by the fact that the parasites strongly prefer young RBCs but can, over long periods of time, adapt to infect older ones.[76] *P. knowlesi*-induced malaria usually presents as uncomplicated, though mortality occurs at a higher frequency than that seen with *P. vivax* and *P. falciparum* proportionally.[75]

1.1.4 Plasmodium species and malaria transmission dynamics in Burkina Faso

Burkina Faso is characterized by regions that are holoendemic (most of the infected population is pediatric) or hyperendemic (high incidence and/or prevalence rates across all age groups equally) for malaria.[77] The disease is responsible for 61% of the country's hospitalizations and 30% of deaths annually, and malaria-induced mortality, especially among

children, has been steadily increasing by more than 4% every year.[78] Starting in 2010, intense and wide-scale distribution of ITNs ensured that by 2014, 89.9% of the population owned at least one ITN and largely complied with bed net use.[78–80] Nevertheless, the lack of significant decrease in the annual number of malaria cases suggests that existing vector control tools, malaria diagnosis methods, and reporting structures are insufficient for malaria elimination.[4]

Three human disease-causing *Plasmodium* species are currently found in Burkina Faso: *P. falciparum, P. ovale,* and *P. malariae*. *P. falciparum* is by far the most prevalent, with studies attributing as much as 98.5% of malaria infections due to this parasite species.[81] When focusing specifically on *P. falciparum,* infection prevalence in children younger than 10 years has been recorded at 57.5%.[82] In general, children bear a high malaria burden in Burkina Faso, with malaria being nearly five times more prevalent in urban pediatric populations (8 months to 5 years old) than adults.[81] However, shifting spatiotemporal distribution of *Anopheles* vectors, environmental factors, and human settlement and migration mean that *Plasmodium* species distribution can also vary significantly over space and time, and also may differ among different demographic populations.[59] *P. malariae* has been on the rise in Burkina Faso, with one study showing increased prevalence from 0.9% to 13.2% over a three year period.[83] Additionally, while *P. falciparum* are typically surveilled across the year, *P. ovale* and *P. malariae* have been documented as more prevalent after the rainy period.[70,83] Coinfections have also been noted in Burkina Faso, with *P. falciparum* interspecies infections with either *P. ovale* or *P. malariae* yielding higher gametocyte prevalence than *P. falciparum* mono-infections.[83]

Notably, *P. vivax* infection is absent or rarely prevalent in Burkina Faso, or even in most parts of Africa, due to the lack of Duffy glycoprotein receptor expression on the surface of red blood cells in the majority (>95%) of the human population.[84] This antigen serves as a receptor

for *P. vivax* parasites, meaning that Duffy-negative individuals are resistant to *P. vivax* invasion.[85] However, recent reports have suggested that *P. vivax* is more widely distributed across Africa than previously believed.[62,86] This could suggest that the parasite is evolving to use alternative receptors for RBC invasion, or a greater percentage of humans in Africa express Duffy receptors than believed.[87,88]

1.1.5 Epidemiology of Plasmodium coinfections and interspecies transmission

At least seven species of *Anopheles* have been shown to carry more than one species of human *Plasmodium* in the wild, and technically all five human malaria species can be transmitted by the *An. gambiae* complex (*An. gambiae* sensu latu or s.l).[89–91] However, the exact mechanisms behind mixed infection rates in mosquitoes in Africa have yet to be fully determined.[89] Because female anopheline mosquitoes sample human blood repeatedly over their lifetime, it is possible for a single mosquito to carry multiple *Plasmodium* species and cause a case of malaria coinfection though simultaneous sporozoite inoculation.[91] However, the consensus on the likelihood of this event is not consistent. Some metanalysis review studies indicate that it is more probable that mixed species infections occur through separate mono-species inoculations.[89] Others have specified that the frequency of mixed malaria parasite species in mosquitoes actually occurs equal to or greater than that predicted from the frequency of single-species infections.[90] Given the variability in spatiotemporal and geographic distribution of both *Plasmodium* and *Anopheles* species, as well as the difficulty in detecting *Plasmodium* in mosquitoes (discussed further in section 1.1.6 below), determining the definitive possibility of multi-species *Plasmodium* transmission from a single mosquito to humans will likely prove exceptionally challenging.[70,83,91–96]

The epidemiology of mixed *Plasmodium* infections is further complicated by the parasite species' ability to cross-interact and potentially engage in mutual suppression. *In vitro* experiments conducted as early as the 1930s have shown that different malaria parasite species interact and/or antagonize each other in the infected host after simultaneous inoculation.[97–99] However, the number of such studies is limited and their generalizability to natural infection in human populations and malaria endemic areas is questionable. There have been some observations in the field, though, showing reciprocal seasonality between different *Plasmodium* species that cannot be easily attributed to mosquito feeding behavior, vector abundance, or chemotherapeutic drug use.[100–102] A leading contemporary hypothesis is that *Plasmodium* species undergo density-dependent regulation of parasitemia in mixed infection scenarios. Studies in asymptomatic children have indicated that total *Plasmodium* density oscillates around an equilibrium threshold.[91,103,104] Growth of one parasite species population above this threshold inhibits minority coinfections and regulatory mechanisms (e.g., the competition for host resources, fever, merozoite clonal phenotypic variation, antigenic variation of red blood cell surface proteins, innate inflammatory responses).[103,105–107] Once the majority population is cleared by chemotherapeutic drugs or species-/genotype-specific host responses, parasitemia levels drop back below threshold, density-dependent regulation ceases, and a minority *Plasmodium* species population has the chance to rise.[103]

The frequency of mixed malaria infections is difficult to determine and highly dependent on the means of detecting them. Conventional, microscopy-based blood smear examination often misses these infections for several reasons: (1) the young ring-form stages of all four malaria parasites are nearly indistinguishable; (2) parasitemia may be too low to detect by microscopy; (3) dormant hypnozoites do not appear in blood smears; (4) observational error can miss cryptic

and rare secondary species after detecting the dominant *Plasmodium* present.[56,91,108] To this latter point, because *P. falciparum* typically produces more severe symptoms than the other three human malaria species, mixed species infections can be easily misdiagnosed as *P. falciparum* mono-species infections.[109]

Failing to identify mixed infections with high sensitivity and specificity has serious consequences for global health. Because secondary malaria parasite species often have milder symptoms and lower parasite prevalence than *P. falciparum,* these infections can remain undetected for long periods of time, enabling patients to serve as reservoirs for ongoing transmission.[109,110] In fact, some studies have shown that in such mixed infection situations, these secondary *Plasmodium* species may transmit gametocytes more efficiency at low parasite density, thereby further thwarting the effort to curb malaria transmission.[111,112] On the therapeutic side, studies have shown failure of parasite clearance after artemisinin-based combination therapy in non–*P. falciparum* infections, leading to the possibility of increased drug resistance formation among *Plasmodium* species present in mixed infections.[110,113,114]

1.1.6 Scoring Plasmodium transmission by mosquitoes: methods, strengths, and weaknesses

Measuring *Plasmodium* transmission in mosquitoes is critical for evaluating the success of vector control and malaria prevention initiatives.[115] Two metrics are typically used: the sporozoite infection rate (SIR; an indicator of vector infectiousness calculated as [number of sporozoite-positive mosquitoes]/[total number of sampled mosquitoes] x100%) and the entomological inoculation rate (EIR; the number of infectious bites per person per time period).[116,117] To calculate EIRs and SIRs, it is crucial that researchers accurately detect infectious sporozoites in field-caught mosquitoes.

The oldest and most traditional method to measure *Plasmodium* presence in mosquitoes is through dissection paired with microscopy. In this approach, adult female mosquitoes are either sectioned or pertinent organs (e.g., salivary glands, midgut) are carefully removed, mounted on slides, examined via light microscopy, and often imaged.[118] In its simplest form, researchers look only for the presence or absence of oocysts on the dissected midgut in order to identify an infected mosquito.[56,119] To date, variations of this protocol remain the standard for tracing and assessing *Plasmodium* dissemination and pathology in the mosquito.[119] However, *Plasmodium* transmission can only be scored by identifying infectious mosquitoes, distinguished by the presence of sporozoites in mosquito salivary glands. Both techniques are challenging (particularly sporozoite detection) since: (1) it is infeasible for high numbers of mosquitoes; (2) it is technically difficult as mosquito body contents are often very delicate and opaque; (3) blood pigment can obscure parasites, thereby biasing observation; (4) objective classification of oocysts and positive identification of sporozoites can be challenging.[119,120] Additionally, imaging and visualization are often hindered by light scattering due to the mosquito cuticle or lipids in cell membranes, thereby necessitating the use of additional tissue clearance and preparation techniques.[121,122] Given these practical challenges, *Plasmodium* scoring is more frequently done using molecular methods.

First developed in the 1980s, the leading molecular method for detecting *Plasmodium* sporozoites in mosquitoes has been an enzyme-linked immunosorbent assay (ELISA) that uses monoclonal antibodies to target circumsporozoite protein (CSP).[123–125] CSP is a glycosylphosphatidylinositol-anchored membrane protein that is profusely expressed along the surface of all human malaria species sporozoites and oocysts, is shed abundantly into the environment, and contains two conserved regions flanking a central repeat region of various

lengths.[34] CSP-ELISA provides several advantages over dissection; it allows for samples to be stored until processed and higher sample throughput, is *Plasmodium* stage-specific, and can provide *Plasmodium* species identification if species-specific monoclonal antibodies are used.[126] However, there are several notable disadvantages to this technique. First, CSP-ELISAs are less sensitive than dissection when sporozoite prevalence in the salivary glands is low.[127] Second, because CSP-ELISAs detect CSP in other tissues besides the salivary glands, the technique tends to overestimate sporozoite rates even if only the mosquito head+thorax is analyzed.[126,127] As an example, one study using CSP-ELISA to detect *P. falciparum* in *An. funestus* salivary glands found that only ~1% of ELISA-positive mosquitoes also tested positive for malaria when reexamined with polymerase chain reaction (PCR) assays.[128] The reason for the high degree of false positives is not fully understood, with some hypotheses pointing to cross reactivity to other vector borne parasites, other *Plasmodium* antigens, and/or other plasma factors in animal blood meals.[126,129] Regardless of the mechanism, the high degree of type 1 error means that exclusively using CSP-ELISA will likely result in an overestimated SIR and EIR, which can seriously affect estimation metrics for malaria transmission, vector control evaluations, and vector identification.[126,130,131]

As an alternative or complimentary method to CSP-ELISAs, quantitative PCR (qPCR) assays are increasingly used to detect and quantify *Plasmodium* in mosquito samples. qPCRs are more sensitive than ELISAs, which typically require at least 100 sporozoites to read positive detection.[132] qPCRs, on the other hand, should be able to detect as few as one sporozoite in theory, but usually need at least 10 in practice.[133] Advantages to qPCR include that it is a highly sensitive, *Plasmodium* species-specific, high-throughput, relatively fast, and affordable technique. It also facilitates storage of samples prior to analysis, making it a preferred method for

detecting *Plasmodium* in mosquitoes.[126] However, because it will detect the presence of all *Plasmodium* DNA and not just sporozoites, qPCR cannot be used to specify *Plasmodium* life stage.[134] Therefore, it is critical that mosquitoes first be bisected between the second and third leg immediately after capture in order to prevent false positive qPCR readings from non-sporozoite *Plasmodium* life stages that migrate into the head+thorax.[135] However, care must be taken when bisecting recently blood fed female anophelines. Blood leakage during dissection can contaminate a head+thorax sample, or even cause carryover contamination to other potentially *Plasmodium*-negative samples.[129] It is also possible that residual blood in the mosquito pharynx could lead to a false positive in a more sensitive PCR assay.[136]

1.2 *Anopheles* mosquitoes

Human malaria is transmitted exclusively by mosquitoes in the genus *Anopheles*, which have a wide global distribution and can be found on every continent except Antarctica.[137,138] As early as 1896, the Italian researcher Amico Bignami first suggested that mosquitoes might transmit malaria by inoculation.[139] However, it wasn't until two years later that he and his collaborator, Giovanni Battista Grassi, proved the theory after feeding local *An. claviger* mosquitoes on malaria-infected human patients and then subsequently allowing those same mosquitoes to feed on uninfected individuals.[140] Ensuing research showed that only anopheline mosquitoes transmitted the disease, and the mosquito-stage life cycle of *P. vivax*, *P. falciparum*, and *P. malariae* were documented in totality.[141] Today, *Anopheles* is known to include 465 formally recognized species, approximately 70 of which have the capacity to transmit *Plasmodium* spp. to humans and 41 are considered as dominant vector species/species complexes capable of transmitting malaria at a level of major epidemiological concern.[142]

1.2.1 Anopheles malaria vectors in Africa

Within Africa, malaria is predominantly transmitted by mosquitoes in one of two species complexes/groups: *Anopheles gambiae* and *Anopheles funestus*.[95,143] In both complexes, individual sibling species are impossible to distinguish based on morphology alone across all life stages of the mosquito.[144] In regards to the *An. gambiae* complex, there is ample research illustrating how the individual species differ based on chromosomal polymorphism, population genetic structure, molecular characterization, ecology, phenotype, behavior, and insecticide resistance mechanisms.[145–154] Although the *An. funestus* group is larger than the *An. gambiae* complex (nine sibling species vs. only seven), it is significantly less researched and only two *An. funestus* group characteristics are used as primary species differentiation markers: insecticide susceptibility status and frequencies of shared polymorphic chromosomal inversions.[155–158] However, *An. funestus* s.s is the dominant malaria transmitting species within the group due to its human feeding preference, wide geographic distribution, and population abundance.[155]

Due to their role in transmitting malaria in Burkina Faso, subsequent sections of this review will focus exclusively on the primary vectors *An. gambiae* s.s, *An. coluzzii*, *An. arabiensis* (all members of the *An. gambiae* s.l species complex) and the secondary vector *An. funestus* s.s.[95,159] Seasonal mosquito population abundance and geographic distributions can vary significantly over time; *An. coluzzii* and *An. gambiae* s.s are normally the prevailing species during the rainy season, *An. funestus* acts as the main vector during the dry cold season, and *An. coluzzii* dominates during the dry hot season.[143,159] Despite these shifts, mosquito abundances typically peak and malaria entomological infection rates (EIRs) are usually highest during the rainy season, which can occur anytime between June-September.[95,160] Studies have shown that small, stagnant water puddles exposed to the sun during the rainy season and at the beginning of

the dry cold season are favorable to *Anopheles* larvae development and survival in urban settings.[161–163] Additional evidence suggests that heavy rainfall, which usually destroys mosquito breeding habitats, does not deter malaria mosquitoes in this region.[162] Mosquito populations do generally decrease significantly during the hot dry season, potentially even disappearing completely for some species.[164,165] However, permanent water structures like dams and agriculture sites maintain low residual mosquito populations, allowing *Plasmodium*-infected mosquitoes to persist throughout the dry season.[95,162]

1.2.2 Anopheles life cycle and pertinent physiology

The entire holometabolous life cycle of an *Anopheles* mosquito, which includes egg hatching, larval and pupal development, and adult emergence, typically takes between nine and 20 days, depending on environmental and temperature conditions.[144,166] Mating is initiated when males form swarms 1-3 meters above the ground, which females fly into and depart paired with a single male.[167,168] Females will likely mate only once in their life as they are able to store spermatozoa to fertilize oocysts in following gonotrophic cycles.[144] Afterwards, female *Anopheles* mosquitoes undergo behavioral changes including induction of egg laying and refractoriness to further insemination.[168,169]

To successfully ovulate, female anophelines must blood feed to gain the energy and protein amino acids needed for ovarian and egg development.[170] Mosquitoes have two ovaries, which consist of a number of ovarioles attached to a central oviduct through which developing eggs are discharged. Ovarioles consist of a series of follicles and culminate in the germarium, a mass of undifferentiated cells that form oocysts, nurse cells, and follicular cells.[144,171] Following a blood meal, these ovarian structures go through four developmental phases: (1) previtellogenic phase – ovarian follicles separate from the germarium, oocytes become capable of incorporating

vitellogenin (an egg yolk precursor), and a minor amount of growth occurs; (2) initiation phase – a few hours immediately after a blood meal, follicle growth reinitiates and vitellogenin synthesis starts; (3) trophic phase – vitellogenin synthesis is completed and oocytes rapidly grow, causing massive ovary expansion; (4) post-trophic phase – oocytes mature and are surrounded by unhardened chorion (the outermost fetal membrane around the embryo).[144,171,172] Specific ovarian morphology observed during these stages can be used to determine the relative age of an adult female mosquito (discussed in greater depth in section 1.3.5).[173] Once ovarian development is complete, female anophelines will oviposit anywhere between 50-150 eggs at one time, and as many as 800-1,000 in their lifetime.[144,170]

Embryos begin to develop and, provided that the eggs stay submerged in water, will hatch into first instar larvae within 2-3 days. Larvae will then go through three additional instar stages, all of which are fully aquatic.[144] Anopheline larvae predominantly feed through collecting-filtering, removing suspended particles within a water column or, more frequently, at the top micrometer of the water surface.[174] This behavior is attributable to the fact that *Anopheles* larvae do not have a siphon and therefore must lie parallel to the water surface to obtain oxygen through spiracular lobes present on the dorsal side of the abdomen.[144] After the fourth instar stage, larvae will undergo a final round of ecdysis and metamorphosize into pupae, a state that they will remain in for 2-5 days. During this time, pupae abstain from all feeding behavior, using their energy instead to develop adult internal and external physiological structures.[144]

During eclosion, the pupal cuticle splits along the mid-dorsal line of the thorax and the adult emerges, thus terminating its aquatic life stages. Approximately 10 minutes after full emergence, the new adult mosquito is able to make short flights, but usually remains on the surface of the water.[144] This is due to the fact that the adult cuticle and wings have not fully

sclerotized, leaving the exoskeleton weakened and diminishing flight capability. Once emergence and sclerotization are complete, adult females can live up to a month or more in a laboratory setting, but typically only live two weeks or less in nature. Females can be ready for mating as soon as one day post-eclosion, but normally need 3-5 days under insectary conditions.[118]

1.2.3 Anopheles blood feeding behavior and its relationship to malaria transmission

All anopheline females are able to navigate towards potential vertebrate hosts using a series of cues, which can consist of: (1) carbon dioxide, water vapor, and volatile organic compounds present in exhaled breath; (2) carbon dioxide, sweat, bacterial decomposition products, and other organic compounds excreted from the eccrine, apocrine, and sebaceous glands found within the inner layers of the host's skin; (3) corporal heat transfer via radiation, conduction, and convection; (4) visual cues such as host movement and size, color contrast, and spectral wavelengths.[168,175–180]

Upon finding a host, *Anopheles* explore and probe the dermal surface, eventually thrusting the proboscis fascicle into the skin and continuing to probe in search of a blood vessel. During this time, the mosquito discharges saliva from the fascicle tip; once she finds a capillary, further saliva is expelled in alternating sequences of postulated suction.[168] In total, mosquitoes typically expectorate ~5 nL of saliva per blood feed.[144] The saliva of hematophagous arthropods contains assorted proteins with anticoagulant, vasodilation, antihemostatic, platelet inhibition, anti-inflammatory, and immune-modulating/immunosuppressive properties.[181] Homologues of anopheline (anticoagulant), salivary peroxidases (vasodilator), apyrase enzymes (platelet aggregation inhibitor), and D7 family proteins (vasodilators, platelet aggregation inhibitors, and

pain inhibitors) are some of the primary proteins identified in *An. gambiae* salivary transcriptomic studies.[144,182,183]

Plasmodium sporozoites that have successfully infiltrated the mosquito salivary gland are ejected into the human blood stream during *Anopheles* salivation and blood feeding.[36] Some studies have indicated that salivary components may actually facilitate malaria transmission and contribute to subsequent disease. Laboratory experiments with mice and chickens have indicated that *Plasmodium* sporozoites were more infectious when inoculation occurs via infected mosquitoes rather than intravenous injection.[182,184–186] However, studies have also reported opposite findings, once again indicating that malaria transmission dynamics are difficult to accurately and consistently model in laboratory settings alone.[187,188] Regardless, the broad hypothesis remains that *Anopheles* saliva components enhance malaria transmission by: (1) inducing rapid skin mast cell activation, which in turn down-regulates antigen-specific immune responses; (2) facilitating *Plasmodium* entry/exit from blood vessels by prompting increased levels of basophil- and mast cell-derived histamine in plasma and tissue, which can enhance vascular permeability and mediate the initial recruitment of inflammatory cells; (3) stimulating immunopathology and allergic inflammatory responses that lead to the dissemination, adherence, and sequestration of parasites in tissues.[189–196]

After obtaining a blood meal, the female mosquito will rest 2-3 days while blood is digested and eggs develop, preferring to stay on dark, cool surfaces such as a house wall, under furniture, or on plant surfaces.[168] Additional feeding behavior and host preferences are unique to individual *Anopheles* species and have direct impacts on malaria disease transmission.

1.2.4 Host seeking and feeding behavior for the primary malaria vectors in Burkina Faso

The primary malaria vectors of Burkina Faso (*An. gambiae* s.s, *An. coluzzii, An. arabiensis,* and *An. funestus),* all exhibit anthropophilic tendencies in host selection, though to different degrees depending on geographic location, host availability, or insecticide pressure.[168] *An. gambiae* s.s and *An. coluzzii* have been shown to exhibit extreme anthropophagy, even in the presence of chemical insecticides.[168,197] A West African field study quantified this host preference in the field, demonstrating a high and similar anthropophagic index (0.97) for these two closely related *Anopheles* species.[198] The remaining *Anopheles* malaria vectors exhibit anthropophilic tendencies as well, but with varying degrees of preference for zoophagy. This has been demonstrated in host seeking studies, as with the case of a Burkina Faso field study involving 3,300 female *An. gambiae* and *An. arabiensis*; 95% were caught in a human-baited trap (roughly even distribution with 52% *An. arabiensis* and 48% *An. gambiae*) while 5% were caught in a calf-baited trap (92% *An. arabiensis* and 8% *An. gambiae*).[199] This result demonstrates that *An. arabiensis* is considered a primarily zoophagic mosquito, a conclusion reinforced by blood meal analyses. A survey of malaria vectors in Kenya showed that most *An. arabiensis* (98.9%) had fed on cattle, with a small number also having fed on sheep, goats, and birds. In the same study, field-collected *An. funestus* were mostly sampled from indoors. Blood meal analyses showed that these mosquitoes had mainly fed on people (93.0%), but taken at least some of their blood meal (20.2%) from cattle.[200] Additional field studies report *An. arabiensis* and *An. funestus* feeding on pigs, fowl, or having mixed blood meals (animal-human or mixed animal).[201,202]

A second distinguishing behavior of these four *Anopheles* species is their preference for either endophagy (biting indoors) or exophagy (biting outdoors). Being the most rigidly anthropogenic, it is unsurprising that *An. gambiae* s.s and *An. coluzzii* exhibit the strongest

endophilic tendencies, though exophily has been reported.[197,203–207] However, significantly higher blood feeding rates have been observed in *An. gambiae* s.s as compared to *An. coluzzii* indoors, potentially indicating that *An. gambiae* s.s has more success in biting and feeding on humans inside houses.[198] *Anopheles funestus* is also usually classified as a more endophilic species but again, exophilic behavior has been observed.[206–210] Being the most zoophagic, *An. arabiensis* tends to feed on outdoor dwelling animal hosts.[204,208,209,211,212] However, field observations indicate that this vector is nevertheless about twice as likely to bite humans indoors as opposed to outdoors.[197]

In perfect conditions, a female *Anopheles* only needs one blood meal to complete one gonotrophic cycle. However, it is more common for females to leave a host having only imbibed a partial blood meal. This interrupted feeding is usually due to movement or defensive behavior of the host. Anophelines will then continue to host seek and feed until a full meal is obtained (~2-3μL).[168] This is evidenced by several human-based studies, which show a nearly equal proportion of *Anopheles* that feed on one or two hosts and, to a lesser extent, more than three.[116,213–215] There are additional reports that some anophelines continue to host seek during the gonotrophic cycle.[216] These feeding behaviors, in combination, have important implications for malaria transmission. Recent evidence indicates that additional blood meals not only increase the potential transmission of malaria among multiple humans, but also accelerate *Plasmodium* development in the mosquito.[217,218]

The last important blood feeding characteristic to consider is the preferred time of feeding. *Anopheles* mosquitoes are known in general for their nocturnality, preferring to bite hosts during the late evening as they sleep.[144] However, biting cycle patterns have been shown to change over the course of the rainy season due to environmental factors, so clear trends in biting

time remain difficult to fully distinguish.[168,219–221] *An. gambiae* s.s and *An. coluzzii* are generally characterized as biting more actively outdoors in the early hours of the evening, increasing indoor biting activity as the night progresses.[222] Similar trends in peak biting activity have been documented with *An. funestus,* with biting peaks occurring between 10:00-11:00pm.[200,223–225] In contrast, *An. arabiensis* is characterized as more likely to bite humans during predawn periods.[197,225,226] Within the context of Burkina Faso, *An. gambiae* s.l mosquitoes have been well documented as having lower biting activity in the early evening until 9:00pm, with two biting peaks observed between 8:00-11:00pm and a second, higher and more expended peak between 12:00-2:00am.[227] However, a more recent study indicates shifts in biting patterns. *An. gambiae* biting activity was documented as moderate within the first two hours after dusk, increasing quickly towards a six hour period of high, plateaued activity.[219] This new observation in sustained biting or, in some cases, in daytime biting is hypothesized to be a result of behavioral adaptation to high ITN use among human populations (see section 1.4.1 for further details).[219,228–230]

1.2.5 Vector competence

In the context of mosquitoes, vector competence is defined as the ability for a female adult to support pathogen survival, development, and transmission.[231] The term was first defined in the early 1900s by Ronald Ross in his effort to conduct malaria modelling.[232] In the context of malaria, vector competence signifies the vector's ability to support the completion of each *Plasmodium* developmental stage, starting from the initial gamete fusion in the midgut blood meal to sporozoite transmission out of the salivary glands. As such, it is a combined estimate of parasite infectivity, development, and transmission alongside vector resistance and tolerance.[233]

The degree of vector competence can vary considerably between different mosquito species, and can even differ considerably between individuals from the same species.[231,233,234] The variability in vector competence is due to many factors. This can include a number of genetic, molecular, cellular, and physiological dynamics such as: (1) internal physiology and tissue resistance/susceptibility to *Plasmodium* invasion; (2) mosquito immune responses (especially the Toll, IMD, Jak-Stat, and complement-like pathways); (3) specific and complex interactions between vector and parasite genotypes.[235–240] Additionally, there are a number of environmentally-mediated factors that affect vector competence, including: (1) ambient temperature; (2) mosquito diet, number of blood feeds, and nutritional status; (3) microbial gut flora; (4) infection history; (5) interactions with other co-infected pathogens; (6) exposures during larval development.[89,234,241–246]

Due to the complexity and number of variables driving vector competence, the variable is usually measured only in laboratory settings via experimental feeding assays.[231,234] These approaches measure vector competence through the success or failure rate of *Plasmodium* infection (e.g., sporozoite prevalence, oocyst prevalence, parasite intensity).[56]

1.3 Vectorial capacity

Although the biological components driving vector competence at times remain elusive, additional parameters that shape an insect's ability to transmit human pathogens from a currently infectious case can be quantified. This metric, which estimates a vector's ability to spread disease based on vector density (*m)*, mosquito biting rate (*a)*, vector competence (*c*), the daily survival probability (*p*), pathogen extrinsic incubation period (EIP; *n*), and lifetime survival ($\frac{1}{-\ln(p)}$), is known as vectorial capacity (*C*, with $C = \frac{ma^2cp^n}{-\ln(p)}$).[231,247] To successfully reduce

pathogen transmission rates, vector control campaigns usually target aspects of mosquito population biology and physiology that drive vectorial capacity.[231] However, it should be noted that, despite their utility, vectorial capacity calculations are intrinsically biased by the methodological difficulties associated with estimating the formula's parameters.[248] As the actual numerical values of *vectorial capacity* estimates will rarely be informative alone, it is recommended that studies instead compare pre-control and post-control vectorial capacity estimates when gauging the efficacy of their programs.[249]

1.3.1 The impact of mosquito age on vectorial capacity

When analyzing the equation for vectorial capacity, it is clear that some metrics drive disease transmission more than others, notably variables related to mosquito survival and aging. As evidenced by the variable for lifetime survival ($\frac{1}{-\ln(p)}$), vectorial capacity increases drastically when the probability of surviving through one day (p) is high. Additionally, since the daily survival probability is raised to an exponential power in the numerator (p^n), the calculated value for vectorial capacity is all the more sensitive to mosquito longevity. As such, mosquito populations with a long average life expectancy overall will contribute to greater disease transmission.[250,251]

Given the importance of age in determining mosquito vectorial capacity, any vector control initiatives that successfully reduce average life expectancy can also significantly reduce disease transmission. In the context of malaria, it is important to remember that the average *Plasmodium* spp. EIP (typically 10-15 days) is long relative to the average lifespan of a wild mosquito (14 days to one month).[34,231,252] Therefore, it is not just crucial to reduce mosquito population sizes overall; rather, timing is a factor. Eliminating female anopheline mosquitoes from the population before they age to the EIP threshold could eliminate the possibility of

humans being exposed to infectious sporozoites.[249,252,253] Therefore, the need to precisely distinguish older anophelines from younger classes of mosquitoes, and the inherent difficulties therein, is tied to the ability to accurately evaluate malaria control programs.

1.3.2 Overview of mosquito age grading

In an effort to study vectorial capacity, researchers have long sought entomological age measures that can be easily translated into measurements of epidemiological importance (e.g., mosquito fitness, evaluation of vector control interventions). The importance of such age measures is further supported by the fact that it is often unrealistic or unwise from a resistance management perspective for mosquito control programs to attempt to eliminate all malaria vectors in a control area. As such, it is both more relevant and efficient to evaluate mosquito population reduction efforts by determining if older classes of mosquitoes, who are the most efficient disease transmitters, have been eliminated.[231,251] However, the difficulties inherent in measuring the age of wild mosquitoes has been an ongoing challenge long acknowledged by entomologists and, consequently, is infrequently attempted under operational conditions.[253–256] Despite decades of effort and research, most age grading tools still have questionable reliability, are inordinately expensive or labor-intensive, require advanced technical expertise, and/or are not generalizable across mosquito species. Likewise, age measurements can be biased significantly due to small sample sizes, sequential sampling techniques, local environmental or geographic factors, or human measurement error or subjective judgement.[257]

The first broad class of age grading techniques rely on assessing morphological characteristics of mosquito physiology. Within this category, one of the most limited techniques is looking for the presence/absence of meconium in the adult midgut (remnants of the larval gut lining) or larval muscle between the gut and abdominal wall.[258] These opaque structures briefly

persist past eclosion before they are degraded by hydrolytic enzymes, and therefore can be used to identify newly emerged (teneral) mosquitoes from non-teneral ones. Only basic equipment and minimal dissection expertise is required for these techniques, making them viable options for limited-resource field studies.[173] However, since these structures typically disappear after 49 hours, these techniques can only be used to identify the youngest classes of mosquitoes, which is not typically relevant for malaria surveillance purposes.[259,260] As a slight improvement, a different dissection-based technique counts the daily layers of cuticular growth in apodemes (inward protrusions of the exoskeleton).[261,262] Apodeme-based age grading studies in both *Aedes* and *Culex* spp. mosquitoes have shown that it is possible to distinguish daily growth layers for periods of up to 10-13 days provided that proper staining procedures are used.[261] This technique allows researchers to calculate mosquito age as a continuous variable, which is the ideal for epidemiological relevance. Nevertheless, it requires more advanced equipment and expert-level dissection and staining skills, and is relatively unreliable since results vary by staining success and environmental conditions.[253]

An additional morphological technique unique to the field of malaria study involves dissecting mosquitoes for sporozoites. Knowing the typical *Plasmodium* EIP for a mosquito species, researchers can use the presence/absence of sporozoites as an indicator that a female is older (>EIP) or younger (<EIP).[263] With the advancement of molecular techniques, sporozoite detection can be accomplished via PCR-based analysis of mosquito head and thorax DNA extracts rather than through dissection.[264–266] However, the efficiency of *Plasmodium* transmission and ability to maintain malaria epidemics despite low to undetectable sporozoite rates in the field limits the usefulness of this technique. In areas of low transmission settings, entomological research teams may rigorously surveil anopheline mosquitoes from the field and

still find <1% that are sporozoite-positive. As such, age grading via sporozoite detection yields data for only a very limited number of collected mosquitoes despite high labor costs.[4,263] Alternative, morphology-based age grading techniques allow researchers to gather data on all captured mosquitoes, in theory, whether they are infected with *Plasmodium* or not. These techniques will be discussed further in section 1.3.4 below.

Currently, one of the most standard and comprehensive tools entomologists use to measure changes in mosquito population age structure are mark-release-recapture (MRR) studies. By releasing a known number of marked mosquitoes and monitoring the number recaptured over time, estimates can be made on mosquito survivorship and age structures.[267,268] MRR studies are often exceptionally difficult to execute in the field for both logistical and financial reasons. A significant limitation is the marking techniques themselves. For mosquito dispersal studies, topical fluorescent powders and paints, ingestible dyes, or larval habitat marking with rubidium or stable isotopes are typically used, all of which are difficult to use when marking large numbers of mosquitoes, may have limited durability in the field, and can introduce biases by negatively affecting mosquito behavior and survivorship.[269] All current MRR designs are considered time-consuming and are expensive due to the large numbers of marked mosquitoes required to achieve a reasonable level of recapture and age estimation accuracy. As such, they often are too cost- and labor-intensive to justify their key attribute – measuring mosquito age as a continuous variable.[253]

A second class of age grading techniques involves chemical analysis of cuticular biomolecules. In one technique, cuticular hydrocarbons are extracted from mosquito legs and time-associated, quantitative changes in molecular composition are measured with gas chromatography and flame-ionization detection.[270,271] Alternatively, pteridine, a fluorescent

pigment, can be extracted from mosquitoes and quantified with high-performance liquid chromatography (HPLC) or spectofluorometry.[272,273] Regression models based on the relative abundance of specific biochemicals can then be used as an age grading tool. Though these techniques can robustly measure mosquito biological age up to ~15 days and have been validated against field-caught mosquitoes, they have not been widely adopted as they require sensitive analyses, advanced technical expertise, and have high equipment and processing costs.[253,271,274]

Another age grading category involves protein and genetic profiling. ELISAs and mass spectrometry have been used to detect age-dependent changes in mosquito protein expression under laboratory conditions.[275,276] Additionally, experiments analyzing global gene transcription profiles across mosquito adult lifespans indicate that transcriptional profiling combined with multivariate modeling could be a future age grading tool.[277–279] However, this latter method requires extensive target identification and optimization, requires advanced laboratory skills and equipment access, is expensive for each sample tested, may be subject to environmental variation, and also likely species-specific.[279,280] Therefore, even though these advanced molecular techniques have the potential to calculate mosquito age as a continuous variable, they are still in their nascent stage and, until significant scientific advancements are made, are likely restricted to laboratory conditions.[253]

The final category of age grading, spectroscopic analysis, as well as additional methods in morphology-based age grading, are the primary subject of this thesis and thus will be expounded upon in greater detail in the subsequent sections.

1.3.3 Wing wear as an age grading technique

Because flight is both a complex and physically taxing process for mosquitoes, it translates into chronic wear on the wing structure. The wing itself is primarily composed of

cuticle, a multilayered, protein matrix of chitin microfibers arranged in tubular supporting veins and thin deformable membranes.[168] Despite their lightweight nature, mosquito wings are strong, durable, and flexible largely due to the wing veins – thickened, strut-like structures embedded in the wing surface – that lace across their surface.[281] These veins have several functions, including: (1) stiffening the wing; (2) resisting crack propagation; (3) transporting hemolymph; (4) forming vertices for wing folds and furrows; (5) sensory structure support; (6) structural bolstering against aerodynamic forces.[281–286] Also importantly, they divide the wing into regions that entomologists can use for taxonomy and wing feature identification.[287] Three layers of stacked wing scales lie within these regions and extend along and off of the distal wing edge. These scales come in various lengths and hinge onto the wing by a single joint. Mosquito wings flap and rotate at remarkably high frequencies (>800 Hz), using leading-edge vortices, trailing-edge vortices, and rotational drag to achieve the aerodynamic force needed for takeoff and flight.[284,288] These movements, as well as friction experienced during other life events (e.g., mating, navigating through narrow spaces) are sufficient for dislodging wing scales and causing other notable sources of wear on wings, which accumulate as mosquitoes age.

Using external wing wear as a method to age grade mosquitoes owes its origins to malaria epidemiology and *Anopheles* vector control. The earliest known record of this technique was documented in 1912, where Major E. L. Perry documented the wing conditions of *Myzomyia (Anopheles) culifacies* captured daily for a month from a cowshed in a village around Jeypore, India.[289] His assessment was qualitative and categorized wing appearances on a 1-4 rating scale (grade 1: "well marked and with the wing fringe practically complete;" grade 2: "fairly well marked but with the wing fringe somewhat worn;" grade 3: "decidedly shabby and the wing fringe very much worn;" grade 4: "actually threadbare"). However, Perry himself noted that this

method relied heavily on human judgment, and that wing grades needed to be correlated to a secondary age grade technique (e.g., egg development stage and ovary assessments).[289]

With this logic, Perry conducted a second round of mosquito sampling in a different Indian village. In total he captured 514 specimens of three different species of *Anopheles*, age graded them with his wing condition categories, and used sporozoite absence/presence from dissected salivary glands as a secondary age grading method.[289] Even though Perry's wing condition grade classes are subjective, results from this study closely fit the expected age distribution of wild female *Anopheles* as determined by sporozoite absence/presence.[263,289,290] As anticipated, mosquitoes with the most worn wings (presumably the oldest age class) not only represented the smallest fraction of the total vector population, but also were the only mosquitoes sampled that were capable of transmitting malaria parasites.[289] Nearly 20 years later, similar findings in correlation between wing wear and sporozoite presence in anophelines was recorded by Gordon et al, who used Perry's technique to age grade wild anophelines in Sierra Leone.[291]

1.3.4 Determining mosquito age from ovary morphology: the Detinova and Polovodova methods

The most widely used methods for age grading mosquitoes involve assessing changes in female reproductive structures. As described in section 1.2.1 above, mosquito ovaries undergo profound physiological changes following the ingestion of a blood meal and subsequent development of eggs. Many of these morphological changes are permanent, and therefore can be used as age indicators for female mosquitoes.[171]

Nevertheless, ovary morphology-based age grading methods have inherent drawbacks. First and foremost, they are intrinsically subjective, requiring researchers to make qualitative judgements on ovary appearances.[253] This can prove challenging, for reasons that will be detailed in greater depth in subsequent paragraphs. As an additional difficulty, some mosquito species

(but not anopheline malaria vectors) can be facultatively autogenous, or rather, they produce a first batch of eggs without needing to blood feed.[144,292] Alternatively, others (including *An. gambiae* s.l) may undergo gonotrophic discordance, needing more than one blood meal to complete a gonotrophic cycle.[45,144,293] In both scenarios, ovary assessments will be confounded; reproductive morphological changes induced by blood feeding will make the ovaries appear as if eggs have been laid (a parous state), though none actually have. Additionally, using these methods forces researchers to assume no age-dependent or gonotrophic cycle-dependent variations in mortality and that the sample mosquito population is at equilibrium, neither of which is truly realistic for wild mosquito populations.[252,253]

Despite these limitations, ovary assessments are frequently used in field studies due to their numerous advantages; they require relatively little equipment, need only modest levels of expertise, are cost-effective, and, though labor intensive, can be used to age grade large numbers of mosquitoes provided that the manpower and dissection expertise is available.[253] Within this category of age grading techniques, two methods have been used by entomologists for decades: the Detinova method and the Polovodova method.

Formally published in 1962, the Detinova method is considered the simplest of the two ovary-based techniques.[294] It is based on the morphological characterization of the "skeins" (coiled ends of tracheoles, the main airways of invertebrates), that surround the ovaries. For virgin females (those in a nulliparous state), these skeins are tightly wound and tangled around the ovary. However, when the ovaries expand (sometimes occupying >50% of the mosquito body cavity) during egg development, these skeins stretch and remain permanently loose and uncoiled.[173,294] The state of these skeins can therefore be used to qualitatively classify mosquitoes in terms of gonotrophic cycles, or rather, categorizing mosquitoes in one of two groups:

nulliparous (never laid eggs and therefore younger) vs. parous (having laid eggs and therefore older).[173,253] Translating these age outcomes to measurements relevant for disease epidemiology is difficult, and sometimes even impossible due to biological factors. However, limited frameworks have been established for applying nulliparous/parous classifications to survivorship estimations.[295,296] Further distinguishing older age classes of mosquitoes with the Detinova method remains challenging, meaning that the method has limited application for mosquito species where, due to feeding behavior or trapping method, the vast majority of field-collected individuals are often parous.[253,270] These limitations, as well as those listed at the beginning of this section, prompted researchers to develop a more precise ovary-based method for age grading mosquitoes.

First published in 1949, the Polovodova method uses ovary morphology to calculate the number of completed, successive egg-laying events.[297] During egg formation, oocytes are formed and descend into the ovarioles, tubes within the ovary that are surrounded by the swelling follicle. After each egg deposition, a bead-like dilatation is observed at the ovariole in the egg's absence.[171] By examining the fine ovariole structures on a dissected ovary, a researcher can count the number of ovariole dilations and determine the number of egg-laying cycles completed. If the average length of the species-specific gonotrophic cycle is known, the researcher can then calculate the mosquito's physiological age, which can then be related to the EIP, mosquito survivorship, and the potential for transmission.[173,297,298] While the Polovodova method offers more quantitative assessment capability than its Detinova counterpart, it has its limitations. The technique is known to be labor intensive, lacks reproducibility, can be highly subjective with results varying across technicians and equipment, and produces inconsistent results across species due to different dilatation morphology.[299]

To overcome these challenges, an annotation to the Polovodova method was made; paraffin oil is injected via micropipette into the ovaries through the oviduct to induce ovary swelling and make dilations easier to observe. Anagonou et al showed that this modified technique was successful in age grading ~91% parous *An. gambiae* s.s mosquitoes.[298] Despite these improvements, challenges remain. Finding ovarioles with intact dilations can be difficult, meaning that gonotrophic cycle interpretations may only be possible on a subset of ovariole structures.[173] Dilations may also be "false" (agonotrophic dilations), resulting from the degeneration or reabsorption of follicles rather than the production of eggs.[171] Similarly, evidence of previous dilations can be erased in due to tissue damage resulting from eggs being passed into the oviduct.[300] All of these biological phenomena can confound subsequent age calculations. Lastly, Anagonou et al admitted that the improved, modified Polovodova technique "was not easy and appeared impossible at the beginning of this study," meaning it is likely an unsuitable technique for investigations involving large-scale mosquito surveillance or field collections.[298]

1.3.5 Near infrared spectroscopy (NIRS) and mid-infrared spectroscopy (MIRS)

NIRS measures the absorption of light by organic molecules within a mosquito exoskeleton cuticle using an electromagnetic spectrum in the near-infrared region (350–2,500 nm). The electromagnetic radiation is absorbed by the covalent bonds present in cuticular biomolecules (typically those composed of lighter weight atoms like carbon, nitrogen, oxygen, and hydrogen), causing them to vibrate, excite, and change energy states. The quantity of biomolecules present influences the amount of near-infrared light absorbed. Likewise, different classes of biomolecules will vibrate in different fashions (either by stretching, bending, rocking, or wagging). Both phenomena combined produce a unique absorption signal that can be read by the NIRS spectrometer.[252,301,302] Because the molecular composition of a mosquito's exoskeleton

changes and degrades over time, a NIRS reading can be used to determine the chronological age of a mosquito.[252,303,304] Along the same lines, cuticular hydrocarbon composition can be species-specific, meaning that NIRS scanning may also be simultaneously used for mosquito species identification as well.[301,305]

Although physically scanning mosquitoes with near-infrared light and generating NIRS data is easy in practice, it does require significant planning. To accurately calculate chronological age from NIRS adult scans, calibration curves must be made from mosquitoes of known age. Larva must be reared, allowed to develop into adult life stages, and then scanned at periods of known age to generate these curves. At least 40 spectra readings are needed for each age and/or species in order to develop a robust calibration curve for downstream age predictions.[252] This can be technically challenging to obtain, especially for *An. gambiae* s.l species that are impossible to distinguish without genetic confirmation.[144] Because calibration curves generated from one population of mosquitoes at one point in time cannot be used to accurately predict age from other NIRS studies, new calibration curves must be generated for every investigation.[252] Also a mosquito's diet during larval stages can influence NIRS absorption readings. Therefore, it is important that all calibration curves be made from larva reared in aquatic conditions native to a field site or representative of later caught adults.[304] Similarly, adult diet, notably the presence or absence of a blood meal, can alter NIRS age predictions significantly.[306–308]

Perhaps the greatest limitation of NIRS is the manner in which it calculates chronological age. Early experiments with field-collected *An. gambiae* s.s were able to classify females into binary age categories of >7 days old and <7 days old with ~80%; with laboratory-reared *An. gambiae* s.s, similar binary age classification achieved almost 100% accuracy. However, further

age distinction was impossible beyond seven days, which limits the ability to tie age to malaria transmission risk as the EIP of *Plasmodium* parasites is >10 days.[309] These limitations in NIRS age prediction have been repeated across NIRS studies, meaning: (1) NIRS-based age grading can only effectively differentiate young mosquitoes as opposed to older ones; (2) NIRS produces high levels of variance in age prediction even for mosquitoes of known age.[252,253,301,308,310,311] In addition, although generating NIRS data and mosquito scanning requires little expertise, analyzing and interpreting NIRS spectral data can be complex since multivariate analytical techniques are required for their interpretation.[312] Because NIRS readings are formed from combinations of dozens of spectral bands, interpretation of results can be difficult as few features stand out against a background of continuous absorption. Lastly, because most NIRS analyses use a dispersive method to collect absorption spectra, the reflectivity of the sample is not controlled. Consequently, the intensity of the spectrum band is highly dependent on the position of the mosquito prior to scanning.[313]

Despite these challenges, NIRS has numerous advantages. Scanning mosquitoes is fairly simple, fast, and high-throughput, meaning it is an easy tool to use in the field despite large upfront costs.[253] Additionally, NIRS-based age grading is robust (>75% accuracy) for mosquitoes that are exposed to chemical insecticides, have various levels of genetic insecticide resistance, or have intracellular *Wolbachia* infections.[310,314] NIRS can even be used to detect *Plasmodium* infection in mosquitoes.[315] Furthermore, little sample preparation is required prior to scanning, scanning isn't destructive to samples, and scanning can also be done on mosquitoes stored long-term in preservative solutions like RNAlater®.[257,301,311]

To improve upon NIRS-based age grading, technological advancements have been made in a new but related spectroscopic method, MIRS. MIRS maintains the same advantages as

NIRS. It is a rapid, high-throughput technique with low continual cost (though high upfront cost) suitable for field studies, and capable of extra benefits like *Plasmodium* detection.[253,316] MIRS differs from NIRS, though, as it involves spectral analysis via an a attenuated total reflectance in the 2,500–25,000 nm wavelength region.[305] Initial investigations, of which there are few, indicate that this wavelength range penetrates less deeply into the mosquito exoskeleton than NIRS. This makes scanned results easier to interpret, less sensitive to biological confounders (e.g., the amount of moisture in the mosquito), and more reproducible.[253,305] MIRS-derived spectral bands are affected significantly by the development of a mosquito, detecting age-related changes in cuticular chitin, proteins, and waxes. However, it is not possible to predict traits by simply monitoring changes in band intensities; instead supervised machine learning analysis techniques are required in order to recognize the complex relationships in changing biochemical composition inherent across mosquito species and ages.[305,317]

Unfortunately, MIRS has its downsides. Because machine learning is required, a high level of computational expertise is needed to conduct MIRS-based age grading. Additionally, MIRS is a "destructive technique;" the mosquito sample must be crushed prior to being scanned, rendering any additional downstream analyses difficult.[318] Furthermore, the accuracy of MIRS-based age grading is yet to be determined due to the current lack of investigative studies.[305,319]

1.4 Reducing malaria transmission through adult mosquito control

1.4.1 Current practices, strengths, and limitations in Anopheles population reduction

Chemical insecticide-based strategies such as ITNs, LLINs, IRS, aerial sprays, and insecticide-treated traps have long been the mainstay of any mosquito vector control effort.[320,321] ITNs, a subset of LLINs, have long been the go-to strategy to combat *Anopheles* mosquitoes,

since the physical barrier protects sleeping individuals from nocturnal biting and the pyrethroid insecticide treatments are not only toxic to mosquitoes, but also repel them.[322] IRS is often a complementary tool used as well, since the insecticide treatments on household walls target mosquitoes that rest within the household after blood feeding.[231] Together these two insecticide-based methods have significantly reduced malaria cases over the past several decades, though their efficacy is much reduced against mosquitoes that are exophilic, bite earlier in the day, and/or have resistance mechanisms against insecticide modes of action.[4,12,323,324]

Chemical-based insecticides typically use neurological toxins that agonistically or antagonistically disrupt normal invertebrate nerve signaling.[325,326] Though a number of chemical classes are used in mosquito vector control, until recently only pyrethroids were approved for use in ITNs and LLINs given their low toxicity to mammals.[321] The resulting low diversity of insecticide classes and accompanying molecular modes of action, plus the widespread use of agricultural insecticides of similar modes of action, have helped select for insecticide resistance mechanisms in *Anopheles* mosquitoes.[327,328] These resistance mechanisms can be genetic and/or phenotypic, and include: (1) single nucleotide point mutations (SNPs) on the sodium-gated chloride channel gene (i.e., a leucine-phenylalanine [L1014F], a leucine-serine [L1014S] substitution, or an asparagine to tyrosine mutation [N1575Y]) or the acetylcholinesterase-1 gene (a guanine to serine substitution [G119S Ace-1]); (2) effects of different repetitions of these SNPs (e.g., homogenous duplications, which can provide a quantitative advantage, or heterogeneous duplications, which may carry two functions simultaneously); (3) metabolic resistance via the upregulated expression of several detoxification enzymes; (4) thickening the exoskeleton cuticle to prevent insecticide penetration; (5) expressing proteins that can bind and sequester insecticide molecules that permeate the cuticle; (6) altering behavior to include new

blood meal hosts, biting time, or biting environmental preferences.[147,197,334–341,222,324,325,329–333] Consequently, many insecticides can no longer adequately control malaria outbreaks by themselves.[321]

New mosquito control methods aim to either reduce vector survival by exploiting mosquito biology or to interfere with mosquito-parasite interactions to disrupt malaria transmission. Thus far, these control efforts fall several broad categories: (1) genetically boosting the mosquito immune system by overexpressing immune effectors or repressing negative regulators of immunity in key transmission tissues (e.g. midgut, fat body, salivary glands); (2) impairing key *Plasmodium* transitions in the mosquito with antibodies or small molecules (e.g., sporozoite invasion of the salivary glands, ookinete penetration into the midgut epithelium); (3) altering *Anopheles* microbiomes by introducing naturally occurring or modified, paratrangenic microbiota that block malaria infection; (4) creating designer mosquito strains by genetically reducing their vector competence (population replacement) or spreading sterility (population suppression); (5) engineering new, non-neurotoxic, chemical insecticide classes that instead disrupt other invertebrate cellular functions.[342,343,352–355,344–351] A novel mosquito control tool, ivermectin, falls within this latter category.

1.4.2 Ivermectin history and use

Ivermectin owes its origin to a random act of discovery. In 1970, microbiologist Satoshi Ōmura isolated and cultured an unknown, Gram-positive bacterium from a soil sample collected near a Japanese golf course. The sample, named NRRL 8165, was identified as an unidentified *Streptomyces* species and sent to William Campbell, a scientist at Merck, to see if the bacteria had any antiparasitic properties.[356] Preliminary investigations showed activity against *Nematospiroides dubius* infection in mice, and the purified active components were identified as

a family of macrocyclic lactones. These naturally occurring compounds were named "avermectins" to reflect their ability to rid parasitic infections (in Latin, "a" – without, "vermis" – worms).[357,358] Of the various avermectin compounds available, the "B" series (having a hydroxy group at position C5) proved the most efficacious in clearing gastrointestinal worms in sheep. Further characterization of the B-class avermectins was made based on the presence of a double bond between C22 and C23 or a hydrogen at C22 and hydroxy group at C23 (designated with superscripts 1 and 2, respectively). Another categorization was made with B-class variants, with "A" variants noted as having secbutyl at C25, while the "B" variants have isopropyl. Today, ivermectin is a chemically modified derivative of naturally produced avermectin B_1, comprised of ~80% 22,23-dihydro-avermectin B_{1a} and ~20% 22,23-dihydro-avermectin B_{1b}.[358,359]

Ivermectin's high activity against parasites meant that it soon became a widely marketed medication by Merck & Co., which created the term "endectocide" and labeled the drug the first of its kind. Ivermectin formulations became the largest selling animal health product in the world starting in the 1980s, particularly for companion animals and livestock.[360] Its efficacy against filarial nematodes spurred its approval for human use in 1988 and motivated the CEO of Merck & Co. to donate ivermectin, licensed as Mectizan®, in order to combat two neglected, parasitic diseases in humans: onchocerciasis and lymphatic filariasis.[360] As a result of these efforts, ivermectin was named a World Health Organization's List of Essential Medicines and Campbell and Ōmura received half of the 2015 Nobel Prize in Physiology or Medicine.[356,361]

For human patients, ivermectin is prescribed most often as an antihelminth medication for *Onchocerca volvulus* and *Wuchereria bancrofti*.[362,363] However, serious adverse effects following ivermectin treatment are common for individuals who are highly infested with *Loa loa* (>30,000 microfilaria per mL of blood), which can include severe inflammation and capillary

blockage following mass microfilaria death. As such, ivermectin cannot be administered in areas where *L. loa* has been detected unless rapid screening programs are implemented.[364] Additional adverse effects are rare since ivermectin's binding targets are restricted to the brain and spinal cord in mammals. Ivermectin exhibits poor penetration of the blood-brain barrier of vertebrate animals due to the presence of a drug-transporting p-glycoprotein.[365] However, individuals who have a variant of the MDR1 gene, which codes for p-glycoprotein production, or ingest drugs that inhibit the cytochrome P450 3A4 (CYP3A4) enzyme, which in turn inhibits p-glycoprotein transport, risk ivermectin absorption past the blood-brain barrier and severe adverse effects.[366,367]

1.4.3 Ivermectin for malaria control: effect on mosquitoes and Plasmodium

Ivermectin has a unique mode of action against invertebrates in comparison to typical, chemical-based insecticides with neurotoxicological properties. The drug has three molecular targets: glutamate-gated chloride (GluCl) channels (nerve signal controllers for locomotion, feeding, and mediating sensory inputs into behavior), glycine and γ- aminobutyric acid (GABA) channels (major determinants of nerve signaling), and Cys-loop ion channels (membrane-spanning neurotransmitter-gated ion channels responsible for fast excitatory and inhibitory nerve signal transmission).[360,368–370] Ivermectin preferentially binds to the channels, forcing them to open slowly but irreversibly. This leads to very long-lasting hyperpolarization or depolarization of the neuron or muscle cell, blocks further neuronal function or muscular contractility, causes flaccid paralysis, and, if the ivermectin concentration is high enough, death.[371–374]

Ivermectin's effect on arthropods is being explored within the context of mosquito-borne disease control, notably with malaria and West Nile virus.[13,360] In-field and pharmacokinetic studies have shown that when mosquitoes feed on humans who have taken the minimum, single oral dose of ivermectin (150 μg/kg) within 24 hours of being bitten, the LC_{50} is surpassed and

significant mosquito mortality is observed.[375,376] However, due to ivermectin's short pharmacokinetic persistence, many vectors will ingest a sublethal dose if they bite people more than two days post treatment.[377] Nevertheless, ivermectin still affects mosquito physiology in a way that reduces its survivability and likelihood of transmitting malaria in the field, notably by delaying refeeding, reducing locomotor activity, inhibiting fertility, and shortening mosquito lifespans.[378] Each of these characteristics will be discussed in subsequent paragraphs.

Since *Anopheles* mosquitoes in particular are known to take multiple blood meals per gonotrophic cycle, disrupting mosquito feeding is a key strategy in preventing malaria transmission.[217,379] Lab experiments have indicated that sublethal concentrations of ivermectin administered through blood-filled membrane feeders have the ability to postpone refeeding. Relatively young (two days old) *An. gambiae* s.s demonstrated delayed refeeding when ingesting a 26.21 ng/mL or a 11.73 ng/mL ivermectin blood meal, while older mosquitoes (eight days old) demonstrated similar behavior only when given a 26.21 ng/mL ivermectin blood meal.[377] These findings were corroborated with experiments with *An. darlingi*, a dominant Amazonian malaria mosquito. In this experiment, various concentrations of ivermectin predicted to occur after a single oral dose of 200 μg/kg were given to *An. darlingi* in laboratory settings and re-feeding was observed with individual mosquitoes every day for 12 days thereafter. Ivermectin significantly delayed time to refeed at the four hour (48.7 ng/mL) and 12 hour (26.9 ng/mL) concentrations, but not at the 36 hour (10.6 ng/mL) or 60 hour (6.3 ng/mL) ones.[380]

Reducing mosquito locomotion is predicted to impact mosquito host seeking, mating, and dispersal. Because expression of GluCl receptors has been shown on *An. gambiae* thoracic ganglia, ivermectin-GluCl binding is hypothesized to disrupt flight and leg muscle control.[381] This was demonstrated quantitatively in laboratory settings. *An. aquasalis* was given ivermectin

at sublethal concentrations at different time points via membrane-based blood feeding, with decreased locomotor activity correlating with increasing ivermectin concentration.[381] This reduced activity and agility could expose mosquitoes to greater risk of predation, thereby reducing mosquito population size and impacting malaria disease transmission.[382] Uncoordinated movements and temporary paralysis has been observed in mosquitoes in less than one hour after sublethal ivermectin exposure through a blood meal.[383] However, maximum reductions in locomotor activity have been observed in the first 30 minutes of simulated dusk and into the following dark hours.[381] Since *Anopheles* spp. tend to lay eggs at night, sub-lethal ivermectin exposure could not only reduce locomotor activity, but also impact reproductive fitness.[144]

A reduction in mosquito fecundity, egg hatching rate, and/or progeny larvae survival would reduce mosquito density in relation to humans, all of which would decrease vector populations and potentially malaria transmission as well. Ivermectin's effect on ovarian development and oviposition has been well documented both in lab and field settings. Female *Aedes aegypti*, another disease-transmitting mosquito, that survived past eight days after a sublethal dose of ivermectin displayed significant changes in ovarian development, including: blood digestion without development of ovarian follicles, degeneration of primary follicles and formation of ovarian dilatations within 24 hours after ivermectin ingestion, significant reduction in the rate of vitellogenesis and follicle development, decreased egg production, reduced egg hatching, abnormal egg size and shape, and increased percentages of unhatched embryonated and sterile eggs.[383] These results have been corroborated by other studies, which also documented that *Aedes* mosquitoes given ivermectin at a concentration within the range found in human and/or domestic animal blood demonstrated reduced egg production, increased sterility in eggs (by as much as 50%), and decreased larval survival from eggs that successfully hatched.[384,385]

Likewise, these results have been replicated with *Anopheles* mosquitoes in both laboratory and field settings, with parity rates significantly reduced in ivermectin-exposed anophelines for more than two weeks after each ivermectin mass drug administration (MDA).[386–389]

Lastly, it is well documented that ivermectin reduces the lifespan of *An. gambiae* s.l and that this reduction in survivorship is likely sufficient to reduce malaria transmission. In laboratory settings, *An. gambiae* have significantly reduced survivorship in comparison to controls when given a series of sublethal ivermectin exposures in human blood.[377] Similar trends have been observed in field studies. *An. gambiae* s.s and *An. arabiensis* demonstrated significantly reduced survival when collected from southeastern Senegalese villages that received ivermectin MDAs as opposed to control villages. It was estimated that the daily probability of mosquito survival dropped by >10% for the six days following ivermectin MDA.[376] Field studies in Burkina Faso, Liberia, and Senegal demonstrated a 33.9% reduction in *An. gambiae* s.l survivorship for one week following an ivermectin MDA.[389] Importantly, ivermectin induces greater mortality in older female mosquitoes than younger ones. Preliminary lab experiments showed decreased survival in eight-day-old *An. gambiae* s.s as compared to two-day-old ones when exposed to 26.21 ng/mL ivermectin in blood meals.[377] These findings have been confirmed in additional lab studies, which found that *An. gambiae* s.s mortality was lowest in younger (two days old) mosquitoes exposed to ivermectin in their first blood meal and highest in older (six days old) mosquitoes exposed on their second blood meal.[390] This age-based susceptibility to ivermectin was hypothesized to be facilitated, in part, by the complex biochemical interactions that occur post-blood feeding. Transcription patterns showed high upregulation in peritrophic matrix-associated genes, and immune-response genes; patterns also differed between mosquito age groups, which may explain the observed susceptibility

differences. It was suggested that ivermectin ingestion likely disrupted blood meal digestion physiological responses, midgut microflora, and innate immune responses, causing reduced survivorship.[390]

Ivermectin has been shown to negatively affect *Plasmodium* development in mosquitoes as well. In a laboratory study, *An. gambiae* s.s were fed two concentrations of ivermectin (LC_{25} and LC_{50}) along with *P. falciparum* in human blood meals at different time points, and then dissected for oocyst or sporozoite prevalence. Results indicated that, even at LC_{25} concentrations, ivermectin significantly reduced the proportion of *An. gambiae* that developed oocysts and sporozoites when it was co-ingested with *Plasmodium.*[391] These results have been further supported by observational epidemiological studies. There was a 79% reduction in the mean proportion of *P. falciparum* sporozoite-infectious *An. gambiae* s.s collected two weeks following ivermectin MDA in Senegalese villages. In contrast, there was a 24% increase in the mean proportion of sporozoite-infectious *An. gambiae* s.s collected in pair-matched control villages at the same time.[392] Likewise, a >77% reduction for up to two weeks in sporozoite rates has been observed post-ivermectin MDAs even in the midst of intense malaria transmission seasons.[393] Unfortunately, the exact mechanism behind sporozoite reduction in mosquitoes remains largely unknown.

As an additional benefit, ivermectin has been shown to potentially inhibit liver infection by impairing *Plasmodium* development inside human hepatocytes. An ~80% inhibition of *P. berghei* liver infection *in vivo* was observed upon treatment with 10 mg/kg ivermectin in mice; paired *in vitro* studies with *P. berghei*-infected human hepatoma cells showed compromised parasite development inside cells once exposed to 2.1 μg/mL ivermectin.[394] Furthermore, *An. aquasalis* and *An. darlingi* that fed on whole blood spiked with ivermectin and *P. vivax* showed

reduced infection rates when compared to those that fed on non-ivermectin-treated blood. These same mosquitoes were infected with *P. vivax* and fed on plasma from healthy volunteers given a single 200 μg/kg oral dose of ivermectin; the result was significantly reduced oocyst development.[395] In conclusion, ivermectin may therefore impact malaria parasite developmental cycles in both human and mosquito hosts.

1.4.4 Repeated Ivermectin Mass Drug Administrations for control of Malaria (RIMDAMAL) studies

Given both its history as an FDA- and WHO-approved drug and its ability to target both *Plasmodium* and *Anopheles*, it was hypothesized that frequently repeated ivermectin MDAs to humans would reduce clinical malaria episodes with few adverse reactions. Numerous studies, both past and ongoing, have tested this hypothesis as well as investigated ivermectin MDAs' impact on other neglected tropical diseases and wild mosquito and *Plasmodium* populations.[375,376,403,404,395–402] However, the 2015-launched RIMDAMAL I study in Burkina Faso was the first cluster-randomized trial to investigate the effects of ivermectin MDAs on clinical malaria.

RIMDAMAL I was founded with the aim to decrease the number of infectious mosquitoes and, consequentially, reduce childhood malaria incidence in children living in MDA-receiving villages.[398] The trial was conducted over a single, 18-week-long rainy season in 2015 and was classified as a single-blind, parallel-assignment, two-arm, cluster-randomized study. At the beginning of the trial, eligible and consenting villages in both study arms (ivermectin and control) received single oral doses of ivermectin (150–200 μg/kg) and albendazole (400 mg). However, those in the intervention group received additional ivermectin doses at three-week intervals thereafter. Although the primary study outcome was the cumulative incidence of

uncomplicated malaria episodes over the 18-week study period, additional entomological indices were measured as secondary objectives. These included: human biting rate, SIR, EIR, proportion of parous mosquitoes, and serological reactivity to an *Anopheles* salivary gland protein. Measurements were made from mosquitoes sampled in up to six houses per village every three weeks.[398]

Over the course of the RIMDAMAL I trial, repeated ivermectin MDA reduced malaria incidence in children by 20%.[398] Furthermore, these ivermectin MDAs caused no obvious drug-related harms to the village populace. However, results for the secondary entomological outcomes were not as forthcoming. No significant difference in human biting rate, SIR, weekly EIR, or proportion of parous mosquitoes was detected between the two study arms. These negative results were not necessarily reflective of ivermectin's inability to affect the mosquito population, but rather likely due to inadequate mosquito sampling procedures. This hypothesis was supported by a notable, positive entomological outcome; participants that received ivermectin had significantly reduced reactivity to an *Anopheles* salivary gland protein, indicating that these participants received fewer mosquito bites, and therefore experienced reduced malaria risk, over the trial than individuals in the control group. The success in reducing pediatric malaria overall, as well as the need for further clinical and entomological outcome reporting, justified additional clinical studies for examining the supposed direct, antimalarial effects of ivermectin MDAs in humans.[398]

RIMDAMAL II was launched during two rainy seasons between 2019 and 2020 as a follow-up to RIMDAMAL I. This second study was a double-blind, cluster-randomized trial that integrated repeated, high-dose ivermectin MDAs into the existing malaria prevention efforts routinely deployed in the Diebougou health district of Burkina Faso. This investigation's

hypothesis was that regular treatment with ivermectin would result in significantly decreased wild *Anopheles* mosquito survivorship, which in turn would reduce parasite transmission. Ultimately, this would result in decreased malaria incidence in children under 10 years of age. Similar to RIMDAMAL I, RIMDAMAL II measured secondary entomological indicators of malaria disease reduction and mosquito field data. These included: taxonomic identification of female *Anopheles,* age grading through parity rates, NIRS scans, wing scale counting, blood-fed mosquito survivorship assays, and follow-up molecular assays to determine SIR.[405] Subsequent chapters of this thesis will analyze and explore entomological and, to a more limited degree, parasitological data derived from this study.

CHAPTER 2: INVESTIGATING WING WEAR AND WING SCALE COUNTING AS AN AGE GRADING TECHNIQUE FOR *ANOPHELES GAMBIAE* MOSQUITOES

2.1 Introduction

An insect's ability to act as a vector for human pathogens is quantitatively understood via vectorial capacity, a mathematical measurement of a vector's ability to spread disease.[254] Among mosquitoes, females are the sole transmitters of pathogens to vertebrates as blood feeding is often required for egg development.[144,171] Most mosquito-borne pathogens ingested in bloodmeals develop and/or replicate in the midgut, and then migrate to the salivary glands or other specific tissues to be transmitted to the next host.[406–408] The time required for this process is known as the extrinsic incubation period (EIP), and it is often long relative to the average mosquito's adult lifespan. Daily and lifetime survival probability are, therefore, the most influential determinants of vectorial capacity.[252,408] As such, to successfully prevent the transmission of mosquito-borne pathogens, control strategies are often designed to shorten mosquito lifespan below the EIP of a given pathogen. Therefore, it is useful for researchers and control programs to accurately measure epidemiologically meaningful changes in the age structure of mosquito populations.

Currently, the most widely accepted and utilized method for mosquito age classification is examining changes in ovary appearance. Although several techniques exist for assessing age based on mosquito reproductive morphology, the Detinova method remains the archetype due to its simplicity. Age assessment is conducted by characterizing the tracheole skeins that supply oxygen to individual ovarioles within each ovary, which remain tightly coiled for virgin females but permanently stretched and uncoiled after a gonotrophic cycle. As such, females can be age characterized as nulliparous or parous.[173,409] Even though the Detinova technique is one of the

most often use methods for age grading wildtype mosquitoes, it presents numerous challenges. First, it only provides an inexact binomial categorical classification of mosquito age based on parity status. Parous females, therefore, could be as young as 3-5 days or several weeks old.[144,171] Consequently, age classification by parity is limited in its ability to yield epidemiologically relevant information relative to a pathogen's EIP. Second, the veracity of the method is questionable in mosquito species capable of gonotrophic discordance and autogeny.[45,173,410] In addition, parity assessment can be subjective. In some species, ovarioles may develop unevenly during gonotrophic cycles. As such, a single ovary may contain tracheole skeins of mixed morphologies, making it difficult to classify parity status in an unbiased fashion.[173,256,411] Lastly, although the dissection techniques and tools needed for the Detinova method are relatively simple, dissecting ovaries from numerous mosquito samples on a regular basis in the field can be labor intensive. Alternative procedures originally developed by Polovodova and modified by others build upon the Detinova method to calculate age from more advanced screenings of ovary morphology. These techniques quantify the number of ovariole dilations and egg sac stages.[256,297,298,412] However, these procedures still measure age in terms of previous gonotrophic cycles. Furthermore, this technique is even more labor intensive than parity dissections, and can also be biased by inconsistent ovariole development in each ovary.

More modern tools for determining mosquito age include chemometrics, transcriptional and protein profiling, biochemical analyses, and alternative physiology-based morphological assessments.[261,270,275,276,301,304,305,309,413,414] These methods present their own technical and cost-benefit challenges and all have biases in being able to accurately measure chronological age, especially from wild-type adults.[253] An ideal mosquito age grading tool should be viable with both laboratory colonies and in field settings using wild-type adults, be neither technically

difficult nor too labor intensive, and allow for rapid processing of many specimens per sampling time point. Similarly, it should be inexpensive, reliable, and accurate across mosquito species, and quantify mosquito age in a manner that is epidemiologically relevant.

The earliest assessments of mosquito age that we are aware of simply documented the external wear of mosquitoes and associated it with sporozoite rates. In 1912, Perry detailed his qualitative categorization of wild *Myzomyia (Anopheles)* spp. mosquitoes based on their wing condition. Calculating sporozoite rates from a subset of these wild-caught mosquitoes showed that all sporozoite-positive mosquitoes were classified as having grade 3 wing wear, which was described as being "decidedly shabby and the wing fringe very much worn."[289] This finding was supported nearly 20 years later by Gordon et al., who used the technique to age grade wild anophelines in Sierra Leone and observed that sporozoite rates increased as wing condition deteriorated.[291] Despite the obvious correlation of wing condition and sporozoite rates, qualitative wing condition grading has been critiqued as being a subjective age-assessment tool and also biased by environmental conditions.[289,294] Recognizing these possible faults but also the potential ease of this assessment, we developed and evaluated quantitative metrics of Perry's original technique. We hypothesized that wing scale loss correlates with time post-eclosion due to normal flying activity, and thus could be used as a quantitative means of estimating mosquito chronological age. To test this hypothesis, we conducted laboratory experiments using *Anopheles gambiae* held as adults in either simple cages or more complex mesocosms that also featured ivermectin treatments. Mosquito age was then assessed by photographing the wings of mosquitoes under a microscope and either manually counting a subset of wing scales in each photograph or analyzing total wing wear through machine learning and pixel intensity algorithms that assessed the entire wing image.

2.2 Results

2.2.1 Age grading using wing scale counting from mosquitoes held in simple cages.

Parity assessments were made for a subset of mosquitoes before their first blood feed (nulliparous), while others were sampled post-blood feed and/or after a designated number of gonotrophic cycles. In all cases, the number of ovipositions and the age was known for all females. The mean age for nulliparous females was 5.6 days (n = 66; 95% CI: 5.4, 5.9) and for parous females was 12.7 days (n = 73; 95%CI: 12.0, 13.4), which were significantly different (t-test: t = 12.1, p-value < 0.0001).

Results indicated that there was a significant linear relationship between the total number of wing scales on the left (n = 133) and right (n = 135) wings (Pearson r: r = 0.65, p-value: < 0.0001), demonstrating that scale loss rate was roughly equal for both wings. For the Poisson modeling analysis, a separate dataset from newly emerged, nulliparous females (n = 20) were added to the cage dataset to analyze chronological mosquito age ranging from one to 18 days post-emergence from pupae. The results showed that counted long wing scales from each wing region decreased on average as mosquitoes aged (Fig. 2.1), however, relatively more wing scales were lost from region Cu1 and relatively few were lost from wing region M2 as the mosquitoes aged. The trend of wing scale loss from aging was clearer when data were summed across all four wing regions (Fig. 2.2).

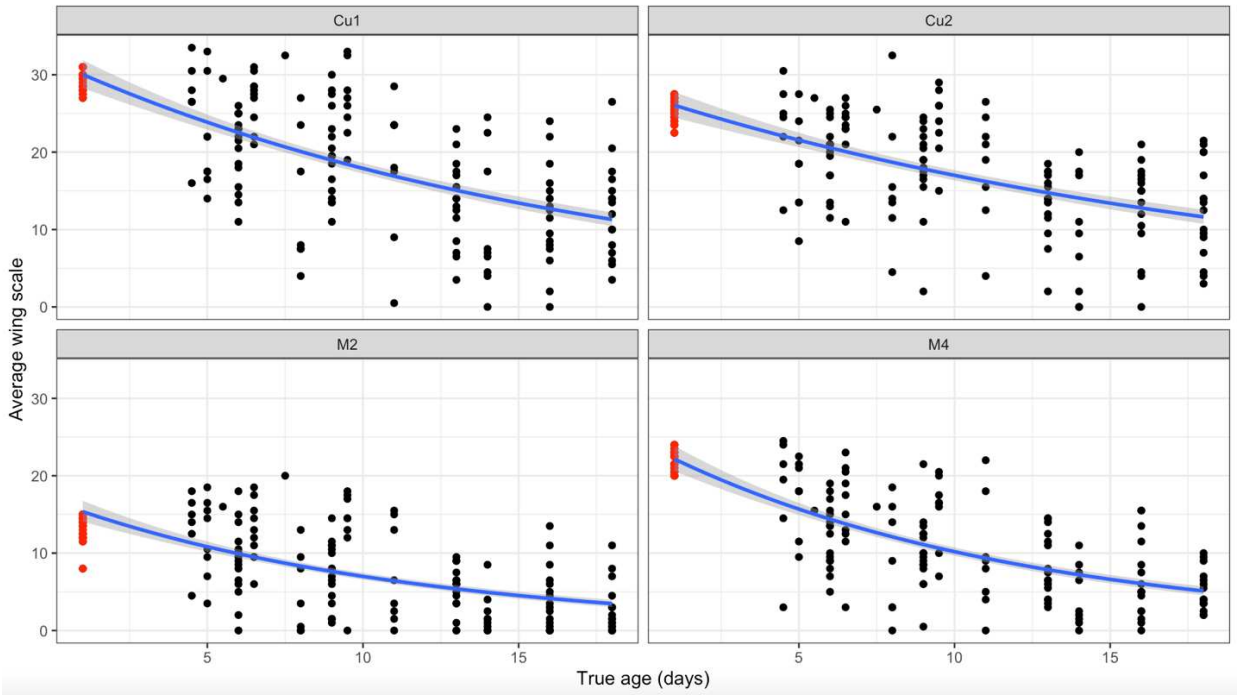

Figure 2.1. Wing scale loss in each counted wing region relative to mosquito age in simple cage experiments. *An. gambiae* mosquitoes were sampled between five and 18 days post-emergence. These time points corresponded with nulliparous and varying stages of parous ovary morphologies. Long wing scales were counted along the posterior, distal wing fringe within four individual wing regions: Cu2, Cu1, M4, and M2. Data from newly emerged females that were sampled from a separate cage at one day post-eclosion are marked in red. Data from all known-aged females sampled from the cage are marked in black. Blue line denotes a Poisson regression model line discerned from the data (gray areas = 95% confidence interval region of the model).

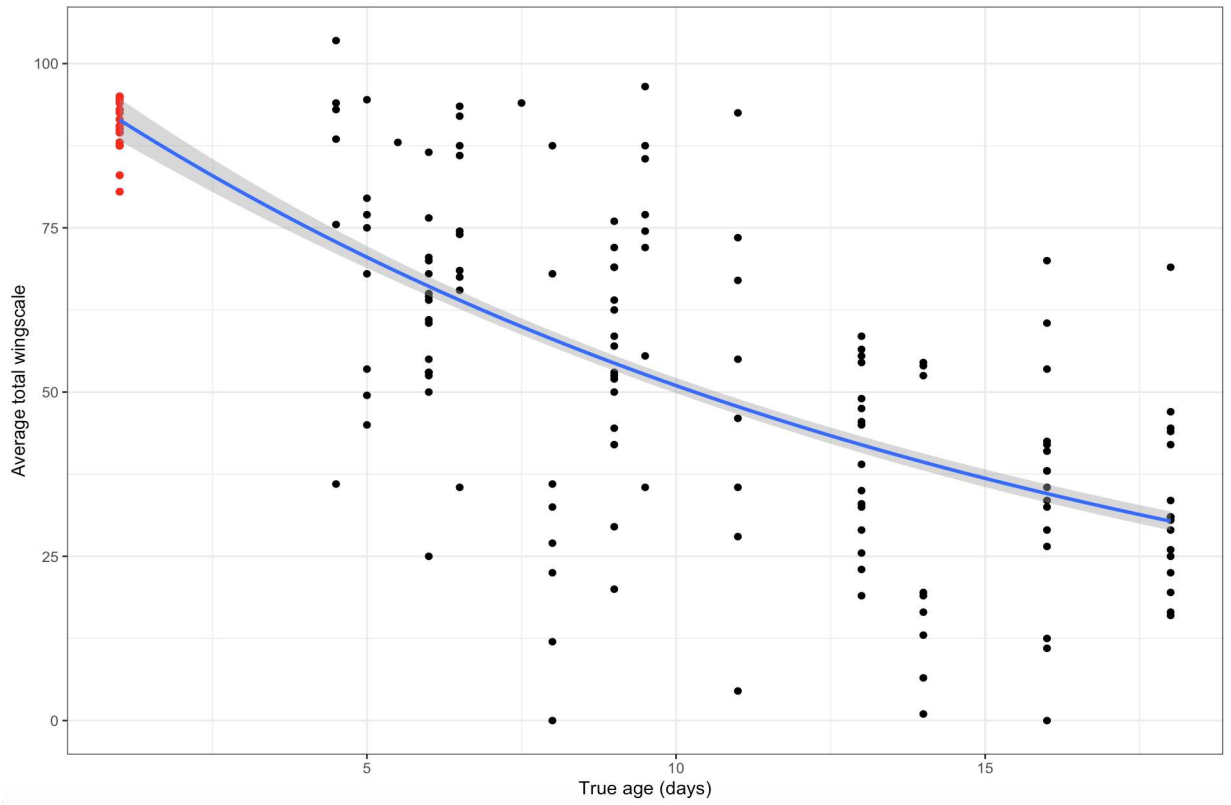

Figure 2.2. Wing scale loss correlates with mosquito age in simple cage experiments. *An. gambiae* mosquitoes were sampled between five and 18 days post-emergence. Long wing scales were counted and summed across all four individual wing regions, Cu2, Cu1, M4, and M2. Data from newly emerged females that were sampled from a separate cage at one day post-eclosion are marked in red. Data from all known-aged females sampled from the cage are marked in black. Blue line denotes the Poisson regression model line discerned from the data (gray areas = 95% confidence interval region of the model).

2.2.2 Age grading using wing scale counting from mosquitoes held in mesocosms.

Poisson regression showed a similar relationship between wing scale loss and average mosquito age in the mesocosm experiments. Results indicated a significant decrease in total long wing scale counts over time in the control mesocosm (Pearson r: r = -0.47. p-value: < 0.0001), but the initial rate of scale loss over time was significantly more pronounced in this experiment relative to the simple cage experiments (F = 32.2, p-value <0.0001; Fig. 2.3).

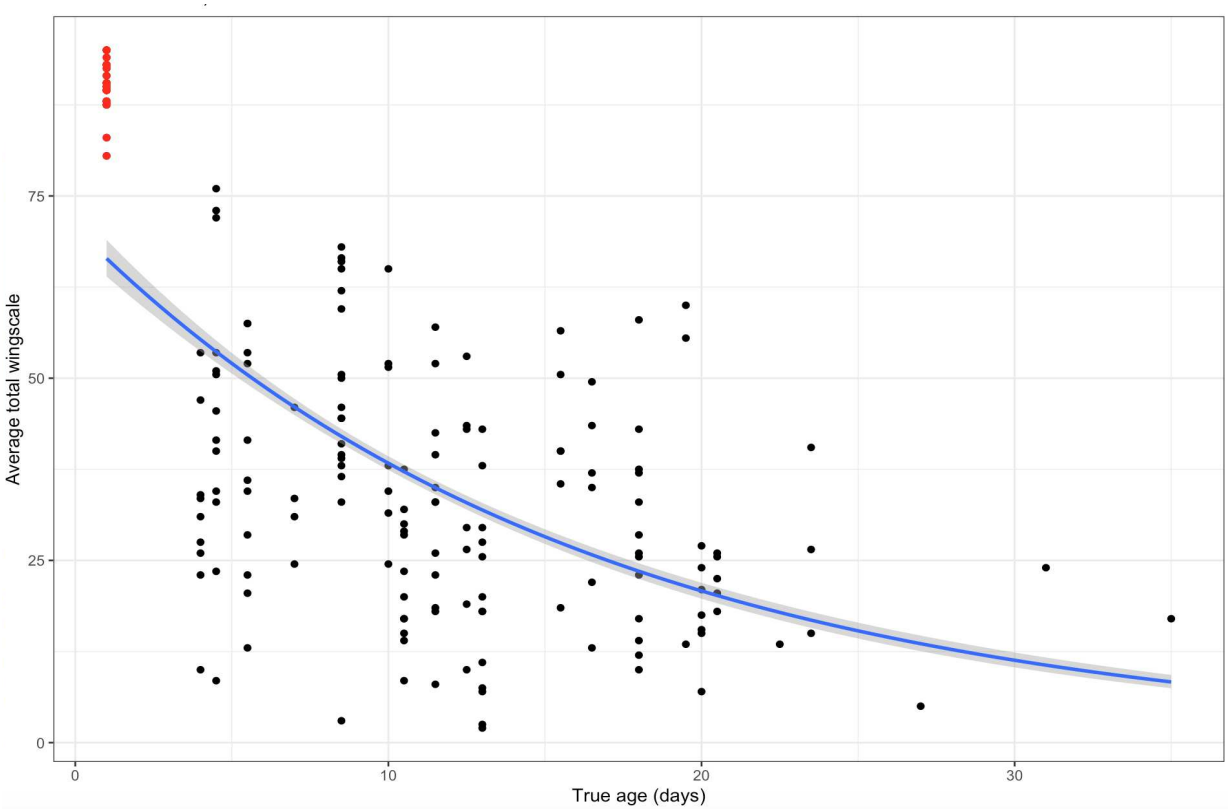

Figure 2.3. Wing scale loss correlates with mosquito age in mesocosm experiments. *An. gambiae* mosquitoes were sampled twice per week from a mesocosm that was continuously replenished with marked mosquitoes over 10 weeks. The total number of wing scales was summed across the Cu2, Cu1, M4, and M2 regions and analyzed against the average age of marked mosquitoes measured in days. Data from newly emerged females that were sampled from a separate cage at one day post-eclosion are marked in red. Data from all known-aged females sampled from the control mesocosm are marked in black. Blue line denotes the Poisson regression model line discerned from the data (gray areas = 95% confidence interval region of the model).

2.2.3 Assessing ivermectin-induced effect on mesocosm age structure.

Parity analyses of females of known age showed significantly different mean ages between nulliparous and parous mosquitoes tested from the control mesocosm (nulliparous = 8.9 days [95% CI: 6.9, 11.0], n = 42; parous = 13.2 [95% CI: 12.2, 14.2], n = 115; t-test: t = 4.2, p-value <0.0001) and the intervention (ivermectin-treated) mesocosm (nulliparous = 7.4 days [95% CI: 5.7, 9.2], n = 32; parous = 11.5 [95% CI: 10.4, 12.6], n = 97; t-test: t = 3.7, p-value = 0.0003). Furthermore, the mean ages of nulliparous and parous mosquitoes were lower in the

intervention mesocosm relative to the control mesocosm. Although parity status proved to be an accurate predictor of chronological age for individual mosquitoes, accuracy decreased when populations of mosquitoes of mixed and unknown ages were analyzed. When analyzing all mosquitoes sampled over the course of the entire 10-week experiment, no significant difference in the proportion of parous mosquitoes could be detected when comparing the control and ivermectin-fed mesocosms (n = 519; chi-square value: 0.26, df = 1, p-value 0.61).

Pearson correlation coefficients indicated a statistically significant negative correlation between the two wings (r: r = -0.67; p-value < 0.001). This indicated that both wings could be treated equally. We next assessed whether wing scale counting could be used to detect the shifts in age structure induced through the ivermectin-containing blood feeds. We conducted two-way t-tests for wing scale counts in each individual wing region, as well as the total sum of wing scales for mosquitoes of both known and unknown ages grouped based on mesocosm. Whether summed across all wing regions or within an individual wing region, the average number of wing scales was always significantly higher for mosquitoes in the ivermectin-treated mesocosm than those in the control mesocosm (Table 2.1).

Table 2.1. Two-way t-test for difference in wing scale counts from mosquitoes of known and unknown ages between both mesocosms

Wing region	Mesocosm	Mean n wing scales	95% CL	T-test value	P-value
Cu2	Control	14.1	(13.3, 14.8)	1.99	0.0477
	Ivermectin	15.1	(14.4, 15.8)		
Cu1	Control	13.3	(12.5, 14.1)	2.61	0.0094
	Ivermectin	14.8	(14.0, 15.6)		
M4	Control	7.7	(7.0, 8.3)	3.87	0.0001
	Ivermectin	9.5	(8.8, 10.1)		
M2	Control	5.3	(4.7, 5.8)	2.98	0.0031
	Ivermectin	6.5	(5.9, 7.0)		
Total wing scale	Control	40.3	(37.8, 42.8)	3.17	0.0016
	Ivermectin	45.7	(43.4, 48.0)		

2.2.4 Age grading by assessing total wing wear using computer vision algorithms.

Lastly, we investigated if computer vision algorithms could correctly classify or quantify mosquito age using wing photos derived from the mesocosm experiments. Machine learning (ML) outputs were first analyzed as a binary outcome of mosquitoes ≤ 10 days old (n = 235) and > 10 days old (n = 253). Early exploration utilizing mosquito wing photos from the simple cage experiment (non-mesocosm) using the ResNet18 convolutional neural network (CNN) showed high 93.7% accuracy on the test set. However, when using images generated from the more complex mesocosm experiment, the accuracy of the ML analysis using resnet18 CNN decreased to 84.2%. It was suspected that this was due to a greater diversification of wing scale states with the addition of environmental stressors in the mesocosm as compared to the cages. We then combined the images from the cage experiment and the mesocosm trial to increase the number of training set data points used in the model. Surprisingly, we saw a substantial decrease in accuracy to 75.7%. This indicates that the increased wing wear from the more complex mesocosm cohort expressed enough differences from the simpler cage experiments to support the need for environments that replicate wildtype ecosystems. To further explore where a natural maximum wing wear threshold occurred, we incrementally adjusted the classification cutoff to a lower time point with just the mesocosm dataset. We achieved the highest score of 88.0% accuracy when using the binary classification ≤ 6 days old and > 6 days old. This suggested that greater differences in the numbers of scales are seen at younger ages and that older aged mosquitoes are harder to differentiate with this method. This is further demonstrated by the non-linear relationship between number of scales and the true age observed in the regression analyses (Fig. 2.3).

To increase the model's accuracy in distinguishing mosquitoes older or younger than the malaria EIP (10 days), we used the combined data from the mesocosm and cage experiments but removed the image data that was taken from days 8-12. In contrast, our test set still contained the images from days 8-12. The pre-trained CNN and support vector machine (SVM) models achieved similar results (75.4% accuracy) as what was seen previously.

Image analysis using pixel intensity began by processing individual wing photos through algorithms to achieve histogram equalization. A linear binary decision threshold analysis was explored to categorize control mesocosm mosquitoes predicted to be above or below the EIP (10 days old). This model achieved an 88.0% accuracy between distinguishing individual mosquitoes of known age above and below this cut-off. In contrast, a human classifier counting only long wing scales in our predetermined wing fringe regions from the same mosquito wing photos correctly classified the age only 56.0% of the time.

In comparing the two mesocosms, the mean pixel intensity scores of all mosquitoes sampled were significantly different from each other (control = 119,162,337; ivermectin = 119,102,006; t-test: $t = 2.8$, $df = 517$, p-value = 0.0061), reflecting a significantly younger age in the ivermectin mesocosm due to a lower pixel intensity score caused by darker pixels on wings with more scales. Subsequently, linear binary decision threshold analysis was applied to mosquitoes sampled from both mesocosm datasets to group them into young and old age classes. By averaging pixel intensity scores of ivermectin and control mesocosm mosquitoes of known age, a single, common threshold value of 119,141,236.5 was applied to the data. This threshold was then used to group mosquitoes of unknown ages into each age class (Fig. 2.4).

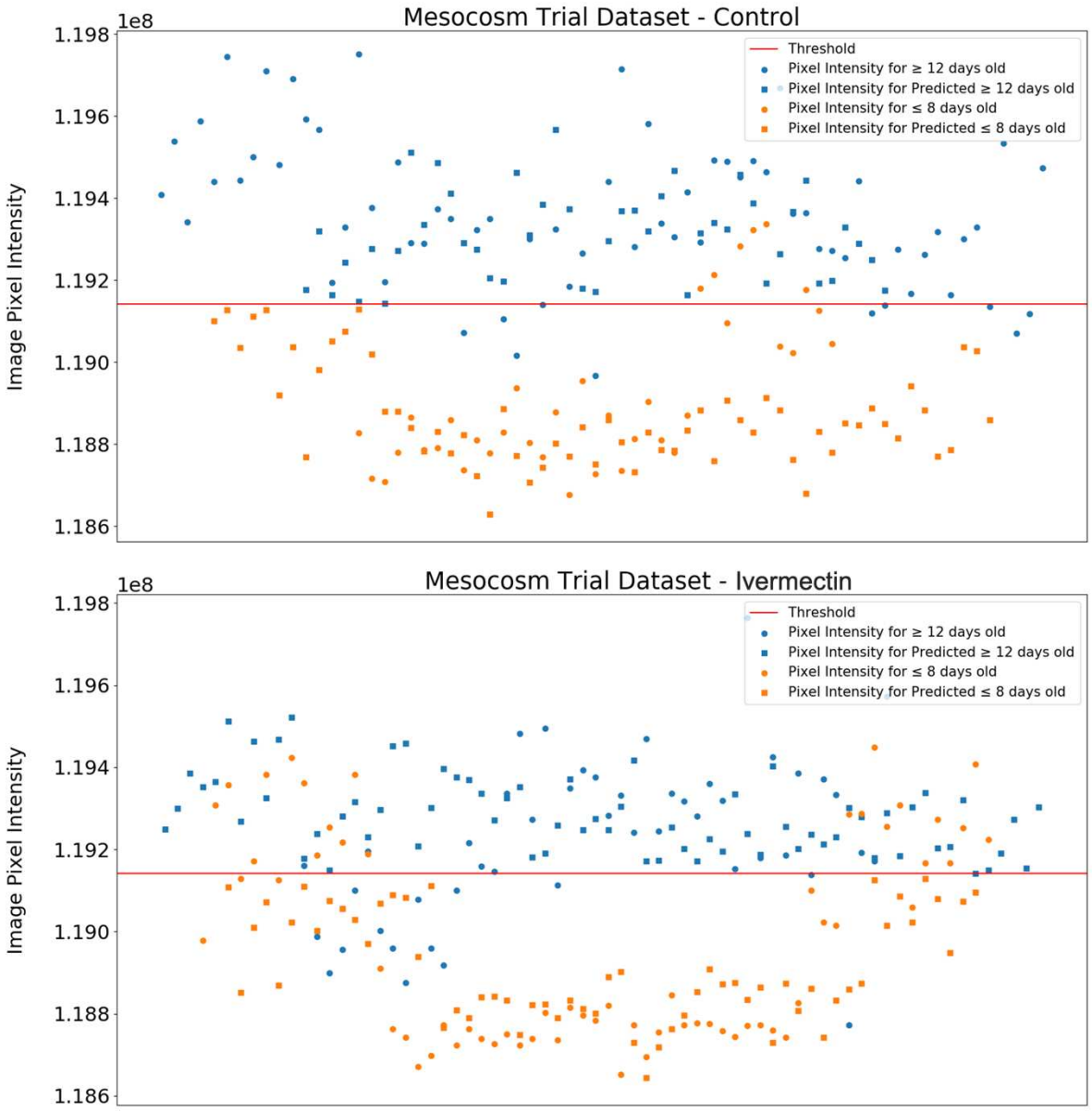

Figure 2.4. Mosquitoes from the control and ivermectin-treated mesocosms classified as young and old based on age and their mean wing image pixel intensity score. Orange dots represent mosquitoes of known age (marked) ≤ 8 days old, while orange squares represent unmarked mosquitoes predicted to be ≤ 8 days old. Blue dots represent mosquitoes of known age (marked) ≥ 8 days old, while blue squares represent unmarked mosquitoes predicted to be ≥ 12 days old. Mosquitoes graded as ages 9-11 were removed from the analysis for greater separation of the age groupings. The threshold was calculated by determining the mean pixel intensity of marked mosquitoes analyzed from both mesocosms.

Based upon the results from the linear binary threshold, linear regression analysis was then performed. Using only images of mosquitoes with known ages from both the control and ivermectin mesocosm cohorts, images were processed by calculating the left and right wing pixel intensity scores averaged per mosquito followed by cross-validation. The average overall test accuracy was 83.4% and the average training accuracy was 89.7%. The results of the six independent cross-validation trials are presented in Supplemental Figure S1.2.

Given the accuracy of the cross-validation tests using image pixel intensity, a summary analysis was made for all control and ivermectin-treated mesocosm mosquitoes of known age, as well as newly emerged mosquitoes (Fig. 2.5). Overall, a higher proportion of mosquitoes from the ivermectin-treated mesocosm (108/257; 0.42 [95% CI: 0.36, 0.48]) were grouped into the younger age class relative to those in the control mesocosm (96/262; 0.37 [95% CI: 0.31, 0.43]), while a higher proportion of control mesocosm mosquitoes were grouped into the older age class (137/262; 0.52 [95% CI: 0.46, 0.58]) relative to the ivermectin-treated mesocosm (113/257; 0.44 [95% CI: 0.38, 0.50]). However, neither comparison was statistically significant.

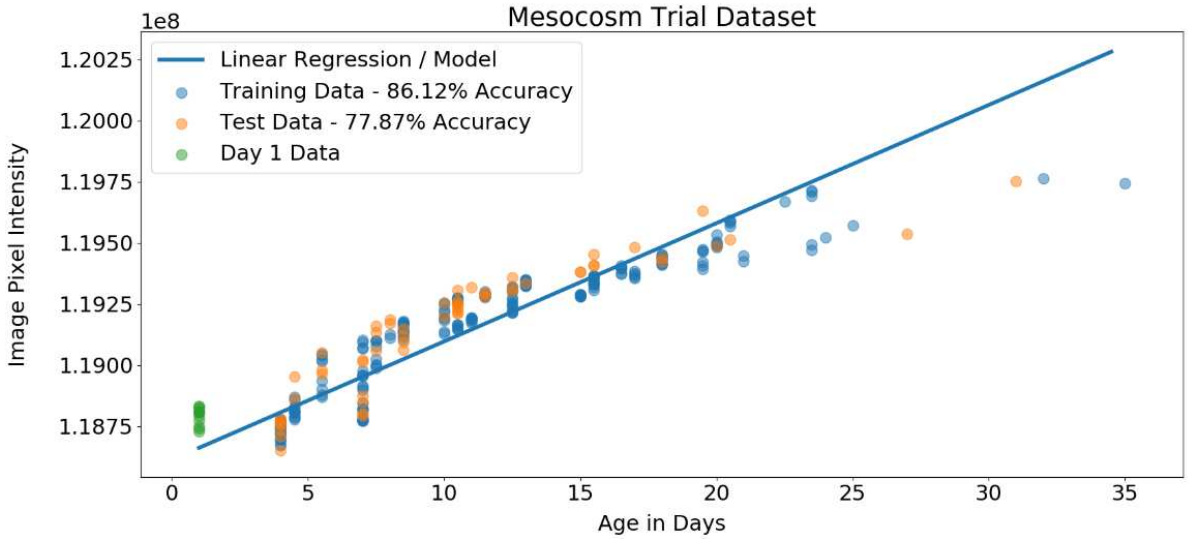

Figure 2.5. Linear regression of mean wing image pixel intensity per individual plotted by age. Each blue and orange dot represents a single marked mosquito. All color-marked mosquitoes from the control and the ivermectin mesocosm were included in the analysis. Image pixel intensity scores were derived from the mean score from averaged left and right wings from an individual mosquito. Added green dots represent the newly-eclosed (day 1) mosquitoes.

2.3 Discussion

Our data represent the critical first steps to developing a robust technique for age grading mosquitoes using wing wear. Assaying mosquitoes in laboratory-based cage experiments indicated that the number of long wing scales across the four predefined wing regions (Cu1, Cu2, M2, and M4) were reduced over time. This relationship was also observed in the mesocosm experiment, but the scale loss over time was more pronounced. While the wing scale counting technique was generally effective, the variance of scale loss per mosquito of known age was high and the process of manually counting scales was tedious and potentially biased. In contrast, computer vision techniques, particularly wing image pixel intensity analysis, showed great promise for grading mosquito chronological age due to its relatively high accuracy, the potential for automation of the process, and lower variance per mosquito of known age. Overall, sub-lethal exposure to ivermectin in one mesocosm led to significant shifts in the age structure towards

younger classes of mosquitoes when compared to the control mesocosm that could be detected with both the wing scale counting technique and wing image pixel intensity analysis.

Mosquito age has long been recognized as a potentially good indicator of vector control efficiency and, more recently, is seen as a viable metric to predict mosquito-borne disease outbreaks.[93,94] However, because mosquito survivorship typically follows complex, age-dependent patterns,[415,416] new techniques are needed that can finely classify mosquitoes by chronological age. Currently, researchers and control personnel are limited in their predictive abilities as only a few age grading methods are able to calculate continuous age, notably gene and protein profiling, mark release recapture (MRR) studies, and chemometric methods (near-infrared spectroscopy [NIRS] and mid-infrared spectroscopy [MIRS]).[253] Of these, NIRS has been the most widely used as NIRS scanning is rapid and field-viable, performs non-destructive analysis, and can also potentially detect *Plasmodium* infections and identify species and sub-species.[315,417] However, measurements of mosquito age from NIRS have comparatively high individual mosquito error.[252] Difficulties are further augmented in the field, as NIRS data variation can be high likely due to the confounding effects of genetic, dietary, and environmental effects on wild mosquitoes.[304] In addition, instrument costs with NIRS-based analyses are also high, the statistical methods of analysis can be difficult for non-specialists, and NIRS scan datasets cannot easily be combined across sites, often necessitating new calibration datasets for each mosquito population tested in time and space.[252] MIRS may allay some of these problems with NIRS. However, the technique is relatively new (and thus less tested) and also requires destructive measurements of the samples.[253]

Our results indicate that wing scale-based age estimation could prove to be a viable, alternative age grading technique. Even as early as 1912, Perry was able to successfully classify

wild mosquitoes into four tiered age groups based on qualitative assessment of their wing.[289] Our cage and mesocosm experiment results expand Perry's original conclusions, showing that wing scale counting can use count-based data, and wing image pixel intensity can use continuous variable data, to calculate chronological age in days. This technique is also non-destructive, only requiring that wings be plucked from the sample during initial identifications under a microscope. Therefore, it allows for downstream processing of all other mosquito tissues. Both wing scale counting and wing image pixel intensity analyses were able to detect the changes in overall age structure between our two mesocosm populations due to natural flying activities of the mosquitoes that led to scale loss over time. The former technique showed relatively more scales in the select regions we counted from mosquitoes of younger age classes; the latter technique showed relatively lower (more black) mean pixel intensity scores of the entire wing images in younger age classes due to the presence of more dark scales on these mosquitoes. Overall, the control mesocosm's population skewed towards older females, while the ivermectin-treated mesocosm skewed towards younger females.

Mosquito populations can be highly variable and change rapidly due to mass larval emergences or quickly changing environmental conditions at field sites. As such, many individuals should ideally be processed per time interval to achieve accurate measurement of population age in that period. This also is often done by field teams who may have limited resources, familiarity with entomology field work, or experience handling mosquito samples.[5] Considering these realities, an ideal age grading technique should be quick, low-cost and be accessible even for novice personnel. Assessing wing wear via scale counting is inexpensive aside from the upfront purchase of a stereoscope with a camera. It is also intuitive and requires little training to master. To save time in the field, wing image analysis could be also done later

from stored, slide-mounted wings, or the images could be immediately scanned and virtually analyzed elsewhere. We have also demonstrated that workloads could be reduced further by reducing the number of wing regions used for counting; based on our goodness-of-fit statistics for Poisson modeling, counting scales in just the M2 and Cu2 regions predicted mosquito age just as accurately as counting long wing scales across all four regions (data not shown). However, focusing on only long wing scales on the distal posterior wing fringe may be biased by limiting analysis to such a small part of the wing. To this point, we observed high variance in scale counts per age in days 4-18. The variance may also be due partially to human error, as the counting process is tedious for the person who had to study many images. While mosquito age grading necessarily should be focused on the population rather than individuals, the two are related and it is significant that individual mosquitoes of known age were only accurately predicted to be above or below the EIP 56% of the time by the wing scale counting technique.[252] We also observed a faster loss of scales in the mesocosm experiments that facilitated more mosquito flying relative to the simple cage experiments. This observation may be even more amplified between laboratory and wild environments, and the link between environmental conditions (e.g., excessive wind) and scale loss could confound comparisons of mosquito age across populations collected in time and space with this technique. As such, it will be crucial for wing scale-based age grading to be performed and validated in field settings. Regardless, some of these limitations in wing scale counting may be resolved by the image analysis approaches we tested.

ML has become the gold standard in image analysis and has broadened the capabilities of scientific research, including in mosquito identification studies.[418,419] Here, we apply ML with image analysis to classify mosquito age. Using a variety of different algorithms, application of

ML to individual mosquitoes' wing images was easily able to outperform mosquito age classification by a human performing wing scale counting on the same images. While the advanced ML algorithms we tested (pre-trained CNNs and SVM) were superior to human-based classification, the algorithm that showed the most promise, wing image pixel intensity quantification followed by simple linear regression, does not use computationally expensive ML algorithms but instead classifies mosquito age based on the intensities of the pixels located within the wing images. The advantage of this approach is that it is intuitive (scales lost equate to higher/more white pixel intensity from the wing image), requires far less computational resources, and can be used on standard computers without investing in costly graphics cards or processors. In contrast, the predictive variables that ML uses are generally unknown or hard to discern and it requires a large amount of data to be used in training, sometimes requiring thousands or more images to generate an accurate model.[420] Failure to collect the appropriate amount and quality of data may result in overfitting the model, increase its susceptibility to noise within the data, or otherwise decrease model performance. Because of the limited number of images available for training our ML classification models, all the concerns mentioned were issues we had to account for. Overall, we conclude that wing image pixel intensity analysis is the most advantageous method to classify the age of mosquitoes we have tested so far, but the more advanced ML models may prove better in time with the accumulation of more images from both the lab and field. In addition, collecting images in this manner allows for potential secondary analyses such as quantifying wing patterning to help in mosquito identification efforts. The pixel intensity data generally fit a linear regression but skewed most from this simple model at the later ages, at approximately 12 days old. Presumably the wing images of the mosquitoes start to reach saturation of whiter pixel intensities as dark scale loss becomes very high in old age.

Analyses of field mosquitoes with similar techniques in the future may be best analyzed with different regression models depending on scale color intensities of wild type populations and the rate of wing scale loss in natural environments. Data could be analyzed on a continuous scale, binned into groups (e.g., 1-5, 6-10, >10) or split into binary groups with a threshold on the most relevant epidemiological age of the mosquitoes, such as the EIP for *Plasmodium* development in *Anopheles gambiae*.

Ovary assessments by the Detinova and Polovodova techniques have been the gold standard tool for entomologists in their effort to age grade mosquitoes. Our results demonstrated that parity was reliable for determining an individual mosquito's age in both our cage and mesocosm experiments. In samples where the true age of the mosquito could be externally verified, the average age for nulliparous and parous females aligned with what has been reported in the literature.[144,171] Yet, from an epidemiological standpoint, it is more productive to judge parity-based age grading in its ability to detect differences in the age structure of a mosquito population rather than of individuals. As evidenced in our mesocosm experiments, the Detinova method failed to detect the significant shifts in age structure induced by ivermectin in mixed populations of known and unknown ages. In the RIMDAMAL clinical trial testing ivermectin for malaria control, no significant reduction in parity rates was observed between mosquitoes collected from control vs. intervention sites. This result was perplexing, as indicators for reduced malaria transmission in ivermectin sites were observed, including participants' exposure to biting anophelines.[398] However, sub-lethal ivermectin exposure is known to interrupt the mosquito reproductive cycle. As shown in a study with *Aedes aegypti,* ivermectin exposure in bloodmeals caused notable dysregulation in ovarian development, including slow blood digestion without development of ovarian follicles, degeneration of primary follicles and formation of ovarian

dilatations within 24 hours post-blood feed, significant reduction in the rate of vitellogenesis and follicle development, and decreased egg production.[383] Additionally, field studies involving *Anopheles* feeding on ivermectin-treated cattle demonstrated that ivermectin exposure reduced mosquito egg production for up to 15 days.[386,421] It is reasonable to conclude that sub-lethal ivermectin exposures result in some parity misclassifications due to the dysregulated ovarian development. This could explain why parity rates in the RIMDAMAL trial did not match other entomological indicators for malaria control in the field, and why parity assessment alone was unable to detect age structure differences between our two mesocosms in this study. As such, having an accurate mosquito age grading technique that does not rely on ovarian development, such as NIRS, MIRS and wing wear analysis, may be more appropriate for analyzing ivermectin-based control approaches. Similarly, other new and developing vector control tools should assess the interventions' sub-lethal effects on mosquito ovarian development to avoid such potential confounders in the future.

In conclusion, assessing wing wear for mosquito age grading has promise to be both an accurate and practical tool to use in evaluating the risk of mosquito borne pathogen transmission and the efficacy of mosquito-control interventions in research and operational settings. Further investigation is needed in other species, and whether wing wear in field settings, either done via human assessments or computational wing image analyses, is a germane alternative to other age grading techniques such as parity assessments and NIRS. Furthermore, it would be both insightful and important to determine in field settings if ovarian-based grading techniques remain a viable tool for vector control efficacy assessments when insecticides/endectocides that impair or delay female mosquito reproduction are utilized.

2.4 Materials and Methods

2.4.1 Mosquito rearing and experimentation design

Mosquitoes. *An. gambiae* (G3 strain) were reared in an insectary at 27-30°C, 60%-80% relative humidity, with a standard photoperiod (16 hours of light: eight hours of dark). Larvae were reared in open-faced plastic bins and fed a diet of ground TetraMin fish food.[118] Pupae were transferred from larval rearing pans to closed, plastic emergence cages. Twenty-four hours post-eclosion, adults were gently aspirated with a ProkoPack and moved to an adult-only colony bin.[422] Adults were binned according to age, with large cohorts of adults of the same age being placed together. In cases of smaller cohorts, adults of mixed ages were grouped together. However, these adults never differed by more than two days in age. Adults were fed 10% sucrose in water *ad libitum*.

Simple cage experiment. For this experiment, parity status was classified per definitions set out by Benedict et al. Nulliparous status was defined not by whether a female mosquito had blood fed or not, but rather by her virgin status. Parous females were those who had oviposited at least once.[118]

Approximately 300, 5- to 6-day-old female *An. gambiae* were transferred into a 30.5 cm x 35.5 cm x 40.5 cm plastic cage via ProkoPack aspiration. Mosquitoes were then fed defibrinated calf blood in a glass membrane feeder for one hour. After 30 minutes of rest, mosquitoes were knocked down with cold. Unfed females were removed and analyzed as unfed nulliparous. Blood-fed females and males were reintroduced into the cage. Three days later, 10 females were removed from the cage with a mouth aspirator and classified as blood-fed nulliparous.

Mosquitoes were then given a second bloodmeal to allow for full ovary development. Afterwards they were provided damp paper towels for egg laying. Twenty-four hours later the egg papers were removed, and 10 females were removed from the cage with a mouth aspirator and classified as uniparous (i.e., completion of one gonotrophic cycle). Remaining mosquitoes were given a third and final bloodmeal. Females that did not feed or fully engorge were removed via cold knock down. Engorged females and males were reintroduced and provided egg papers. Twenty-four hours later, egg papers were removed along with 10 biparous (i.e., completion of two gonotrophic cycles) females via mouth aspiration. The experiment was repeated three more times to have four replicates and 139 females sampled in total. In one replicate, enough mosquitoes remained after biparous sampling to go through a third blood feed and egg laying (triparous - completion of three gonotrophic cycles). Additionally, 20 teneral females were sampled < 24 hours after emergence to determine the base number of scales present along wing edges (described below).

Mesocosm experiments. Two mesocosms (122 cm long x 61 cm wide x 96.5 cm height) were constructed using plastic containers (Fig. 2.6). At the front of the mesocosm, mosquitoes had to pass through 2.5 cm holes cut into a Tupperware container (15 cm long x 15 cm wide x 15 cm height) to feed on sugar cubes. They had to enter a separate but identical container to lay eggs on damp paper. To obtain water and bloodmeals, mosquitoes had to traverse the length of the mesocosm, navigate through a tall, artificial plant, and enter a separate chamber in the back upper section of the cage. Initially, approximately 400 3- to 5-day-old male and non-blood fed female *An. gambiae* were placed into each mesocosm. The age distribution between both mesocosms was approximately equal. Mosquitoes in both mesocosms were offered two

defibrinated calf bloodmeals every week for 10 weeks. However, the intervention mesocosm received a bloodmeal containing 5 ng/μL ivermectin every other week. This concentration, which is less than the lethal concentration to kill 50% (LC_{50}) of this species, was previously shown to significantly reduce mosquito fecundity and affect survivorship but not induce mortality across the entire mosquito population.[377,386,423]

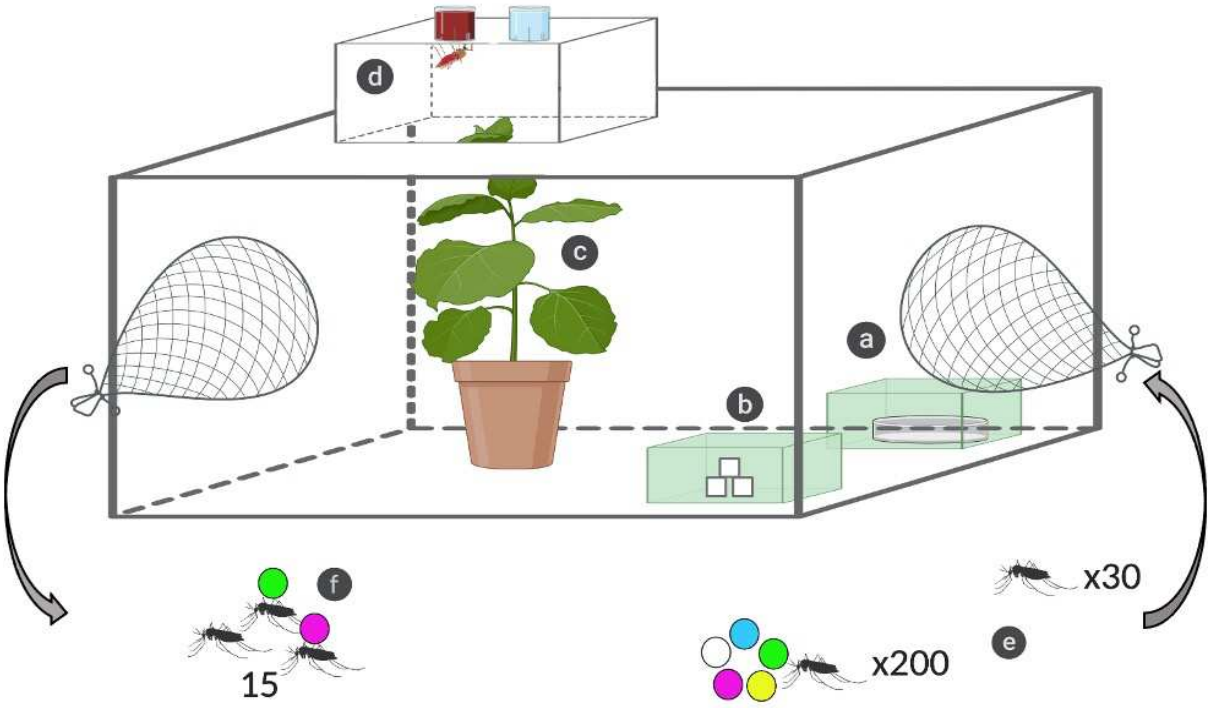

Figure 2.6. Cage design and procedural overview for mesocosm-based experiments. *An. gambiae* G3 mosquitoes were reared in two separate mesocosms for 10 weeks. Navigational flight was encouraged by placing egg papers (a), sugar (b), and blood/water (d) in different locations and chambers covered with small entry/exit holes. The control mesocosm received untreated blood, while the intervention mesocosm received a sub-lethal 5 ng/μL dose of ivermectin in its blood feed every other week. Every two weeks 200 fluorescent powder-marked mosquitoes were added to each mesocosm; twice each week, 30 unmarked mosquitoes were added to each mesocosm (e). Twice each week, 15 females were removed from each mesocosm for parity and wing wear analyses (f).

The day before a blood feed, 30 unmarked mosquitoes (a mix of newly emerged male and female) were added to each mesocosm. To simulate a mass emergence event, every other week a normal input of 30 unmarked mosquitoes were replaced by a batch of 200 newly emerged, mixed male and female mosquitoes (Supplemental Figure S1.1). However, due to uncontrollable and unpredictable irregularities in mosquito emergence rates, there were some instances where an emergence group had < 200 adults. As such, some emergence groups had to be combined to have the required sample numbers. In these instances, mosquitoes added to each mesocosm were not all the same age but differed by no more than 1-2 days. When analyzing data from these mosquitoes, the average of the age groups was taken to have a single, numerical variable to use for analysis (i.e., if the group was 10-11 days old when sampled from a mesocosm, the average age was logged as 10.5). These mosquitoes were first collected from emergence bins with a ProkoPack aspirator, placed in a large Ziplock bag, knocked down with carbon dioxide, coated in a light dusting of fluorescent pigment powder (Shannon Luminous Materials, Inc.), and then transferred to a mesocosm. In total, five different colors were used, with each color used only once. As such, the exact age of a mosquito could be determined based on its color mark alone. The day after a blood feed, 15 females were removed from each mesocosm via mouth aspiration (total sampled: n = 537). Each group of removed females constituted a replicate. Females were selected in a random fashion, resulting in a mixed selection of unmarked mosquitoes of unknown ages and color-marked mosquitoes of known ages. Due to the long duration of the experiment (10 weeks) and complexity of the continuously sampled and restocked mesocosms, only a single replicate was undertaken (one control and one treatment mesocosm).

2.4.2 Age assessment techniques conducted for mesocosm and cage experiment mosquitoes

Parity and wing assessments for both experiments. Selected females were knocked down with cold and held on ice. For the simple cage experiments, these included newly emerged, unfed nulliparous, blood-fed nulliparous, uniparous, biparous, and triparous females. For the mesocosm experiments, 30 mosquitoes (15 from each mesocosm) were analyzed, and the color mark of each mosquito was also noted. Wings were carefully removed by first pinching the lateral sides of the scutum. This contracted the thoracic muscles, forcing the wings to flare away from the thorax at 90° or more. Wings were then removed by gently pulling the exposed wing at the basal junction to the thorax with a fine pair of forceps. Dissected wings were placed on a ~5 μL drop of 10% sugar water on a glass slide, which was allowed to dry. The sugar water acted as an adherent, preventing the wings from shifting or losing scales when the slide was photographed at 30X with a Leica EZ4 W stereo microscope. Wing photos were later analyzed by counting long wing scales present along the distal-posterior edge of the wing, as this is likely subject to the greatest rate of scale loss due to aerodynamic forces experienced during wing beats.[288] We only counted the tallest, long wing scales because they are the easiest to differentiate with the human eye. To further focus our effort, we only counted long wing scales within four wing cell regions defined by branches of the cubital (Cu) and medial (M) longitudinal veins that reached the wing margin: Cu1, Cu2, M2, and M4 (Fig. 2.7).[424] Ovaries were dissected from the same mosquitoes in water. Parity assessments were made according to the Detinova method with a Leica DM500 microscope.[8]

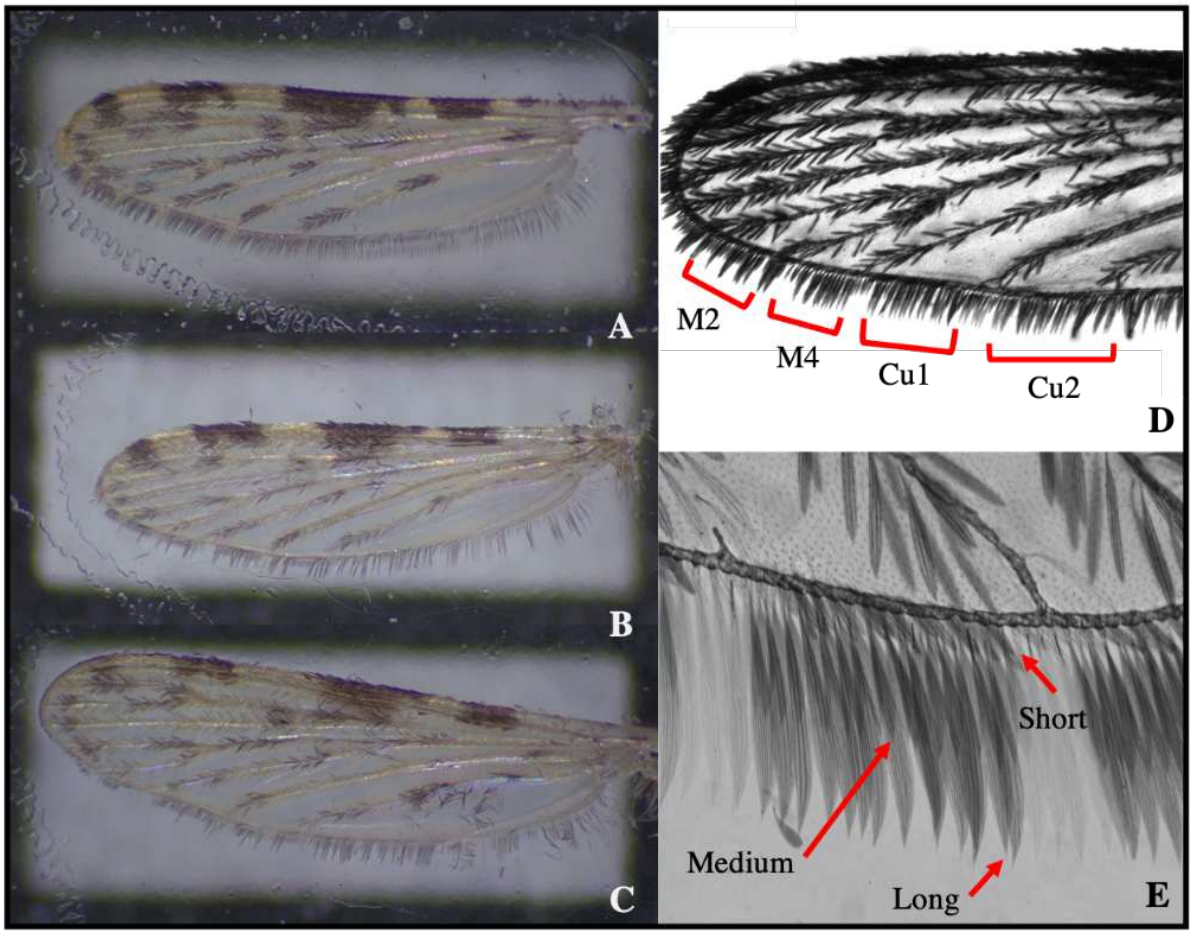

Figure 2.7. Wing wear patterns and scale counting methods for age grading**.** Photos of female, lab-reared, G3 strain *Anopheles gambiae* wings at one day (A), eight days (B), and 14 days post-emergence (C) show that wing scales are lost as mosquitoes age. Wing scales vary in length along the wing edge (D), but only long wing scales were counted in four specific wing regions, Cu2, Cu1, M4 and M2 in our manual counting experiments (D & E).

Computational wing photo analyses. In addition to manually counting wing scales in the pre-described regions, wing photos were also analyzed by computer algorithms to classify or measure total wing wear. First, ML techniques were used to classify adult female *An. gambiae* s.l mosquitoes based on the malaria EIP. Although the EIP for malaria can depend on climatic conditions, it commonly ranges from 10 to 15 days for malaria.[2,425] In order to have the largest sample size possible for older class females, mosquitoes were categorized based on the lowest estimate for EIP (10-days-old or older vs. younger ages). All ML models were trained using

PyTorch version 1.3.1 ML library in Python 3.6.10 version on an NVIDIA GeForce GTX 1060 GPU. There were 997 original images used but image augmentation using the computer programming library OpenCV (www.opencv.org; version 3.4.1) was implemented to increase the dataset size. This included image rotation, horizontal and vertical flipping, Gaussian blurring (5x5), and mean denoising. The initial ML classifier schema and test dataset did include all images, however, removing days 9-11 to distinguish mosquitoes more easily from young vs. old groupings showed increased accuracy of the final algorithm when compared to training with all images. After image augmentation there were 1,917 images for the > 10 days classification and 1,950 images for the ≤ 10 days classification. During the initial training we explored combining both the cage and mesocosm data, but the final algorithm only included the mesocosm original and augmented images. The first ML algorithm techniques explored a variety of pre-trained neural networks, which included ResNet-18, ResNet-50, ResNet-152, Densenet-121 and VGG-16.[426–428] The second approach explored was support vector machine algorithms using the same PyTorch library.

Our last approach used traditional computer vision methodology, using OpenCV and NumPy to create a simpler and more robust classification model by computing overall pixel intensities of wing images. With each wing photo (left and right for each mosquito), pre-processing in the form of histogram equalization was performed. Afterwards, pixel intensity scores for each image were obtained by summing pixel intensities across the entire image. Initially, a binary decision threshold model was created from the means of these pixel intensities to classify mosquitoes ≥ 12 days old and ≤ 8 days old, with 9- to 11-day-old mosquito samples being discarded.[429] This test showed that there was a marked difference between the old and young groups, and that using

the pixel intensity method may even work for creating a linear regression model. Subsequently, the 9- to 11-day-old mosquito samples were re-inserted into the dataset, and a linear regression model was generated for the entire dataset (control and ivermectin-treated mesocosms), with left- and right-wing pixel intensities averaged. Newly eclosed (day 1) mosquitoes were additionally included. To test the reliability of our promising results, cross-validations were performed six times to evaluate the linear regression age grading model, with a training-test distribution of 80% - 20%. Results of this cross-validation are available in Supplemental Figure S1.2. Given the high accuracy of the cross-validation tests, a final linear regression model was used for age grading with the control and ivermectin-treated mesocosms.

2.4.3 Statistical analyses

Any observation for which one wing region was not able to be counted (i.e., the wing folded on itself, scales were pulled away from the wing, photograph was slightly blurry, etc.) was removed from the dataset. For each remaining mosquito processed via wing scale counting, the values of the four wing regions (Cu2, Cu1, M4, M2) were averaged over the left and right wing. Left and right wing counts were averaged when both values were available or taken as the value solely for the left or right wing otherwise. For wing scale counts from cage data, 139 mosquitoes sampled were included in the final analyses. Additionally, 519 mosquitoes were sampled from the mesocosm and included in the final analyses.

To determine if mosquitoes displayed unequal rates of wing scale loss between left and right wings on any given individual, we conducted a basic correlation analysis comparing the total number of counted wing scales between the left and right wing for all mosquitoes. This was done

for mosquitoes sampled from the cage experiments as well as the mesocosm. A univariate Poisson regression model was used to quantify the relationship between wing scale counts and age, by regressing age on the sum of all long wing scales across the Cu2, Cu1, M4, and M2 regions. For total wing wear quantification using wing photo pixel intensity, linear regression models were used to quantify the relationship between pixel intensity scores and age by interpolation. The proportions of young vs. old mosquitoes of known and predicted ages in each mesocosm were analyzed using Fisher's exact tests. To compare the initial rate of scale loss between the cage and mesocosm (control mesocosm only) experiment data, we used an F-test to compare the linear regression slopes between common early age points of the two experiments (day = 1 and day = 4.5). All analyses were performed using SAS statistical software (v9.4), GraphPad Prism (v8.1.1), and R (v6.3.1).

CHAPTER 3: COMPARING WING SCALE COUNTING, PARITY, AND NEAR INFRARED SPECTROSCOPY AGE GRADING TECHNIQUES USED WITHIN THE FIRST SEASON OF RIMDAMAL II

3.1 Introduction

Malaria is a devastating, arthropod-borne disease that affects nearly 200 million people and produces hundreds of thousands of deaths each year.[4,430] The disease is caused by unicellular protists of the genus *Plasmodium,* of which there are five species known to infect humans (*Plasmodium falciparum*, *P. vivax*, *P. ovale*, *P. malariae,* and *P. knowlesi*).[15] In West Africa, malaria transmission is facilitated by female mosquitoes in the genus *Anopheles*, which become infected with *Plasmodium* gametocytes when feeding on an infected human.[143] Given the vital role mosquitoes play in transmitting malaria, adult mosquito population reduction is a core component of malaria control efforts.

A significant amount of time relative to the adult mosquito lifespan is needed for *Plasmodium* to successfully infect the mosquito, complete sporogony, and reach the saliva glands to be transmitted to humans in a subsequent bite. It is estimated that at its most rapid, the entire process (called the extrinsic incubation period; EIP) lasts 10 days in the *Anopheles gambiae* mosquito complex (*An. gambiae* sensu latu, or s.l).[40,431] Therefore, older female mosquitoes have the greatest likelihood of transmitting malaria to humans, as these mosquitoes have likely lived long enough for incubating malaria parasites to complete and surpass the required EIP.[231,253] Additionally, the probability of a mosquito being infected with malaria gametocytes is relatively low, meaning that it is far more common for most blood feeding mosquitoes to only become successfully infected in their later blood feeds. Age, therefore,

becomes a significant factor in mosquito population dynamics before infection even occurs and the malaria EIP begins. Consequently, from the perspective of mosquito-borne disease surveillance and prevention, this means that it is crucial for field entomologists to routinely monitor the relative ages of local mosquito vector populations to determine if females are aging to the point where transmission to humans is likely.[253]

Tools and techniques for determining ages of wild mosquitoes should accommodate the realities entomologists face in field work, while also providing age measurements that are epidemiologically relevant. In regards to the former point, techniques are favored if they can be conducted with minimal technical resources, require little technical expertise, provide results quickly and accurately, and have minimal associated costs.[5] Additionally, methods should calculate mosquito age in a unit that can easily be correlated to the surveilled pathogen's EIP.[252,253] Given these needs, two grading techniques are frequently used by field entomologists: the Detinova parity technique and near-infrared spectroscopy (NIRS).

The Detinova parity technique examines the morphology of tracheole skeins surrounding the mosquito ovary. These tracheoles remain tightly coiled for virgin females but permanently stretched and uncoiled after egg production. As such, age can be measured in gonotrophic cycles and females can be classified as nulliparous (typically less than three days old) or parous (typically older than 3 days).[409]

NIRS uses the near-infrared region of the electromagnetic spectrum to quantitatively measure organic compound functional groups within the mosquito exoskeleton.[304,417] The spectrum collected is proportional to the amount of these functional groups present in samples, which change as mosquitoes age.[303] This technique allows for mosquito age to be measured as continuous days.[417]

A third, long under-utilized technique that broadly predicts mosquito age classes from wing wear also meets the aforementioned requirements.[289] We have recently demonstrated that wing wear as mosquitoes age can be quantified by counting scale loss on wings or performing machine vision learning techniques on computer images of the whole wing. Age predictions for mosquitoes of unknown ages can then be made by comparing these counts or images to similar data taken from mosquitoes of known age. This technique has been shown to be relatively accurate in laboratory- and mesocosm-based settings and, like NIRS, measures age as continuous days (unpublished data, see Chapter 2 for results).

To date, no direct comparison has been made between these three age grading methods using wild-caught mosquitoes. This is in part because it is difficult to accurately age wild mosquitoes in comparison to their lab-reared counterparts. Field entomologists have no way of knowing wild mosquitoes' true ages with certainty, meaning age must be predicted by either a) comparing the physiological status (e.g., ovary morphology) of wild mosquitoes to those of known ages, or b) generating age regression models from counts and/or measurements of biological factors (e.g., number of wing scales) from mosquitoes of known age that can be applied to mosquitoes of unknown ages. In both cases, additional, labor-intensive steps must be taken to generate calibration curves and other comparative tools using mosquitoes captured from the wild as larvae and reared in insectaries. The difficulties of age grading wild mosquitoes are compounded by the fact that environmental factors such as larval diet and aquatic environments, physiological condition of the mosquito, and weather can result in a high degree of variability in age readings.[173,256,304,306–308] Similarly, *An. gambiae* s.l is a species complex of seven sibling species, all of which are morphologically identical.[145,146,432,433] Although NIRS can potentially be used to identify these sibling species, genetic and other biological differences between

mosquitoes in the *An. gambiae* s.l complex can still impact age readings and results.[434] Despite these obstacles, the need to reliably age wild mosquitoes is still highly needed in order to monitor malaria prevention and vector control efforts.

Our Repeated Ivermectin Mass Drug Administrations for control of Malaria II (RIMDAMAL II) trial provided an opportunity to compare the Detinova parity method, NIRS, and wing scale counting in both a true field environment and an area hyperendemic for malaria.[77,435] RIMDAMAL II is a NIH-funded, double-blind, cluster-randomized trial that integrates repeated high-dose ivermectin mass drug administrations (MDAs) into the existing monthly seasonal malaria chemoprevention (SMC) delivery platform and distribution of long lasting insecticidal nets (LLINs). The hypothesis of the study is that regular treatment of most of the cluster participants in the intervention arm with ivermectin MDAs will result in significantly decreased survivorship of the malaria vectors that blood feed on these people, which will decrease parasite transmission in the community and thus malaria in the community's children. This trial was conducted over two rainy seasons between 2019 and 2020 in Burkina Faso's Diebougou health district to provide definitive evidence on ivermectin efficacy in malaria prevention in children under 10 years of age. One of the expected entomological outcomes from this trial is that the predicted median age of the mosquito populations from intervention clusters will be significantly lower compared to the predicted median age of the mosquito population from control clusters. Due to the timing of RIMDAMAL II relative to my thesis completion, this age grading study analyzes data generated from female *Anopheles gambiae* s.l sampled during the 2019 field season only, offering a comparative analysis of these age grading methods' accuracy and feasibility. Furthermore, because the machine vision learning techniques to age grade mosquito populations from wing images were not fully developed and validated until early

2021, we only used the wing scale counting method developed and described in Chapter 2 on the 2019 field samples from RIMDAMAL II.

3.2 Results

3.2.1 Mosquito demographics

Taxonomic identification indicated that *An. gambiae* s.l represented 83.8% of all malaria mosquito vectors captured across the six sampled villages, while 12.4% were *An. funestus*, and minor vector species (*An. coustani, An. pharoensis, An. rufipes*) made up 1.3%. The number of *An. gambiae* s.l captured within each RIMDAMAL II cross-sectional village cluster at each sampling time point under different trapping methods can be viewed in Table 3.1, while the corresponding total number of mosquitoes caught per village and time point is seen in Figure 3.1. Table 3.2 shows the number of *An. gambiae* s.l tested with each different age grading method within each village cluster at each sampling time point among the six RIMDAMAL II villages.

Table 3.1. Number of *An. gambiae* s.l captured across six sampled villages in RIMDAMAL II according to sampling time point and trapping method

Village	MDA1+1		MDA1+3		MDA2+1		MDA2+3	
	LTC	ASP	LTC	ASP	LTC	ASP	LTC	ASP
DB	1	52	8	47	13	134	20	165
DL	24	64	3	133	16	227	23	211
KP	22	127	7	22	27	166	25	72
KS	28	33	18	51	0	48	19	29
SG	9	18	6	55	20	125	14	136
TG	7	23	8	28	3	129	7	87
Total per trap type	91	317	50	336	79	829	108	700
Total per time point	408		386		908		808	

Village	MDA3+1		MDA3+3		MDA4+1		MDA4+3	
	LTC	ASP	LTC	ASP	LTC	ASP	LTC	ASP
DB	20	98	12	103	12	178	9	49
DL	18	109	18	148	26	201	6	71
KP	10	39	4	71	23	70	6	26
KS	10	41	6	27	4	28	4	21
SG	12	65	26	136	25	82	2	74
TG	12	98	2	49	7	83	4	38
Total per trap type	82	450	68	534	97	635	31	279
Total per time point	532		602		732		310	

Mosquito sampling methods: LTC = CDC-mini light trap catches with UV light left overnight (1 placed outdoors under the rain tarp of an occupied tent and 1 placed indoors next to an occupied bednet); ASP = indoor, morning aspiration of resting mosquitoes with a ProkoPack. Villages: DB = Dangbara; DL = Dialanpozu; KP = Kolepar, KS = Konsabla; SG = Segri; TG = Tampé-Gougougré.

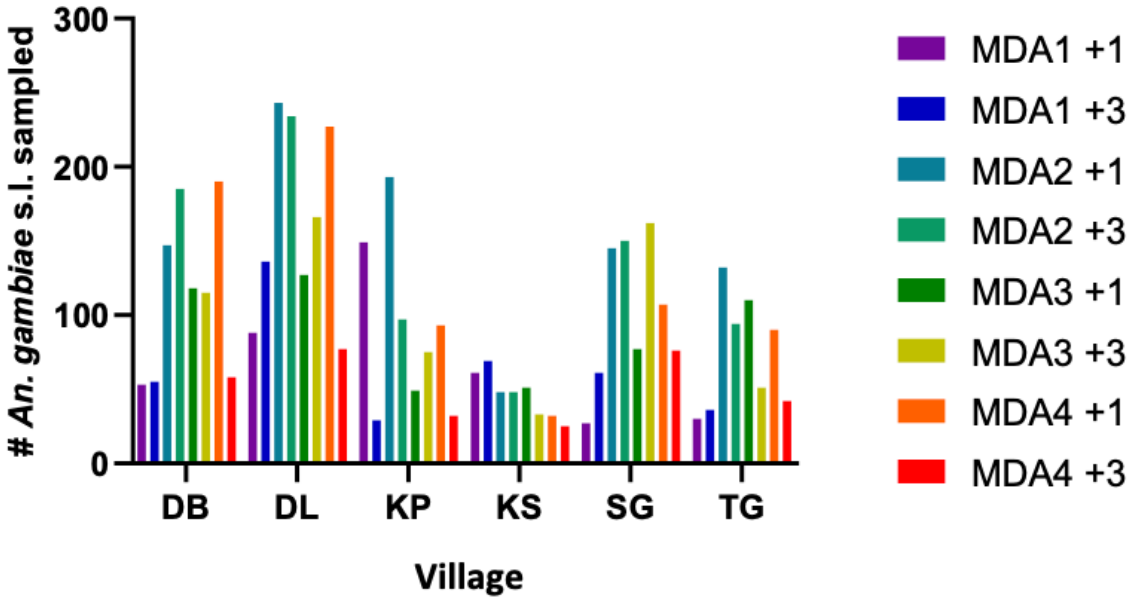

Figure 3.1. Number of mosquitoes captured across all methods (light trap and aspirator) by time point in the six sampled RIMDAMAL II villages.

Table 3.2. Number of *An. gambiae* s.l captured across six sampled villages in RIMDAMAL II by age grading method

Village	MDA1+1			MDA1+3			MDA2+1			MDA2+3		
	WS	**NIRS**	**Par**	**WS**	**NIRS**	**Par**	**WS**	**NIRS**	**Par**	**WS**	**NIRS**	**Par**
DB	25	26	0	25	25	0	33	34	0	29	30	11
DL	23	17	12	31	38	0	33	34	14	28	34	14
KP	35	35	14	18	19	0	26	31	16	24	25	19
KS	13	14	19	10	23	0	26	27	0	10	17	15
SG	10	11	4	12	26	0	18	24	15	25	29	10
TG	18	19	3	16	19	0	32	35	3	29	33	4
Total per method	124	122	52	112	150	0	168	185	48	145	168	73
Total per time point		298			262			401			386	

Village	MDA3+1			MDA3+3			MDA4+1			MDA4+3		
	WS	**NIRS**	**Par**	**WS**	**NIRS**	**Par**	**WS**	**NIRS**	**Par**	**WS**	**NIRS**	**Par**
DB	12	25	14	31	33	9	35	35	10	20	23	7
DL	18	30	12	29	34	14	35	35	22	20	29	2
KP	17	20	7	27	29	2	25	27	15	15	20	5
KS	23	25	8	20	21	4	17	22	1	16	21	3
SG	9	22	9	30	35	19	23	29	18	21	32	2
TG	27	34	11	29	31	2	29	31	6	10	21	1
Total per method	106	156	61	166	183	50	164	179	72	102	146	20
Total per time point		323			399			415			268	

Mosquito testing methods: WS = wing scale; NIRS = near infrared spectroscopy; Par = parity determination by the Detinova method. Villages: DB = Dangbara; DL = Dialanpozu; KP = Kolepar, KS = Konsabla; SG = Segri; TG = Tampé-Gougougré.

3.2.2 Parity analyses for wild-caught mosquitoes from RIMDAMAL II villages

As seen in Table 3.3, the percentage of parous mosquitoes is highest at the beginning of the trial (MDA1+1), steadily decreases through the middle of season 1 of the trial (MDA2+1 through MDA3+1), and then begins to increase again at the season's end (MDA3+3 though MDA4+1). Unfortunately, the data are too few to make strong analyses and, therefore, we cannot examine parity rate in the individual RIMDAMAL II villages. Additionally, Table 3.3 shows that many of the parity rates calculated for each MDA sampling time have overlapping confidence intervals and therefore are not significantly different. The exceptions are MDA1+1 vs. the middle time points (MDA2+3 through MDA4 + 1; all Fisher's exact test p-values <0.001) and MDA4+3 vs. MDA3+1 (Fisher's exact test p-value <0.01). Due to the low sample numbers and mostly statistically insignificant results, parity rates were excluded from subsequent comparative modeling efforts between age grading techniques.

3.2.3 Wing scale-based age grading from wild An. gambiae s.l

Pearson correlation analyses indicated that there was a weak, positive but statistically significant correlation between all left and right wing scale count comparisons (Table 3.4). Therefore, we could assume no differential loss of wing scales on one wing versus the other and treat left and right wings from the same mosquito as approximately equal to one another.

Table 3.3. Parity data from wild *An. gambiae* s.l mosquitoes sampled in RIMDAMAL II villages per MDA time point

	MDA1+1	**MDA1+3**	**MDA2+1**	**MDA2+3**	**MDA3+1**	**MDA3+3**	**MDA4+1**	**MDA4+3**
% Parity*	86	-	61	52	41	52	55	100
[95%CI]	[93,74]	-	[74,46]	[64,41]	[57,28]	[68,35]	[67,43]	[100,63]
(n)	(44/51)	-	(28/46)	(36/69)	(17/41)	(17/33)	(34/62)	(8/8)

*Because so few were scored for parity by village per timepoint, data across all six villages was summed.

Table 3.4. Pearson correlation analyses between wing scale counts on left and right wings

Left vs. right wing comparison	**N left wing**	**N right wing**	**N XY pairs**	**Pearson r**	**95% CI**	**P-value**
Cu2 wing scale count	1,319	1,341	1,256	0.3541	0.3048, 0.4016	<0.0001
M2 wing scale count	1,279	1,336	1,218	0.3689	0.3193, 0.4164	<0.0001
Total wing scale (Cu2 + M2)	1,357	1,364	1,315	0.3944	0.3477, 0.4391	<0.0001

Age was predicted from wing scale count data using a Poisson model generated from mosquitoes of known age in the control mesocosm described in Chapter 2. When analyzing mosquitoes of known age from the control mesocosm only, this same model predicted sample median age of 7.89 compared to the observed sample median age of 10, indicating moderate model accuracy but perhaps a slight tendency to underestimate age. This same Poisson model was then used to predict the age of field mosquito (of unknown true age) based on their wing scale count data. Results are shown as a median age of the population of mosquitoes sampled as the distribution of true ages is likely to be non-normally distributed (Fig. 3.2). The median wing scale values vary over sampling period, with a range between 17 and 37. Note that wing scales are lost over time post-eclosion, and thus a higher median scale number indicates a younger population of mosquitoes and a lower median scale number indicates an older population. A general trend of lower median wing scale number is observed across villages at the earliest timepoint, while a gradual but uneven trend towards mosquitoes with a higher median total captured in the middle-to-late season sampling periods. This trend mirrors those observed in the overall parity data (Table 3.3). Additionally, the median total wing scales more often increased from week +1 to week +3 following each MDA (in 14/24 samplings during MDAs conducted over the 6 villages), suggesting the mosquito populations more often became younger over the spans of weeks after each MDA, especially in Dialanpozou (DL) and Tampé-Gougougré (TG).

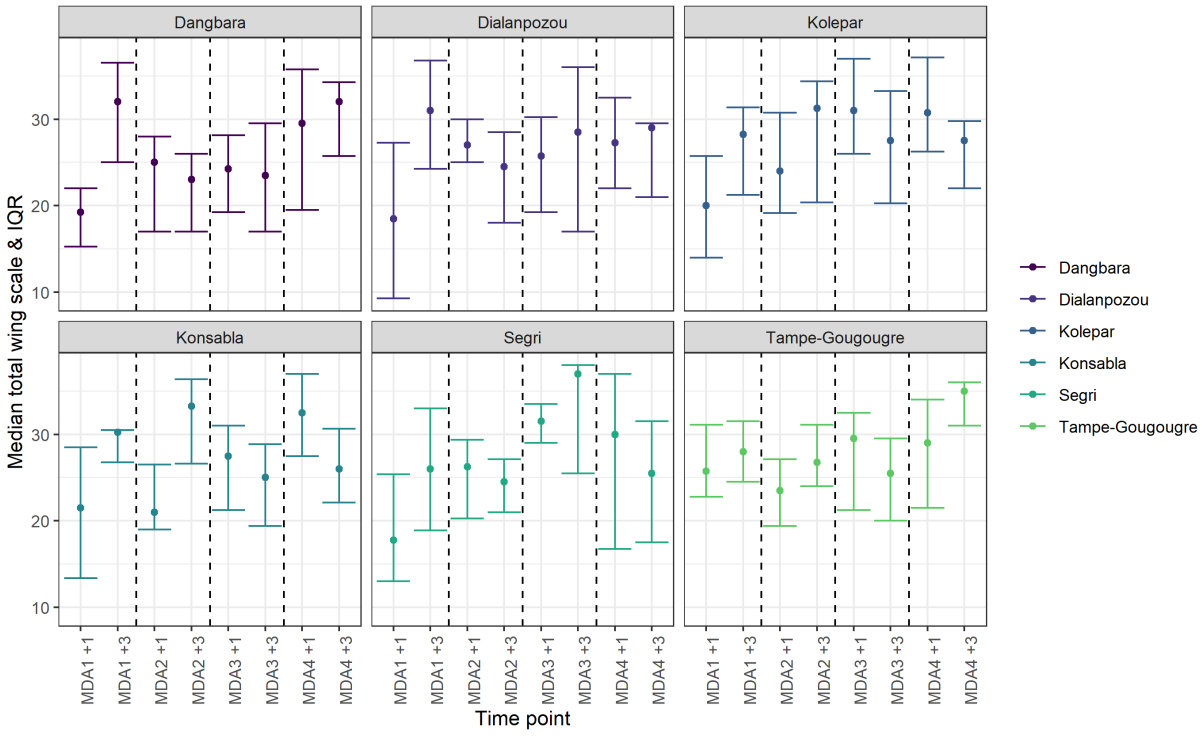

Figure 3.2. Median total wing scales and interquartile range for field mosquitoes captured in the six RIMDAMAL II villages at the different sampling time points post-MDAs.

3.2.4 Comparison of NIRS- and wing scale-based age grading methods against wild caught An. gambiae s.l of unknown age

The wing scale model was developed with marked lab mosquitoes of known ages held together in mesocosms and sampled at set times over 10 weeks, while the NIRS model was developed with wild mosquitoes caught as larvae and held in cages to known ages post-eclosion until scanned with a spectrometer (Table 3.5).

Table 3.5. Number of wild adult female *An. gambiae* s.l used for the NIRS calibration curve

Age (days) of wild mosquitoes held post-eclosion prior to NIRS scanning	3	6	9	12	15
Number of wild mosquitoes scanned	99	100	98	72	35

Predicted age structure varied substantially by village and timepoint, with no obvious visible trends. As seen in Figure 3.3, wing scale predicted age structure exhibited a Poisson-type distribution, with most mosquitoes predicted to be young and a longer tail trailing off to the right of fewer mosquitoes predicted to be old. This distribution generally fits similar age distributions assessed from field mosquitoes and matches the age distributions of marked mosquitoes held in our laboratory mesocosms (Chapter 2, Figure 2.2). On the other hand, NIRS-predicted age structure more often exhibited a Gaussian-type distribution with long tails trailing off to both the left (young to negative ages) and to the right (old). Both predictions of mosquito age should be interpreted as relative age in days because the relationship between true age and the different measures (number of wing scale or NIRS linear predictor) is non-linear.

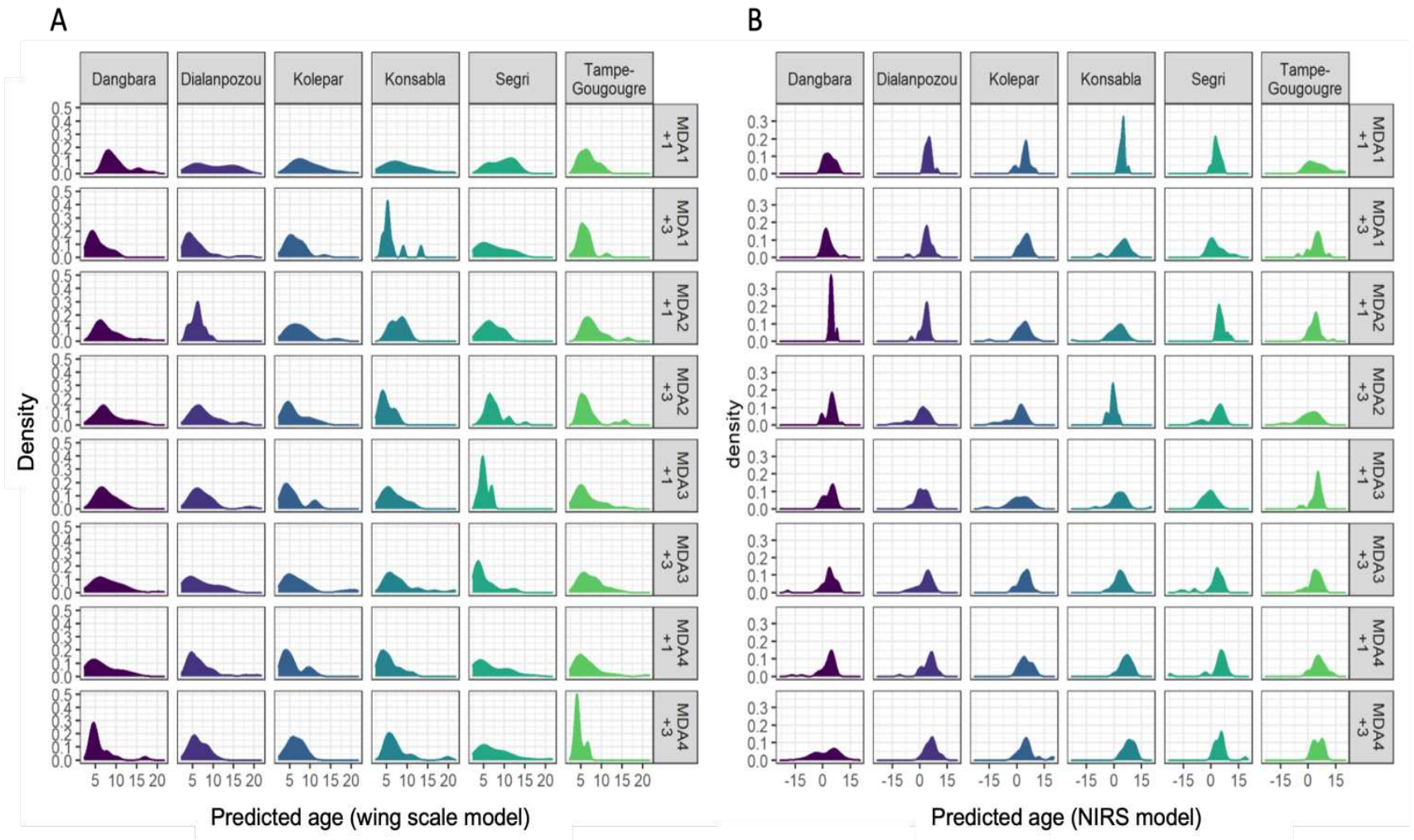

Figure 3.3. Distributions of the *An. gambiae* s.l age structure in sampled RIMDAMAL II villages by village and timepoint as predicted with the wing scale (A) and NIRS (B) models.

The population structure data were then converted to median age predictions with 95% CIs plotted by village and time point (Fig. 3.4), as well as in a side-by-side comparison (Fig. 3.5). Overall, the predicted age of the wild mosquitoes differed between the models. Median age of all mosquitoes was predicted to be younger 4.04 (3.85-4.25 95% CI) when using the NIRS model and older 6.26 (6.1-6.47 95% CI) when using the wing scale model. The two predicted datasets reflect each other in some village-time estimates (e.g., Dangbara), in others they noticeably diverge (e.g., in MDAs 2 and 3 in Dialanpozou). Although overall, they tend to match each other in age predictions trending up or down across village time points and more often median predicted age of the mosquito population is predicted to be higher in the sampling week immediately after the MDA (MDAx+1) but lower in the sampling week that occurred three weeks after each MDA (MDAx+3).

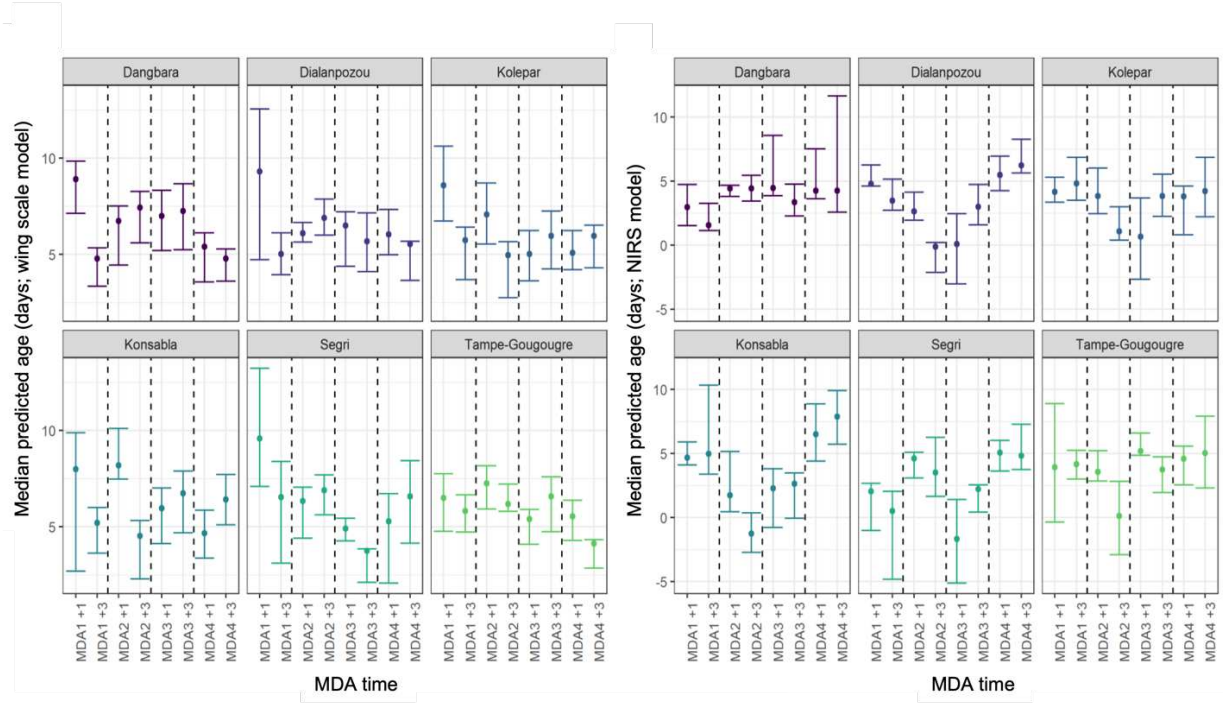

Figure 3.4. Wing scale (A) and NIRS (B) models predictions of *An. gambiae* s.l median age and 95% CIs sampled by RIMDAMAL II village and timepoint in 2019.

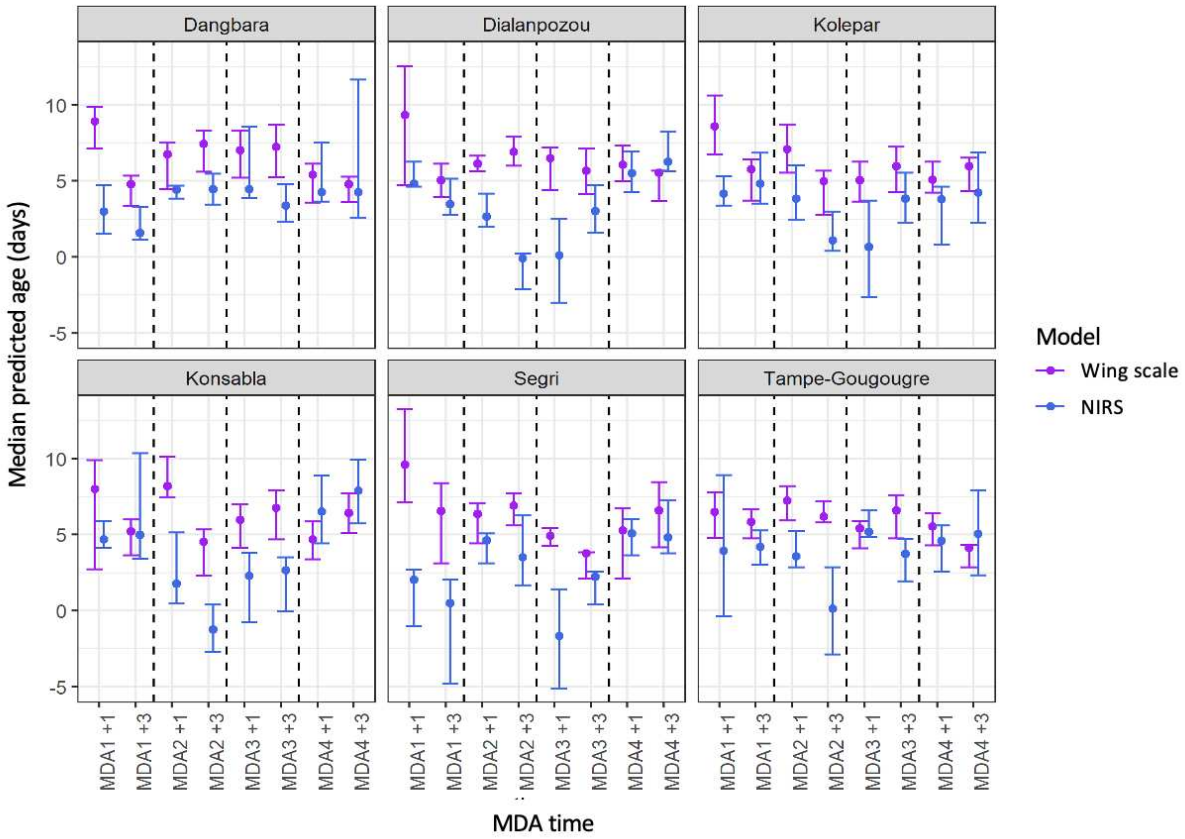

Figure 3.5. Side-by-side comparison of wing scale and NIRS model predictions of *An. gambiae* s.l median age and 95% CIs sampled by RIMDAMAL II village and timepoint in 2019.

3.3 Discussion

Ovary assessments by the Detinova and Polovodova techniques have been the gold standard tools for entomologists in their effort to age grade mosquitoes. Numerous studies in both the laboratory and field have indicated that these methods are not only accurate, but also can be used as a low cost and efficient means of age grading wild type mosquitoes.[173,253,294,298,299] Our prior results demonstrated that parity was reliable for determining an individual mosquito's age in standard insectary-based and mesocosm experiments as mosquitoes of known age had parity statuses aligned with what has been reported in the literature (see section 2.3 in Chapter 2).[144,171]

Results presented in this study continue to confirm that the Detinova method has its merits in field settings as well. During the 2015 RIMDAMAL I trial, we observed that parity rates for mosquitoes collected across all villages were initially high during the start of the malaria transmission season, but then dropped significantly mid-season once mosquito populations peaked.[398] Parity rates then increased again at the trial's end as older mosquitoes persisted but fewer new mosquitoes were born due to a reduction in seasonal rains. Our present results roughly match those observed in 2015, demonstrating not only corroboration of findings, but also reveal important trends in mosquito population dynamics in this hyperendemic Sahelian region. At the beginning of the rainy season, wild anopheline populations are older. As the season progresses, the rains and mosquito productivity in the environment reaches its peak. During this time, the age demographic shifts to younger classes of mosquitoes. Mosquito populations then become older again in the late season when populations are significantly reduced.

Because ivermectin has been shown in lab studies to have a stronger mortality effect against older mosquitoes who have taken >1 blood meal, we would expect decreased parity rates in villages that received ivermectin MDAs and increased nulliparity in villages that only received standard SMC and vector control.[377,390] However, no significant reduction in parity rates was observed between mosquitoes collected from control vs. intervention sites in our RIMDAMAL I trial. This result was perplexing, as reduced malaria transmission (indicating ivermectin's lethal effect on mosquitoes) and decreased exposure to biting anophelines (demonstrating mosquito mortality and/or reduced feeding due to ivermectin) were observed in ivermectin sites.[398] Entomological indicators of malaria transmission are known to vary widely over time and space, even over short geographic distances.[436,437] As such, the lack of parity distinctions between our

villages could be due to our small sample sizes or to sampling methods used in the field. Additionally, sub-lethal ivermectin exposure is known to disrupt normal ovarian development in mosquitoes, producing undeveloped ovarian follicles and nulliparous morphology even post-blood digestion.[383] Therefore, ivermectin exposure may have confounded parity analyses in the RIMDAMAL I study and, subsequently, the 2019 RIMDAMAL II study as well.

Unfortunately, we are limited in our ability to further discern ivermectin's impact on anopheline ovarian development and the Detinova method's efficacy in age grading mosquitoes exposed to the drug. Comparisons may become clearer when the study is unblinded and we are able to group data across villages by whether they received placebo or ivermectin. Even then, we will still be restricted by the small sample size of mosquitoes analyzed for parity. The rigor of field sampling, high number of anophelines that were collected and required immediate processing on a daily basis, and the limited number of field staff forced us to reduce our sampling. The Detinova method proved to be too taxing and time consuming to handle with large sample sizes, and therefore had to be reduced considerably, a critique of the method that has been referenced before by entomologists.[173] Our work highlights the practical limitations of the Detinova technique, and the arguably even more labor-intensive Polovodova method by extension. Although still considered a gold-standard method in age grading, this study's outcomes indicate that researchers must be cognizant of the time needed to perform ovary dissections and assessments on a regular basis in large-scale field studies.

Determining age via wing scale counting alleviated some of the limitations of parity-based assessments, with our RIMDAMAL II trial indicating that it is a relatively fast and intuitive method that requires little training to master. Furthermore, it performed well in field sampling conditions since images could be taken quickly of wings from field-collected

anophelines. Wing scales could be counted from these images at a later date, thereby reducing workloads considerably. Previous explorations of this technique in laboratory-based settings indicated that wing scale-based age grading could detect shifts in mosquito population age structures, with greater wing scale loss observed when mosquitoes were reared in mesocosms that mimicked natural environments (see sections 2.2. and 2.3 in Chapter 2). In RIMDAMAL II, similar evaluations in age structure cannot be fully assessed due to the fact that the trial remains blinded. However, wing scale-based predicted age structures generated from field data indicated that most mosquitoes were predicted to be young and fewer mosquitoes were predicted to be older, a Poisson-based distribution that generally fits similar age distributions assessed from field mosquitoes of previous field studies.[252,305,310,438] As such, we have preliminary evidence that the wing scale method originally proposed by Perry could be revitalized and potentially used in contemporary mosquito field surveillance efforts.

The primary challenge we encountered while using the wing scale method was accounting for the high degree of variance in scale counts for each individual mosquito. This may be a result of human error resulting from fatigue generated after analyzing multiple mosquito wing images over time, or could be a product of bias by limiting analysis to such a small part of the wing. Given the wide range of wing scale counts for any given true age, predictions of the age of individual mosquitoes will be relatively poor. There is, however, a clear statistical trend with the number of wing scales diminishing as the mosquito ages indicating that population age predictions are likely to be more robust, a metric which has far more epidemiological relevance than accurate age prediction for individual mosquitoes.[231,253]

NIRS had many of the same advantages overall as wing scale counting, proving to be a relatively easy technique to use in the field. However, subsequent data analyses were challenging

and produced results that were difficult to interpret. The Gaussian-type age population distribution across our sample villages predicted by NIRS indicates a significant presence of both younger and older mosquitoes, results which contradict previous field data for mosquitoes collected across control and ivermectin MDA villages.[398] Furthermore, the NIRS and wing scale datasets noticeably diverged across space and time in some villages, with NIRS predicting an overall younger median age for all mosquitoes. This discrepancy may be due to some of the inherent limitations in the NIRS technique, as it can only reliably classify mosquitoes that are very young (<7 days old) or old (>7 days old).[253] Prior inconsistencies with NIRS-based age grading were experienced previously with wild-caught mosquitoes from Burkina Faso (independent test sets of unknown ages), which could only be grouped into broadly young and old age classes by using a non-standard regression algorithm and robust, labor-intensive calibration curves.[304] Despite this study's dissimilarities between NIRS- and wing scale-based age grading, both techniques indicated that the median predicted age of the mosquito population was higher in the sampling week immediately after an ivermectin MDA and lower three weeks after each MDA. This matches expectations in the literature, showing decreased mosquito mortality and sublethal effects as blood concentration of ivermectin decreases due to human pharmacokinetics.[377]

Presently, it is still difficult to conclude that one age grading method is better than the other in the current analysis given several limiting factors. The relatively sparse and homogenous training datasets used for wing scale- and NIRS-predictive modeling (wing scale: 274 adult females of known ages; NIRS: 404 adult females of known ages) likely limited the precision of the predicted ages. Larger numbers of samples collected from a more diverse set of mosquitoes will be needed to improve predictions in field mosquitoes, though, this may be accomplished

moving forward once data from RIMDAMAL II over the 2020 season is added to the existing dataset. Secondly, it should be noted that the average age of a mosquito population is highly sensitive to sampling variability.[252,301,310] At the number of mosquitoes sampled here, this sampling variability is likely to be larger than the variability induced by the measurement error of the technique used to predict mosquito age.[252]

In summary, our preliminary analysis of the entomological data derived from RIMDAMAL II is one of the few studies that directly compares age grading techniques for field-caught mosquitoes. Admittedly, our ability to accurately evaluate the Detinova technique and parity assessments within this study is limited due to the fact that the difficulty of this technique in a large-scale field trial necessitated a greatly reduced sample size; additionally, results were potentially biased due to sub-lethal effects of ivermectin exposure. However, the data show that age grading with wing scales can be relatively fast and thus can be performed on large datasets, done inexpensively, and analyzed without complex modeling. By contrast, although NIRS is also rapid and capable of processing of large datasets, the cost of the spectrometer is a downside as well as the complicated processing and modeling required for age grading. Overall, the present data indicate that wing scale and NIRS age grading show relatively similar prediction trends across village and time points using median age, but the distributions of predicted ages were noticeably different between the two methods, a trend we cannot completely explain until RIMDAMAL II is fully unblinded.

3.4 Materials and Methods

3.4.1 Field study design

Village cluster and household selection: Villages or spatially-delineated village sectors in the Diebougou district were considered for study enrollment based on: being within a 30 minute drive from our Diebougou field station, possessing sufficient road infrastructures so that villages were accessible by car and motorcycle during the rainy season, having at least one kilometer of distance from any neighboring villages in order to minimize contamination effects from human and *Anopheles* migration, being located sufficiently far away from any gold mining activity and therefore reducing security risks, and containing between 21-49 households. The latter qualification was chosen as the range of households facilitated a potential cohort of children between 0-10 years old that not only was necessary to adequately power our study, but also was a manageable sample group for a single nurse to perform regular clinical sampling. Based on these qualifications, 14 villages (or clusters) were selected as study locations: Bamako-Gourée, Dangbara (DB), Dialanpozu (DL), Djinkargo, Dolo Toundja Djegergo, Goumbori, Kolepar (KP), Konsabla (KS), Moutori, Niaba, Nouvielgane, Segri (SG), Tampé-Gougougré (TG), and Tiedja (Supplemental Fig. S2.1).

MDA distribution, standard of care, and routine vector control: SMC with sulfadoxine-pyrimethamine (SP) plus amodiaquine (AQ) (SP+AQ (SPAQ-CO™ , Guilin Pharmaceutical; 500/25 mg SP and 153 mg AQ for children 12-59 months; 250/12.5 mg SP and 76.5 mg AQ for children 3-11 months) was provided for children aged 3-59 months. Ivermectin or placebo (Iver P®, Elea Labs; 6 mg tablet) was administered to most other individuals not receiving SMC. Both drugs were administered as 3-day course of 300 μg/kg/day. Per package insert, dosing of

ivermectin or placebo was determined by participant height (90-119 cm = 1 tablet/day for 3 days; 120-140 cm = 2 tablets/day for 3 days; 141-158 cm = 3 tablets/day for 3 days; >158 cm = 4 tablet/day for 3 days). This dose and schedule were selected based on previous findings that showed it to be safe in adult trials and its ability to produce mosquitocidal ivermectin serum levels up to a month after each treatment round.[396,397] Ivermectin and placebo were given monthly over four months of the rainy season (July-October) to the eligible village population.

For routine mosquito vector control, standard pyrethroid-based LLINs were distributed to the villages to achieve coverage of one per sleeping space. Interceptor® G2 nets to were distributed in all RIMDAMAL II villages in early October 2019 just prior to MDA4. These LLINs are treated with a combination of alpha-cypermethrin, which repels mosquitoes, and chlorfenapyr, a new, non-neurotoxic, slow-acting insecticide that disrupts metabolic respiratory pathways in mitochondria. This new mode of action means that the nets are able to kill both insecticide resistant and susceptible mosquitoes.[439,440]

3.4.2 Mosquito field sampling

Mosquito capture and field schedule: Six of the villages were chosen for entomological surveillance throughout the rainy season: DB, DL, KP, KS, SG, and TG. Three of these villages were randomized to receive ivermectin, while three others received placebo. The randomization of each was unknown to the villager and the study team, with the exception of the study pharmacist who was unblinded and allocated the respective drugs to the proper villages each MDA. In each village, eight household were selected for weekly mosquito sampling. These households were chosen by making one east-west and one north-south transect across the village.

The four innermost and the four outermost households lying on or closest to these transects were selected for entomological sampling (Supplemental Fig. S2.2). Sampling occurred approximately one and three weeks following each MDA and include the following date ranges: July 29-August 3 (first MDA, one week after; MDA1+1), August 12-August 18 (first MDA, three weeks after; MDA1+3), August 26-September 1 (MDA2+1), September 9-September 15 (MDA2 3), September 23-September 29 (MDA3+1), October 7-October 13 (MDA3+3), October 21-October 27 (MDA4+1), and November 4-November 10 (MDA4+3). All entomological surveillance villages were sampled one time each MDA sampling week in a randomized order for the week. For each sampling day, entomology team members visited each cluster the evening prior and positioned two CDC-mini light trap catches with UV light (LTC) to catch host-seeking mosquitoes. One LTC was placed outdoors at the feet of a volunteer sleeping in a zipped camping tent while the second was located indoors at the feet of an individual sleeping under a bednet. Both LTCs were placed at household sites at the center of each village transect. At dawn, the team returned to collect the LTCs and proceed to aspirate primarily blood fed mosquitoes resting in sleeping houses of each of the eight households using a ProkoPack aspirator (ASP). Using a mouth aspirator, mosquitoes were transferred from LTC and ProkoPack catches into labeled transportation cups, placed in a container, covered with a moist towel, and transported back to the Diebougou field station.

Mosquito processing for age grading: Once at the field station, unfed and blood fed female mosquitoes were knocked down with chloroform and separated by species based on taxonomic identification methods. *An. gambiae* s.l we placed in our age grading comparison pipeline. If the mosquito was collected via aspiration, the wings were first removed and photographed at 30X

using a stereoscope (Leica EZ4 W, which also has a built-in digital camera) as described in Chapter 2 section 2.4. LTC-caught mosquito wings were not processed due to damage from the trap's fan motor. Next, all female *An. gambiae* s.l mosquito were placed on their side on a white, spectralon disk and scanned at their thorax using a LabSpec 4 Standard NIRS machine (ASD Inc., Boulder, CO).[304] Spectra were recorded with RS3 spectral acquisition software (ASD Inc., Boulder, CO). The head and thorax scanning with the NIRS machine in order to omit any introduced biases due to blood in the abdomen.[308] The NIRS machine was optimized and baseline scans (white reference) performed against the disk background before each days' use, and continuous spectra were first examined on all samples to ensure proper placement under the NIRS probe. The final data on each sample consisted of the average of 20 spectra taken. Finally, if the mosquito was unfed, the ovaries were dissected and the slide read for parity status using the Detinova method and a Leica DM500 standing microscope.[173,409] Parity was only scored on up to 10 unfed *An. gambiae* s.l mosquitoes collected either from ASP or LTC collections because the blood meals in mosquitoes (which dominated ASP collections) influences parity scoring. Nearly all are scored parous because the of the time difference between the blood meal in the night and the dissection in the late morning results in already swollen ovarioles. Because of this, mosquitoes scored for parity were most often not the same samples that were processed for wing scale or by NIRS. Furthermore, fewer mosquitoes were processed in parity dissections per village and timepoint than planned because of the time-consuming nature of the procedure.

NIRS calibration curve generation: The NIRS model for predicting the age of the wild mosquitoes was developed using NIRS scans of wild adult mosquitoes that were captured as larvae in the field in the Diebougou region. These larvae were reared to eclosion with

supplemental ground TetraMin fish food and maintained as adults in cages under standard field insectary conditions with access to water and 10% sucrose.[118] These 404 adult female mosquitoes were held for three, six, nine, 12 or 15 days prior to NIRS scanning. The scans produced spectra functions across a range of 2151 wavelengths (350-2500nm) to calibrate the model.

Manual wing scale counting and data cleaning: Wing photos were uploaded onto a cloud drive for later analysis. In total, 2,421 photos of *An. gambiae* s.l left and right wings were taken over the course of the field season. Analysis consisted of visual counting of only long fringe scales on the distal-posterior wing fringe and within the boundaries of the Cu2 and M2 wing vein cells (bounded by the anal [A] vein and the posterior branch of the cubital vein [Cu_2], and the posterior branch of the medial vein [M_{3+4}] vein and the anterior branch of the medial vein [M_{1+2}], respectively; see Fig. 2.7 in Chapter 2 for reference). For each mosquito, the average between wing scale counts on the left and right wing was taken and then summed (Cu2 + M2) to give the total wing scale value. If only one set of measures (i.e., left Cu2 and left M2) was reported then these values were taken as the total value without any averaging. If a mosquito had either one measurement missing from one side, then only the side with both reported metrics was included in the calculation to ensure the consistency of this variable. Finally, 29 mosquitoes which only had one of the four possible measurements were excluded from any wing scale calculation. The final field dataset consisted of count data from 1,213 mosquito wing images.

3.4.3 Statistical analyses

NIRS age prediction: Spectra readings were trimmed to values corresponding to 500-2,350 nm to remove the excess noise arising from the sensitivity of the spectrometer at the ends of the

near-infrared range.[257] Multiple candidate models were fit using partial least squares linear regression over a parameter grid with 160 combinations.[312] The optimal model was chosen by considering the top 10 most accurate models and selecting the smoothest coefficient function within this sample. The final model deployed spectral smoothing through the use of B-spline functions in order to make the model more generalizable to independent samples. The final model was fit with 50 different sampling replicates, and thus the age predicted for each mosquito was taken as the median of these replicates. Scans that noticeably diverged from the norm (those that are conspicuously flat across wavelengths or have non-normal spikes at certain wavelengths) were not pulled from the training or the prediction datasets, even though these can be common when scanning many samples in the field due to simply poor alignment of the mosquito under the probe.[304] Analyses and figure generation were completed with R script in R studio (RStudio Team, version 3.6.3, *http://www.rstudio.com/*) using the mlevcm (*https://github.com/pmesperanca/mlevcm*) package.

Wing scale-based age prediction: Pearson correlation analyses were done before any preliminary data cleaning to ensure left and right wings could be treated equally. Analyses included comparing left and right Cu2 wing scale counts, left and right M2 wing scale counts, and left and right total wing scale counts (Cu2 + M2 on a given wing). For the latter analysis, if only the Cu2 or M2 count on a wing was given, then that value was used as the total wing scale count. Analyses were performed in GraphPad Prism (GraphPad Software, La Jolla California USA) and SAS statistical software (Version 9.4).

Predictions of field *An. gambiae* s.l age came from wing scale counts of adult mosquitoes that were aged in a laboratory mesocosm constructed at Colorado State University (see section 2.4 in Chapter 2 for reference). A Poisson regression model of mosquito age was fit to the count of long wing per independent sample with known age. To test the age prediction accuracy of this model, it was used to estimate the sample median age of all mosquitoes of known age within the control mesocosm. This was then compared against the sample median age calculated by hand. This same model was then used to predict the age of field-collected *An. gambiae* s.l female mosquitoes of unknown age based on their wing scale count data. Modeling and figure generation were performed in R script in R Studio (RStudio Team, version 3.6.3, *http://www.rstudio.com/*); dplyr ('1.0.2'), ggplot2 ('3.3.2'), and reshape ('1.4.4') packages were used.

CHAPTER 4: SPATIOTEMPORAL DYNAMICS AND ENTOMOLOGICAL INDICATORS OF MALARIA TRANSMISSION DURING RIMDAMAL II

4.1 Introduction

In sub-Saharan Africa, malaria remains a major cause of morbidity and mortality. In 2019, when the current study was initiated, approximately 405 million malaria cases were recorded worldwide, with most (94%) occurring in Africa.[4] When tallying the top 21 countries that accounted for nearly 85% of malaria deaths globally, all but one were African nations; within the list, Burkina Faso, a country of only ~20 million people, accounted for 3% of the 85% total.[4,441]

Plasmodium transmission in Burkina Faso is complex with several *Anopheles* spp. mosquito species serving as primary and secondary vectors throughout the region. Members of the *An. gambiae* complex, including *An. coluzzii*, *An. gambiae* s.s and *An. arabiensis*, serve as the dominant malaria vectors in Burkina Faso with *An. funestus* acting as a secondary but still prevalent vector.[95,143,159] Population abundance and geographic distributions can vary significantly over time depending on environmental conditions, availability of natural and artificial water structures, and human migration and settlement.[78,95,143,159,162] The resulting shifts in spatiotemporal distribution of *Anopheles* vectors mean that *Plasmodium* species distribution can also vary significantly over space and time.[59] Presently, three human disease-causing *Plasmodium* species are found in Burkina Faso: *P. falciparum*, *P. ovale*, and *P. malariae*. *P. falciparum* is by far the most prevalent and is estimated to cause as much as 98.5% of malaria infections in the country.[81] However, increased prevalence of *P. ovale*, and *P. malariae* has been

documented within Burkina Faso, and *P. vivax* has recently been detected across the African continent.[62,70,83,86]

Malaria control programs that target mosquito vectors and/or *Plasmodium* parasites have been a disease prevention staple in Africa for decades. These efforts have included indoor residual spraying of insecticides (IRS), insecticide-treated bed nets (ITNs), long-lasting insecticidal nets (LLINs), rapid diagnostic tests (RDTs), and effective anti-malaria medicines.[250,442] Although these interventions have been largely successful, the increasing problem of multi-drug resistance, insecticide resistance, and mosquito behavioral adaptation highlights the need for new tools, especially in areas of moderate-to-high malaria transmission intensity like Burkina Faso.[110,113,114,229,321,327,328] Novel vector control tools that simultaneously target *Plasmodium* and *Anopheles* species, bypass resistance mechanisms via new modes of action, and also work against outdoor malaria transmission are urgently needed to support malaria disease elimination efforts.

To date, ivermectin has proven effective in inducing mortality among a dozen *Anopheles* species.[443] Laboratory studies, field studies, and clinical trials have all successfully demonstrated that ivermectin is lethal to *Anopheles gambiae* s.l.[376,377,387,389,399,444,445] Additionally, it is one of the few vector control measures capable of efficiently targeting outdoor malaria transmission.[13] Ivermectin mass drug administrations (MDAs) in West African field conditions have also resulted in reduced *P. falciparum* transmission by *An. gambiae* s.l.[389,392] The drug has also been shown to suppress *P. falciparum* developmental cycles in anopheline mosquitoes.[391,446]

Our Repeated Ivermectin Mass Drug Administrations for control of Malaria II (RIMDAMAL II) trial launched in Burkina Faso provides the opportunity to quantify the drug's impact on true malaria transmission dynamics in the field. RIMDAMAL II is a NIH-funded,

double-blind, cluster-randomized trial that integrates repeated high-dose ivermectin MDAs into the existing monthly seasonal malaria chemoprevention (SMC) delivery platform and distribution of LLINs. This trial was conducted over two rainy seasons in 2019 and 2020 in Burkina Faso's Diebougou health district to provide definitive evidence on ivermectin's efficacy in malaria prevention in children under 10 years of age. Although we are still blinded and therefore cannot yet quantify ivermectin's effect on disease transmission, this chapter still uses data collected from RIMDAMAL II to assess changes in *Plasmodium* spp. and *Anopheles* spp. population dynamics over space and time, yielding important insights into *Anopheles* vector competence.

4.2 Results

4.2.1 Mosquito and Plasmodium demographics

Across the two years of RIMDAMAL II, 2,928 malaria vectors (*An. gambiae* s.l and *An. funestus*) were collected over the two field seasons from six different villages. Of those, we tested a total of 2,722 mosquitoes (93.0% of the total collected) belonging to the *An. gambiae* s.l (n = 2,450, representing 90.0% of tested samples) and *An. funestus* species complexes (n = 272, representing 10.0% of tested samples). Using qPCR only on the head+thorax-derived DNA extracts, 100 *An. gambiae* s.l (4.1% of all *An. gambiae* s.l collected from the field and 3.7% of all anophelines tested) and 38 *An. funestus* (14.0% of all *An. funestus* collected from the field and 1.4% of all anophelines tested) were positive for *Plasmodium* sporozoites.

Most *An. gambiae* s.l head+thoraces that tested positive for *Plasmodium* were determined to be *P. falciparum* (n of total tested = 69/2,450), with *P. ovale* (n of total tested = 21/2,450) and *P. malariae* (n of total tested = 10/2,450) being less prevalent. Speciation of the sporozoite-

positive mosquitoes into members of the *An. gambiae* complex revealed that the majority of *P. falciparum*-positives were *An. gambiae* s.s (n of total positive = 54/85; 63.5%) (Fig. 4.2). Tested *An. coluzzii* and *An. arabiensis* samples were only positive for *P. falciparum* sporozoites. Interestingly, most sporozoite-positive *An. funestus* were positive for *P. ovale* (n of total positive = 21/38; 55.3%).

An. funestus head+thorax tissues were positive for *P. falciparum, P. ovale,* and *P. malariae* sporozoites. In comparison to *An. gambiae* s.l, a significantly higher percentage of *An. funestus* were infected with sporozoites (4.1% vs. 14.0%; $X^2 = 49.8$; df = 1; p-value <0.0001), and *P. ovale* infections were nearly ten times more prevalent (7.7%) in this species (Fig. 4.1). Overall, while *P. falciparum* was the predominate species among the sporozoite positive samples from *An. gambiae* s.l, *P. ovale* was even more predominant relative to the other plasmodia among the sporozoite-positive samples from *An. funestus*.

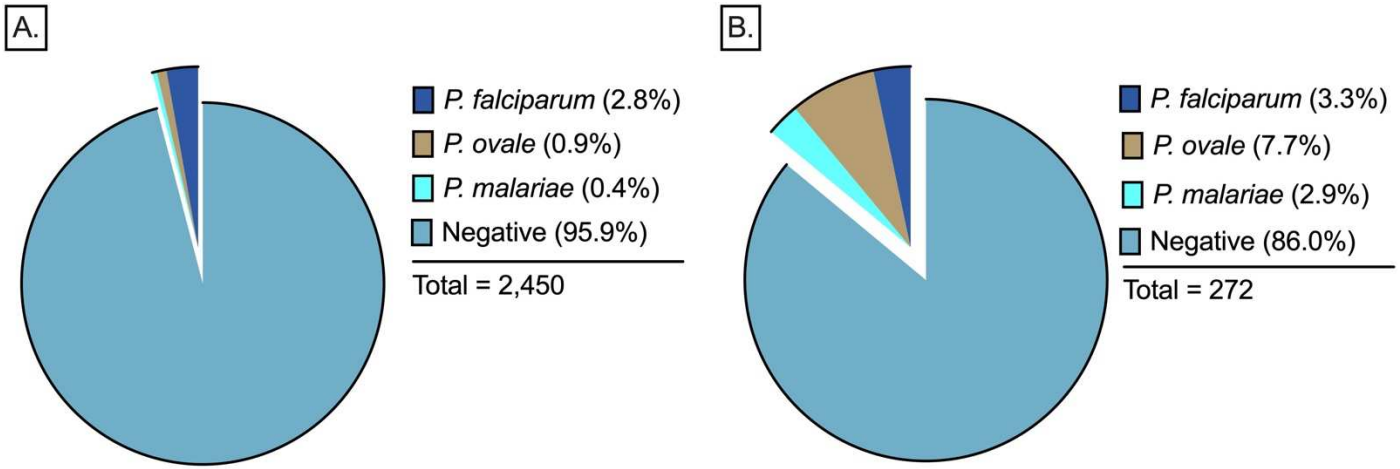

Figure 4.1. Prevalence of sporozoite *Plasmodium* species detected in (A) *An. gambiae* s.l and (B) *An. funestus* mosquito species tested from RIMDAMAL II across all time points and villages.

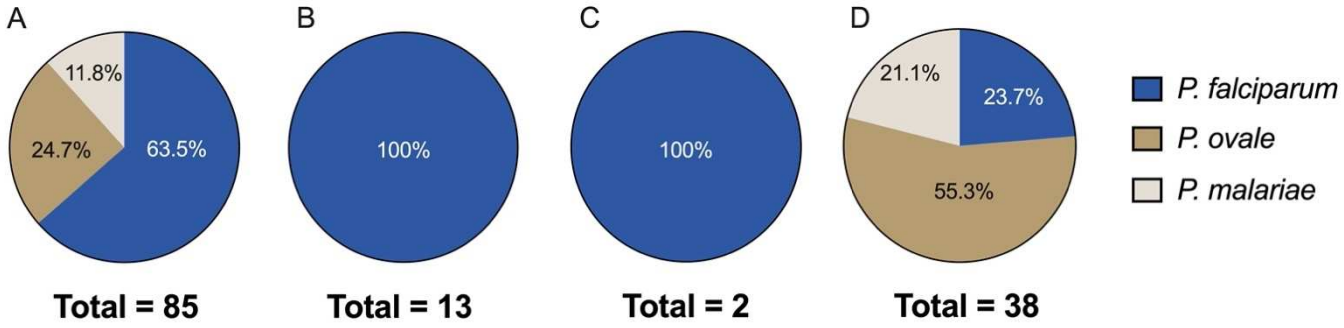

Figure 4.2. Percentages of *Plasmodium* spp. detected in (A) *An. gambiae* s.l, (B) *An. coluzzii*, (C) *An. arabiensis*, and (D) *An. funestus* head+thorax DNA extracts across all RIMDAMAL II time points and villages.

During qPCR analyses, mosquitoes were also analyzed for *Plasmodium* sporozoite co-infections. Only three coinfected samples were identified (Table 4.1). Two were positive for *P. falciparum* and *P. ovale;* both of these samples originated from the same village. The third co-infected sample was positive for *P. ovale* and *P. malariae*. Two out of three detected co-infections were from *An. funestus* samples. All co-infected samples were collected during the late stages of RIMDAMAL II sampling in 2019.

Table 4.1. *Plasmodium* coinfections detected in *Anopheles* spp. mosquitoes collected across RIMDAMAL II

Study year	**MDA time**	**Village**	**Mosquito species**	***P. falciparum***	***P. ovale***	***P. malariae***
2019	MDA4+1	DB	*An. gambiae* s.s	X	X	
2019	MDA4+3	DB	*An. funestus*	X	X	
2019	MDA4+3	DL	*An. funestus*		X	X

Villages: DB = Dangbara; DL = Dialanpozu.

4.2.2 Spatiotemporal changes in mosquito and Plasmodium population dynamics

Across RIMDAMAL II sampling clusters, 1,471 *An. gambiae* s.l were tested in total during 2019, but the number collected dropped in 2020 to only 979. Despite reduced sample sizes, mosquito population trends across villages in 2019 and 2020 remained broadly the same. Sample numbers were typically at their lowest during the beginning of each season (2019: MDA1+1 and MDA1+3, 2020: MDA5+1 and MDA5+3) and at the end of each season of the study (2019: MDA4+1 and MDA4+3, 2020: MDA8+1 and MDA8+3) (Fig. 4.3). Conversely, sample numbers usually reached their peak in the middle of each season of the study (2019: MDA2+3 and MDA3+1, 2020:MDA6+3 and MDA7+1).

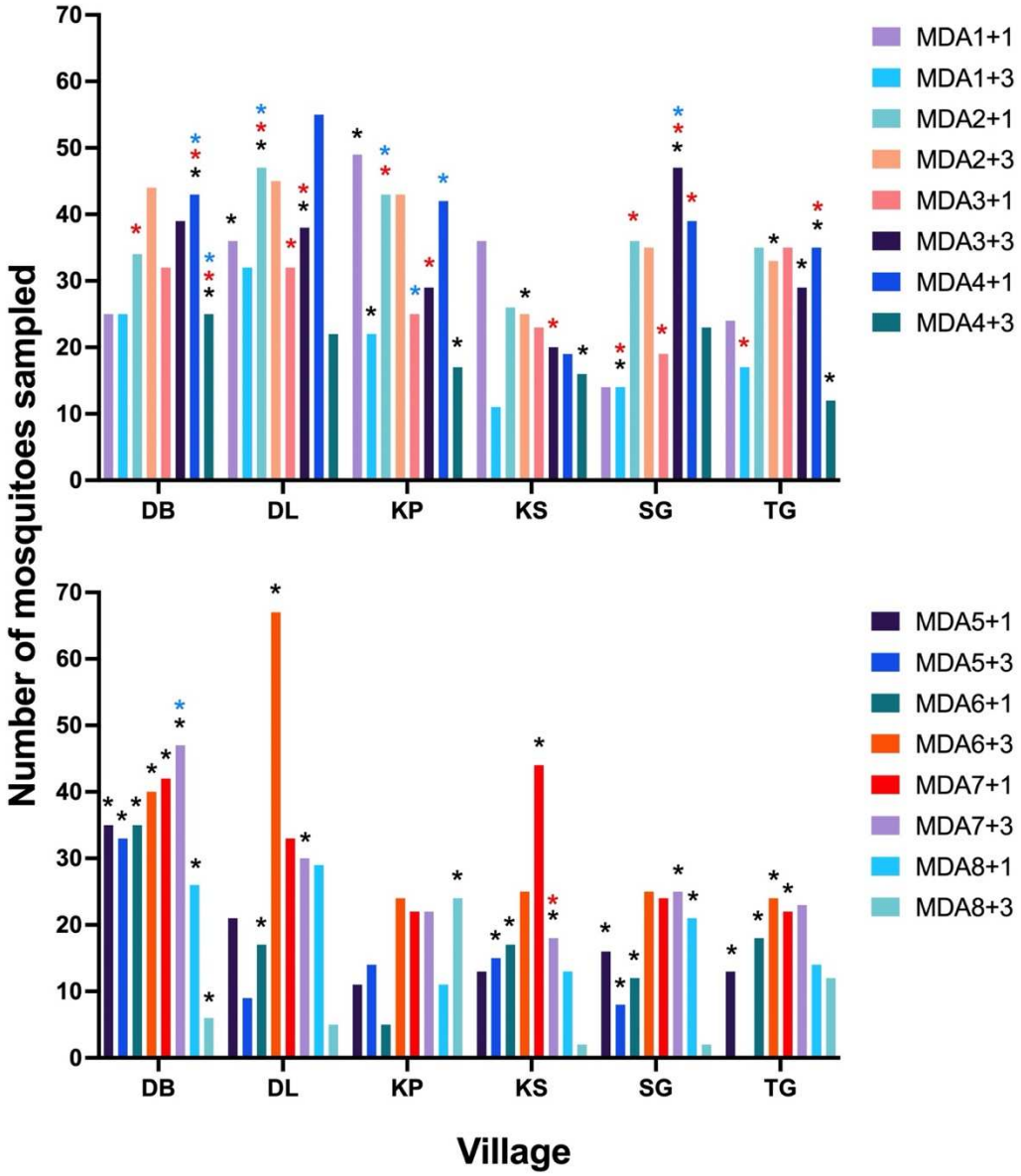

Figure 4.3. Number of *An. gambiae* s.l female mosquitoes sampled across RIMDAMAL II by MDA time points and villages. Stars (*) indicate that *Plasmodium* sporozoites were detected via qPCR analyses of head+thorax DNA extracts derived from a portion of the mosquitoes sampled within a given village and MDA timepoint. Black stars representing the presence of *P. falciparum*, red stars representing *P. ovale,* and blue stars representing *P. malariae*.

In comparison to *An. gambiae* s.l, *An. funestus* population dynamics were more variable over time due to lower sample numbers across both study seasons and a near absence of *An. funestus* sampled in 2020 (total sampled in 2019: n = 242, total sampled in 2020: n = 30). Like

An. gambiae s.l, sample numbers were typically at their lowest during the beginning of the season (2019: MDA1+1 and MDA1+3, 2020: MDA5+1 and MDA5+3; Fig. 4.4). However, rather than peaking mid-trial, the number of *An. funestus* sampled generally increased across every subsequent MDA timepoint, reaching their apex at the final sampling times (2019: MDA4+1 and MDA4+3, 2020: MDA8+1 and MDA8+3).

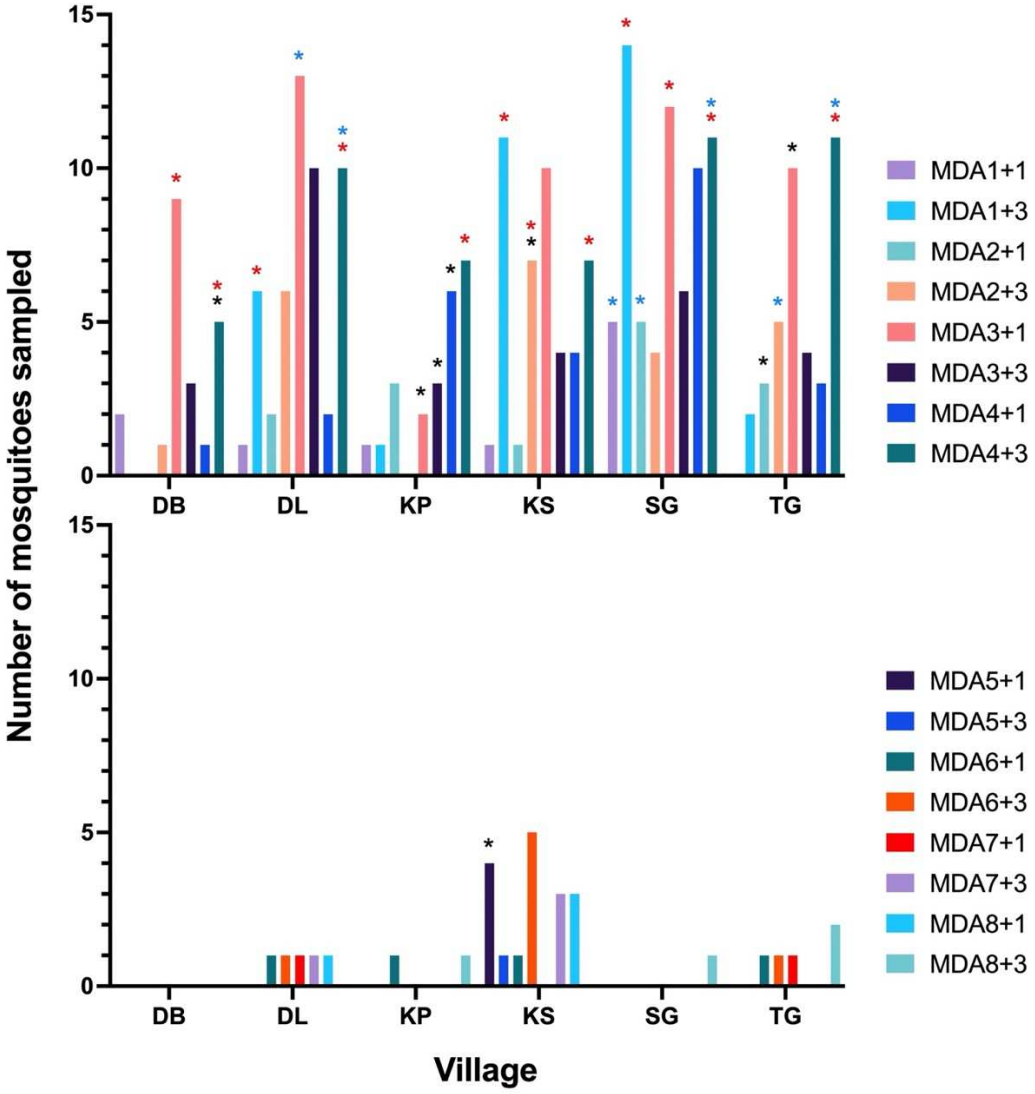

Figure 4.4. Number of *An. funestus* female mosquitoes sampled across RIMDAMAL II by MDA time points and villages. Stars (*) indicate that *Plasmodium* sporozoites were detected via qPCR analyses of head+thorax DNA extracts derived from a portion of the mosquitoes sampled within a given village and MDA timepoint. Black stars representing the presence of *P. falciparum*, red stars representing *P. ovale*, and blue stars representing *P. malariae*.

Table 4.2 illustrates that across RIMDAMAL II, the total number of sporozoite-positive mosquitoes is similar among most villages; DL, KS, SG, and TG all had 21 or 22 positive mosquitoes total, with most being positive for *P. falciparum*. The number of *P. ovale* and *P. malariae* infected mosquitoes is also roughly equivalent across all villages. An apparent exception is the village DB, which not only had a large number of sporozoite-positive mosquitoes overall (grant total: n = 40), but also accounted for a considerable number of *P. falciparum* sporozoite positives (n = 28). Further comparisons may become clearer when the study is unblinded and we are able to group data across villages by whether they received placebo or ivermectin. No sample tested positive for *P. vivax*.

Table 4.2. Number of *Plasmodium* spp. detected from *An. funestus* and *An. gambiae* s.l head+thoraces sampled across six villages during RIMDAMAL II

Time		Village																	
		DB			DL			KP			KS			SG			TG		
Year	**MDA time**	**P.f**	**P.o**	**P.m**	**P.f**	**P.o**	**P.m**	**P.f**	**P.o**	**P.m**	**P.f**	**P.o**	**P.m**	**P.f**	**P.o**	**P.m**	**P.f**	**P.o**	**P.m**
2019	MDA1+1				1			1								1			
	MDA1+3					1		1				2		1	2			1	
	MDA2+1		1		1	1	1		1	1					1	1	1		
	MDA2+3										2		1				1		1
	MDA3+1		1			1	1	1		1					3		1		
	MDA3+3	1			2	1			1			2		1	1	1	2		
	MDA4+1	4	2	1				1		1					1		1	1	
	MDA4+3	3	3	1		3	1	1	2		2	3			1	1	1	3	3
2020	MDA5+1	2									1						1		
	MDA5+3	4									3			1					
	MDA6+1	7			1						2			1			2		
	MDA6+3	1			5						1						1		
	MDA7+1	3															1		
	MDA7+3	1		3	1						1	2		1					
	MDA8+1	1												3					
	MDA8+3	1						1											
RIMDAMAL II Subtotal		27	7	5	11	7	3	5	4	3	12	9	1	8	9	4	12	5	4
RIMDAMAL II Grand Total:			39			21			12			22			21			21	

Plasmodium spp. sporozoite detected: P.f = *P. falciparum;* P.o = *P. ovale*; P.m = *P. malariae*. Villages: DB = Dangbara; DL = Dialanpozu; KP = Kolepar, KS = Konsabla; SG = Segri; TG = Tampé-Gougougré.

4.2.3 Analysis of sporozoite quantifications across RIMDAMAL II

Comparing the number of genomes per sample in *P. falciparum-*, *P. ovale-*, and *P. malariae*-positive samples indicated a notably wide range of sporozoite quantity for each *Plasmodium* species. This is best illustrated in the results for *P. falciparum,* with a range of genomes per sample that exceeded 200,000 (Table 4.3 as well as Supplemental Tables S3.3, S3.4, and S3.5). One-way ANOVA analyses with multiple comparisons on log-transformed genomes per sample indicated no significant difference in sporozoite quantity between the three malaria species, even when stratified by mosquito species.

Table 4.3. Descriptive statistics for qPCR-determined genomes per sample for all mosquito species across RIMDAMAL II

***Plasmodium* species**	**n**	**Min.**	**Median**	**Max.**	**Range**	**Mean (95% CI)**
P. falciparum	78	153.04	3,829.07	233,145.61	232,992.57	16,252.96 (8,814.35, 23,691.57)
P. ovale	43	25.82	1,306.32	23,386.15	23,360.34	1,861.46 (796.59, 2,926.34)
P. malariae	18	748.82	1,494.48	66,246.63	65,497.81	10,043.45 (463,38, 19,623.53)

4.2.4 Entomological indicators for malaria infection and transmission for RIMDAMAL II

Overall sporozoite infection (SIR) rates for RIMDAMAL II showed that SIR was highest for *P. falciparum* (2.8% [95%CI: 3.5, 2.3]; [n of total = 77/2,722]), followed by *P. ovale* (1.5% [95%CI: 2.1, 1.1]; [n of total = 42/2,722]) and *P. malariae* (0.6% [95%CI: 1.0, 0.4]; [n of total = 17/2,722]). The SIR for *P. falciparum* significantly increased from 2019 (1.8% [95%CI: 2.5, 1.2]; [30/1,703]) to 2020 (4.7% [95%CI: 6.1, 3.5]; [47/1,009]) (X^2 = 18.4; df = 1; p-value <0.0001). The SIR for *P. ovale* in 2019 (2.3% [95%CI: 3.2, 1.7]; [40/1,703]) was higher than

expected according to the literature, but decreased in 2020 (0.2% [95%CI: 0.7, 0.04];[2/1,009]). *P. malariae* SIR also decreased from 2019 (0.8% [95%CI: 1.4, 0.5; 14/1,703]) to 2020 (0.3% [95%CI: 0.9, 0.08]; [3/1,009]). However, the sample sizes for both *P. ovale* and *P. malariae* were too small to calculate statistical significance.

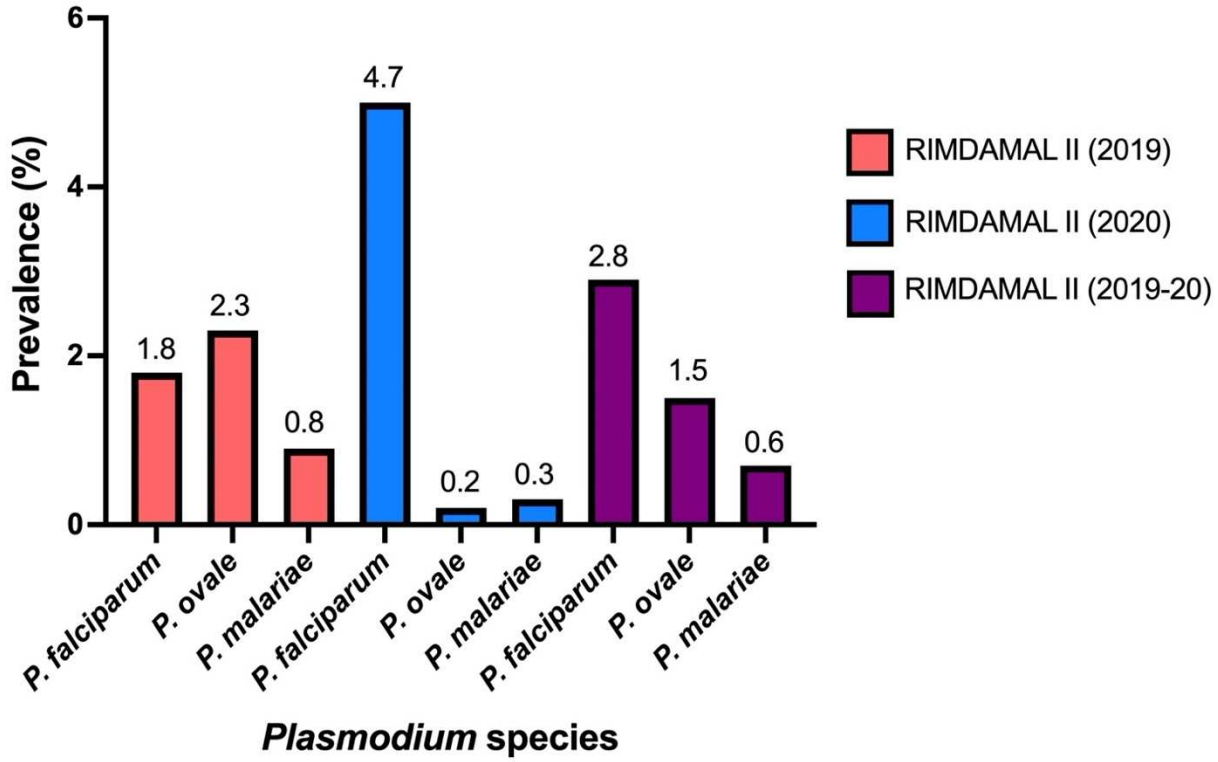

Figure 4.5. Sporozoite infection rate (SIR) calculated throughout RIMDAMAL II according to *Plasmodium* species and study year.

Somewhat contrary to the SIR data, the proportion of the *An. gambiae* s.l population within each village that reached an epidemiologically dangerous age for malaria transmission (P_d) remained notably low (see Supplemental Table S3.6). A full interpretation of these results is limited due to overall low sample sizes and a lack of data from certain villages and MDA timepoints, particularly in 2020. However, the parity rate and P_d were both at their highest at the

first and last MDA time points for both 2019 and 2020, a trend also observed in the RIMDAMAL trial in 2015.[398]

4.3 Discussion

The sibling species *An. gambiae* s.s and *An. coluzzii* have been regularly identified as sub-Saharan Africa's major malaria vectors.[4,46] Within Burkina Faso's Diebougou region, the site of our RIMDAMAL II trial, a past study shows that these two subspecies are dominant during the rainy season, with *An. coluzzii* being up to three times more prevalent than *An. gambiae* s.s; *An. arabiensis* population densities are much lower than either.[159] Our findings across RIMDAMAL II corroborate some of these past trends. The vast majority of our tested samples were from the *An. gambiae* s.l clade. However, most were *An. gambiae* s.s, not *An. coluzzii*. Additionally, *An. gambiae* s.l mosquitoes were the dominant *Plasmodium* sporozoite transmitters in our study, though we admittedly only speciated samples that were sporozoite-positive.

An earlier investigation conducted in the Burkina Faso savannah indicated that although *An. funestus* could supplement *An. gambiae* s.l in malaria transmission, its role as a human disease vector was minimal.[447] More recent evidence suggests that *An. funestus* may be a major malaria vector in this region, capable of higher human biting and sporozoite rates than vectors within the *An. gambiae* s.l complex. However, these studies are limited and usually confined to only analyzing the mosquito's vectorial capacity for *P. falciparum* alone.[158,159] Efforts to investigate *An. funestus'* role in malaria transmission have been thwarted by the difficulties of colonizing this mosquito species under laboratory conditions. To date, only two strains from southern Africa have been successfully colonized from wild populations due to the mosquitoes' poor larval and short adult survival rates, low mating success and fecundity, and overall low

fitness (as determined by wing length and body size).[448–451] However, although *An. funestus* has been regarded as physically weaker than other members of *An. gambiae* s.l when colonized, survivorship and fitness levels between the two clades may be comparable in the wild.[299,448]

Our study shows that the comparatively small number of *An. funestus* collected in RIMDAMAL II were not only more infectious than anticipated, but also were highly infectious for *P. ovale.* Cumulative surveillance studies have shown that it is typical for 3-5% of a competent mosquito vector population to be infected with *Plasmodium.*[59,89] While our results fell within that range for *P. falciparum* and *P. malariae,* 7.7% of sampled *An. funestus* were positive for *P. ovale. An. funestus* has been shown to be a major malaria vector in other areas of Africa, notably Kenya, Tanzania, and Cameroon, due in part to high levels of insecticide resistance present in the population.[452–454] Similar results are somewhat rare in Burkina Faso, though they have been noted in the past. One early 1990s study noted parasite rates in *An. funestus* between 2.8-14.6% outside the capital city Ouagadougou, with one sampled village recording up to 50% *An. funestus* (n = 56) positive for *P. falciparum* circumsporozoite protein via ELISA testing.[455] Because previous studies have indicated that *An. funestus* is the dominant mosquito in Burkina Faso during the dry cold season (December to February), these historical findings as well as our detection of highly infectious *An. funestus* may hint at the mosquito's role in sustaining malaria transmission outside of the rainy season when *An. gambiae* populations decrease.[159]

These previous findings in addition to own results may reflect *An. funestus'* ecological preferences or shifting vector competence factors within the region. Unlike *An. gambiae* s.l, which is often widely distributed due its ability to thrive in diverse, shallow, small, and temporary aquatic environments, *An. funestus* prefers permanent and semi-permanent larval habitats characterized by slow-moving, clear, deep waters.[456,457] Further investigation in our

study's fine-scale geographic data may reveal a correlation between *Plasmodium*-infected *An. funestus,* high densities of houses and/or people outdoors, and proximity to standing water bodies.[457–459] Additionally, our findings could indicate an increased *An. funestus* vector competence for malaria parasites, *P. ovale* in particular. These parasite species may have developed the ability to circumvent the *Plasmodium* population bottleneck that occurs in the mosquito haemocoel (e.g., enhanced or new immune system evasion capabilities, the ability to move more quickly through hemolymph and reach the salivary glands) or gained salivary gland invasion capabilities (e.g., enhanced receptor-ligand interactions between sporozoites and salivary gland receptor proteins).[44,460] Further vector competence and molecular assays are required to explore these hypotheses.

On a similar note, results from our RIMDAMAL II *Plasmodium* and entomological surveillance indicated a higher prevalence for *P. ovale* and *P. malariae* than expected. Previous surveillance efforts within Africa indicated that *P. malariae* and *P. ovale* infections are more prevalent in the sub-Saharan and southwest Pacific region, though both are still regarded as relatively uncommon.[70] However, recent clinical studies in Uganda and Kenya have reported increases in non-*P. falciparum* malaria cases, particularly *P. ovale* and *P. malariae,* in symptomatic patients even in the face of regular chemopreventive therapy MDAs and treatment.[102,113] Similarly, persistent transmission of *P. ovale* and, to a lesser extent, *P. malariae* has been reported in Tanzania despite a continued decline in *P. falciparum* transmission.[461] Within Burkina Faso, high gametocyte prevalence in non-*P. falciparum* malaria species has been documented with increasing prevalence of *P. malariae* and *P. ovale* being reported over time, particularly after the rainy season.[83] From an epidemiological standpoint, these trends and our own findings are worrisome as both *Plasmodium* species can result in chronic disease. *P. ovale*

parasites can form dormant hypnozoites capable of reactivation anywhere from several weeks to years after initial infection, causing multiple secondary infections if not properly treated.[68] Similarly, *P. malariae* can recrudesce years after the period of initial exposure to cause malaria disease.[70] Without treatment, blood-stage parasites can endure for extremely long periods of time (sometimes for the lifetime of the human host), concluding in an irreversible, immune-mediated, nephrotic syndrome.[71–73] Given the severity of these disease outcomes, our detection of elevated *P. ovale* and *P. malariae* prevalence in both *An. gambiae* s.l and *An. funestus* mosquitoes warrants further follow-up investigations.

Although a relatively high prevalence of *P. ovale* and *P. malariae* was detected in RIMDAMAL II, *P. falciparum* had the highest SIR overall. Our results indicated that a cumulative SIR of 2.8% was recorded over the two-year study, which falls within the expected range for this region of Burkina Faso given the dominance of *P. falciparum* during the rainy season in particular.[159] However, it is unusual that the SIR for *P. falciparum* increased between 2019 and 2020. Furthermore, our qPCR analyses indicated that of the three parasite species, *P. falciparum* had the highest median number of genomes per anopheline mosquito sample. Interpreting these results may prove difficult and ineffectual, though, given the epidemiology of malaria transmission.

The probability of malaria transmission from mosquito to human is dose dependent to an extent; the greater the number of parasites within the salivary gland of the mosquito following blood-feeding, the more likely it is to transmit the disease.[462,463] Nevertheless, minimum thresholds also exist; mosquito salivary gland infections resulting from a natural median of one or two oocysts have been shown to successfully result in human infection, though in theory human infection is possible if just one sporozoite is transmitted from a mosquito.[462,464,465] For

this reason, all of the mosquitoes represented in Table 4.3 could potentially contribute to malaria disease, even though their degree of *Plasmodium* infectiousness varies widely. Given this complex relationship between sporozoite dose and malaria disease response, it is increasingly acknowledged that SIR and entomological inoculation rates, though still widely considered the gold standard metrics of malaria transmission, have limited precision and accuracy.[466] As such, different, and more standardized, methods of measuring malaria transmission, vector competence, and vectorial capacity are required.

Recent modeling studies argue that estimations of transmission rates are more accurate when they not only include sporozoite and oocyst rates, but mosquito age and parity rates as well. The likelihood of *Plasmodium* infection in mosquitoes shows a strong association with the average age or parity of mosquitoes, both of which differ in growing, stable, and declining populations.[263,467] As such, the proportion of mosquitoes that are infectious reflects the age structure of a mosquito population; it peaks where old mosquitoes are found and when mosquito population density is declining, and decreases when younger adult mosquitoes, who are not yet infected nor past the malaria extrinsic incubation period, dominate the population and thereby reduce the overall sporozoite rates.[468,469] Our previous parity rates calculated in the 2015 RIMDAMAL trial, as well as the RIMDAMAL II parity rate results and subsequent estimation of the proportion of the vector population that reached an epidemiologically dangerous age, all mirror this trend. Parity rates for mosquitoes collected across all villages were initially high during the start of the malaria transmission season, but then dropped significantly mid-season once mosquito populations peaked.[398] This is likely due to new, younger mosquitoes being added to the population structure through mass emergence, as well as elimination of older mosquitoes from the population due to ivermectin.[390] Parity rates peaked again at the trial's end as older

mosquitoes persisted but fewer new mosquitoes were born due to the start of the dry season. Given this overall trend and its alignment with mathematical theories concerning malaria transmission dynamics, our data may further indicate that measuring the age structure of a mosquito population, not just the SIR and *Plasmodium* quantity, could prove a more accurate metric of malaria disease transmission potential.

In summary, our preliminary analysis of the entomological data derived from RIMDAMAL II showcases entomological malaria transmission dynamics that have noteworthy and surprising implications for future malaria control efforts. The data show that *An. funestus,* a relatively overlooked mosquito complex in Burkina Faso, may play a significant role in *Plasmodium* transmission during and, potentially, outside of the rainy season. Furthermore, our demographic data indicate that *An. funestus* may be more responsible than anticipated for transmitting all malaria species (especially *P. ovale,* which was detected at relatively high prevalence). This could suggest the need for altered vector and malaria control strategies that do not just focus on *An. gambiae* s.l population reduction and *P. falciparum* prevention. Lastly, our data indicate the need for entomologists to move beyond standard entomological measurements of malaria disease transmission, arguing that other metrics, such as parity rate, be utilized as well.

4.4 Materials and Methods

4.4.1 RIMDAMAL II field design

RIMDAMAL II study conditions and *Anopheles* spp. mosquito sampling:

The 2020 RIMDAMAL II field trial followed the same MDA administration protocol, field site visitation strategy, vector control interventions, and mosquito collection techniques as described in the previous chapter (see sections 3.4.1 and 3.4.2 for further details). Additionally, the same

villages remained enrolled in this second year of study, and received the same MDA intervention (ivermectin or placebo) as they received in 2019. The first four MDAs and accompanying mosquito field sampling occurred in 2019. Additional entomology sampling occurred in 2020 approximately one and three weeks following each MDA and include the following date ranges: July 29-August 3 (fifth MDA, one week after; MDA5+1), August 12-August 17 (fifth MDA, three weeks after; MDA5+3), August 28-August 30 (MDA6+1), September 7-September 13 (MDA6+3), September 21-September 23 (MDA7+1), October 7-October 12 (MDA7+3), October 20-October 22 (MDA8+1), and November 6 (MDA8+3). In total, 1,897 anophelines were collected in 2019 and 1,031 were collected in 2020 (see Supplemental Tables S3.1 and S3.2).

Mosquito processing and storage for *Plasmodium* detection

As described in the previous chapter, mosquitoes underwent a series of processing steps once they were collected from villages and returned to the field station (see section 3.4.2 for further details). Female mosquitoes belonging to the *An. gambiae* s.l and *An. funestus* species clades were taxonomically identified based on morphological features. For these *Anopheles* females, the head and thorax were scanned, avoiding the abdomen in order to omit any introduced biases due to blood feeds.[308] The head+thoraces were then separated from the abdomen, individually placed in 1.5mL Eppendorf tubes filled with RNALater®, and stored in a -20°F freezer for the duration of the field trial. Abdomens were stored separately and not analyzed for this thesis. In total, 2,722 mosquitoes were processed in this fashion. However, due to the high number of mosquitoes collected from the field, a portion of mosquitoes were left intact, taxonomically identified, and vialed in RNALater® by mosquito clade in pools of up to 25 mosquitoes (n = 206

or 7.0% of total anophelines collected). These samples were not analyzed in this thesis, though their numbers are reported in the total number of mosquitoes sampled from the field (n = 2,928). All samples were shipped to Colorado State University and, upon arrival, stored at -80°F until processed. All head+thorax samples that were vialed individually underwent further molecular analyses (described below).

4.4.2 DNA extractions from Anopheles head+thorax samples

Female *An. gambiae* s.l and *An. funestus* head+thoraces were removed from tubes and blotted on absorbent paper to remove excess RNALater®. Samples were then individually placed in new tubes containing 300 µL mosquito diluent containing 20% of FBS, 100 μg/ml of streptomycin, 100 units/ml of penicillin, 50 μg/ml gentamicin, and 2.5 μg/ml fungizone in PBS. Samples were homogenized by a single zinc-plated, steel 4.5 mm bead for 1.5 minutes at 24 Hz before being centrifuged for 5 minutes at 14000 x g and 4°C. DNA was extracted from all samples using the Mag-Bind Viral DNA/RNA 96 kit (Omega Bio-Tek) on the KingFisher Flex Magnetic Particle Processor (Thermo Fisher Scientific). DNA was eluted in 30 μL nuclease-free water and stored at -20°F until processed.

4.4.3 Plasmodium sporozoite detection from wildtype Anopheles mosquitoes collected in 2019

DNA extracts from anopheline head+thorax samples collected in 2019 were preliminarily analyzed via a multiplex qPCR protocol designed by Bass et al (see Supplemental Figure S3.1 for a complete overview of qPCR experimental pipelines).[118,266] Probes bound to the 18S small subunit ribosomal RNA (ssrRNA) gene sequences of the four *Plasmodium* species. For *P. falciparum,* this region contains two single nucleotide polymorphisms (SNPs) four base pairs

apart flanked by an area of conserved sequence. The *P. falciparum* probe (5'-TCTGAATACGAATGTC-3') was labelled with 6-FAM at the 5' end and the probe for *P. malariae, P. ovale* or *P. vivax* (5'-CTGAATACAAATGCC-3') was labelled with VIC. Each probe also carried a 3' nonfluorescent quencher and a minor groove binder at the 3' end. Forward (5'-GCTTAGTTACGATTAATAGGAGTAGCTTG-3') and reverse (5'-GAAAATCTAAGAATTTCACCTCTGACA-3') primers flanked the probe binding site. Samples that showed a logarithmic amplification curve before 40 cycles were labeled as tentatively positive. These samples, as well as any sample with an undeterminable result, were run through the same qPCR protocol again to confirm or clarify results (see Supplemental Figure S3.4).

Nuclease-free water served as a negative control. Positive controls included plasmid clones (MRA number 177–180) carrying a PCR insert of the 18S ssrRNA gene amplified from either *P. falciparum, P. vivax, P. malariae* or *P. ovale* were obtained from BEI Resources. These inserts were linearized through single and double enzyme digests and purified using the QIAquick PCR purification kit. These same controls were also diluted and used for standard curve generation.

4.4.4 Plasmodium sporozoite detection from wildtype Anopheles mosquitoes collected in 2020 and verification of 2019 positives

***P. ovale, P. vivax,* and *P. malariae* detection via qPCR**

DNA extracts from anopheline head+thorax samples collected in 2020 were analyzed via an adapted version of the Bass et al qPCR protocol used to analyze 2019 samples. The *P. falciparum* probe was removed and replaced with an equivalent volume of nuclease-free water,

converting the multiplex qPCR into a singleplex qPCR. The same positive and negative controls, as well as qPCR cutoff values, were used. However, no standard curves were generated as the goal was to identify and remove true *P. ovale-, P. vivax-,* and *P. malariae*-negative samples from the dataset.

Samples identified as possible *P. ovale-, P. vivax-,* and *P. malariae*-positive samples from 2020 using the revised, singleplex Bass et al protocol, or from 2019 using two rounds of the original, multiplex Bass et al protocol, were rerun and quantified using a revised, multiplex qPCR protocol described by Phuong et al.[264,470] The probe for *P. falciparum* was removed and replaced with an equivalent volume of nuclease-free water. *P. ovale, P. vivax,* and *P. malariae* species identification were determined with species-specific forward primers probes (*P. ovale*: 5'-CCGACTAGGTTTTGGATGAAAGATTTTT-3'; *P. vivax*: 5'-CCGACTAGGCTTTGGATGAAAGATTTTA-3'; *P. malariae*: 5'-CCGACTAGGTGTTGGATGATAGAGTAAA-3') targeting the 18S ssrRNA region. *P. ovale* was identified using a probe (5'- CGAAAGGAATTTTCTTATT-3') labeled with VIC at the 5' end and a minor groove binding quencher at the 3' end. *P. vivax* was identified using a probe (5'-AGCAATCTAAGAATAAACTCCGAAGAGAAAATT CT-3') labeled with TAMRA at the 5' end and a BHQ-2 quencher at the 3' end. *P. malariae* was identified using a probe (5'-CTATCTAAAAGAAACACTCAT-3') labeled with FAM at the 5' end and a minor groove binding quencher at the 3' end. The same reverse primer was used for all species identification (5'-AACCCAAAGACTTTGATTTCTCATAA-3'). Nuclease-free water served as the negative control, while linearized, clean DNA from the plasmid clones (MRA number 177–180) mentioned previously acted as both positive controls and material used for generating standard

curves. Samples that amplified before 35 cycles and showed a logarithmic amplification curve were considered positive (see Supplemental Figures S3.5 and S3.6).

P. falciparum detection via qPCR

DNA extracts from anopheline head+thorax samples collected in 2020 were analyzed via a singleplex qPCR protocol designed by Hofmann et al.[265] This qPCR used primers and probes targeting the *var* gene acidic terminal sequence (varATS, 59 copies/genome) and was shown to be ten times more sensitive than a standard 18S ssrRNA qPCR approach. *P. falciparum* detection was accomplished with a single forward (5'-CCCATACACAACCAAYTGGA-3') and reverse (5'-TTCGCACATATCTCTATGTCTATCT-3') primer and a probe (5'-TRTTCCATAAATGGT-3') labeled with FAM at the 5' end and a minor groove binding quencher at the 3' end. Samples that amplified before 36 cycles and showed a logarithmic amplification curve were labeled as potential positives (see Supplemental Figure S3.5). All potential positives from 2020 and any 2019 *P. falciparum* sample identified by the Bass et al protocol was run through the Hofmann et al qPCR protocol a second time to confirm and quantify results.

Positive controls consisted of DNA extracts from *Plasmodium*-infected dried blood spots of various ranges of parasitemia on Whatman paper. A biopsy punch was used to 3mm holes, which were then placed in PCR tubes with 70 µL RNA Rapid Extraction Solution (Thermo Fisher Scientific) and rocked overnight at 4°C before going through the DNA extraction protocols listed above (see section 4.4.2). Negative controls were DNA extracts from malaria-negative dried blood samples.

4.4.5 Anopheles cryptic species identification for Plasmodium-positive samples

DNA extracts for *An. gambiae* s.l head+thorax samples that were definitively positive for *P. falciparum, P. ovale, P. vivax,* and/or *P. malariae* underwent additional analyses to determine cryptic species identities. A modified PCR protocol originally designed by Wilkins et al was used that only included the universal forward primer (5'-GCTGCGAGTTGTAGAGATGCG-3') and reverse primers for *An. arabiensis* (5'-GTGTTAAGTGTCCTTCTCCGTC-3'), *An. gambiae* s.l (5'-GCTTACTGGTTTGGTCGGCATGT-3'), *An. gambiae* s.s (5'-CCAGACCAAGATGGTTCGCTG-3'), and *An. coluzzii* (5'-TAGCCAGCTCTTGTCCACTAGTTTT-3').[118,471] Eliminated primers were either specific to species not observed in Burkina Faso and/or were not relevant to this study.[95]

PCR-amplified samples were run on a 1.5% agarose gel at 60V for 1 hour and 40 minutes. The protocol created fragments of 387 base pairs (bp) for *An. arabiensis* and 463 bp for *An. gambiae* s.l with a second, additional band at 333 bp for *An. coluzzii* or 221 bp for *An. gambiae* s.s. As a negative control, the Wilkins et al PCR protocol was followed using nuclease-free water in place of a DNA extract. For a positive control, we amplified DNA extracts from previously identified *An. arabiensis, An. coluzzii,* and *An. gambiae* s.s collected from Burkina Faso in 2015. *An. funestus* subspecies were not identified since prior, recent studies out of Burkina Faso indicate that nearly all *An. funestus* in this area are *An. funestus* s.s.[159]

4.4.6 Statistical analyses

To measure vector infectiousness, the SIR was calculated for both the 2019 and 2020 RIMDAMAL II datasets according to the standard formula ([number of sporozoite-positive

mosquitoes]/[total number of sampled mosquitoes] x100%).[94] Genomes per sample results were assessed for normal and lognormal distributions via the Anderson-Darling, D'Agostino-Pearson, Shapiro-Wilk, and Kolmogorov-Smirnov tests. All normalcy tests were failed, but the four tests showed the data followed a lognormal distribution. Parous rates (PR; the proportion of parous females over the total dissected) were calculated for *An. gambiae* s.l sampled in both 2019 and 2020. Further analysis into subspecies was omitted due to the dominance of *An. gambiae* s.s and few sample numbers for *An. coluzzii* and *An. arabiensis*. Because only a very small number of *An. funestus* were dissected, no PRs were calculated for this clade. MDA sampling periods (e.g., MDA1+3) and villages (e.g., DB in MDA1+1) that had no parity data recorded were omitted from Supplemental Table S3.6. Daily survival rates (p) were deduced from *An. gambiae* s.l PRs according to Davidson's method ($p = \sqrt[g]{PR}$).[295] Because the gonotrophic cycle (g) lasts 2-5 days for *An. gambiae* s.l, an average of 3.5 days was used for calculating p.[472,473] The proportion of the vector population that reached an epidemiologically dangerous age (P_d) was determined from p according to MacDonald's formula ($P_d = p^n$).[255] The EIP (n in the preceding formula) for *An. gambiae* s.l was assumed to be 10 days according to the literature.[2,255] Statistical significance was primarily determined through contingency table analyses and chi-square tests, unpaired t-tests, or one-way ANOVA with ad hoc Tukey's multiple-comparison tests in GraphPad Prism (GraphPad Software, La Jolla California USA).

CHAPTER 5: SUMMARY AND FUTURE CONSIDERATIONS

Methods of assessing mosquito survivorship, the most significant driver of vectorial capacity, were tested for *An. gambiae* s.l mosquitoes. The first goal was to determine the viability of a long-underutilized technique for age grading mosquitoes originally based on qualitatively assessing wing wear. It was found that counting long wing scales along the distal edge of the wing, specifically between the Cu2, Cu1, M2, and M4 vein-divided wing sections, could potentially be an accurate and field-viable means of determining malaria mosquito age. We showed that wing scales are lost in a non-linear fashion over time, which we hypothesize is a result of the force exerted on wings during flight as well as friction experienced when mosquito wings come into contact with surfaces.[284,288] Because of this correlation, we could calculate age in numerical days, a valuable metric when correlating mosquito age to malaria extrinsic incubation periods. However, our manual assessment of wing wear was dependent on just one morphological feature – wing scales. Longstanding taxonomy practices show that several wing structures and characteristics are significant for differentiating mosquito species.[144,174] These features may also be affected over time, and therefore could be investigated further as additional wing wear-based age indicators. However, given the need for high-throughput age grading techniques, such features would be best analyzed through machine learning and other computational, image-based analysis techniques.

The accuracy of the wing-based technique was increased when we used computational analysis algorithms to process images of mosquito wings. Therefore, wing-based age grading could not only be a viable tool for researchers moving forward, but could also be a new, collaborative area of research merging medical entomology with computer science. Using

machine and deep learning techniques to classify mosquito sex and species based on wing images is both a promising and budding area of present research.[418,474–476] However, these efforts have yet to be paired with age grading. Our results indicate that these two endeavors could perhaps be merged, leading to innovative technology developments for malaria vector surveillance. Additional technology applications could include: (1) measuring wing length, which is used as a proxy for mosquito body size and therefore indicate levels of fitness and fecundity; (2) direct malaria detection, as sporozoites are carried by the circulation of hemolymph to all tissues of the mosquito, even to the legs and wing veins.[34,41,477,478] However, further work is first needed to validate the pixel intensity-based methods we utilized and assess other machine learning strategies as alternative, viable options. Additionally, although wing scale counting has been used to age grade wild mosquito populations, no such effort has yet been undertaken for pixel intensity- or machine learning-based methods.

Measuring mosquito age is even more complicated when investigating wild mosquitoes in comparison to their lab-reared counterparts. Wild-caught mosquitoes have unknown life histories, and their pre-exposure to environmental and weather factors combined with their genetic and physiological conditions can all impact age readings and results.[173,256,304,306–308,434] Given these challenges, we compared three age grading techniques – Detinova parity assessments, NIRS, and wing scale counting – and considered their accuracy, technicality, and cost and labor efficiency with samples derived from the first year of RIMDAMAL II. Ultimately, we determined that the latter two methods were the best for processing the large sample sizes needed for age grading, though no firm conclusions could be made given our study limitations. Larger numbers of samples collected from a more diverse set of mosquitoes will be needed to improve and accurately compare our NIRS- and wing scale-based age prediction models, which

may be accomplished moving forward once data from the 2020 RIMDAMAL II season is added to the existing analyses. However, parity data is still limited in our 2020 dataset. If possible, future field efforts could be made to augment our parity data and achieve the sample numbers required for a robust three-way comparison between the techniques.

Additionally, future research is perhaps warranted to investigate the Detinova method's efficacy in age grading ivermectin-exposed mosquitoes as well as the drug's impact on normal ovarian development. Because ivermectin has been shown to have a stronger mortality effect against older mosquitoes that have taken more than one blood meal, we would expect mosquito populations that ingest the drug to exhibit increased nulliparity as older mosquitoes are eliminated from the population.[377,390] We have corroborated these findings to an extent. As evidenced in our mesocosm experiments, the Detinova method failed to detect the ivermectin-induced shifts in age structure in mixed mosquito populations of known and unknown ages. Similarly, parity rates between control and treatment villages during RIMDAMAL I were not significantly different.[398] We hypothesize that ivermectin exposure may confound parity analyses. This idea could either be tested in subsequent laboratory experiments or determined by reassessing our RIMDAMAL II data after we are unblinded, group villages by study arm, and correlate parity results to our survivorship data.

Our original hypothesis was that mosquito age populations would be shifted to younger classes in ivermectin-treated villages which, if proven correct after unblinding the study, would usher in several new avenues of potential exploration. Several studies have already shown that blood feeding on ivermectin-treated humans and animals significantly reduces mosquito survival; others have demonstrated that ivermectin MDAs can reduce sporozoite transmission within communities.[13,376,378,393,479,480] As such, an initial area of research would be to merge these

two efforts, comparing entomological and clinical data from our study arms and assessing whether reduced malaria incidence was experienced in treated villages that had younger mosquito populations as compared to untreated villages with older mosquito populations. This investigation will be critical, particularly if ivermectin is used regularly as a malaria control tool in the future. A recent modeling investigation indicated that (1) control strategies that manipulate mosquito reproduction with the aim of suppressing *Anopheles* populations may inadvertently favor malaria transmission, and (2) that younger anopheline females potentially contribute significantly to malaria transmission.[217] With these findings in mind, our future surveillance efforts and RIMDAMAL II data analyses should investigate whether potential, ivermectin-induced shifts in mosquito population age structure facilitate new malaria transmission dynamics in Burkina Faso. To do so, the SIR of young mosquitoes should be monitored and compared to malaria clinical disease incidence.

Within the context of RIMDAMAL II, our examinations of mosquito age structure changes should also be paired with parallel explorations into shifts in insecticide resistance profiles. One study showed that permethrin-resistant strains of *Ae. aegypti* were significantly less susceptible to ivermectin bloodmeals than standard reference strains. Furthermore, a correlation analysis of log-transformed LC_{50} among strains suggested that permethrin and ivermectin cross-resistance may occur.[481] This might be due to enhanced metabolic resistance mechanisms; the upregulated expression of several detoxification enzymes could be used to break down ivermectin as well as standard malaria control insecticides. Because insecticide resistance can potentiate the vector competence of *An. gambiae* s.s, a future endeavor could include analyzing our *Anopheles* samples for genetic and metabolic resistance via protein expression assays, RNA sequencing, and PCR-based analyses.[482,483] Furthermore, field studies have shown that

insecticide susceptibility is restored when mosquitoes age, and insecticide-resistant mosquitoes are more likely to be nulliparous (in other words, younger).[483–487] Determining if and how ivermectin MDAs affect insecticide resistance profiles and levels among malaria mosquitoes, and how that impacts malaria disease incidence, will therefore be crucial.

In addition to measuring mosquito age and its correlation to vector competence, we analyzed entomological and limited parasitological data from RIMDAMAL II to explore changing vector competence dynamics in Burkina Faso. Our results first indicated that *An. funestus* may play a significant role in *Plasmodium* transmission during and, potentially, outside of the rainy season. Similarly, our findings suggest that *An. funestus* may be more responsible than anticipated for transmitting *P. ovale*. Ideally, these discoveries would be verified with follow-up, laboratory vector competence studies. However, only two *An. funestus* strains have been successfully colonized from wild populations, meaning that these studies would be extremely difficult to execute.[448–451] Furthermore, lab strain-derived results would likely not be generalizable to the wild *An. funestus* populations and malaria transmission dynamics of our Burkina Faso study region. Working with wildtype, locally captured *An. funestus* would prove a more viable, though still difficult, means of conducting a vector competence assay. Limited protocols exist detailing how wild-caught *An. funestus* larvae can be reared to adulthood and propagated through a limited number of generations in insectary conditions.[118] These adult mosquitoes could then be fed blood drawn from gametocytaemic human volunteers and, afterwards, processed via molecular and salivation assays to determine malaria infection, dissemination, and transmission.

In an effort to explore *An. funestus* vector competence further, future RIMDAMAL II analysis efforts could determine: (1) molecular measurements of transmission efficiency by

calculating dissemination rates (proportion of mosquitoes with virus in their legs, irrespective to their infection status) and transmission rates (proportion of mosquitoes with a disseminated infection that transmit the virus during refeeding); (2) changes in endophilic and exophilic feeding behavior by comparing proportions of mosquitoes collected in indoor vs. outdoor light traps; (3) alterations in host species preference by using PCR-based analyses to identify the origin of mosquito blood meals.[488,489] To this latter point, future research in our lab will explore host preference for specific human individuals. Prior studies have shown that a small number of individuals within households receive potentially more infectious bites than others.[221] This indicates that some individuals may be "super-transmitters," having a higher malaria transmission potential due to heterogeneous mosquito exposure (among other factors like high gametocytemia and high gametocyte infectiousness).[221,490] Molecular blood fingerprinting could be used to identify human DNA in mosquito blood meals, which could then be correlated with human clinical samples and matched to paired demographic (e.g., sex, pregnancy status, weight) and housing (e.g., the room each individual slept in, whether they use a bednet or not, housing structure type, etc.) data. This analysis would not only elucidate essential factors of vector competence, namely host seeking behavior and host preference, but could also yield information critical for designing tailored malaria control strategies in the future.

As a final analysis, we used our 2019 and 2020 RIMDAMAL II data to calculate entomological indicators pertinent to vectorial capacity and malaria transmission risk. Notably, we deduced daily survival rates using Davidson's method and estimated the proportion of the vector population that reached the epidemiologically dangerous age according to MacDonald's formula.[255,295] Recent modeling studies argue that estimations of this nature, notably those that include variables related to mosquito age in addition to sporozoite and oocyst rates, potentially

provide more accurate estimates for malaria transmission risks.[263,467–469] It should be noted, though, that MacDonald and Davidson's formulae use parity rates as an indicator for mosquito age. As highlighted in this thesis, parity determination is often a subjective technique and is logistically challenging when used for large-scale mosquito surveillance efforts.[173] However, our comparisons of other age grading techniques show that NIRS and wing wear evaluation are viable alternatives and produce relatively accurate age predictions for mosquito populations. What remains to be explored, however, is whether MacDonald and Davidson's formulae could be adapted to include age determinations derived from these two methods instead of from parity assessments. To our knowledge, no such study has yet been undertaken. However, the benefits of doing so could be significant. We hypothesize that NIRS- and wing wear-based age derivations could be substituted in place of parity rates, though not necessarily in a 1:1 fashion. If proven true, researchers would have a means of incorporating age metrics that are high-throughput and accurate into MacDonald and Davidson's formulae, thereby generating important disease transmission risk estimates from larger and more robust datasets.

REFERENCES

1. Jackson P. *The Lord of the Rings: The Two Towers*. USA: New Line Cinema; 2002.
2. Beier JC. Malaria Parasite Development in Mosquitoes. *Annu Rev Entomol*. 1998;43(1):519-543. doi:10.1146/annurev.ento.43.1.519.
3. Drugs I of M (US) C on the E of A, Arrow KJ, Panosian C, Gelband H. A Brief History of Malaria. 2004. https://www.ncbi.nlm.nih.gov/books/NBK215638/. Accessed July 30, 2021.
4. Global Malaria Programme - WHO Global. *World Malaria Report 2019*.; 2019. https://www.who.int/publications/i/item/9789241565721.
5. World Health Organization. *Global Vector Control Response 2017-2030*.; 2017. http://www.who.int/malaria/global-vector-control-response/en/.
6. Barat LM, Palmer N, Basu S, Worrall E, Hanson K, Mills A. Do Malaria Control Interventions Reach the Poor? A View through the Equity Lens. 2004. https://www.ncbi.nlm.nih.gov/books/NBK3767/. Accessed July 1, 2021.
7. Devine A, Battle KE, Meagher N, Howes RE, Dini S, Gething PW, Simpson JA, Price RN, Lubell Y. Global economic costs due to vivax malaria and the potential impact of its radical cure: A modelling study. Rosen S, ed. *PLOS Med*. 2021;18(6):e1003614. doi:10.1371/journal.pmed.1003614.
8. Vlassoff C. Gender Differences in Determinants and Consequences of Health and Illness. *J Health Popul Nutr*. 2007;25(1):47. https://www.ncbi.nlm.nih.gov/pmc/articles/PMC3013263/. Accessed July 1, 2021.
9. Schantz-Dunn J, Nour NM. Malaria and Pregnancy: A Global Health Perspective. *Rev Obstet Gynecol*. 2009;2(3):186. https://www.ncbi.nlm.nih.gov/pmc/articles/PMC2760896/. Accessed July 1, 2021.
10. Schumacher R-F, Spinelli E. Malaria in Children. *Mediterr J Hematol Infect Dis*. 2012;4(1). doi:10.4084/MJHID.2012.073.
11. Okiro EA, Al-Taiar A, Reyburn H, Idro R, Berkley JA, Snow RW. Age patterns of severe paediatric malaria and their relationship to Plasmodium falciparum transmission intensity. *Malar J*. 2009;8(1):4. doi:10.1186/1475-2875-8-4.
12. WHO. Global technical strategy for malaria 2016-2030. *World Heal Organ*. 2015:1-35. http://apps.who.int/iris/bitstream/10665/176712/1/9789241564991_eng.pdf?ua=1.
13. Foy BD, Kobylinski KC, Silva IM da, Rasgon JL, Sylla M. Endectocides for malaria control. *Trends Parasitol*. 2011;27(10):423-428. doi:10.1016/j.pt.2011.05.007.
14. Centers for Disease Control and Prevention. CDC - Malaria - About Malaria - Biology. 2020. https://www.cdc.gov/malaria/about/biology/#tabs-1-6. Accessed July 2, 2021.
15. Miller LH, Baruch DI, Marsh K, Doumbo OK. The pathogenic basis of malaria. *Nature*. 2002;415(6872):673-679. doi:10.1038/415673a.
16. Sato S. Plasmodium—a brief introduction to the parasites causing human malaria and their basic biology. *J Physiol Anthropol*. 2021;40(1):1. doi:10.1186/s40101-020-00251-9.
17. Amino R, Thiberge S, Martin B, Celli S, Shorte S, Frischknecht F, Ménard R. Quantitative imaging of Plasmodium transmission from mosquito to mammal. *Nat Med*. 2006;12(2):220-224. doi:10.1038/nm1350.
18. Frischknecht F, Baldacci P, Martin B, Zimmer C, Thiberge S, Olivo-Marin JC, Shorte SL,

Ménard R. Imaging movement of malaria parasites during transmission by Anopheles mosquitoes. *Cell Microbiol*. 2004;6(7):687-694. doi:10.1111/j.1462-5822.2004.00395.x.
19. Ponnudurai T, Lensen A, van Gemert G, Bensink M, Bolmer M, Meuwissen J. Sporozoite load of mosquitoes infected with Plasmodium falciparum. *Trans R Soc Trop Med Hyg*. 1989;83(1). doi:10.1016/0035-9203(89)90708-6.
20. Medica D, Sinnis P. Quantitative dynamics of Plasmodium yoelii sporozoite transmission by infected anopheline mosquitoes. *Infect Immun*. 2005;73(7). doi:10.1128/IAI.73.7.4363-4369.2005.
21. Rosenberg R, Wirtz RA, Schneider I, Burge R. An estimation of the number of malaria sporozoites ejected by a feeding mosquito. *Trans R Soc Trop Med Hyg*. 1990;84(2):209-212. doi:10.1016/0035-9203(90)90258-g.
22. Prudêncio M, Rodriguez A, Mota MM. The silent path to thousands of merozoites: the Plasmodium liver stage. *Nat Rev Microbiol*. 2006;4(11):849-856. doi:10.1038/nrmicro1529.
23. Sultan AA, Thathy V, Frevert U, Robson KJ, Crisanti A, Nussenzweig V, Nussenzweig RS, Ménard R. TRAP is necessary for gliding motility and infectivity of plasmodium sporozoites. *Cell*. 1997;90(3):511-522. doi:10.1016/s0092-8674(00)80511-5.
24. Mota MM, Pradel G, Vanderberg JP, Hafalla JCR, Frevert U, Nussenzweig RS, Nussenzweig V, Rodrı´guez A. Migration of Plasmodium Sporozoites Through Cells Before Infection. *Science (80-)*. 2001;291(5501):141-144. doi:10.1126/SCIENCE.291.5501.141.
25. Meis JF, Verhave JP, Jap PH, Sinden RE, Meuwissen JH. Ultrastructural observations on the infection of rat liver by Plasmodium berghei sporozoites in vivo. *J Protozool*. 1983;30(2):361-366. doi:10.1111/j.1550-7408.1983.tb02931.x.
26. Sturm A, Amino R, Sand C van de, Regen T, Retzlaff S, Rennenberg A, Krueger A, Pollok J-M, Menard R, Heussler VT. Phosphatidylserine Receptor Is Required for Clearance of Apoptotic Cells. *Science (80-)*. 2006;302(5650):1560-1563. doi:10.1126/science.1087621.
27. Tarun AS, Baer K, Dumpit RF, Gray S, Lejarcegui N, Frevert U, Kappe SHI. Quantitative isolation and in vivo imaging of malaria parasite liver stages. *Int J Parasitol*. 2006;36(12):1283-1293. doi:10.1016/j.ijpara.2006.06.009.
28. Wanderley JLM, DaMatta RA, Barcinski MA. Apoptotic mimicry as a strategy for the establishment of parasitic infections: parasite- and host-derived phosphatidylserine as key molecule. *Cell Commun Signal*. 2020;18(1):10. doi:10.1186/s12964-019-0482-8.
29. Matthews H, Duffy CW, Merrick CJ. Checks and balances? DNA replication and the cell cycle in Plasmodium. *Parasit Vectors*. 2018;11(1):216. doi:10.1186/s13071-018-2800-1.
30. Arnot D, Ronander E, Bengtsson D. The progression of the intra-erythrocytic cell cycle of Plasmodium falciparum and the role of the centriolar plaques in asynchronous mitotic division during schizogony. *Int J Parasitol*. 2011;41(1). doi:10.1016/J.IJPARA.2010.07.012.
31. Cowman AF, Healer J, Marapana D, Marsh K. Malaria: Biology and Disease. *Cell*. 2016;167(3):610-624. doi:10.1016/j.cell.2016.07.055.
32. Josling GA, Llinás M. Sexual development in Plasmodium parasites: knowing when it's time to commit. *Nat Rev Microbiol*. 2015;13(9):573-587. doi:10.1038/nrmicro3519.
33. Bancells C, Llorà-Batlle O, Poran A, Nötzel C, Rovira-Graells N, Elemento O, Kafsack BFC, Cortés A. Revisiting the initial steps of sexual development in the malaria parasite

Plasmodium falciparum. *Nat Microbiol*. 2019;4(1):144-154. doi:10.1038/s41564-018-0291-7.
34. Frischknecht F, Matuschewski K. Plasmodium Sporozoite Biology. doi:10.1101/cshperspect.a025478.
35. Billker O, Lindo V, Panico M, Etienne AE, Paxton T, Dell A, Rogers M, Sinden RE, Morris HR. Identification of xanthurenic acid as the putative inducer of malaria development in the mosquito. *Nature*. 1998;392(6673):289-292. doi:10.1038/32667.
36. Matuschewski K. Getting infectious: formation and maturation of Plasmodium sporozoites in the Anopheles vector. *Cell Microbiol*. 2006;8(10):1547-1556. doi:10.1111/j.1462-5822.2006.00778.x.
37. Smith RC, Vega-Rodríguez J, Jacobs-Lorena M. The Plasmodium bottleneck: malaria parasite losses in the mosquito vector. *Mem Inst Oswaldo Cruz*. 2014;109(5):644-661. doi:10.1590/0074-0276130597.
38. Janse CJ, Van der Klooster PF, Van der Kaay HJ, Van der Ploeg M, Overdulve JP. Rapid repeated DNA replication during microgametogenesis and DNA synthesis in young zygotes of Plasmodium berghei. *Trans R Soc Trop Med Hyg*. 1986;80(1):154-157. doi:10.1016/0035-9203(86)90219-1.
39. Kawamoto F, Alejo-Blanco R, Fleck S, Sinden R. Plasmodium berghei: ionic regulation and the induction of gametogenesis. *Exp Parasitol*. 1991;72(1). doi:10.1016/0014-4894(91)90118-G.
40. Beier JC. Malaria parasite development. *Annu Rev Entomol*. 1998.
41. Aly ASI, Vaughan AM, Kappe SHI. Malaria parasite development in the mosquito and infection of the mammalian host. *Annu Rev Microbiol*. 2009;63:195-221. doi:10.1146/annurev.micro.091208.073403.
42. Han YS, Thompson J, Kafatos FC, Barillas-Mury C. Molecular interactions between Anopheles stephensi midgut cells and Plasmodium berghei: the time bomb theory of ookinete invasion of mosquitoes. *EMBO J*. 2000;19(22):6030. doi:10.1093/EMBOJ/19.22.6030.
43. Wang Y-H, Chang M-M, Wang X-L, Zheng A-H, Zou Z. The immune strategies of mosquito Aedes aegypti against microbial infection. *Dev Comp Immunol*. 2018;83:12-21. doi:10.1016/j.dci.2017.12.001.
44. Hillyer JF, Barreau C, Vernick KD. Efficiency of salivary gland invasion by malaria sporozoites is controlled by rapid sporozoite destruction in the mosquito haemocoel. *Int J Parasitol*. 2007;37(6):673-681. doi:10.1016/j.ijpara.2006.12.007.
45. Beier JC. Frequent Blood-Feeding and Restrictive Sugar-Feeding Behavior Enhance the Malaria Vector Potential of Anopheles gambiae s.l. and An. funestus (Diptera: Culicidae) in Western Kenya. *J Med Entomol*. 1996. doi:10.1093/jmedent/33.4.613.
46. World Health Organization. *World Malaria Report 2015*.; 2015. https://books.google.com/books?hl=en&lr=&id=rg4LDgAAQBAJ&oi=fnd&pg=PP1&dq=WHO+.++2015++World+malaria+report+2015.+World+Health+Organization,+Geneva+.+&ots=XTiENTN0IF&sig=Nh89_yvRXuPIqXdFWIF5JxvSzq4#v=onepage&q=WHO . 2015 World malaria repo. Accessed July 3, 2021.
47. Milner DA, Jr. Malaria Pathogenesis. *Cold Spring Harb Perspect Med*. 2018;8(1). doi:10.1101/cshperspect.a025569.
48. Ansar W, Mukhopadhyay Nee Bandyopadhyay S, Chowdhury S, Hasan Habib SK, Mandal C, Ansar W, Mukhopadhyay Nee Bandyopadhyay · S, Chowdhury · S, Habib SH,

Mandal · C. Role of C-reactive protein in complement-mediated hemolysis in Malaria. *Glycoconj J*. 2006;23:233-240. doi:10.1007/s10719-006-7928-0.
49. Oakley MS, Gerald N, McCutchan TF, Aravind L, Kumar S. Clinical and molecular aspects of malaria fever. *Trends Parasitol*. 2011;27(10):442-449. doi:10.1016/J.PT.2011.06.004.
50. Hafalla JC, Silvie O, Matuschewski K. Cell biology and immunology of malaria. *Immunol Rev*. 2011;240(1):297-316. doi:10.1111/j.1600-065X.2010.00988.x.
51. Wassmer SC, Taylor TE, Rathod P, Mishra S, Mohanty S, Arevalo-Herrera M, Duraisingh M, Smith J. Investigating the Pathogenesis of Severe Malaria: A Multidisciplinary and Cross-Geographical Approach. *Am J Trop Med Hyg*. 2015;93(3 Suppl). doi:10.4269/AJTMH.14-0841.
52. White NJ. Anaemia and malaria. *Malar J*. 2018;17. doi:10.1186/S12936-018-2509-9.
53. Wassmer SC, Grau GER. Severe malaria: what's new on the pathogenesis front? *Int J Parasitol*. 2017;47(2-3):145. doi:10.1016/J.IJPARA.2016.08.002.
54. Grau GER, Craig A. Cerebral malaria pathogenesis: revisiting parasite and host contributions. *Future Microbiol*. 2012;7(2). doi:10.2217/FMB.11.155.
55. Manning L, Laman M, Davis WA, Davis TME. Clinical features and outcome in children with severe Plasmodium falciparum malaria: a meta-analysis. *PLoS One*. 2014;9(2):e86737. doi:10.1371/journal.pone.0086737.
56. Ansong D, Seydel KB, Taylor TE. Malaria. In: Ryan ET, Hill DR, Solomon T, Aronson NE, Endy TP, eds. *Hunter's Tropical Medicine and Emerging Infectious Diseases*. 10th ed. Elsevier; 2020:734-754. doi:https://doi.org/10.1016/C2016-0-01879-X.
57. Ayres Pereira M, Mandel Clausen T, Pehrson C, Mao Y, Resende M, Daugaard M, Riis Kristensen A, Spliid C, Mathiesen L, E. Knudsen L, Damm P, G. Theander T, R. Hansson S, A. Nielsen M, Salanti A. Placental Sequestration of Plasmodium falciparum Malaria Parasites Is Mediated by the Interaction Between VAR2CSA and Chondroitin Sulfate A on Syndecan-1. Rowe JA, ed. *PLOS Pathog*. 2016;12(8):e1005831. doi:10.1371/journal.ppat.1005831.
58. Rénia L, Howland SW, Claser C, Charlotte Gruner A, Suwanarusk R, Hui Teo T, Russell B, Ng LFP. Cerebral malaria: mysteries at the blood-brain barrier. *Virulence*. 2012;3(2):193-201. doi:10.4161/viru.19013.
59. Nkumama IN, O'Meara WP, Osier FHA. Changes in Malaria Epidemiology in Africa and New Challenges for Elimination. *Trends Parasitol*. 2017;33(2). doi:10.1016/j.pt.2016.11.006.
60. Adams JH, Mueller I. The Biology of Plasmodium vivax. *Cold Spring Harb Perspect Med*. 2017;7(9). doi:10.1101/CSHPERSPECT.A025585.
61. Flannery EL, Markus MB, Vaughan AM. Plasmodium vivax. *Trends Parasitol*. 2019;35(7):583-584. doi:10.1016/j.pt.2019.04.005.
62. Dayananda KK, Achur RN, Gowda DC. Epidemiology, drug resistance, and pathophysiology of Plasmodium vivax malaria. *J Vector Borne Dis*. 2018;55(1):1-8. doi:10.4103/0972-9062.234620.
63. Chitnis CE, Sharma A. Targeting the Plasmodium vivax Duffy-binding protein. *Trends Parasitol*. 2008;24(1):29-34. doi:10.1016/j.pt.2007.10.004.
64. Mahittikorn A, Masangkay FR, Kotepui KU, Milanez GDJ, Kotepui M. Comparison of Plasmodium ovale curtisi and Plasmodium ovale wallikeri infections by a meta-analysis approach. *Sci Rep*. 2021;11(1):6409. doi:10.1038/s41598-021-85398-w.

65. Stephens JWW. A New Malaria Parasite of Man. *Ann Trop Med Parasitol*. 1922;16(4):383-388. doi:10.1080/00034983.1922.11684331.
66. Sutherland CJ, Tanomsing N, Nolder D, Oguike M, Jennison C, Pukrittayakamee S, Dolecek C, Hien TT, Do Rosário VE, Arez AP, Pinto J, Michon P, Escalante AA, Nosten F, Burke M, Lee R, Blaze M, Otto TD, Barnwell JW, Pain A, Williams J, White NJ, Day NPJ, Snounou G, Lockhart PJ, Chiodini PL, Imwong M, Polley SD. Two nonrecombining sympatric forms of the human malaria parasite plasmodium ovale occur globally. *J Infect Dis*. 2010;201(10):1544-1550. doi:10.1086/652240.
67. Ansari HR, Templeton TJ, Subudhi AK, Ramaprasad A, Tang J, Lu F, Naeem R, Hashish Y, Oguike MC, Benavente ED, Clark TG, Sutherland CJ, Barnwell JW, Culleton R, Cao J, Pain A. Genome-scale comparison of expanded gene families in Plasmodium ovale wallikeri and Plasmodium ovale curtisi with Plasmodium malariae and with other Plasmodium species. *Int J Parasitol*. 2016;46(11):685-696. doi:10.1016/J.IJPARA.2016.05.009.
68. Collins WE, Jeffery GM. Plasmodium ovale: parasite and disease. *Clin Microbiol Rev*. 2005;18(3):570-581. doi:10.1128/CMR.18.3.570-581.2005.
69. Golgi C. Sulla infezione malarica. 1886. https://scholar.google.com/scholar_lookup?title=Sul%27 infezione malarica&journal=Arch Sci Med Torino&volume=10&pages=109-135&publication_year=1886&author=Golgi%2CC. Accessed July 3, 2021.
70. Mueller I, Zimmerman PA, Reeder JC. Plasmodium malariae and Plasmodium ovale--the "bashful" malaria parasites. *Trends Parasitol*. 2007;23(6):278-283. doi:10.1016/j.pt.2007.04.009.
71. WE C, GM J. Plasmodium malariae: parasite and disease. *Clin Microbiol Rev*. 2007;20(4). doi:10.1128/CMR.00027-07.
72. Sutherland CJ. Persistent Parasitism: The Adaptive Biology of Malariae and Ovale Malaria. *Trends Parasitol*. 2016;32(10):808-819. doi:10.1016/J.PT.2016.07.001.
73. Hendrickse RG, Adeniyi A. Quartan malarial nephrotic syndrome in children. *Kidney Int*. 1979;16(1):64-74. doi:10.1038/ki.1979.103.
74. Müller M, Schlagenhauf P. Plasmodium knowlesi in travellers, update 2014. *Int J Infect Dis*. 2014;22:55-64. doi:10.1016/j.ijid.2013.12.016.
75. Singh B, Daneshvar C. Human infections and detection of Plasmodium knowlesi. *Clin Microbiol Rev*. 2013;26(2). doi:10.1128/CMR.00079-12.
76. Lim C, Hansen E, DeSimone TM, Moreno Y, Junker K, Bei A, Brugnara C, Buckee CO, Duraisingh MT. Expansion of host cellular niche can drive adaptation of a zoonotic malaria parasite to humans. *Nat Commun*. 2013;4:1638. doi:10.1038/ncomms2612.
77. Stich A, Oster N, Abdel-Aziz I, Stieglbauer G, Coulibaly B, Wickert H, McLean J, Kouyaté B, Becher H, Lanzer M. Malaria in a holoendemic area of Burkina Faso: a cross-sectional study. *Parasitol Res*. 2006;98(6). doi:10.1007/S00436-005-0104-9.
78. Tourre YM, Vignolles C, Viel C, Faruque FS, Malone JB. Malaria in Burkina Faso (West Africa) during the twenty-first century. *Environ Monit Assess*. 2019;191(S2):273. doi:10.1007/s10661-019-7410-7.
79. Guglielmo F, Ranson H, Sagnon N, Jones C. The issue is not 'compliance': exploring exposure to malaria vector bites through social dynamics in Burkina Faso. *Anthropol Med*. May 2021:1-18. doi:10.1080/13648470.2021.1884185.
80. Samadoulougou S, Pearcy M, Yé Y, Kirakoya-Samadoulougou F. Progress in coverage of

bed net ownership and use in Burkina Faso 2003–2014: evidence from population-based surveys. *Malar J*. 2017;16(1):302. doi:10.1186/s12936-017-1946-1.
81. Soma DD, Kassié D, Sanou S, Karama FB, Ouari A, Mamai W, Ouédraogo GA, Salem G, Dabiré RK, Fournet F. Uneven malaria transmission in geographically distinct districts of Bobo-Dioulasso, Burkina Faso. *Parasit Vectors*. 2018;11(1):296. doi:10.1186/s13071-018-2857-x.
82. Diallo A, Sié A, Sirima S, Sylla K, Ndiaye M, Bountogo M, Ouedraogo E, Tine R, Ndiaye A, Coulibaly B, Ouedraogo A, Faye B, Ba EH, Compaore G, Tiono A, Sokhna C, Yé M, Diarra A, Bahmanyar ER, De Boer M, Pirçon J-Y, Usuf EA. An epidemiological study to assess Plasmodium falciparum parasite prevalence and malaria control measures in Burkina Faso and Senegal. *Malar J*. 2017;16(1):63. doi:10.1186/s12936-017-1715-1.
83. Gnémé A, Guelbéogo WM, Riehle MM, Tiono AB, Diarra A, Kabré GB, Sagnon N, Vernick KD. Plasmodium species occurrence, temporal distribution and interaction in a child-aged population in rural Burkina Faso. *Malar J*. 2013;12(1):67. doi:10.1186/1475-2875-12-67.
84. Guerra CA, Snow RW, Hay SI. Mapping the global extent of malaria in 2005. *Trends Parasitol*. 2006;22(8):353-358. doi:10.1016/j.pt.2006.06.006.
85. Langhi DM, Orlando Bordin J. Duffy blood group and malaria. *Hematology*. 2006;11(5-6):389-398. doi:10.1080/10245330500469841.
86. Twohig KA, Pfeffer DA, Baird JK, Price RN, Zimmerman PA, Hay SI, Gething PW, Battle KE, Howes RE. Growing evidence of Plasmodium vivax across malaria-endemic Africa. *PLoS Negl Trop Dis*. 2019;13(1):e0007140. doi:10.1371/journal.pntd.0007140.
87. Poirier P, Doderer-Lang C, Atchade PS, Lemoine J-P, de l'Isle M-LC, Abou-bacar A, Pfaff AW, Brunet J, Arnoux L, Haar E, Filisetti D, Perrotey S, Chabi NW, Akpovi CD, Anani L, Bigot A, Sanni A, Candolfi E. The hide and seek of Plasmodium vivax in West Africa: report from a large-scale study in Beninese asymptomatic subjects. *Malar J*. 2016;15(1):570. doi:10.1186/s12936-016-1620-z.
88. Mendes C, Dias F, Figueiredo J, Mora VG, Cano J, de Sousa B, do Rosário VE, Benito A, Berzosa P, Arez AP. Duffy negative antigen is no longer a barrier to Plasmodium vivax--molecular evidences from the African West Coast (Angola and Equatorial Guinea). *PLoS Negl Trop Dis*. 2011;5(6):e1192. doi:10.1371/journal.pntd.0001192.
89. Imwong M, Nakeesathit S, Day NPJ, White NJ. A review of mixed malaria species infections in anopheline mosquitoes. *Malar J*. 2011;10. doi:10.1186/1475-2875-10-253.
90. McKenzie FE, Bossert WH. Multispecies Plasmodium infections of humans. *J Parasitol*. 1999;85(1):12-18. http://www.ncbi.nlm.nih.gov/pubmed/10207356. Accessed July 7, 2021.
91. Mayxay M, Pukrittayakamee S, Newton PN, White NJ. Mixed-species malaria infections in humans. *Trends Parasitol*. 2004;20(5):233-240. doi:10.1016/J.PT.2004.03.006.
92. Barry AE, Waltmann A, Koepfli C, Barnadas C, Mueller I. Uncovering the transmission dynamics of Plasmodium vivax using population genetics. *Pathog Glob Health*. 2015;109(3):142-152. doi:10.1179/2047773215Y.0000000012.
93. Li R, Xu L, Bjørnstad ON, Liu K, Song T, Chen A, Xu B, Liu Q, Stenseth NC. Climate-driven variation in mosquito density predicts the spatiotemporal dynamics of dengue. *Proc Natl Acad Sci U S A*. 2019. doi:10.1073/pnas.1806094116.
94. Smith DL, McKenzie FE. Statics and dynamics of malaria infection in Anopheles mosquitoes. *Malar J*. 2004. doi:10.1186/1475-2875-3-13.

95. Epopa PS, Collins CM, North A, Millogo AA, Benedict MQ, Tripet F, Diabate A. Seasonal malaria vector and transmission dynamics in western Burkina Faso. *Malar J*. 2019;18(1):113. doi:10.1186/s12936-019-2747-5.
96. Zollner GE, Ponsa N, Garman GW, Poudel S, Bell JA, Sattabongkot J, Coleman RE, Vaughan JA. Population dynamics of sporogony for Plasmodium vivax parasites from western Thailand developing within three species of colonized Anopheles mosquitoes. *Malar J*. 2006;5(1):68. doi:10.1186/1475-2875-5-68.
97. Boyd MF, Kitchen SF. Vernal Vivax Activity in Persons Simultaneously Inoculated with Plasmodium Vivax and Plasmodium Falciparum. *Am J Trop Med Hyg*. 1938;s1-18(5):505-514. doi:10.4269/ajtmh.1938.s1-18.505.
98. Kitchen SF, Boyd MF. Simultaneous Inoculation with Plasmodium Vivax and Plasmodium Falciparum. *Am J Trop Med Hyg*. 1937;s1-17(6):855-861. doi:10.4269/ajtmh.1937.s1-17.855.
99. Mayne B, Young MD. Antagonism between Species of Malaria Parasites in Induced Mixed Infections. *Public Heal Reports*. 1938;53(30):1289. doi:10.2307/4582611.
100. Paul RE, Packer MJ, Walmsley M, Lagog M, Ranford-Cartwright LC, Paru R, Day KP. Mating patterns in malaria parasite populations of Papua New Guinea. *Science*. 1995;269(5231):1709-1711. doi:10.1126/science.7569897.
101. McKenzie FE, Killeen GF, Beier JC, Bossert WH. Seasonality, Parasite Diversity, and Local Extinctions in Plasmodium Falciparum Malaria. *Ecology*. 2001;82(10):2673-2681. doi:10.1890/0012-9658(2001)082[2673:spdale]2.0.co;2.
102. Akala HM, Watson OJ, Mitei KK, Juma DW, Verity R, Ingasia LA, Opot BH, Okoth RO, Chemwor GC, Juma JA, Mwakio EW, Brazeau N, Cheruiyot AC, Yeda RA, Maraka MN, Okello CO, Kateete DP, Managbanag JR, Andagalu B, Ogutu BR, Kamau E. Plasmodium interspecies interactions during a period of increasing prevalence of Plasmodium ovale in symptomatic individuals seeking treatment: an observational study. *The Lancet Microbe*. 2021;2(4):e141-e150. doi:10.1016/S2666-5247(21)00009-4.
103. Bruce MC, Day KP. Cross-species regulation of malaria parasitaemia in the human host. *Curr Opin Microbiol*. 2002;5(4):431-437. doi:10.1016/S1369-5274(02)00348-X.
104. Bruce MC, Donnelly CA, Alpers MP, Galinski MR, Barnwell JW, Walliker D, Day KP. Cross-species interactions between malaria parasites in humans. *Science (80-)*. 2000;287(5454):845-848. doi:10.1126/science.287.5454.845.
105. Kwiatkowski D. Febrile temperatures can synchronize the growth of Plasmodium falciparum in vitro. *J Exp Med*. 1989;169(1):357-361. doi:10.1084/jem.169.1.357.
106. Kwiatkowski D, Nowak M. Periodic and chaotic host-parasite interactions in human malaria. *Proc Natl Acad Sci U S A*. 1991;88(12):5111-5113. doi:10.1073/pnas.88.12.5111.
107. Read AF, Taylor LH. The ecology of genetically diverse infections. *Science*. 2001;292(5519):1099-1102. doi:10.1126/science.1059410.
108. Mayxay M, Pukrittayakamee S, Chotivanich K, Imwong M, Looareesuwan S, White NJ. Identification of cryptic coinfection with Plasmodium falciparum in patients presenting with vivax malaria. *Am J Trop Med Hyg*. 2001;65(5):588-592. doi:10.4269/ajtmh.2001.65.588.
109. Dalrymple U, Cameron E, Arambepola R, Battle KE, Chestnutt EG, Keddie SH, Twohig KA, Pfeffer DA, Gibson HS, Weiss DJ, Bhatt S, Gething PW. The contribution of non-malarial febrile illness co-infections to Plasmodium falciparum case counts in health facilities in sub-Saharan Africa. *Malar J*. 2019;18(1):195. doi:10.1186/s12936-019-2830-

y.
110. White NJ. The role of anti-malarial drugs in eliminating malaria. *Malar J*. 2008;7(S1):S8. doi:10.1186/1475-2875-7-S1-S8.
111. Bousema JT, Drakeley CJ, Mens PF, Arens T, Houben R, Omar SA, Gouagna LC, Schallig H, Sauerwein RW. *Increased Plasmodium Falciparum Gametocyte Production in Mixed Infections with P. Malariae*.; 2008. www.controlled-trials.com/ISRCTN31291803. Accessed July 8, 2021.
112. Vaccines T malERA CG on. A Research Agenda for Malaria Eradication: Vaccines. *PLoS Med*. 2011;8(1):e1000398. doi:10.1371/journal.pmed.1000398.
113. Betson M, Sousa-Figueiredo JC, Atuhaire A, Arinaitwe M, Adriko M, Mwesigwa G, Nabonge J, Kabatereine NB, Sutherland CJ, Stothard JR. Detection of persistent Plasmodium spp. infections in Ugandan children after artemether-lumefantrine treatment. *Parasitology*. 2014;141(14):1880-1890. doi:10.1017/S003118201400033X.
114. Dinko B, Oguike MC, Larbi JA, Bousema T, Sutherland CJ. Persistent detection of Plasmodium falciparum, P. malariae, P. ovale curtisi and P. ovale wallikeri after ACT treatment of asymptomatic Ghanaian school-children. *Int J Parasitol Drugs drug Resist*. 2013;3:45-50. doi:10.1016/j.ijpddr.2013.01.001.
115. Burkot TR, Graves PM. The value of vector-based estimates of malaria transmission. *Ann Trop Med Parasitol*. 1995;89(2):125-134. doi:10.1080/00034983.1995.11812943.
116. Das S, Muleba M, Stevenson JC, Pringle JC, Norris DE. Beyond the entomological inoculation rate: characterizing multiple blood feeding behavior and Plasmodium falciparum multiplicity of infection in Anopheles mosquitoes in northern Zambia. *Parasit Vectors*. 2017;10(1):45. doi:10.1186/s13071-017-1993-z.
117. Christie M. The Statistical Treatment of the Sporozoite Rate in Anopheline Mosquitoes. *Ann Trop Med Parasitol*. 1956;50(4):350-354. doi:10.1080/00034983.1956.11685776.
118. Benedict M. *Methods in Anopheles Research*.; 2007. https://www.beiresources.org/Publications/MethodsinAnophelesResearch.aspx%0A.
119. Griffin P, Pasay C, Elliott S, Sekuloski S, Sikulu M, Hugo L, Khoury D, Cromer D, Davenport M, Sattabongkot J, Ivinson K, Ockenhouse C, McCarthy J. Safety and Reproducibility of a Clinical Trial System Using Induced Blood Stage Plasmodium vivax Infection and Its Potential as a Model to Evaluate Malaria Transmission. *PLoS Negl Trop Dis*. 2016;10(12):e0005139. doi:10.1371/journal.pntd.0005139.
120. Mori T, Hirai M, Mita T. See-through observation of malaria parasite behaviors in the mosquito vector. *Sci Rep*. 2019;9(1):1768. doi:10.1038/s41598-019-38529-3.
121. Sorosjinda-Nunthawarasilp P, Bhumiratana A. Ecotope-based entomological surveillance and molecular xenomonitoring of multidrug resistant malaria parasites in anopheles vectors. *Interdiscip Perspect Infect Dis*. 2014;2014:969531. doi:10.1155/2014/969531.
122. De Niz M, Kehrer J, Brancucci NMB, Moalli F, Reynaud EG, Stein J V, Frischknecht F. 3D imaging of undissected optically cleared Anopheles stephensi mosquitoes and midguts infected with Plasmodium parasites. *PLoS One*. 2020;15(9):e0238134. doi:10.1371/journal.pone.0238134.
123. Wirtz RA, Sattabongkot J, Hall T, Burkot TR, Rosenberg R. Development and evaluation of an enzyme-linked immunosorbent assay for Plasmodium vivax-VK247 sporozoites. *J Med Entomol*. 1992;29(5):854-857. doi:10.1093/jmedent/29.5.854.
124. Burkot TR, Williams JL, Schneider I. Identification of Plasmodium falciparum-infected mosquitoes by a double antibody enzyme-linked immunosorbent assay. *Am J Trop Med*

Hyg. 1984;33(5):783-788. doi:10.4269/ajtmh.1984.33.783.
125. Wirtz RA, Burkot TR, Andre RG, Rosenberg R, Collins WE, Roberts DR. Identification of Plasmodium vivax sporozoites in mosquitoes using an enzyme-linked immunosorbent assay. *Am J Trop Med Hyg*. 1985;34(6):1048-1054. doi:10.4269/ajtmh.1985.34.1048.
126. Durnez L, Van Bortel W, Denis L, Roelants P, Veracx A, Trung HD, Sochantha T, Coosemans M. False positive circumsporozoite protein ELISA: a challenge for the estimation of the entomological inoculation rate of malaria and for vector incrimination. *Malar J*. 2011;10:195. doi:10.1186/1475-2875-10-195.
127. Beier JC, Perkins P V, Koros JK, Onyango FK, Gargan TP, Wirtz RA, Koech DK, Roberts CR. Malaria sporozoite detection by dissection and ELISA to assess infectivity of afrotropical Anopheles (Diptera: Culicidae). *J Med Entomol*. 1990;27(3):377-384. doi:10.1093/jmedent/27.3.377.
128. Koekemoer LL, Rankoe EM, La Grange JP, Govere J, Coetzee M. False detection of Plasmodium falciparum sporozoites in Anopheles marshallii group mosquitoes. *J Am Mosq Control Assoc*. 2001;17(3):160-165.
129. Somboon P, Morakote N, Koottathep S, Trisanarom U. Detection of sporozoites of Plasmodium vivax and Plasmodium falciparum in mosquitoes by ELISA: false positivity associated with bovine and swine blood. *Trans R Soc Trop Med Hyg*. 1993;87(3):322-324. doi:10.1016/0035-9203(93)90148-j.
130. Graumans W, Tadesse FG, Andolina C, van Gemert G-J, Teelen K, Lanke K, Gadisa E, Yewhalaw D, van de Vegte-Bolmer M, Siebelink-Stoter R, Reuling I, Sauerwein R, Bousema T. Semi-high-throughput detection of Plasmodium falciparum and Plasmodium vivax oocysts in mosquitoes using bead-beating followed by circumsporozoite ELISA and quantitative PCR. *Malar J*. 2017;16(1):356. doi:10.1186/s12936-017-2011-9.
131. Póvoa MM, Machado RL, Segura MN, Vianna GM, Vasconcelos AS, Conn JE. Infectivity of malaria vector mosquitoes: correlation of positivity between ELISA and PCR-ELISA tests. *Trans R Soc Trop Med Hyg*. 2000;94(1):106-107. doi:10.1016/s0035-9203(00)90457-7.
132. Beier JC, Perkins P V, Wirtz RA, Whitmire RE, Mugambi M, Hockmeyer WT. Field evaluation of an enzyme-linked immunosorbent assay (ELISA) for Plasmodium falciparum sporozoite detection in anopheline mosquitoes from Kenya. *Am J Trop Med Hyg*. 1987;36(3):459-468. doi:10.4269/ajtmh.1987.36.459.
133. Tassanakajon A, Boonsaeng V, Wilairat P, Panyim S. Polymerase chain reaction detection of Plasmodium falciparum in mosquitoes. *Trans R Soc Trop Med Hyg*. 1993;87(3). doi:10.1016/0035-9203(93)90124-9.
134. Hendershot AL. A Comparison of PCR and ELISA Methods to Detect Different Stages of Plasmodium Vivax in Anopheles Arabiensis. doi:10.21203/rs.3.rs-589001/v1.
135. Foley DH, Harrison G, Murphy JR, Dowler M, Rueda LM, Wilkerson RC. Mosquito bisection as a variable in estimates of PCR-derived malaria sporozoite rates. *Malar J*. 2012;11:145. doi:10.1186/1475-2875-11-145.
136. Echeverry DF, Deason NA, Makuru V, Davidson J, Xiao H, Niedbalski J, Yu X, Stevenson JC, Bugoro H, Aparaimo A, Reuben H, Cooper R, Burkot TR, Russell TL, Collins FH, Lobo NF. Fast and robust single PCR for Plasmodium sporozoite detection in mosquitoes using the cytochrome oxidase I gene. *Malar J*. 2017;16(1):230. doi:10.1186/s12936-017-1881-1.
137. Sinka ME, Bangs MJ, Manguin S, Rubio-Palis Y, Chareonviriyaphap T, Coetzee M,

Mbogo CM, Hemingway J, Patil AP, Temperley WH, Gething PW, Kabaria CW, Burkot TR, Harbach RE, Hay SI. A global map of dominant malaria vectors. *Parasit Vectors*. 2012;5:69. doi:10.1186/1756-3305-5-69.
138. Kiszewski A, Mellinger A, Spielman A, Malaney P, Sachs SE, Sachs J. A global index representing the stability of malaria transmission. *Am J Trop Med Hyg*. 2004;70(5):486-498. doi:10.4269/ajtmh.2004.70.486.
139. Cox FE. History of the discovery of the malaria parasites and their vectors. *Parasit Vectors*. 2010;3(1):5. doi:10.1186/1756-3305-3-5.
140. Grassi G, Bignami A, Bastianelli G. Ulteriori ricerche sul ciclo dei parassiti malarici umani nel corpo del zanzarone. 1899.
141. Grassi B. *Studio Di Uno Zoologo Sulla Malaria*.; 1900.
142. Centers for Disease Control and Prevention. CDC - Malaria - FAQs. https://www.cdc.gov/malaria/about/faqs.html. Published 2021. Accessed July 12, 2021.
143. Sinka ME, Bangs MJ, Manguin S, Coetzee M, Mbogo CM, Hemingway J, Patil AP, Temperley WH, Gething PW, Kabaria CW, Okara RM, Van Boeckel T, Godfray HCJ, Harbach RE, Hay SI. The dominant Anopheles vectors of human malaria in Africa, Europe and the Middle East: occurrence data, distribution maps and bionomic précis. *Parasit Vectors*. 2010;3(1):117. doi:10.1186/1756-3305-3-117.
144. Clements AN. *The Biology of Mosquitoes: Development, Nutrition and Reproduction*. CABI Publishing; 1992.
145. Hunt R, Coetzee M, Fettene M. The Anopheles gambiae complex: a new species from Ethiopia. *Trans R Soc Trop Med Hyg*. 1998;92(2). doi:10.1016/S0035-9203(98)90761-1.
146. Coluzzi M, Sabatini A, Petrarca V, Di Deco M. Chromosomal differentiation and adaptation to human environments in the Anopheles gambiae complex. *Trans R Soc Trop Med Hyg*. 1979;73(5). doi:10.1016/0035-9203(79)90036-1.
147. Paine MJI, Hemingway J, Stevenson BJ, Ranson H, Egyir-Yawson A, Muller P, Mitchell SN, Donnelly MJ, Field SG, Wilding CS. Identification and validation of a gene causing cross-resistance between insecticide classes in Anopheles gambiae from Ghana. *Proc Natl Acad Sci*. 2012. doi:10.1073/pnas.1203452109.
148. Miles A, Harding NJ, Bottà G, Clarkson CS, Antão T, Kozak K, Schrider DR, Kern AD, Redmond S, Sharakhov I, Pearson RD, Bergey C, Fontaine MC, Donnelly MJ, Lawniczak MKN, Ayala D, Besansky NJ, Burt A, Caputo B, Torre A Della, Godfray HCJ, Hahn MW, Midega J, Neafsey DE, O'Loughlin S, Pinto J, Riehle MM, Vernick KD, Weetman D, Wilding CS, White BJ, Troco AD, Diabaté A, Costantini C, Rohatgi KR, Elissa N, Coulibaly B, Dinis J, Mbogo C, Bejon P, Mawejje HD, Stalker J, Rockett K, Drury E, Mead D, Jeffreys A, Hubbart C, Rowlands K, Isaacs AT, Jyothi D, Malangone C, Vauterin P, Jeffery B, Wright I, Hart L, Kluczyński K, Cornelius V, Macinnis B, Henrichs C, Giacomantonio R, Kwiatkowski DP. Genetic diversity of the African malaria vector anopheles gambiae. *Nature*. 2017;552. doi:10.1038/nature24995.
149. Lawniczak MKN, Emrich SJ, Holloway AK, Regier AP, Olson M, White B, Redmond S, Fulton L, Appelbaum E, Godfrey J, Farmer C, Chinwalla A, Yang SP, Minx P, Nelson J, Kyung K, Walenz BP, Garcia-Hernandez E, Aguiar M, Viswanathan LD, Rogers YH, Strausberg RL, Saski CA, Lawson D, Collins FH, Kafatos FC, Christophides GK, Clifton SW, Kirkness EF, Besansky NJ. Widespread divergence between incipient Anopheles gambiae species revealed by whole genome sequences. *Science (80-)*. 2010. doi:10.1126/science.1195755.

150. Lee Y, Cornel AJ, Meneses CR, Fofana A, Andrianarivo AG, Mcabee RD, Fondjo E, Traoré SF, Lanzaro GC. Ecological and genetic relationships of the Forest-M form among chromosomal and molecular forms of the malaria vector Anopheles gambiae sensu stricto. *Malar J*. 2009. doi:10.1186/1475-2875-8-75.
151. Lee Y, Collier TC, Sanford MR, Marsden CD, Fofana A, Cornel AJ, Lanzaro GC. Chromosome Inversions, Genomic Differentiation and Speciation in the African Malaria Mosquito Anopheles gambiae. *PLoS One*. 2013. doi:10.1371/journal.pone.0057887.
152. Favia G, Lanfrancotti A, Spanos L, Sidén-Kiamos I, Louis C. Molecular characterization of ribosomal DNA polymorphisms discriminating among chromosomal forms of Anopheles gambiae s.s. *Insect Mol Biol*. 2001. doi:10.1046/j.1365-2583.2001.00236.x.
153. Lehmann T, Diabate A. The molecular forms of Anopheles gambiae: A phenotypic perspective. *Infect Genet Evol*. 2008. doi:10.1016/j.meegid.2008.06.003.
154. White BJ, Lawniczak MKN, Cheng C, Coulibaly MB, Wilson MD, Sagnon N, Costantini C, Simard F, Christophides GK, Besansky NJ. Adaptive divergence between incipient species of Anopheles gambiae increases resistance to Plasmodium. *Proc Natl Acad Sci*. 2011. doi:10.1073/pnas.1013648108.
155. Coetzee M, Fontenille D. Advances in the study of Anopheles funestus, a major vector of malaria in Africa. *Insect Biochem Mol Biol*. 2004;34(7):599-605. doi:10.1016/J.IBMB.2004.03.012.
156. Coetzee M, Koekemoer LL. Molecular Systematics and Insecticide Resistance in the Major African Malaria Vector *Anopheles funestus*. *Annu Rev Entomol*. 2013;58(1):393-412. doi:10.1146/annurev-ento-120811-153628.
157. Guelbeogo WM, Sagnon N, Liu F, Besansky NJ, Costantini C. Behavioural divergence of sympatric Anopheles funestus populations in Burkina Faso. *Malar J*. 2014;13(1):65. doi:10.1186/1475-2875-13-65.
158. Dabiré KR, Baldet T, Diabaté A, Dia I, Costantini C, Cohuet A, Guiguemdé TR, Fontenille D. *Anopheles funestus* (Diptera: Culicidae) in a Humid Savannah Area of Western Burkina Faso: Bionomics, Insecticide Resistance Status, and Role in Malaria Transmission. *J Med Entomol*. 2007;44(6):990-997. doi:10.1093/jmedent/44.6.990.
159. Soma DD, Zogo BM, Somé A, Tchiekoi BN, Hien DF de S, Pooda HS, Coulibaly S, Gnambani JE, Ouari A, Mouline K, Dahounto A, Ouédraogo GA, Fournet F, Koffi AA, Pennetier C, Moiroux N, Dabiré RK. Anopheles bionomics, insecticide resistance and malaria transmission in southwest Burkina Faso: A pre-intervention study. *PLoS One*. 2020;15(8):e0236920. doi:10.1371/journal.pone.0236920.
160. Tourre YM, Vignolles C, Viel C, Mounier F. Climate impact on malaria in northern Burkina Faso. *Geospat Health*. 2017;12(2). doi:10.4081/gh.2017.600.
161. Teklehaimanot HD, Lipsitch M, Teklehaimanot A, Schwartz J. Weather-based prediction of Plasmodium falciparum malaria in epidemic-prone regions of Ethiopia I. Patterns of lagged weather effects reflect biological mechanisms. *Malar J*. 2004;3:41. doi:10.1186/1475-2875-3-41.
162. Ouedraogo B, Inoue Y, Kambiré A, Sallah K, Dieng S, Tine R, Rouamba T, Herbreteau V, Sawadogo Y, Ouedraogo LSLW, Yaka P, Ouedraogo EK, Dufour J-C, Gaudart J. Spatio-temporal dynamic of malaria in Ouagadougou, Burkina Faso, 2011–2015. *Malar J*. 2018;17(1):138. doi:10.1186/s12936-018-2280-y.
163. Abeku TA, De Vlas SJ, Borsboom GJJM, Tadege A, Gebreyesus Y, Gebreyohannes H, Alamirew D, Seifu A, Nagelkerke NJD, Habbema JDF. Effects of meteorological factors

on epidemic malaria in Ethiopia: a statistical modelling approach based on theoretical reasoning. *Parasitology*. 2004;128(Pt 6):585-593. doi:10.1017/s0031182004005013.
164. Dao A, Yaro AS, Diallo M, Timbiné S, Huestis DL, Kassogué Y, Traoré AI, Sanogo ZL, Samaké D, Lehmann T. Signatures of aestivation and migration in Sahelian malaria mosquito populations. *Nature*. 2014;516(7531):387-390. doi:10.1038/nature13987.
165. Yaro AS, Traoré AI, Huestis DL, Adamou A, Timbiné S, Kassogué Y, Diallo M, Dao A, Traoré SF, Lehmann T. Dry season reproductive depression of Anopheles gambiae in the Sahel. *J Insect Physiol*. 2012;58(8):1050-1059. doi:10.1016/j.jinsphys.2012.04.002.
166. Christiansen-Jucht C, Parham PE, Saddler A, Koella JC, Basáñez M-G. Temperature during larval development and adult maintenance influences the survival of Anopheles gambiae s.s. *Parasit Vectors*. 2014;7(1):489. doi:10.1186/s13071-014-0489-3.
167. Dao A, Adamou A, Yaro AS, Maïga HM, Kassogue Y, Traoré SF, Lehmann T. Assessment of alternative mating strategies in Anopheles gambiae: Does mating occur indoors? *J Med Entomol*. 2008;45(4):643-652. doi:10.1603/0022-2585(2008)45[643:aoamsi]2.0.co;2.
168. Clements AN. *The Biology of Mosquitoes: Sensory Reception and Behavior*. London, UK: CABI Publishing; 1999.
169. Thailayil J, Gabrieli P, Caputo B, Bascuñán P, South A, Diabate A, Dabire R, della Torre A, Catteruccia F. Analysis of natural female post-mating responses of Anopheles gambiae and Anopheles coluzzii unravels similarities and differences in their reproductive ecology. *Sci Rep*. 2018;8(1):6594. doi:10.1038/s41598-018-24923-w.
170. Scaraffia PY. *Disruption of Mosquito Blood Meal Protein Metabolism*. Elsevier Inc.; 2016. doi:10.1016/B978-0-12-800246-9.00012-0.
171. Clements AN, Boocock MR. Ovarian development in mosquitoes: stages of growth and arrest, and follicular resorption. *Physiol Entomol*. 1984;9(1):1-8. doi:10.1111/j.1365-3032.1984.tb00675.x.
172. Troy S, Anderson WA, Spielman A. Lipid content of maturing ovaries of Aedes aegypti mosquitoes. *Comp Biochem Physiol Part B Comp Biochem*. 1975;50(3):457-461. doi:10.1016/0305-0491(75)90258-8.
173. Hugo LE, Quick-miles S, Kay BH, Ryan PA. Evaluations of Mosquito Age Grading Techniques Based on Morphological Changes. *J Med Entomol*. 2008;45(3):353-369. doi:10.1093/jmedent/45.3.353.
174. Williams J, Pinto J, Macdonald M, O'sullivan J. *Training Manual on Malaria Entomology For Entomology and Vector Control Technicians (Basic Level) Integrated Vector Management of Malaria and Other Infectious Diseases*. www.rti.org. Accessed July 14, 2021.
175. Smallegange RC, van Gemert G-J, van de Vegte-Bolmer M, Gezan S, Takken W, Sauerwein RW, Logan JG. Malaria Infected Mosquitoes Express Enhanced Attraction to Human Odor. Dimopoulos G, ed. *PLoS One*. 2013;8(5):e63602. doi:10.1371/journal.pone.0063602.
176. Montell C, Zwiebel LJ. *Mosquito Sensory Systems*. Vol 51. 1st ed. Elsevier Ltd.; 2016. doi:10.1016/bs.aiip.2016.04.007.
177. van Loon JJA, Smallegange RC, Bukovinszkiné-Kiss G, Jacobs F, De Rijk M, Mukabana WR, Verhulst NO, Menger DJ, Takken W. Mosquito Attraction: Crucial Role of Carbon Dioxide in Formulation of a Five-Component Blend of Human-Derived Volatiles. *J Chem Ecol*. 2015;41(6):567-573. doi:10.1007/s10886-015-0587-5.

178. Wright RH, Kellogg FE. Host Size as a Factor in the Attraction of Malaria Mosquitoes. *Nature*. 1964;202(4929):321-322. doi:10.1038/202321a0.
179. Verhulst NO, Weldegergis BT, Menger D, Takken W. Attractiveness of volatiles from different body parts to the malaria mosquito Anopheles coluzzii is affected by deodorant compounds. *Sci Rep*. 2016;6:27141. doi:10.1038/srep27141.
180. Kline D. Olfactory responses and field attraction of mosquitoes to volatiles from limburger cheese and human foot odor. *J Vector Ccology*. 1998;23(2):186-194.
181. Torre A Della, Arca B, Favia G, Petrarca V, Coluzzi M. The role of research in molecular entomology in the fight against malaria vectors. *Parassitologia*. 2008;50(1-2):137-140.
182. Lombardo F, Lanfrancotti A, Mestres-Simón M, Rizzo C, Coluzzi M, Arcà B. At the interface between parasite and host: The salivary glands of the African malaria vector Anopheles gambiae. *Parassitologia*. 2006;48(4):573-580.
183. Kalume DE, Okulate M, Zhong J, Reddy R, Suresh S, Deshpande N, Kumar N, Pandey A. A proteomic analysis of salivary glands of femaleAnopheles gambiae mosquito. *Proteomics*. 2005;5(14):3765-3777. doi:10.1002/pmic.200401210.
184. Vaughan JA, Scheller LF, Wirtz RA, Azad AF. Infectivity of *Plasmodium berghei* Sporozoites Delivered by Intravenous Inoculation versus Mosquito Bite: Implications for Sporozoite Vaccine Trials. Kaufmann SHE, ed. *Infect Immun*. 1999;67(8):4285-4289. doi:10.1128/IAI.67.8.4285-4289.1999.
185. Da Rocha ACVM, Braga ÉM, Araújo MSS, Franklin BS, Pimenta PFP. Effect of the Aedes fluviatilis saliva on the development of Plasmodium gallinaceum infection in Gallus (gallus) domesticus. *Mem Inst Oswaldo Cruz*. 2004;99(7):709-715. doi:10.1590/s0074-02762004000700008.
186. Leitner WW, Bergmann-Leitner ES, Angov E. Comparison of Plasmodium berghei challenge models for the evaluation of pre-erythrocytic malaria vaccines and their effect on perceived vaccine efficacy. *Malar J*. 2010;9:145. doi:10.1186/1475-2875-9-145.
187. Kebaier C, Voza T, Vanderberg J. Neither mosquito saliva nor immunity to saliva has a detectable effect on the infectivity of Plasmodium sporozoites injected into mice. *Infect Immun*. 2010;78(1):545-551. doi:10.1128/IAI.00807-09.
188. Conteh S, Chattopadhyay R, Anderson C, Hoffman SL. Plasmodium yoelii-infected A. stephensi inefficiently transmit malaria compared to intravenous route. *PLoS One*. 2010;5(1):e8947. doi:10.1371/journal.pone.0008947.
189. Srichaikul T, Archararit N, Siriasawakul T, Viriyapanich T. Histamine changes in Plasmodium falciparum malaria. *Trans R Soc Trop Med Hyg*. 1976;70(1):36-38. doi:10.1016/0035-9203(76)90004-3.
190. Bhattacharya U, Roy S, Kar PK, Sarangi B, Lahiri SC. Histamine & kinin system in experimental malaria. *Indian J Med Res*. 1988;88:558-563. http://www.ncbi.nlm.nih.gov/pubmed/3072298. Accessed July 15, 2021.
191. Mecheri S. Contribution of allergic inflammatory response to the pathogenesis of malaria disease. *Biochim Biophys Acta - Mol Basis Dis*. 2012;1822(1):49-56. doi:10.1016/J.BBADIS.2011.02.005.
192. Perlmann P, Perlmann H, ElGhazali G, Blomberg MT. IgE and tumor necrosis factor in malaria infection. *Immunol Lett*. 1999;65(1-2):29-33. doi:10.1016/S0165-2478(98)00120-5.
193. Baptista JL, Vanham G, Wery M, Van Marck E. Cytokine levels during mild and cerebral falciparum malaria in children living in a mesoendemic area. *Trop Med Int Heal*.

1997;2(7):673-679. doi:10.1046/j.1365-3156.1997.d01-355.x.
194. Kossodo S, Monso C, Juillard P, Velu T, Goldman M, Grau GE. Interleukin-10 modulates susceptibility in experimental cerebral malaria. *Immunology*. 1997;91(4):536-540. doi:10.1046/j.1365-2567.1997.00290.x.
195. Saeftel M, Krueger A, Arriens S, Heussler V, Racz P, Fleischer B, Brombacher F, Hoerauf A. Mice Deficient in Interleukin-4 (IL-4) or IL-4 Receptor α Have Higher Resistance to Sporozoite Infection with *Plasmodium berghei* (ANKA) than Do Naive Wild-Type Mice. *Infect Immun*. 2004;72(1):322-331. doi:10.1128/IAI.72.1.322-331.2004.
196. Amani V, Vigário AM, Belnoue E, Marussig M, Fonseca L, Mazier D, Rénia L. Involvement of IFN-γ receptor-mediated signaling in pathology and anti-malarial immunity induced by Plasmodium berghei infection. *Eur J Immunol*. 2000;30(6):1646-1655. doi:10.1002/1521-4141(200006)30:6<1646::AID-IMMU1646>3.0.CO;2-0.
197. Githeko AK, Adungo NI, Karanja DM, Hawley WA, Vulule JM, Seroney IK, Ofulla AVO, Atieli FK, Ondijo SO, Genga IO, Odada PK, Situbi PA, Oloo JA. Some observations on the biting behavior of Anopheles gambiae s.s., Anopheles arabiensis, and Anopheles funestus and their implications for malaria control. *Exp Parasitol*. 1996;82(3):306-315. doi:10.1006/expr.1996.0038.
198. Akogbéto MC, Salako AS, Dagnon F, Aïkpon R, Kouletio M, Sovi A, Sezonlin M. Blood feeding behaviour comparison and contribution of Anopheles coluzzii and Anopheles gambiae, two sibling species living in sympatry, to malaria transmission in Alibori and Donga region, northern Benin, West Africa. *Malar J*. 2018;17(1):307. doi:10.1186/s12936-018-2452-9.
199. Costantini C, Sagnon N, Torre A Della, Diallo M, Brady J, Gibson G, Coluzzi M. Odor-mediated host preferences of West African mosquitoes, with particular reference to malaria vectors. *Am J Trop Med Hyg*. 1998;58(1):56-63. doi:10.4269/ajtmh.1998.58.56.
200. Githeko AK, Service MW, Mbogo CM, Atieli FK, Juma FO. Origin of blood meals in indoor and outdoor resting malaria vectors in western Kenya. *Acta Trop*. 1994;58(3-4):307-316. doi:10.1016/0001-706x(94)90024-8.
201. Ekoko WE, Awono-Ambene P, Bigoga J, Mandeng S, Piameu M, Nvondo N, Toto J-C, Nwane P, Patchoke S, Mbakop LR, Binyang JA, Donelly M, Kleinschmidt I, Knox T, Mbida AM, Dongmo A, Fondjo E, Mnzava A, Etang J. Patterns of anopheline feeding/resting behaviour and Plasmodium infections in North Cameroon, 2011–2014: implications for malaria control. *Parasit Vectors*. 2019;12(1):297. doi:10.1186/s13071-019-3552-2.
202. Ototo EN, Mbugi JP, Wanjala CL, Zhou G, Githeko AK, Yan G. Surveillance of malaria vector population density and biting behaviour in western Kenya. *Malar J*. 2015;14:244. doi:10.1186/s12936-015-0763-7.
203. Highton RB, Bryan JH, Boreham PFL, Chandler JA. Studies on the sibling species *Anopheles gambiae* Giles and *Anopheles arabiensis* Patton (Diptera: Culicidae) in the Kisumu area, Kenya. *Bull Entomol Res*. 1979;69(1):43-53. doi:10.1017/S0007485300017879.
204. Mnzava AE, Rwegoshora RT, Wilkes TJ, Tanner M, Curtis CF. Anopheles arabiensis and An. gambiae chromosomal inversion polymorphism, feeding and resting behaviour in relation to insecticide house-spraying in Tanzania. *Med Vet Entomol*. 1995;9(3):316-324. doi:10.1111/j.1365-2915.1995.tb00140.x.
205. Faye O, Konate L, Mouchet J, Fontenille D, Sy N, Hebrard G, Herve JP. Indoor resting by

outdoor biting females of Anopheles gambiae complex (Diptera:Culicidae) in the Sahel of northern Senegal. *J Med Entomol*. 1997;34(3):285-289. doi:10.1093/jmedent/34.3.285.
206. Bockarie MJ, Service MW, Barnish G, Maude GH, Greenwood BM. Malaria in a rural area of Sierra Leone. III. Vector ecology and disease transmission. *Ann Trop Med Parasitol*. 1994;88(3):251-262. doi:10.1080/00034983.1994.11812865.
207. Githeko A, Mbogo C, Parassitologia FA-, 1996 undefined. Resting behaviour, ecology and genetics of malaria vectors in large scale agricultural areas of Western Kenya. *europepmc.org*. https://europepmc.org/article/med/9257337. Accessed July 16, 2021.
208. Fontenille D, Lepers JP, Campbell GH, Coluzzi M, Rakotoarivony I, Coulanges P. Malaria transmission and vector biology in Manarintsoa, high plateaux of Madagascar. *Am J Trop Med Hyg*. 1990;43(2):107-115. doi:10.4269/ajtmh.1990.43.107.
209. Rajaonarivelo V, Le Goff G, Cot M, Brutus L. [Anopheles and malaria transmission in Ambohimena, a village in the Occidental fringe of Madagascar Highlands]. *Parasite*. 2004;11(1):75-82. doi:10.1051/parasite/200411175.
210. Clarke J, Pradhan G, … GJ-J of M, 1980 undefined. Assessment of the Grain Store as an Unbaited Outdoor Shelter for Mosquitoes of the Anopheles Gambiae Complex and Anopheles Funestus (Diptera: Culicidae) At. *academic.oup.com*. https://academic.oup.com/jme/article-abstract/17/1/100/2219712. Accessed July 16, 2021.
211. Mahande A, Mosha F, Mahande J, Kweka E. Feeding and resting behaviour of malaria vector, Anopheles arabiensis with reference to zooprophylaxis. *Malar J*. 2007;6:100. doi:10.1186/1475-2875-6-100.
212. Tirados I, Costantini C, Gibson G, Torr SJ. Blood-feeding behaviour of the malarial mosquito Anopheles arabiensis: implications for vector control. *Med Vet Entomol*. 2006;20(4):425-437. doi:10.1111/j.1365-2915.2006.652.x.
213. Tedrow RE, Rakotomanga T, Nepomichene T, Howes RE, Ratovonjato J, Ratsimbasoa AC, Svenson GJ, Zimmerman PA. Anopheles mosquito surveillance in Madagascar reveals multiple blood feeding behavior and Plasmodium infection. Milon G, ed. *PLoS Negl Trop Dis*. 2019;13(7):e0007176. doi:10.1371/journal.pntd.0007176.
214. Boreham PF, Lenahan JK, Boulzaguet R, Storey J, Ashkar TS, Nambiar R, Matsushima T. Studies on multiple feeding by Anopheles gambiae s.l. in a Sudan savanna area of north Nigeria. *Trans R Soc Trop Med Hyg*. 1979;73(4):418-423. doi:10.1016/0035-9203(79)90167-6.
215. Amerasinghe PH, Amerasinghe FP. Multiple host feeding in field populations of Anopheles culicifacies and An. subpictus in Sri Lanka. *Med Vet Entomol*. 1999;13(2):124-131. doi:10.1046/j.1365-2915.1999.00160.x.
216. Klowden MJ, Briegel H. Mosquito gonotrophic cycle and multiple feeding potential: contrasts between Anopheles and Aedes (Diptera: Culicidae). *J Med Entomol*. 1994;31(4):618-622. doi:10.1093/jmedent/31.4.618.
217. Shaw WR, Holmdahl IE, Itoe MA, Werling K, Marquette M, Paton DG, Singh N, Buckee CO, Childs LM, Catteruccia F. Multiple blood feeding in mosquitoes shortens the Plasmodium falciparum incubation period and increases malaria transmission potential. Billker O, ed. *PLOS Pathog*. 2020;16(12):e1009131. doi:10.1371/journal.ppat.1009131.
218. Tedrow RE, Zimmerman PA, Abbott KC. Multiple Blood Feeding: A Force Multiplier for Transmission. *Trends Parasitol*. 2019;35(12):949-952. doi:10.1016/j.pt.2019.08.004.
219. Dambach P, Schleicher M, Korir P, Ouedraogo S, Dambach J, Sié A, Dambach M, Becker N. Nightly Biting Cycles of Anopheles Species in Rural Northwestern Burkina Faso. *J*

Med Entomol. 2018;55(4):1027-1034. doi:10.1093/jme/tjy043.
220. Reddy MR, Overgaard HJ, Abaga S, Reddy VP, Caccone A, Kiszewski AE, Slotman MA. Outdoor host seeking behaviour of Anopheles gambiae mosquitoes following initiation of malaria vector control on Bioko Island, Equatorial Guinea. *Malar J*. 2011;10(184). doi:10.1186/1475-2875-10-184.
221. Guelbéogo WM, Gonçalves BP, Grignard L, Bradley J, Serme SS, Hellewell J, Lanke K, Zongo S, Sepúlveda N, Soulama I, Wangrawa DW, Yakob L, Sagnon N, Bousema T, Drakeley C. Variation in natural exposure to anopheles mosquitoes and its effects on malaria transmission. *Elife*. 2018;7:e32625. doi:10.7554/eLife.32625.
222. Degefa T, Yewhalaw D, Zhou G, Lee M, Atieli H, Githeko AK, Yan G. Indoor and outdoor malaria vector surveillance in western Kenya: implications for better understanding of residual transmission. *Malar J*. 2017;16(1):443. doi:10.1186/s12936-017-2098-z.
223. Sande S, Zimba M, Chinwada P, Masendu HT, Makuwaza A. Biting behaviour of anopheles funestus populations in Mutare and Mutasa districts, Manicaland province, Zimbabwe: Implications for the malaria control programme. *J Vector Borne Dis*. 2016;53(2):118-126.
224. Kabbale FG, Akol AM, Kaddu JB, Onapa AW. Biting patterns and seasonality of Anopheles gambiae sensu lato and Anopheles funestus mosquitoes in Kamuli District, Uganda. *Parasit Vectors*. 2013;6:340. doi:10.1186/1756-3305-6-340.
225. Doucoure S, Thiaw O, Wotodjo AN, Bouganali C, Diagne N, Parola P, Sokhna C. Anopheles arabiensis and Anopheles funestus biting patterns in Dielmo, an area of low level exposure to malaria vectors. *Malar J*. 2020;19(1):230. doi:10.1186/s12936-020-03302-9.
226. Braack LEO, Coetzee M, Hunt RH, Biggs H, Cornel A, Gericke A. Biting Pattern and Host-Seeking Behavior of Anopheles arabiensis (Diptera: Culicidae) in Northeastern South Africa. *J Med Entomol*. 1994;31(3):333-339. doi:10.1093/jmedent/31.3.333.
227. Yé Y. *Environmental Factors and Malaria Transmission Risk: Modelling the Risk in a Holoendemic Area of Burkina Faso*.; 2008.
228. Sougoufara S, Diédhiou SM, Doucouré S, Diagne N, Sembène PM, Harry M, Trape J-F, Sokhna C, Ndiath MO. Biting by Anopheles funestus in broad daylight after use of long-lasting insecticidal nets: a new challenge to malaria elimination. *Malar J*. 2014;13(1):125. doi:10.1186/1475-2875-13-125.
229. Thomsen EK, Koimbu G, Pulford J, Jamea-Maiasa S, Ura Y, Keven JB, Siba PM, Mueller I, Hetzel MW, Reimer LJ. Mosquito Behavior Change After Distribution of Bednets Results in Decreased Protection Against Malaria Exposure. *J Infect Dis*. 2017;215(5):790-797. doi:10.1093/infdis/jiw615.
230. Carrasco D, Lefèvre T, Moiroux N, Pennetier C, Chandre F. Behavioural adaptations of mosquito vectors to insecticide control. *Curr Opin Insect Sci*. 2019;34:48-54. doi:10.1016/J.COIS.2019.03.005.
231. Shaw WR, Catteruccia F. Vector biology meets disease control: using basic research to fight vector-borne diseases. *Nat Microbiol*. 2019. doi:10.1038/s41564-018-0214-7.
232. Ross R. *The Prevention of Malaria*. 2nd ed.; 1911.
233. Cohuet A, Harris C, Robert V, Fontenille D. Evolutionary forces on Anopheles: what makes a malaria vector? *Trends Parasitol*. 2010;26(3):130-136. doi:10.1016/j.pt.2009.12.001.

234. Lefèvre T, Vantaux A, Dabiré KR, Mouline K, Cohuet A. Non-Genetic Determinants of Mosquito Competence for Malaria Parasites. Chitnis CE, ed. *PLoS Pathog*. 2013;9(6):e1003365. doi:10.1371/journal.ppat.1003365.
235. Cirimotich CM, Dong Y, Garver LS, Sim S, Dimopoulos G. Mosquito immune defenses against Plasmodium infection. *Dev Comp Immunol*. 2010. doi:10.1016/j.dci.2009.12.005.
236. Marois E. The multifaceted mosquito anti-Plasmodium response. *Curr Opin Microbiol*. 2011;14(4):429-435. doi:10.1016/J.MIB.2011.07.016.
237. Mitri C, Vernick KD. Anopheles gambiae pathogen susceptibility: the intersection of genetics, immunity and ecology. *Curr Opin Microbiol*. 2012;15(3):285-291. doi:10.1016/J.MIB.2012.04.001.
238. Harris C, Lambrechts L, Rousset F, Abate L, Nsango SE, Fontenille D, Morlais I, Cohuet A. Polymorphisms in Anopheles gambiae Immune Genes Associated with Natural Resistance to Plasmodium falciparum. Schneider DS, ed. *PLoS Pathog*. 2010;6(9):e1001112. doi:10.1371/journal.ppat.1001112.
239. Lambrechts L, Halbert J, Durand P, Gouagna LC, Koella JC. Host genotype by parasite genotype interactions underlying the resistance of anopheline mosquitoes to Plasmodium falciparum. *Malar J*. 2005;4(1):3. doi:10.1186/1475-2875-4-3.
240. Lambrechts L. Dissecting the Genetic Architecture of Host–Pathogen Specificity. Rall GF, ed. *PLoS Pathog*. 2010;6(8):e1001019. doi:10.1371/journal.ppat.1001019.
241. Murdock CC, Paaijmans KP, Cox-Foster D, Read AF, Thomas MB. Rethinking vector immunology: the role of environmental temperature in shaping resistance. *Nat Rev Microbiol*. 2012;10(12):869-876. doi:10.1038/nrmicro2900.
242. Cirimotich CM, Ramirez JL, Dimopoulos G. Native Microbiota Shape Insect Vector Competence for Human Pathogens. *Cell Host Microbe*. 2011;10(4):307-310. doi:10.1016/j.chom.2011.09.006.
243. Okech BA, Gouagna LC, Yan G, Githure JI, Beier JC. Larval habitats of Anopheles gambiae s.s. (Diptera: Culicidae) influences vector competence to Plasmodium falciparum parasites. *Malar J*. 2007;6(1):50. doi:10.1186/1475-2875-6-50.
244. Aliota MT, Chen C-C, Dagoro H, Fuchs JF, Christensen BM. Filarial Worms Reduce Plasmodium Infectivity in Mosquitoes. Dinglasan RR, ed. *PLoS Negl Trop Dis*. 2011;5(2):e963. doi:10.1371/journal.pntd.0000963.
245. Blanford S, Chan BHK, Jenkins N, Sim D, Turner RJ, Read AF, Thomas MB. Fungal pathogen reduces potential for malaria transmission. *Science*. 2005;308(5728):1638-1641. doi:10.1126/science.1108423.
246. Okech BA, Gouagna LC, Kabiru EW, Beier JC, Yan G, Githure JI. Influence of age and previous diet of Anopheles gambiae on the infectivity of natural Plasmodium falciparum gametocytes from human volunteers. *J Insect Sci*. 2004;4:33. doi:10.1093/jis/4.1.33.
247. MACDONALD G. Epidemiological basis of malaria control. *Bull World Health Organ*. 1956.
248. Dye C. *The Analysis of Parasite Transmission by Bloodsucking Insects*. Vol 37.; 1992. doi:10.1146/annurev.ento.37.1.1.
249. Bellan SE. The Importance of Age Dependent Mortality and the Extrinsic Incubation Period in Models of Mosquito-Borne Disease Transmission and Control. Cornell SJ, ed. *PLoS One*. 2010;5(4):e10165. doi:10.1371/journal.pone.0010165.
250. World Health Organization. *The Evaluation Process for Vector Control Products*.; 2017. www.who.int/%0Ahttp://apps.who.int/iris/bitstream/handle/10665/255644/WHO-HTM-

GMP-2017.13-eng.pdf?sequence=1.
251. Wilson AL, Courtenay O, Kelly-Hope LA, Scott TW, Takken W, Torr SJ, Lindsay SW. The importance of vector control for the control and elimination of vector-borne diseases. Barrera R, ed. *PLoS Negl Trop Dis*. 2020;14(1):e0007831. doi:10.1371/journal.pntd.0007831.
252. Lambert B, Sikulu-Lord MT, Mayagaya VS, Devine G, Dowell F, Churcher TS. Monitoring the Age of Mosquito Populations Using Near-Infrared Spectroscopy. *Sci Rep*. 2018;8(1):5274. doi:10.1038/s41598-018-22712-z.
253. Johnson BJ, Hugo LE, Churcher TS, Ong OTW, Devine GJ. Mosquito Age Grading and Vector-Control Programmes. *Trends Parasitol*. 2020;36(1):39-51. doi:10.1016/j.pt.2019.10.011.
254. Garrett-Jones C. Prognosis for interruption of malaria transmission through assessment of the mosquito's vectorial capacity. *Nature*. 1964. doi:10.1038/2041173a0.
255. Macdonald G. Epidemiological basis of malaria control. *Bull World Health Organ*. 1956;15(3-5):613-626. http://www.ncbi.nlm.nih.gov/pubmed/13404439. Accessed July 22, 2021.
256. Charlwood JD, Tomás EVE, Andegiorgish AK, Mihreteab S, LeClair C. "We like it wet": A comparison between dissection techniques for the assessment of parity in Anopheles arabiensis and determination of sac stage in mosquitoes alive or dead on collection. *PeerJ*. 2018. doi:10.7717/peerj.5155.
257. Sikulu M, Dowell KM, Hugo LE, Wirtz RA, Michel K, Peiris KH, Moore S, Killeen GF, Dowell FE. Evaluating RNAlater® as a preservative for using near-infrared spectroscopy to predict Anopheles gambiae age and species. *Malar J*. 2011;10(1):186. doi:10.1186/1475-2875-10-186.
258. Service MW. Estimation of the Mortalities of the Immature Stages and Adults. In: *Mosquito Ecology*. ; 1993. doi:10.1007/978-94-015-8113-4_10.
259. Romoser WS, Moll RM, Moncayo AC, Lerdthusnee K. The Occurrence and Fate of the Meconium and Meconial Peritrophic Membranes in Pupal and Adult Mosquitoes (Diptera: Culicidae). *J Med Entomol*. 2000;37(6):893-896. doi:10.1603/0022-2585-37.6.893.
260. Rosay B. Anatomical Indicators for Assessing the Age of Mosquitoes: The Teneral Adult (Diptera: Culicidae). *Ann Entomol Soc Am*. 1961;54(4):526-529. doi:10.1093/aesa/54.4.526.
261. Schlein Y, Gratz NG. Determination of the age of some anopheline mosquitos by daily growth layers of skeletal apodemes. *Bull World Health Organ*. 1973.
262. Ellison JR, Hampton EN. Age determination using the apodeme structure in adult screwworm flies (Cochliomyia hominivorax). *J Insect Physiol*. 1982;28(9):731-736. doi:10.1016/0022-1910(82)90132-9.
263. Lines JD, Wilkes TJ, Lyimo EO. Human malaria infectiousness measured by age-specific sporozoite rates in Anopheles gambiae in Tanzania. *Parasitology*. 1991;102(2):167-177. doi:10.1017/S0031182000062454.
264. Phuong M, Lau R, Ralevski F, Boggild AK. Sequence-based optimization of a quantitative real-time PCR assay for detection of Plasmodium ovale and Plasmodium malariae. *J Clin Microbiol*. 2014;52(4):1068-1073. doi:10.1128/JCM.03477-13.
265. Hofmann N, Mwingira F, Shekalaghe S, Robinson LJ, Mueller I, Felger I. Ultra-Sensitive Detection of Plasmodium falciparum by Amplification of Multi-Copy Subtelomeric Targets. *PLoS Med*. 2015;12(3):1-21. doi:10.1371/journal.pmed.1001788.

266. Bass C, Nikou D, Blagborough AM, Vontas J, Sinden RE, Williamson MS, Field LM. PCR-based detection of Plasmodium in Anopheles mosquitoes: A comparison of a new high-throughput assay with existing methods. *Malar J*. 2008. doi:10.1186/1475-2875-7-177.
267. Vavassori L, Saddler A, Müller P. Active dispersal of Aedes albopictus: a mark-release-recapture study using self-marking units. *Parasit Vectors*. 2019;12(1):583. doi:10.1186/s13071-019-3837-5.
268. Harrington LC, Françoisevermeylen F, Jones JJ, Kitthawee S, Sithiprasasna R, Edman JD, Scott TW. Age-dependent survival of the dengue vector Aedes aegypti (Diptera: Culicidae) demonstrated by simultaneous release-recapture of different age cohorts. *J Med Entomol*. 2008;45(2):307-313. doi:10.1603/0022-2585(2008)45[307:asotdv]2.0.co;2.
269. Guerra CA, Reiner RC, Perkins TA, Lindsay SW, Midega JT, Brady OJ, Barker CM, Reisen WK, Harrington LC, Takken W, Kitron U, Lloyd AL, Hay SI, Scott TW, Smith DL. A global assembly of adult female mosquito mark-release-recapture data to inform the control of mosquito-borne pathogens. *Parasit Vectors*. 2014;7(1):276. doi:10.1186/1756-3305-7-276.
270. Desena ML, Clark JM, Edman JD, Symington SB, Scott TW, Clark GG, Peters TM. Potential for aging female Aedes aegypti (Diptera: Culicidae) by gas chromatographic analysis of cuticular hydrocarbons, including a field evaluation. *J Med Entomol*. 1999. doi:10.1093/jmedent/36.6.811.
271. Desena ML, Edman JD, Clark JM, Symington SB, Scott TW. *Aedes aegypti* (Diptera: Culicidae) Age Determination by Cuticular Hydrocarbon Analysis of Female Legs. *J Med Entomol*. 1999;36(6):824-830. doi:10.1093/jmedent/36.6.824.
272. Mail TS, Chadwick J, Lehane MJ. Determining the age of adults of Stomoxys calcitrans (L.) (Diptera: Muscidae). *Bull Entomol Res*. 1983;73(3):501-525. doi:10.1017/S0007485300009123.
273. Lardeux F, Ung A, Chebret M. Spectrofluorometers Are Not Adequate for Aging <I>Aedes</I> and <I>Culex</I> (Diptera: Culicidae) Using Pteridine Fluorescence. *J Med Entomol*. 2000;37(5):769-773. doi:10.1603/0022-2585-37.5.769.
274. Gerade BB, Lee SH, Scott TW, Edman JD, Harrington LC, Kitthawee S, Jones JW, Clark JM. Field Validation of *Aedes aegypti* (Diptera: Culicidae) Age Estimation by Analysis of Cuticular Hydrocarbons. *J Med Entomol*. 2004;41(2):231-238. doi:10.1603/0022-2585-41.2.231.
275. Hugo LE, Monkman J, Dave KA, Wockner LF, Birrell GW, Norris EL, Kienzle VJ, Sikulu MT, Ryan PA, Gorman JJ, Kay BH. Proteomic Biomarkers for Ageing the Mosquito Aedes aegypti to Determine Risk of Pathogen Transmission. *PLoS One*. 2013. doi:10.1371/journal.pone.0058656.
276. Sikulu MT, Monkman J, Dave KA, Hastie ML, Dale PE, Kitching RL, Killeen GF, Kay BH, Gorman JJ, Hugo LE. Proteomic changes occurring in the malaria mosquitoes Anopheles gambiae and Anopheles stephensi during aging. *J Proteomics*. 2015. doi:10.1016/j.jprot.2015.06.008.
277. Cook PE, Sinkins SP. Transcriptional profiling of *Anopheles gambiae* mosquitoes for adult age estimation. *Insect Mol Biol*. 2010;19(6):745-751. doi:10.1111/j.1365-2583.2010.01034.x.
278. Cook PE, Hugo LE, Iturbe-Ormaetxe I, Williams CR, Chenoweth SF, Ritchie SA, Ryan

PA, Kay BH, Blows MW, O'Neill SL. The use of transcriptional profiles to predict adult mosquito age under field conditions. *Proc Natl Acad Sci U S A*. 2006;103(48):18060-18065. doi:10.1073/pnas.0604875103.
279. Cook PE, Hugo LE, Iturbe-Ormaetxe I, Williams CR, Chenoweth SF, Ritchie SA, Ryan PA, Kay BH, Blows MW, O'Neill SL. Predicting the age of mosquitoes using transcriptional profiles. *Nat Protoc*. 2007;2(11):2796-2806. doi:10.1038/nprot.2007.396.
280. Hugo LE, Kay BH, O'neill SL, Ryan PA. Investigation of Environmental Influences on a Transcriptional Assay for the Prediction of Age of Aedes aegypti (Diptera: Culicidae) Mosquitoes. *J Med Entomol*. 2010. doi:10.1603/me10030.
281. Hoffmann J, Donoughe S, Li K, Salcedo MK, Rycroft CH. A simple developmental model recapitulates complex insect wing venation patterns. *Proc Natl Acad Sci U S A*. 2018;115(40):9905-9910. doi:10.1073/pnas.1721248115.
282. Wootton RJ. *Functional Morphology of Insect Wings*. Vol 37.; 1992. doi:10.1146/annurev.en.37.010192.000553.
283. Rees CJC. Form and function in corrugated insect wings. *Nature*. 1975;256(5514):200-203. doi:10.1038/256200a0.
284. Bomphrey RJ, Nakata T, Phillips N, Walker SM. Smart wing rotation and trailing-edge vortices enable high frequency mosquito flight. *Nature*. 2017;544(7648):92-95. doi:10.1038/nature21727.
285. Dirks J-H, Taylor D. Veins improve fracture toughness of insect wings. *PLoS One*. 2012;7(8):e43411. doi:10.1371/journal.pone.0043411.
286. Chintapalli RT V., Hillyer JF. Hemolymph circulation in insect flight appendages: physiology of the wing heart and circulatory flow in the wings of the mosquito, *Anopheles gambiae*. *J Exp Biol*. 2016;219(24):3945-3951. doi:10.1242/jeb.148254.
287. Medlock JM, Vaux AGC. *Morphological Separation of the European Members of the Genus Culiseta (Diptera, Culicidae)*. https://www.researchgate.net/profile/Alexander-Vaux/publication/259964367_Morphological_separation_of_the_European_members_of_the_genus_Culiseta_Diptera_Culicidae/links/54ad7e900cf24aca1c6f5eed/Morphological-separation-of-the-European-members-of-the-genus-Culiseta-Diptera-Culicidae.pdf. Accessed July 26, 2021.
288. Dickinson MH, Lehmann FO, Sane SP. Wing rotation and the aerodynamic basis of insect flight. *Science (80-)*. 1999. doi:10.1126/science.284.5422.1954.
289. Perry M. Malaria in the Jeypore Hill Tract and Adjoining Coastland. *Paludism*. 1912;5:32-40.
290. Killeen GF, McKenzie FE, Foy BD, Schieffelin C, Billingsley PF, Beier JC. A simplified model for predicting malaria entomologic inoculation rates based on entomologic and parasitologic parameters relevant to control. *Am J Trop Med Hyg*. 2000;62(5):535-544. doi:10.4269/ajtmh.2000.62.535.
291. Gordon RM, Hicks EP, Davey TH, Watson M. A Study of the House-Haunting Culicidae Occurring in Freetown, Sierra Leone; and of the Part Played by them in the Transmission of Certain Tropical Diseases, Together with Observations on the Relationship of Anophelines to Housing, and the Effects of Anti. *Ann Trop Med Parasitol*. 1932;26(3):273-345. doi:10.1080/00034983.1932.11684720.
292. O'Meara GF. Gonotrophic Interactions in Mosquitoes: Kicking the Blood-Feeding Habit. *Florida Entomol*. 1985;68(1):122. doi:10.2307/3494335.
293. Scott TW, Clark GG, Lorenz LH, Amerasinghe PH, Reiter P, Edman JD. Detection of

Multiple Blood Feeding in Aedes aegypti (Diptera: Culicidae) During a Single Gonotrophic Cycle Using a Histologic Technique. *J Med Entomol*. 1993;30(1):94-99. doi:10.1093/jmedent/30.1.94.
294. Detinova TS. Age-grouping methods in Diptera of medical importance with special reference to some vectors of malaria. *Monogr Ser World Health Organ*. 1962. doi:10.2307/3275215.
295. Davidson G. Estimation of the survival-rate of anopheline mosquitoes in nature. *Nature*. 1954;174(4434):792-793. doi:10.1038/174792a0.
296. Birley M. Estimation, tactics, and disease transmission. In: Conway G, ed. *Pest and Pathogen Control: Strategy, Tactics and Policy Models*. Chinchester, United Kingdom: Wiley Interscience; 1984:272-289. https://agris.fao.org/agris-search/search.do?recordID=US201301469157. Accessed July 28, 2021.
297. Polovodova VP. The determination of the physiological age of female Anopheles by the number of gonotrophic cycles completed. *Med Parazitol (Mosk)*. 1949.
298. Anagonou R, Agossa F, Azondékon R, Agbogan M, Oké-Agbo F, Gnanguenon V, Badirou K, Agbanrin-Youssouf R, Attolou R, Padonou GG, Sovi A, Ossè R, Akogbéto M. Application of Polovodova's method for the determination of physiological age and relationship between the level of parity and infectivity of Plasmodium falciparum in Anopheles gambiae s.s, south-eastern Benin. *Parasit Vectors*. 2015;8:117. doi:10.1186/s13071-015-0731-7.
299. Gillies MT, Wilkes TJ. A study of the age-composition of populations of Anopheles gambiae Giles and A. funestus Giles in North-Eastern Tanzania. *Bull Entomol Res*. 1965;56(2):237-262. doi:10.1017/S0007485300056339.
300. Hoc TQ, Wilkes TJ. The ovariole structure of Anopheles gambiae (Diptera: Culicidae) and its use in determining physiological age. *Bull Entomol Res*. 1995. doi:10.1017/S0007485300052020.
301. Sikulu M, Killeen GF, Hugo LE, Ryan PA, Dowell KM, Wirtz RA, Moore SJ, Dowell FE. Near-infrared spectroscopy as a complementary age grading and species identification tool for African malaria vectors. *Parasit Vectors*. 2010;3(1):49. doi:10.1186/1756-3305-3-49.
302. Hugo LE, Kay BH, Eaglesham GK, Holling N, Ryan PA. Investigation of cuticular hydrocarbons for determining the age and survivorship of Australasian mosquitoes. *Am J Trop Med Hyg*. 2006;74(3):462-474. doi:10.4269/ajtmh.2006.74.462.
303. Caputo B, Dani FR, Horne GL, Petrarca V, Turillazzi S, Coluzzi M, Priestman AA, della Torre A. Identification and composition of cuticular hydrocarbons of the major Afrotropical malaria vector Anopheles gambiae s.s. (Diptera: Culicidae): analysis of sexual dimorphism and age-related changes. *J Mass Spectrom*. 2005;40(12):1595-1604. doi:10.1002/jms.961.
304. Krajacich BJ, Meyers JI, Alout H, Dabiré RK, Dowell FE, Foy BD. Analysis of near infrared spectra for age-grading of wild populations of Anopheles gambiae. *Parasit Vectors*. 2017;10(1):552. doi:10.1186/s13071-017-2501-1.
305. González Jiménez M, Babayan SA, Khazaeli P, Doyle M, Walton F, Reedy E, Glew T, Viana M, Ranford-Cartwright L, Niang A, Siria DJ, Okumu FO, Diabaté A, Ferguson HM, Baldini F, Wynne K. Prediction of mosquito species and population age structure using mid-infrared spectroscopy and supervised machine learning. *Wellcome Open Res*. 2019. doi:10.12688/wellcomeopenres.15201.3.
306. Liebman K, Swamidoss I, Vizcaino L, Lenhart A, Dowell F, Wirtz R. Advancements and

challenges in using near infrared spectroscopy (NIRS) to determine the age of female Aedes Aegypti mosquitoes with varying larval and adult diets. *Am J Trop Med Hyg*. 2014.
307. Dowell F, Lenhart A, Vizcaino L, Swamidoss I, Liebman K, Wirtz R. The Influence of Diet on the Use of Near-Infrared Spectroscopy to Determine the Age of Female Aedes aegypti Mosquitoes. *Am J Trop Med Hyg*. 2015;92(5):1070-1075. doi:10.4269/ajtmh.14-0790.
308. Ntamatungiro AJ, Mayagaya VS, Rieben S, Moore SJ, Dowell FE, Maia MF. The influence of physiological status on age prediction of Anopheles arabiensis using near infra-red spectroscopy. *Parasit Vectors*. 2013;6(1):298. doi:10.1186/1756-3305-6-298.
309. Ferguson HM, Killeen GF, Michel K, Wirtz RA, Benedict MQ, Dowell FE, Mayagaya VS. Non-destructive Determination of Age and Species of Anopheles gambiae s.l. Using Near-infrared Spectroscopy. *Am J Trop Med Hyg*. 2009;81(4):622-630. doi:10.4269/ajtmh.2009.09-0192.
310. Sikulu MT, Majambere S, Khatib BO, Ali AS, Hugo LE, Dowell FE. Using a Near-Infrared Spectrometer to Estimate the Age of Anopheles Mosquitoes Exposed to Pyrethroids. Beebe NW, ed. *PLoS One*. 2014;9(3):e90657. doi:10.1371/journal.pone.0090657.
311. Dowell FE, Noutcha AEM, Michel K. Short report: The effect of preservation methods on predicting mosquito age by near infrared spectroscopy. *Am J Trop Med Hyg*. 2011;85(6):1093-1096. doi:10.4269/ajtmh.2011.11-0438.
312. Esperança PM, Da DF, Lambert B, Dabiré RK, Churcher TS. Functional data analysis techniques to improve the generalizability of near-infrared spectral data for monitoring mosquito populations. *bioRxiv*. April 2020:2020.04.28.058495. doi:10.1101/2020.04.28.058495.
313. Lin-Vien D, Colthup NB, Fateley WG, Grasselli JG (Professor). *The Handbook of Infrared and Raman Characteristic Frequencies of Organic Molecules*. Academic Press; 1991. https://books.google.com/books?hl=en&lr=&id=bYWNSi6abvwC&oi=fnd&pg=PP1&dq=+Lin-Vien+D+Colthup+NB+Fateley+WG+:+The+Handbook+of+Infrared+and+Raman+Characteristic+Frequencies+of+Organic+Molecules+.+(Academic+Press+Inc.,).+1991++Reference+Source++&ots=yp6y6Nr6o5&sig=YGP8fSi1jE4C7VCrN8GL__nJxvQ#v=onepage&q&f=false. Accessed July 29, 2021.
314. Sikulu-Lord MT, Milali MP, Henry M, Wirtz RA, Hugo LE, Dowell FE, Devine GJ. Near-Infrared Spectroscopy, a Rapid Method for Predicting the Age of Male and Female Wild-Type and Wolbachia Infected Aedes aegypti. Barrera R, ed. *PLoS Negl Trop Dis*. 2016;10(10):e0005040. doi:10.1371/journal.pntd.0005040.
315. Esperança PM, Blagborough AM, Da DF, Dowell FE, Churcher TS. Detection of Plasmodium berghei infected Anopheles stephensi using near-infrared spectroscopy. *bioRxiv*. February 2018:195925. doi:10.1101/195925.
316. Mwanga EP, Minja EG, Mrimi E, Jiménez MG, Swai JK, Abbasi S, Ngowo HS, Siria DJ, Mapua S, Stica C, Maia MF, Olotu A, Sikulu-Lord MT, Baldini F, Ferguson HM, Wynne K, Selvaraj P, Babayan SA, Okumu FO. Detection of malaria parasites in dried human blood spots using mid-infrared spectroscopy and logistic regression analysis. *Malar J*. 2019;18(1):341. doi:10.1186/s12936-019-2982-9.
317. Peiris KHS, Dowell F, Killeen G, Hugo L, Drolet BS, Cohnstaedt LW, Dowell FE.

Infrared Absorption Characteristics of Culicoides sonorensis in Relation to Insect Age. *Columbia Int Publ Am J Agric Sci Technol*. 2014;2(2):49-61. doi:10.7726/ajast.2014.1006.
318. González Jiménez M, Babayan SA, Khazaeli P, Doyle M, Walton F, Reedy E, Glew T, Viana M, Ranford-Cartwright L, Niang A, Siria DJ, Okumu FO, Diabaté A, Ferguson HM, Baldini F, Wynne K. Prediction of mosquito species and population age structure using mid-infrared spectroscopy and supervised machine learning. *Wellcome open Res*. 2019;4:76. doi:10.12688/wellcomeopenres.15201.3.
319. Khoshmanesh A, Christensen D, Perez-Guaita D, Iturbe-Ormaetxe I, O'Neill SL, McNaughton D, Wood BR. Screening of *Wolbachia* Endosymbiont Infection in *Aedes aegypti* Mosquitoes Using Attenuated Total Reflection Mid-Infrared Spectroscopy. *Anal Chem*. 2017;89(10):5285-5293. doi:10.1021/acs.analchem.6b04827.
320. Alout H, Roche B, Dabiré RK, Cohuet A. Consequences of insecticide resistance on malaria transmission. *PLoS Pathog*. 2017;13(9). doi:10.1371/journal.ppat.1006499.
321. Hemingway J. The role of vector control in stopping the transmission of malaria: Threats and opportunities. *Philos Trans R Soc B Biol Sci*. 2014. doi:10.1098/rstb.2013.0431.
322. Bibbs CS, Kaufman PE. Volatile Pyrethroids as a Potential Mosquito Abatement Tool: A Review of Pyrethroid-Containing Spatial Repellents. *J Integr Pest Manag*. 2017;8(1). doi:10.1093/jipm/pmx016.
323. Bhatt S, Weiss DJ, Cameron E, Bisanzio D, Mappin B, Dalrymple U, Battle K, Moyes CL, Henry A, Eckhoff PA, Wenger EA, Briët O, Penny MA, Smith TA, Bennett A, Yukich J, Eisele TP, Griffin JT, Fergus CA, Lynch M, Lindgren F, Cohen JM, Murray CLJ, Smith DL, Hay SI, Cibulskis RE, Gething PW. The effect of malaria control on Plasmodium falciparum in Africa between 2000 and 2015. *Nature*. 2015;526(7572):207-211. doi:10.1038/nature15535.
324. Toé KH, Jones CM, N'Fale S, Ismail HM, Dabiré RK, Ranson H. Increased pyrethroid resistance in malaria vectors and decreased bed net effectiveness, Burkina Faso. *Emerg Infect Dis*. 2014;20(10):1691-1696. doi:10.3201/eid2010.140619.
325. Martinez-Torres D, Chandre F, Williamson MS, Darriet F, Bergé JB, Devonshire AL, Guillet P, Pasteur N, Pauron D. Molecular characterization of pyrethroid knockdown resistance (kdr) in the major malaria vector Anopheles gambiae s.s. *Insect Mol Biol*. 1998. doi:10.1046/j.1365-2583.1998.72062.x.
326. Senthil-Nathan S. A Review of Resistance Mechanisms of Synthetic Insecticides and Botanicals, Phytochemicals, and Essential Oils as Alternative Larvicidal Agents Against Mosquitoes. *Front Physiol*. 2019;10:1591. doi:10.3389/fphys.2019.01591.
327. Hien AS, Soma DD, Hema O, Bayili B, Namountougou M, Gnankiné O, Baldet T, Diabaté A, Dabiré KR. Evidence that agricultural use of pesticides selects pyrethroid resistance within Anopheles gambiae s.l. populations from cotton growing areas in Burkina Faso, West Africa. *PLoS One*. 2017;12(3). doi:10.1371/journal.pone.0173098.
328. Ranson H, N'guessan R, Lines J, Moiroux N, Nkuni Z, Corbel V. Pyrethroid resistance in African anopheline mosquitoes: what are the implications for malaria control? *Trends Parasitol*. 2011;27(2):91-98. doi:10.1016/j.pt.2010.08.004.
329. Ranson H, Jensen B, Vulule JM, Wang X, Hemingway J, Collins FH. Identification of a point mutation in the voltage-gated sodium channel gene of Kenyan Anopheles gambiae associated with resistance to DDT and pyrethroids. *Insect Mol Biol*. 2000. doi:10.1046/j.1365-2583.2000.00209.x.

330. Edi AVC, N'Dri BP, Chouaibou M, Kouadio FB, Pignatelli P, Raso G, Weetman D, Bonfoh B. First detection of N1575Y mutation in pyrethroid resistant Anopheles gambiae in Southern Côte d'Ivoire. *Wellcome Open Res*. 2017. doi:10.12688/wellcomeopenres.12246.1.
331. Namountougou M, Simard F, Baldet T, Diabaté A, Ouédraogo JB, Martin T, Dabiré RK. Multiple Insecticide Resistance in Anopheles gambiae s.l. Populations from Burkina Faso, West Africa. *PLoS One*. 2012. doi:10.1371/journal.pone.0048412.
332. Weill M, Malcolm C, Chandre F, Mogensen K, Berthomieu A, Marquine M, Raymond M. The unique mutation in ace-1 giving high insecticide resistance is easily detectable in mosquito vectors. *Insect Mol Biol*. 2004. doi:10.1111/j.1365-2583.2004.00452.x.
333. Assogba BS, Alout H, Koffi A, Penetier C, Djogbénou LS, Makoundou P, Weill M, Labbé P. Adaptive deletion in resistance gene duplications in the malaria vector Anopheles gambiae. *Evol Appl*. 2018. doi:10.1111/eva.12619.
334. Aïzoun N, Aïkpon R, Padonou GG ermain, Oussou O, Oké-Agbo F, Gnanguenon V, Ossè R, Akogbéto M. Mixed-function oxidases and esterases associated with permethrin, deltamethrin and bendiocarb resistance in Anopheles gambiae s.l. in the south-north transect Benin, West Africa. *Parasit Vectors*. 2013. doi:10.1186/1756-3305-6-223.
335. Weetman D, Wilding CS, Neafsey DE, Müller P, Ochomo E, Isaacs AT, Steen K, Rippon EJ, Morgan JC, Mawejje HD, Rigden DJ, Okedi LM, Donnelly MJ. Candidate-gene based GWAS identifies reproducible DNA markers for metabolic pyrethroid resistance from standing genetic variation in East African Anopheles gambiae. *Sci Rep*. 2018. doi:10.1016/S0301-0104(01)00220-8.
336. Edi C V, Djogbénou L, Jenkins AM, Regna K, Muskavitch MAT, Poupardin R, Jones CM, Essandoh J, Kétoh GK, Paine MJI, Koudou BG, Donnelly MJ, Ranson H, Weetman D. CYP6 P450 enzymes and ACE-1 duplication produce extreme and multiple insecticide resistance in the malaria mosquito Anopheles gambiae. Zhang J, ed. *PLoS Genet*. 2014;10(3):e1004236. doi:10.1371/journal.pgen.1004236.
337. Ingham VA, Anthousi A, Douris V, Harding NJ, Lycett G, Morris M, Vontas J, Ranson H. A sensory appendage protein protects malaria vectors from pyrethroids. *Nature*. 2020;577(7790):376-380. doi:10.1038/s41586-019-1864-1.
338. Balabanidou V, Kampouraki A, MacLean M, Blomquist GJ, Tittiger C, Juárez MP, Mijailovsky SJ, Chalepakis G, Anthousi A, Lynd A, Antoine S, Hemingway J, Ranson H, Lycett GJ, Vontas J. Cytochrome P450 associated with insecticide resistance catalyzes cuticular hydrocarbon production in Anopheles gambiae. *Proc Natl Acad Sci*. 2016. doi:10.1073/pnas.1608295113.
339. Yahouédo GA, Chandre F, Rossignol M, Ginibre C, Balabanidou V, Mendez NGA, Pigeon O, Vontas J, Cornelie S. Contributions of cuticle permeability and enzyme detoxification to pyrethroid resistance in the major malaria vector Anopheles gambiae. *Sci Rep*. 2017;7(1). doi:10.1038/s41598-017-11357-z.
340. Balabanidou V, Kefi M, Aivaliotis M, Koidou V, Girotti JR, Mijailovsky SJ, Juárez MP, Papadogiorgaki E, Chalepakis G, Kampouraki A, Nikolaou C, Ranson H, Vontas J. Mosquitoes cloak their legs to resist insecticides. *Proc R Soc B Biol Sci*. 2019;286(1907):20191091. doi:10.1098/rspb.2019.1091.
341. Norris LC, Main BJ, Lee Y, Collier TC, Fofana A, Cornel AJ, Lanzaro GC. Adaptive introgression in an African malaria mosquito coincident with the increased usage of insecticide-treated bed nets. *Proc Natl Acad Sci*. 2015;112(3).

doi:10.1073/pnas.1418892112.
342. Kim W, Koo H, Richman AM, Seeley D, Vizioli J, Klocko AD, O'Brochta DA. Ectopic expression of a cecropin transgene in the human malaria vector mosquito Anopheles gambiae (Diptera: Culicidae): effects on susceptibility to Plasmodium. *J Med Entomol*. 2004;41(3):447-455. doi:10.1603/0022-2585-41.3.447.
343. Thorpe HM, Smith MC, Tretiakov M, Thiery I, Zettor A, Bourgouin C, James AA. In vitro site-specific integration of bacteriophage DNA catalyzed by a recombinase of the resolvase/invertase family. *Proc Natl Acad Sci U S A*. 1998;95(10):5505-5510. doi:10.1073/pnas.95.10.5505.
344. Garver LS, Dong Y, Dimopoulos G. Caspar Controls Resistance to Plasmodium falciparum in Diverse Anopheline Species. Ribeiro JMC, ed. *PLoS Pathog*. 2009;5(3):e1000335. doi:10.1371/journal.ppat.1000335.
345. Clayton AM, Cirimotich CM, Dong Y, Dimopoulos G. Caudal is a negative regulator of the Anopheles IMD pathway that controls resistance to Plasmodium falciparum infection. *Dev Comp Immunol*. 2013;39(4):323-332. doi:10.1016/j.dci.2012.10.009.
346. Frolet C, Thoma M, Blandin S, Hoffmann JA, Levashina EA. Boosting NF-κB-Dependent Basal Immunity of Anopheles gambiae Aborts Development of Plasmodium berghei. *Immunity*. 2006;25(4):677-685. doi:10.1016/J.IMMUNI.2006.08.019.
347. Ito J, Ghosh A, Moreira LA, Wimmer EA, Jacobs-Lorena M. Transgenic anopheline mosquitoes impaired in transmission of a malaria parasite. *Nature*. 2002;417(6887):452-455. doi:10.1038/417452a.
348. Yoshida S, Shimada Y, Kondoh D, Kouzuma Y, Ghosh AK, Jacobs-Lorena M, Sinden RE. Hemolytic C-type lectin CEL-III from sea cucumber expressed in transgenic mosquitoes impairs malaria parasite development. *PLoS Pathog*. 2007;3(12):e192. doi:10.1371/journal.ppat.0030192.
349. Bando H, Okado K, Guelbeogo WM, Badolo A, Aonuma H, Nelson B, Fukumoto S, Xuan X, Sagnon N, Kanuka H. Intra-specific diversity of Serratia marcescens in Anopheles mosquito midgut defines Plasmodium transmission capacity. *Sci Rep*. 2013;3:1641. doi:10.1038/srep01641.
350. Wang S, Dos-Santos ALA, Huang W, Liu KC, Oshaghi MA, Wei G, Agre P, Jacobs-Lorena M. Driving mosquito refractoriness to Plasmodium falciparum with engineered symbiotic bacteria. *Science*. 2017;357(6358):1399-1402. doi:10.1126/science.aan5478.
351. Dong Y, Manfredini F, Dimopoulos G. Implication of the Mosquito Midgut Microbiota in the Defense against Malaria Parasites. Schneider DS, ed. *PLoS Pathog*. 2009;5(5):e1000423. doi:10.1371/journal.ppat.1000423.
352. Bian G, Joshi D, Dong Y, Lu P, Zhou G, Pan X, Xu Y, Dimopoulos G, Xi Z. Wolbachia invades Anopheles stephensi populations and induces refractoriness to Plasmodium infection. *Science (80-)*. 2013;340(6133):748-751. doi:10.1126/science.1236192.
353. Burt A. Site-specific selfish genes as tools for the control and genetic engineering of natural populations. *Proc R Soc B Biol Sci*. 2003;270(1518):921. doi:10.1098/RSPB.2002.2319.
354. Windbichler N, Menichelli M, Papathanos PA, Thyme SB, Li H, Ulge UY, Hovde BT, Baker D, Monnat RJ, Burt A, Crisanti A. A synthetic homing endonuclease-based gene drive system in the human malaria mosquito. *Nature*. 2011;473(7346):212-215. doi:10.1038/nature09937.
355. Black BC, Hollingworth RM, Ahammadsahib KI, Kukel CD, Donovan S. Insecticidal

Action and Mitochondrial Uncoupling Activity of AC-303,630 and Related Halogenated Pyrroles. *Pestic Biochem Physiol*. 1994;50(2):115-128. doi:10.1006/PEST.1994.1064.
356. Van Voorhis WC, Hooft van Huijsduijnen R, Wells TNC. Profile of William C. Campbell, Satoshi Ōmura, and Youyou Tu, 2015 Nobel Laureates in Physiology or Medicine. *Proc Natl Acad Sci U S A*. 2015;112(52):15773-15776. doi:10.1073/pnas.1520952112.
357. Lasota JA, Dybas RA. Avermectins, a novel class of compounds: implications for use in arthropod pest control. *Annu Rev Entomol*. 1991;36:91-117. doi:10.1146/annurev.en.36.010191.000515.
358. Campbell WC. An introduction to the avermectins. *N Z Vet J*. 1981;29(10):174-178. doi:10.1080/00480169.1981.34836.
359. Campbell WC, Fisher MH, Stapley EO, Albers-Schönberg G, Jacob TA. Ivermectin: a potent new antiparasitic agent. *Science*. 1983;221(4613):823-828. doi:10.1126/science.6308762.
360. Laing R, Gillan V, Devaney E. Ivermectin - Old Drug, New Tricks? *Trends Parasitol*. 2017;33(6):463-472. doi:10.1016/j.pt.2017.02.004.
361. World Health Organization. *World Health Organization Model List of Essential Medicines*. Vol 21.; 2019. https://apps.who.int/iris/bitstream/handle/10665/325771/WHO-MVP-EMP-IAU-2019.06-eng.pdf?ua=1.
362. Taylor HR, Greene BM. The status of ivermectin in the treatment of human onchocerciasis. *Am J Trop Med Hyg*. 1989;41(4):460-466. doi:10.4269/ajtmh.1989.41.460.
363. Ottesen EA, Duke BO, Karam M, Behbehani K. Strategies and tools for the control/elimination of lymphatic filariasis. *Bull World Health Organ*. 1997;75(6):491-503. http://www.ncbi.nlm.nih.gov/pubmed/9509621. Accessed July 19, 2021.
364. Pion SD, Tchatchueng-Mbougua JB, Chesnais CB, Kamgno J, Gardon J, Chippaux J-P, Ranque S, Ernould J-C, Garcia A, Boussinesq M. Effect of a Single Standard Dose (150-200 μg/kg) of Ivermectin on Loa loa Microfilaremia: Systematic Review and Meta-analysis. *Open forum Infect Dis*. 2019;6(4):ofz019. doi:10.1093/ofid/ofz019.
365. Omura S, Crump A. Ivermectin: panacea for resource-poor communities? *Trends Parasitol*. 2014;30(9):445-455. doi:10.1016/j.pt.2014.07.005.
366. Guzzo CA, Furtek CI, Porras AG, Chen C, Tipping R, Clineschmidt CM, Sciberras DG, Hsieh JYK, Lasseter KC. Safety, tolerability, and pharmacokinetics of escalating high doses of ivermectin in healthy adult subjects. *J Clin Pharmacol*. 2002;42(10):1122-1133. http://www.ncbi.nlm.nih.gov/pubmed/12362927. Accessed May 10, 2018.
367. Boussinesq M, Kamgno J, Pion SD, Gardon J. What are the mechanisms associated with post-ivermectin serious adverse events? *Trends Parasitol*. 2006;22(6):244-246. doi:10.1016/j.pt.2006.04.006.
368. Wolstenholme AJ. Glutamate-gated chloride channels. *J Biol Chem*. 2012;287(48):40232-40238. doi:10.1074/jbc.R112.406280.
369. Thompson AJ, Lester HA, Lummis SCR. The structural basis of function in Cys-loop receptors. *Q Rev Biophys*. 2010;43(4):449-499. doi:10.1017/S0033583510000168.
370. Kasaragod VB, Schindelin H. Structure–Function Relationships of Glycine and GABAA Receptors and Their Interplay With the Scaffolding Protein Gephyrin. *Front Mol Neurosci*. 2018;11:317. doi:10.3389/fnmol.2018.00317.
371. Meyers JI, Gray M, Kuklinski W, Johnson LB, Snow CD, Black WC, Partin KM, Foy BD. Characterization of the target of ivermectin, the glutamate-gated chloride channel,

from Anopheles gambiae. *J Exp Biol*. 2015;218(10):1478-1486. doi:10.1242/jeb.118570.
372. Wolstenholme AJ, Rogers AT. Glutamate-gated chloride channels and the mode of action of the avermectin/milbemycin anthelmintics. *Parasitology*. 2005;131(SUPPL. 1):S85. doi:10.1017/S0031182005008218.
373. Adelsberger H, Lepier A, Dudel J. Activation of rat recombinant α1β2γ2S GABAA receptor by the insecticide ivermectin. *Eur J Pharmacol*. 2000;394(2-3):163-170. doi:10.1016/S0014-2999(00)00164-3.
374. Lynagh T, Lynch JW. Molecular mechanisms of Cys-loop ion channel receptor modulation by ivermectin. *Front Mol Neurosci*. 2012;5:60. doi:10.3389/fnmol.2012.00060.
375. Kobylinski KC, Ubalee R, Ponlawat A, Nitatsukprasert C, Phasomkulsolsil S, Wattanakul T, Tarning J, Na-Bangchang K, McCardle PW, Davidson SA, Richardson JH. Ivermectin susceptibility and sporontocidal effect in Greater Mekong Subregion Anopheles. *Malar J*. 2017. doi:10.1186/s12936-017-1923-8.
376. Sylla M, Kobylinski KC, Gray M, Chapman PL, Sarr MD, Rasgon JL, Foy BD. Mass drug administration of ivermectin in south-eastern Senegal reduces the survivorship of wild-caught, blood fed malaria vectors. *Malar J*. 2010;9(1):365. doi:10.1186/1475-2875-9-365.
377. Kobylinski KC, Deus KM, Butters MP, Hongyu T, Gray M, da Silva IM, Sylla M, Foy BD. The effect of oral anthelmintics on the survivorship and re-feeding frequency of anthropophilic mosquito disease vectors. *Acta Trop*. 2010;116(2):119-126. doi:10.1016/j.actatropica.2010.06.001.
378. Chaccour CJ, Kobylinski KC, Bassat Q, Bousema T, Drakeley C, Alonso P, Foy BD. Ivermectin to reduce malaria transmission: a research agenda for a promising new tool for elimination. *Malar J*. 2013;12(153). doi:10.1186/1475-2875-12-153.
379. Charlwood JD, Pinto J, Sousa CA, Ferreira C, Petrarca V, Do V, Rosario E. "A mate or a meal" – Pre-gravid behaviour of female Anopheles gambiae from the islands of São Tomé and Príncipe, West Africa. *Malar J*. 2003;2(2). http://www.malariajournal.com/content/2/1/9. Accessed May 31, 2018.
380. Kobylinski KC, Escobedo-Vargas KS, López-Sifuentes VM, Durand S, Smith ES, Baldeviano GC, Gerbasi R V., Ballard SB, Stoops CA, Vásquez GM. Ivermectin susceptibility, sporontocidal effect, and inhibition of time to re-feed in the Amazonian malaria vector Anopheles darlingi. *Malar J*. 2017;16(1). doi:10.1186/s12936-017-2125-0.
381. Sampaio V de S, Rivas GB da S, Kobylinski K, Pinilla YT, Pimenta PFP, Lima JBP, Bruno RV, Lacerda MVG, Monteiro WM. What does not kill it makes it weaker: effects of sub-lethal concentrations of ivermectin on the locomotor activity of Anopheles aquasalis. *Parasit Vectors*. 2017;10(1):623. doi:10.1186/s13071-017-2563-0.
382. Roitberg BD, Mondor EB, Tyerman JGA. Pouncing spider, flying mosquito: blood acquisition increases predation risk in mosquitoes. *Behav Ecol*. 2003;14(5):736-740. doi:10.1093/beheco/arg055.
383. Mahmood F, Walters LL, Guzman H, Tesh RB. Effect of ivermectin on the ovarian development of Aedes aegypti (Diptera: Culicidae). *J Med Entomol*. 1991. doi:10.1093/jmedent/28.5.701.
384. Tesh RB, Guzman H. Mortality and infertility in adult mosquitoes after the ingestion of blood containing ivermectin. *Am J Trop Med Hyg*. 1990;43(3):229-233. doi:10.4269/ajtmh.1990.43.229.

385. Focks DA, McLaughlin RE, Linda SB. Effects of ivermectin (MK-933) on the reproductive rate of Aedes aegypti (Diptera: Culicidae). *J Med Entomol*. 1991;28(4):501-505. doi:10.1093/jmedent/28.4.501.
386. Fritz ML, Walker ED, Miller JR. Lethal and sublethal effects of avermectin/milbemycin parasiticides on the African malaria vector, anopheles arabiensis. *J Med Entomol*. 2012. doi:10.1603/ME11098.
387. Fritz ML, Siegert PY, Walker ED, Bayoh MN, Vulule JR, Miller JR. Toxicity of bloodmeals from ivermectin-treated cattle to Anopheles gambiae s.l. *Ann Trop Med Parasitol*. 2009;103(6):539-547. doi:10.1179/000349809X12459740922138.
388. Gardner K, Meisch M V, Meek4 CL, Biven5 WS. *Effects of Ivermectin in Canine Blood on Anopheles Quadrimaculatus, Aedes Albopicuts and Culex Salinarius*. Vol 9. https://www.biodiversitylibrary.org/content/part/JAMCA/JAMCA_V09_N4_P400-402.pdf. Accessed July 21, 2021.
389. Alout H, Krajacich BJ, Meyers JI, Grubaugh ND, Brackney DE, Kobylinski KC, Diclaro JW, Bolay FK, Fakoli LS, Diabaté A, Dabiré RK, Bougma RW, Foy BD. Evaluation of ivermectin mass drug administration for malaria transmission control across different West African environments. *Malar J*. 2014;13(417). doi:10.1186/1475-2875-13-417.
390. Seaman JA, Alout H, Meyers JI, Stenglein MD, Dabiré RK, Lozano-Fuentes S, Burton TA, Kuklinski WS, Black WC, Foy BD. Age and prior blood feeding of Anopheles gambiae influences their susceptibility and gene expression patterns to ivermectin-containing blood meals. *BMC Genomics*. 2015;16(797). doi:10.1186/s12864-015-2029-8.
391. Kobylinski KC, Foy BD, Richardson JH. Ivermectin inhibits the sporogony of Plasmodium falciparum in Anopheles gambiae. *Malar J*. 2012;11(381). doi:10.1186/1475-2875-11-381.
392. Kobylinski KC, Sylla M, Chapman PL, Sarr MD, Foy BD. Ivermectin mass drug administration to humans disrupts malaria parasite transmission in Senegalese villages. *Am J Trop Med Hyg*. 2011;85(1):3-5. doi:10.4269/ajtmh.2011.11-0160.
393. Alout H, Krajacich BJ, Meyers JI, Grubaugh ND, Brackney DE, Kobylinski KC, Diclaro JW, Bolay FK, Fakoli LS, Diabaté A, Dabiré RK, Bougma RW, Foy BD. Evaluation of ivermectin mass drug administration for malaria transmission control across different West African environments. *Malar J*. 2014;13(1):417. doi:10.1186/1475-2875-13-417.
394. Mendes AM, Albuquerque IS, Machado M, Pissarra J, Meireles P, Prudêncio M. Inhibition of Plasmodium Liver Infection by Ivermectin. *Antimicrob Agents Chemother*. 2017;61(2):AAC.02005-16. doi:10.1128/AAC.02005-16.
395. Pinilla YT, C. P. Lopes S, S. Sampaio V, Andrade FS, Melo GC, Orfanó AS, Secundino NFC, Guerra MGVB, Lacerda MVG, Kobylinski KC, Escobedo-Vargas KS, López-Sifuentes VM, Stoops CA, Baldeviano GC, Tarning J, Vasquez GM, Pimenta PFP, Monteiro WM. Promising approach to reducing Malaria transmission by ivermectin: Sporontocidal effect against Plasmodium vivax in the South American vectors Anopheles aquasalis and Anopheles darlingi. *PLoS Negl Trop Dis*. 2018;12(2). doi:10.1371/journal.pntd.0006221.
396. Smit MR, Ochomo EO, Aljayyoussi G, Kwambai TK, Abong'o BO, Chen T, Bousema T, Slater HC, Waterhouse D, Bayoh NM, Gimnig JE, Samuels AM, Desai MR, Phillips-Howard PA, Kariuki SK, Wang D, Ward SA, Ter Kuile FO. Safety and mosquitocidal efficacy of high-dose ivermectin when co-administered with dihydroartemisinin-piperaquine in Kenyan adults with uncomplicated malaria (IVERMAL): a randomised,

double-blind, placebo-controlled trial. *Lancet Infect Dis*. 2018;0(0). doi:10.1016/S1473-3099(18)30163-4.
397. Smit MR, Ochomo E, Aljayyoussi G, Kwambai T, Abong'o B, Bayoh N, Gimnig J, Samuels A, Desai M, Phillips-Howard PA, Kariuki S, Wang D, Ward S, Ter Kuile FO. Efficacy and Safety of High-Dose Ivermectin for Reducing Malaria Transmission (IVERMAL): Protocol for a Double-Blind, Randomized, Placebo-Controlled, Dose-Finding Trial in Western Kenya. *JMIR Res Protoc*. 2016;5(4):e213. doi:10.2196/resprot.6617.
398. Foy BD, Alout H, Seaman JA, Rao S, Magalhaes T, Wade M, Parikh S, Soma DD, Sagna AB, Fournet F, Slater HC, Bougma R, Drabo F, Diabaté A, Coulidiaty AG V., Rouamba N, Dabiré RK. Efficacy and risk of harms of repeat ivermectin mass drug administrations for control of malaria (RIMDAMAL): a cluster-randomised trial. *Lancet*. 2019;393(10180):1517-1526. doi:10.1016/S0140-6736(18)32321-3.
399. Ouédraogo AL, Bastiaens GJH, Tiono AB, Guelbéogo WM, Kobylinski KC, Ouédraogo A, Barry A, Bougouma EC, Nebie I, Ouattara MS, Lanke KHW, Fleckenstein L, Sauerwein RW, Slater HC, Churcher TS, Sirima SB, Drakeley C, Bousema T. Efficacy and safety of the mosquitocidal drug ivermectin to prevent malaria transmission after treatment: A double-blind, randomized, clinical trial. *Clin Infect Dis*. 2015. doi:10.1093/cid/ciu797.
400. Dabira ED, Soumare HM, Lindsay SW, Conteh B, Ceesay F, Bradley J, Kositz C, Broekhuizen H, Kandeh B, Fehr AE, Nieto-Sanchez C, Ribera JM, Peeters Grietens K, Smit MR, Drakeley C, Bousema T, Achan J, D'Alessandro U. Mass Drug Administration With High-Dose Ivermectin and Dihydroartemisinin-Piperaquine for Malaria Elimination in an Area of Low Transmission With High Coverage of Malaria Control Interventions: Protocol for the MASSIV Cluster Randomized Clinical Trial. *JMIR Res Protoc*. 2020;9(11):e20904. doi:10.2196/20904.
401. Federal RePORTER - A Novel Vector Control Measure to Combat the Spread of Artemisinin Resistance in the Greater Mekong Subregion (PR150881). https://federalreporter.nih.gov/Projects/Details/?projectId=893768. Accessed September 5, 2021.
402. BOHEMIA - Broad One Health Endectocide-based Malaria Intervention in Africa. https://www.isglobal.org/en/-/bohemia. Accessed September 5, 2021.
403. Insecticide Resistance Management in Burkina Faso and Côte d'Ivoire. ClinicalTrials.gov. https://clinicaltrials.gov/ct2/show/NCT03074435. Accessed September 5, 2021.
404. Adjunctive Ivermectin Mass Drug Administration for Malaria Control. ClinicalTrials.gov. https://clinicaltrials.gov/ct2/show/NCT04844905. Accessed September 5, 2021.
405. Repeat Ivermectin Mass Drug Administrations for MALaria Control II. ClinicalTrials.gov. https://clinicaltrials.gov/ct2/show/NCT03967054. Accessed September 5, 2021.
406. Conway MJ, Colpitts TM, Fikrig E. Role of the Vector in Arbovirus Transmission. *Annu Rev Virol*. 2014. doi:10.1146/annurev-virology-031413-085513.
407. Schorderet-Weber S, Noack S, Selzer PM, Kaminsky R. Blocking transmission of vector-borne diseases. *Int J Parasitol Drugs Drug Resist*. 2017. doi:10.1016/j.ijpddr.2017.01.004.
408. Shaw WR, Catteruccia F. Vector biology meets disease control: using basic research to fight vector-borne diseases. *Nat Microbiol*. 2019;4(1):20-34. doi:10.1038/s41564-018-0214-7.
409. Detinova TS. Determination of the physiological Age of the Females of Anopheles by the

Changes in the tracheal System of the Ovaries. *Med Parasitol*. 1945;14(2). https://www.cabdirect.org/cabdirect/abstract/19461000329. Accessed May 24, 2018.
410. Briegel H, Horler E. Multiple blood meals as a reproductive strategy in Anopheles (Diptera: Culicidae).[Erratum appears in J Med Entomol 1994 Mar;31(2):following 321]. *J Med Entomol*. 1993.
411. Beklemishev WN, Detinova TS, Polovodova VP. Determination of physiological age in anophelines and of age distribution in anopheline populations in the USSR. *Bull World Health Organ*. 1959;21(2):223-232. http://www.ncbi.nlm.nih.gov/pubmed/13798390. Accessed May 24, 2018.
412. Hoc TQ, Charlwood JD. Age determination of Aedes cantans using the ovarian oil injection technique. *Med Vet Entomol*. 1990. doi:10.1111/j.1365-2915.1990.tb00281.x.
413. Wang MH, Marinotti O, Zhong D, James AA, Walker E, Guda T, Kweka EJ, Githure J, Yan G. Gene Expression-Based Biomarkers for Anopheles gambiae Age Grading. *PLoS One*. 2013. doi:10.1371/journal.pone.0069439.
414. Wu D, Lehane MJ. Pteridine fluorescence for age determination of Anopheles mosquitoes. *Med Vet Entomol*. 1999. doi:10.1046/j.1365-2915.1999.00144.x.
415. Styer LM, Carey JR, Wang JL, Scott TW. Mosquitoes do senesce: Departure from the paradigm of constant mortality. *Am J Trop Med Hyg*. 2007. doi:10.4269/ajtmh.2007.76.111.
416. Harrington LC, Buonaccorsi JP, Edman JD, Costero A, Kittayapong P, Clark GG, Scott TW. Analysis of Survival of Young and Old Aedes aegypti (Diptera: Culicidae) from Puerto Rico and Thailand . *J Med Entomol*. 2001. doi:10.1603/0022-2585-38.4.537.
417. Sikulu M, Killeen GF, Hugo LE, Ryan PA, Dowell KM, Wirtz RA, Moore SJ, Dowell FE. Near-infrared spectroscopy as a complementary age grading and species identification tool for African malaria vectors. *Parasites and Vectors*. 2010. doi:10.1186/1756-3305-3-49.
418. Kittichai V, Pengsakul T, Chumchuen K, Samung Y, Sriwichai P, Phatthamolrat N, Tongloy T, Jaksukam K, Chuwongin S, Boonsang S. Deep learning approaches for challenging species and gender identification of mosquito vectors. *Sci Rep*. 2021;11(1):4838. doi:10.1038/s41598-021-84219-4.
419. Couret J, Moreira DC, Bernier D, Loberti AM, Dotson EM, Alvarez M. Delimiting cryptic morphological variation among human malaria vector species using convolutional neural networks. *PLoS Negl Trop Dis*. 2020;14(12):e0008904. doi:10.1371/journal.pntd.0008904.
420. Moen E, Bannon D, Kudo T, Graf W, Covert M, Van Valen D. Deep learning for cellular image analysis. *Nat Methods*. 2019;16(12):1233-1246. doi:10.1038/s41592-019-0403-1.
421. Lyimo IN, Kessy ST, Mbina KF, Daraja AA, Mnyone LL. Ivermectin-treated cattle reduces blood digestion, egg production and survival of a free-living population of Anopheles arabiensis under semi-field condition in south-eastern Tanzania. *Malar J*. 2017. doi:10.1186/s12936-017-1885-x.
422. Vazquez-Prokopec GM, Galvin WA, Kelly R, Kitron U. A New, Cost-Effective, Battery-Powered Aspirator for Adult Mosquito Collections. *J Med Entomol*. 2009. doi:10.1603/033.046.0602.
423. Pasay CJ, Yakob L, Meredith HR, Stewart R, Mills PC, Dekkers MH, Ong O, Llewellyn S, Hugo RLE, McCarthy JS, Devine GJ. Treatment of pigs with endectocides as a complementary tool for combating malaria transmission by Anopheles farauti (s.s.) in Papua New Guinea. *Parasit Vectors*. 2019;12(1):124. doi:10.1186/s13071-019-3392-0.

424. Darsie RF, Ward RA. *Identification and Geographical Distribution of The Mosquito of North America, North of Mexico*. Fresno, CA: American Mosquito Control Association; 1981.
425. Kamiya T, Greischar MA, Wadhawan K, Gilbert B, Paaijmans K, Mideo N. Temperature-dependent variation in the extrinsic incubation period elevates the risk of vector-borne disease emergence. *Epidemics*. 2020. doi:10.1016/j.epidem.2019.100382.
426. He K, Zhang X, Ren S, Sun J. Deep Residual Learning for Image Recognition. December 2015. http://arxiv.org/abs/1512.03385. Accessed June 6, 2021.
427. Simonyan K, Zisserman A. Very Deep Convolutional Networks for Large-Scale Image Recognition. September 2014. http://arxiv.org/abs/1409.1556. Accessed June 13, 2021.
428. Huang G, Liu Z, van der Maaten L, Weinberger KQ. Densely Connected Convolutional Networks. August 2016. http://arxiv.org/abs/1608.06993. Accessed June 13, 2021.
429. Liyuan Li, Ran Gong, Weinan Chen. Gray level image thresholding based on fisher linear projection of two-dimensional histogram. *Pattern Recognit*. 1997;30(5):743-749. doi:10.1016/S0031-3203(96)00100-8.
430. World Health Organization. *A Global Brief on Vector-Borne Diseases*.; 2014. http://apps.who.int/iris/bitstream/10665/111008/1/WHO_DCO_WHD_2014.1_eng.pdf.
431. Ohm JR, Baldini F, Barreaux P, Lefevre T, Lynch PA, Suh E, Whitehead SA, Thomas MB. Rethinking the extrinsic incubation period of malaria parasites. *Parasites and Vectors*. 2018. doi:10.1186/s13071-018-2761-4.
432. Coetzee M. Distribution of the African malaria vectors of the Anopheles gambiae complex. *Am J Trop Med Hyg*. 2004;70(2):103-104. www.malaria.org. Accessed June 30, 2021.
433. Favia G, Della Torre A, Bagayoko M, Lanfrancotti A, Sagnon NF, Touré YT, Coluzzi M. Molecular identification of sympatric chromosomal forms of Anopheles gambiae and further evidence of their reproductive isolation. *Insect Mol Biol*. 1997;6(4):377-383. doi:10.1046/j.1365-2583.1997.00189.x.
434. Sikulu M, Killeen GF, Hugo LE, Ryan PA, Dowell KM, Wirtz RA, Moore SJ, Dowell FE. Near-infrared spectroscopy as a complementary age grading and species identification tool for African malaria vectors. *Parasit Vectors*. 2010;3(1):49. doi:10.1186/1756-3305-3-49.
435. Diboulo E, Sié A, Vounatsou P. Assessing the effects of malaria interventions on the geographical distribution of parasitaemia risk in Burkina Faso. *Malar J*. 2016;15(1):228. doi:10.1186/s12936-016-1282-x.
436. Rumisha SF, Smith T, Abdulla S, Masanja H, Vounatsou P. Modelling heterogeneity in malaria transmission using large sparse spatio-temporal entomological data. *Glob Health Action*. 2014;7(1):22682. doi:10.3402/gha.v7.22682.
437. Drakeley C, Schellenberg D, Kihonda J, Sousa CA, Arez AP, Lopes D, Lines J, Mshinda H, Lengeler C, Schellenberg JA, Tanner M, Alonso P. An estimation of the entomological inoculation rate for Ifakara: a semi-urban area in a region of intense malaria transmission in Tanzania. *Trop Med Int Heal*. 2003;8(9):767-774. doi:10.1046/j.1365-3156.2003.01100.x.
438. Ryan SJ, Ben-Horin T, Johnson LR. Malaria control and senescence: the importance of accounting for the pace and shape of aging in wild mosquitoes. *Ecosphere*. 2015;6(9):art170. doi:10.1890/ES15-00094.1.
439. N'Guessan R, Ngufor C, Odjo A, Vigninou E, Akogbeto M, Rowland M. Efficacy of LLIN mixtures of chlorfenapyr and alphacypermethrin against pyrethroid resistant

anopheles Gambiae: An experimental hut trial in Benin. *Am J Trop Med Hyg*. 2014.
440. Bayili K, N'do S, Namountougou M, Sanou R, Ouattara A, Dabiré RK, Ouédraogo AG, Malone D, Diabaté A. Evaluation of efficacy of Interceptor® G2, a long-lasting insecticide net coated with a mixture of chlorfenapyr and alpha-cypermethrin, against pyrethroid resistant Anopheles gambiae s.l. in Burkina Faso. *Malar J*. 2017. doi:10.1186/s12936-017-1846-4.
441. The World Bank. Population growth (annual %) - Burkina Faso | Data. https://data.worldbank.org/indicator/SP.POP.GROW?locations=BF. Accessed July 25, 2021.
442. Benelli G. Managing mosquitoes and ticks in a rapidly changing world – Facts and trends. *Saudi J Biol Sci*. 2019;26(5):921-929. doi:10.1016/j.sjbs.2018.06.007.
443. Chaccour CJ, Rabinovich NR, Slater H, Canavati SE, Bousema T, Lacerda M, ter Kuile F, Drakeley C, Bassat Q, Foy BD, Kobylinski K. Establishment of the Ivermectin Research for Malaria Elimination Network: updating the research agenda. *Malar J*. 2015;14(243). doi:10.1186/s12936-015-0691-6.
444. Chaccour C, Lines J, Whitty CJM. Effect of ivermectin on Anopheles gambiae mosquitoes fed on humans: the potential of oral insecticides in malaria control. *J Infect Dis*. 2010;202(1):113-116. doi:10.1086/653208.
445. Derua YA, Kisinza WN, Simonsen PE. Differential effect of human ivermectin treatment on blood feeding Anopheles gambiae and Culex quinquefasciatus. *Parasit Vectors*. 2015;8:130. doi:10.1186/s13071-015-0735-3.
446. Kobylinski KC, Alout H, Foy BD, Clements A, Adisakwattana P, Swierczewski BE, Richardson JH. Rationale for the Coadministration of Albendazole and Ivermectin to Humans for Malaria Parasite Transmission Control. *Am J Trop Med Hyg*. 2014;91(4):655-662. doi:10.4269/ajtmh.14-0187.
447. Robert V, Gazin P, Boudin C, Molez J, Ouedraogo V, Carnevale P. La Transmission du Paludisme en Zone de Savane Arboree et en Zone Rizicole des Environs de Bobo Dioulasso (Burkina Faso). *Ann Soc Belg Med Trop*. 1985;65(2):201-214.
448. Ngowo HS, Hape EE, Matthiopoulos J, Ferguson HM, Okumu FO. Fitness characteristics of the malaria vector Anopheles funestus during an attempted laboratory colonization. *Malar J*. 2021;20(1):148. doi:10.1186/s12936-021-03677-3.
449. Nepomichene TN, Andrianaivolambo L, Boyer S, Bourgouin C. Efficient method for establishing F1 progeny from wild populations of Anopheles mosquitoes. *Malar J*. 2017;16(1):21. doi:10.1186/s12936-017-1681-7.
450. Tchigossou G, Akoton R, Yessoufou A, Djegbe I, Zeukeng F, Atoyebi SM, Tossou E, Moutairou K, Djouaka R. Water source most suitable for rearing a sensitive malaria vector, Anopheles funestus in the laboratory. *Wellcome open Res*. 2017;2:109. doi:10.12688/wellcomeopenres.12942.2.
451. Okoye PN, Brooke BD, Hunt RH, Coetzee M. Relative developmental and reproductive fitness associated with pyrethroid resistance in the major southern African malaria vector, Anopheles funestus. *Bull Entomol Res*. 2007;97(6):599-605. doi:10.1017/S0007485307005317.
452. McCann RS, Ochomo E, Bayoh MN, Vulule JM, Hamel MJ, Gimnig JE, Hawley WA, Walker ED. Reemergence of Anopheles funestus as a vector of Plasmodium falciparum in western Kenya after long-term implementation of insecticide-treated bed nets. *Am J Trop Med Hyg*. 2014;90(4):597-604. doi:10.4269/ajtmh.13-0614.

453. Cohuet A, Dia I, Simard F, Raymond M, Rousset F, Antonio-Nkondjio C, Awono-Ambene PH, Wondji CS, Fontenille D. Gene flow between chromosomal forms of the malaria vector Anopheles funestus in Cameroon, Central Africa, and its relevance in malaria fighting. *Genetics*. 2005;169(1):301-311. doi:10.1534/genetics.103.025031.
454. Pinda PG, Eichenberger C, Ngowo HS, Msaky DS, Abbasi S, Kihonda J, Bwanaly H, Okumu FO. Comparative assessment of insecticide resistance phenotypes in two major malaria vectors, Anopheles funestus and Anopheles arabiensis in south-eastern Tanzania. *Malar J*. 2020;19(1):408. doi:10.1186/s12936-020-03483-3.
455. Costantini C, Sagnon N, Ilboudo-Sanogo E, Coluzzi M, Boccolini D. Chromosomal and bionomic heterogeneities suggest incipient speciation in Anopheles funestus from Burkina Faso. *Parassitologia*. 1999;41(4):595-611. http://www.ncbi.nlm.nih.gov/pubmed/10870569. Accessed August 31, 2021.
456. Sinka ME, Bangs MJ, Manguin S, Coetzee M, Mbogo CM, Hemingway J, Patil AP, Temperley WH, Gething PW, Kabaria CW, Okara RM, Van Boeckel T, Godfray HCJ, Harbach RE, Hay SI. The dominant Anopheles vectors of human malaria in Africa, Europe and the Middle East: occurrence data, distribution maps and bionomic précis. *Parasit Vectors*. 2010;3(1):117. doi:10.1186/1756-3305-3-117.
457. Nambunga IH, Ngowo HS, Mapua SA, Hape EE, Msugupakulya BJ, Msaky DS, Mhumbira NT, Mchwembo KR, Tamayamali GZ, Mlembe S V., Njalambaha RM, Lwetoijera DW, Finda MF, Govella NJ, Matoke-Muhia D, Kaindoa EW, Okumu FO. Aquatic habitats of the malaria vector Anopheles funestus in rural south-eastern Tanzania. *Malar J*. 2020;19(1):219. doi:10.1186/s12936-020-03295-5.
458. Kaindoa EW, Matowo NS, Ngowo HS, Mkandawile G, Mmbando A, Finda M, Okumu FO. Interventions that effectively target Anopheles funestus mosquitoes could significantly improve control of persistent malaria transmission in south–eastern Tanzania. Brooke B, ed. *PLoS One*. 2017;12(5):e0177807. doi:10.1371/journal.pone.0177807.
459. Mmbando AS, Kaindoa EW, Ngowo HS, Swai JK, Matowo NS, Kilalangongono M, Lingamba GP, Mgando JP, Namango IH, Okumu FO, Nelli L. Fine-scale distribution of malaria mosquitoes biting or resting outside human dwellings in three low-altitude Tanzanian villages. Carvalho LH, ed. *PLoS One*. 2021;16(1):e0245750. doi:10.1371/journal.pone.0245750.
460. Ghosh AK, Jacobs-Lorena M. Plasmodium sporozoite invasion of the mosquito salivary gland. *Curr Opin Microbiol*. 2009;12(4):394-400. doi:10.1016/j.mib.2009.06.010.
461. Yman V, Wandell G, Mutemi DD, Miglar A, Asghar M, Hammar U, Karlsson M, Lind I, Nordfjell C, Rooth I, Ngasala B, Homann MV, Färnert A. Persistent transmission of plasmodium malariae and plasmodium ovale species in an area of declining plasmodium falciparum transmission in Eastern Tanzania. *PLoS Negl Trop Dis*. 2019;13(5):1-16. doi:10.1371/journal.pntd.0007414.
462. Graumans W, Jacobs E, Bousema T, Sinnis P. When Is a Plasmodium-Infected Mosquito an Infectious Mosquito? *Trends Parasitol*. 2020;36(8):705-716. doi:10.1016/J.PT.2020.05.011.
463. Churcher TS, Sinden RE, Edwards NJ, Poulton ID, Rampling TW, Brock PM, Griffin JT, Upton LM, Zakutansky SE, Sala KA, Angrisano F, Hill AVS, Blagborough AM. Probability of Transmission of Malaria from Mosquito to Human Is Regulated by Mosquito Parasite Density in Naïve and Vaccinated Hosts. Wenger E, ed. *PLOS Pathog*. 2017;13(1):e1006108. doi:10.1371/journal.ppat.1006108.

464. Wang CYT, McCarthy JS, Stone WJ, Bousema T, Collins KA, Bialasiewicz S. Assessing Plasmodium falciparum transmission in mosquito-feeding assays using quantitative PCR. *Malar J*. 2018;17(1):249. doi:10.1186/s12936-018-2382-6.
465. Rungsiwongse J, Rosenberg R. The Number of Sporozoites Produced by Individual Malaria Oocysts. *Am J Trop Med Hyg*. 1991;45(5):574-577. doi:10.4269/ajtmh.1991.45.574.
466. Tusting LS, Bousema T, Smith DL, Drakeley C. Measuring changes in Plasmodium falciparum transmission: precision, accuracy and costs of metrics. *Adv Parasitol*. 2014;84:151-208. doi:10.1016/B978-0-12-800099-1.00003-X.
467. Aron JL, May RM. The population dynamics of malaria. In: *The Population Dynamics of Infectious Diseases: Theory and Applications*. Boston, MA: Springer US; 1982:139-179. doi:10.1007/978-1-4899-2901-3_5.
468. Smith DL, Dushoff J, McKenzie FE. The Risk of a Mosquito-Borne Infectionin a Heterogeneous Environment. Andy P. Dobson, ed. *PLoS Biol*. 2004;2(11):e368. doi:10.1371/journal.pbio.0020368.
469. Reiner RC, Guerra C, Donnelly MJ, Bousema T, Drakeley C, Smith DL. Estimating malaria transmission from humans to mosquitoes in a noisy landscape. *J R Soc Interface*. 2015;12(111):20150478. doi:10.1098/rsif.2015.0478.
470. Shokoples SE, Ndao M, Kowalewska-Grochowska K, Yanow SK. Multiplexed real-time PCR assay for discrimination of Plasmodium species with improved sensitivity for mixed infections. *J Clin Microbiol*. 2009;47(4):975-980. doi:10.1128/JCM.01858-08.
471. Wilkins EE, Howell PI, Benedict MQ. Malaria Journal IMP PCR primers detect single nucleotide polymorphisms for Anopheles gambiae species identification, Mopti and Savanna rDNA types, and resistance to dieldrin in Anopheles arabiensis. *Centers Dis Control Prev*. 2006;(2). doi:10.1186/1475-2875-5-125.
472. Olayemi IK, Ande & AT. *Life Table Analysis of Anopheles Gambiae (Diptera: Culicidae) in Relation to Malaria Transmission*. Vol 46.; 2009. http://www.mrcindia.org/journal/issues/464295.pdf. Accessed August 21, 2021.
473. Gillies MT. *The East African Medical Journal : The Organ of the Medical Association of East Africa*. Vol 30. Medical Association of East Africa; 1953. https://www.cabdirect.org/cabdirect/abstract/19541000205. Accessed August 21, 2021.
474. Wilke ABB, Christe R de O, Multini LC, Vidal PO, Wilk-da-Silva R, de Carvalho GC, Marrelli MT. Morphometric Wing Characters as a Tool for Mosquito Identification. Moreira LA, ed. *PLoS One*. 2016;11(8):e0161643. doi:10.1371/journal.pone.0161643.
475. Vyas-Patel N, Ravela S, Mafra-Neto A, Mumford JD. Insect Wing Classification of Mosquitoes and Bees Using CO1 Image Recognition. *bioRxiv*. 2015. doi:10.1101/034819.
476. Mulchandani P, Siddiqui MU, Kanani P. Real-Time Mosquito Species Identification using Deep Learning Techniques. *Int J Eng Adv Technol*. 2019;(9):2249-8958. doi:10.35940/ijeat.B2929.129219.
477. Yeap HL, Endersby NM, Johnson PH, Ritchie SA, Hoffmann AA. Body size and wing shape measurements as quality indicators of Aedes aegypti mosquitoes destined for field release. *Am J Trop Med Hyg*. 2013;89(1):78-92. doi:10.4269/ajtmh.12-0719.
478. Armbruster P, Hutchinson RA. Pupal Mass and Wing Length as Indicators of Fecundity in *Aedes albopictus* and *Aedes geniculatus* (Diptera: Culicidae). *J Med Entomol*. 2002;39(4):699-704. doi:10.1603/0022-2585-39.4.699.
479. Sarr MD, Sylla M, Foy BD, Chapman PL, Kobylinski KC. Ivermectin Mass Drug

Administration to Humans Disrupts Malaria Parasite Transmission in Senegalese Villages. *Am J Trop Med Hyg*. 2011;85(1):3-5. doi:10.4269/ajtmh.2011.11-0160.
480. Slater HC, Walker PGT, Bousema T, Okell LC, Ghani AC. The potential impact of adding ivermectin to a mass treatment intervention to reduce malaria transmission: a modelling study. *J Infect Dis*. 2014;210(12):1972-1980. doi:10.1093/infdis/jiu351.
481. Deus KM, Saavedra-Rodriguez K, Butters MP, Black WC, Foy BD. The effect of ivermectin in seven strains of Aedes aegypti (Diptera: Culicidae) including a genetically diverse laboratory strain and three permethrin resistant strains. *J Med Entomol*. 2012;49(2):356-363. http://www.ncbi.nlm.nih.gov/pubmed/22493855. Accessed March 21, 2018.
482. Alout H, Ndam NT, Sandeu MM, Djégbe I, Chandre F, Dabiré RK, Djogbénou LS, Corbel V, Cohuet A. Insecticide Resistance Alleles Affect Vector Competence of Anopheles gambiae s.s. for Plasmodium falciparum Field Isolates. Vontas J, ed. *PLoS One*. 2013;8(5):e63849. doi:10.1371/journal.pone.0063849.
483. Collins E, Vaselli NM, Sylla M, Beavogui AH, Orsborne J, Lawrence G, Wiegand RE, Irish SR, Walker T, Messenger LA. The relationship between insecticide resistance, mosquito age and malaria prevalence in Anopheles gambiae s.l. from Guinea. *Sci Rep*. 2019;9(1):8846. doi:10.1038/s41598-019-45261-5.
484. Jones CM, Sanou A, Guelbeogo WM, Sagnon N, Johnson PC, Ranson H. Aging partially restores the efficacy of malaria vector control in insecticide-resistant populations of Anopheles gambiae s.l. from Burkina Faso. *Malar J*. 2012;11(1):24. doi:10.1186/1475-2875-11-24.
485. Lines JD, Nassor NS. DDT resistance in Anopheles gambiae declines with mosquito age. *Med Vet Entomol*. 1991;5(3):261-265. doi:10.1111/j.1365-2915.1991.tb00550.x.
486. Rajatileka S, Burhani J, Ranson H. Mosquito age and susceptibility to insecticides. *Trans R Soc Trop Med Hyg*. 2011;105(5):247-253. doi:10.1016/j.trstmh.2011.01.009.
487. Hodjati MH, Curtis CF. Evaluation of the effect of mosquito age and prior exposure to insecticide on pyrethroid tolerance in *Anopheles* mosquitoes (Diptera: Culicidae). *Bull Entomol Res*. 1999;89(4):329-337. doi:10.1017/S0007485399000462.
488. Oliveira ARS, Strathe E, Etcheverry L, Cohnstaedt LW, McVey DS, Piaggio J, Cernicchiaro N. Assessment of data on vector and host competence for Japanese encephalitis virus: A systematic review of the literature. *Prev Vet Med*. 2018;154:71-89. doi:10.1016/J.PREVETMED.2018.03.018.
489. Golnar AJ, Turell MJ, LaBeaud AD, Kading RC, Hamer GL. Predicting the Mosquito Species and Vertebrate Species Involved in the Theoretical Transmission of Rift Valley Fever Virus in the United States. Barker CM, ed. *PLoS Negl Trop Dis*. 2014;8(9):e3163. doi:10.1371/journal.pntd.0003163.
490. Cooper L, Kang SY, Bisanzio D, Maxwell K, Rodriguez-Barraquer I, Greenhouse B, Drakeley C, Arinaitwe E, G Staedke S, Gething PW, Eckhoff P, Reiner RC, Hay SI, Dorsey G, Kamya MR, Lindsay SW, Grenfell BT, Smith DL, Smith DL. Pareto rules for malaria super-spreaders and super-spreading. *Nat Commun*. 2019;10(1):3939. doi:10.1038/s41467-019-11861-y.

APPENDIX A: SUPPLEMENTAL MATERIAL

S1. Chapter 2 Supplemental Material

Weeks 1, 3, 5, 7, 9

TASK	MONDAY	TUESDAY	WEDNESDAY	THURSDAY	FRIDAY	SATURDAY	SUNDAY
Blood feed		✓			✓		
IVM blood feed (for IVM mesocosm only)							
Remove 15 females			✓			✓	
Add 200 color-tagged females to each mesocosm	✓						
Add 30 untagged mosquitoes to each mesocom				✓			

Weeks 2, 4, 6, 8, 10

TASK	MONDAY	TUESDAY	WEDNESDAY	THURSDAY	FRIDAY	SATURDAY	SUNDAY
Blood feed		✓					
IVM blood feed (for IVM mesocosm only)					✓		
Remove 15 females			✓			✓	
Add 200 color-tagged females to each mesocosm							
Add 30 untagged mosquitoes to each mesocom	✓			✓			

Figure S1.1. Visual representation of mesocosm experimental schedule. Male and female G3 *Anopheles gambiae* s.l mosquitoes were added to each mesocosm 24 hours before any blood feed. During a two-week period, 30 newly emerged, unmarked mosquitoes were added. To simulate a mass emergence event, every other week one of these normal inputs was replaced by a batch of ~200 newly emerged, mixed male and female mosquitoes. These mosquitoes were marked with a fluorescent powder prior to entry. Fifteen female mosquitoes were sampled from each mesocosm twice a week. Blood feeding occurred twice a week. For the ivermectin-exposed mesocosm, every fourth bloodmeal contained 5 ng/μL ivermectin.

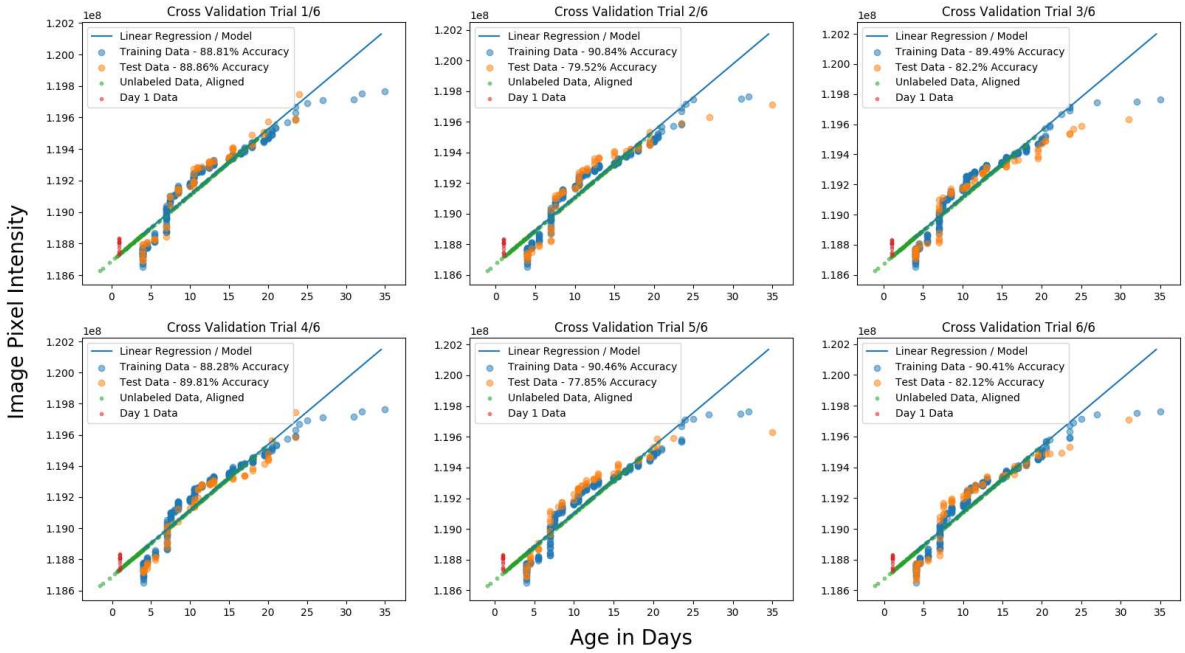

Figure S1.2. Linear regression analyses plotting mosquito age vs. pixel intensity score for wing images using training and testing datasets. Each regression used average pixel intensity score data from left and right wings of individual mosquitoes of known and unknown age from the control mesocosm only. The Y-axis refers to the pixel intensity score obtained from the wing photos of each mosquito (lower values are more black and higher values are whiter; as a mosquito ages in the mesocosm, it loses scales from flying and thus the mean pixel intensity of the wings becomes whiter). Blue dots are the training dataset (80% of the marked mosquitoes, randomly selected), that were used to predict the age of the remaining 20% of marked mosquitoes (orange dots – test dataset) for model validation. Data from mosquitoes of unknown age are included as green dots aligned to linear regression line based on their predicted age using the model. Pixel intensity from newly emerged mosquitoes (day= 1) is represented by red dots on each graph.

S2. Chapter 3 Supplemental Material

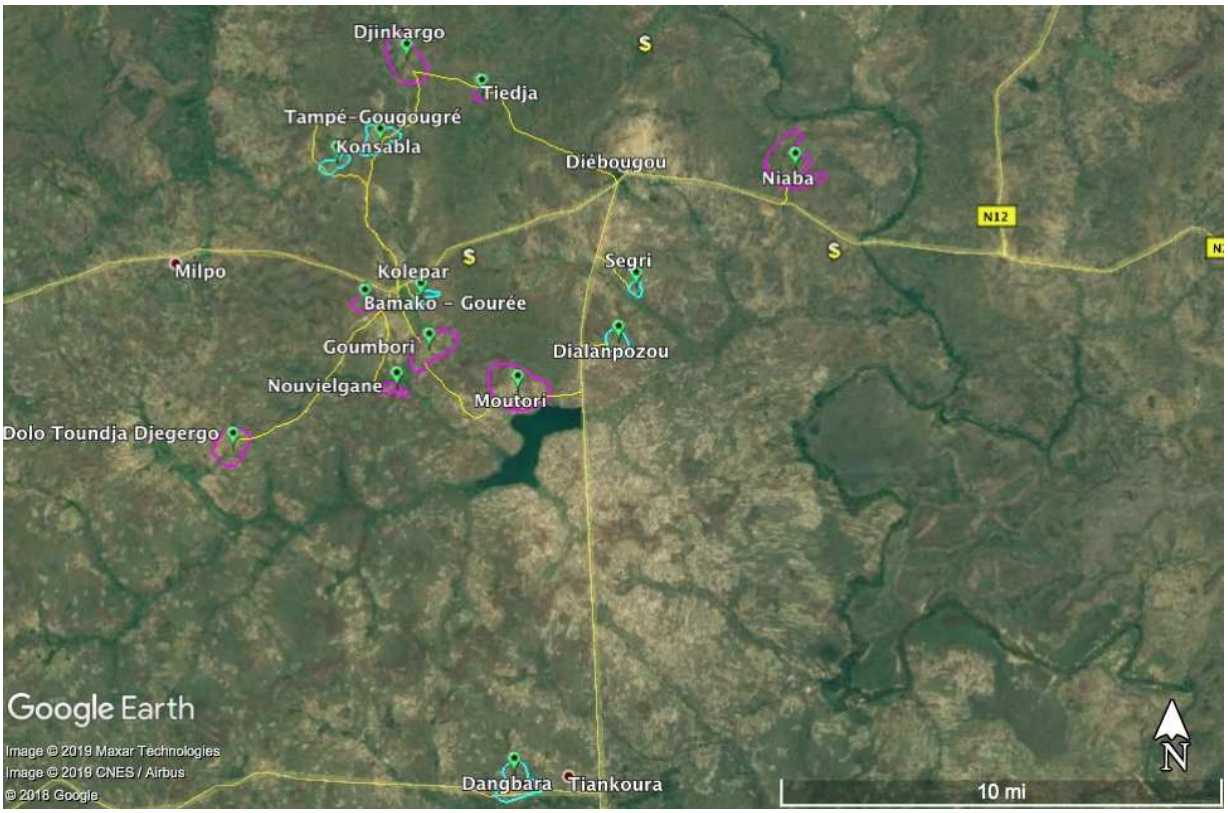

Figure S2.1. Map of the 14 villages within the Diebougou health district enrolled in RIMDAMAL II: Bamako-Gourée, Dangbara, Dialanpozu, Djinkargo, Dolo Toundja Djegergo, Goumbori, Kolepar, Konsabla, Moutori, Niaba, Nouvielgane, Segri, Tampé-Gougougré, and Tiedja. Fuchsia and teal lines represent village borders while yellow lines represent major roadways. All villages participated in clinical surveillance, while only those outlined in teal were regularly sampled for mosquitoes. Yellow dollar signs indicate known locations of gold mining, which were sites of potential security risk.

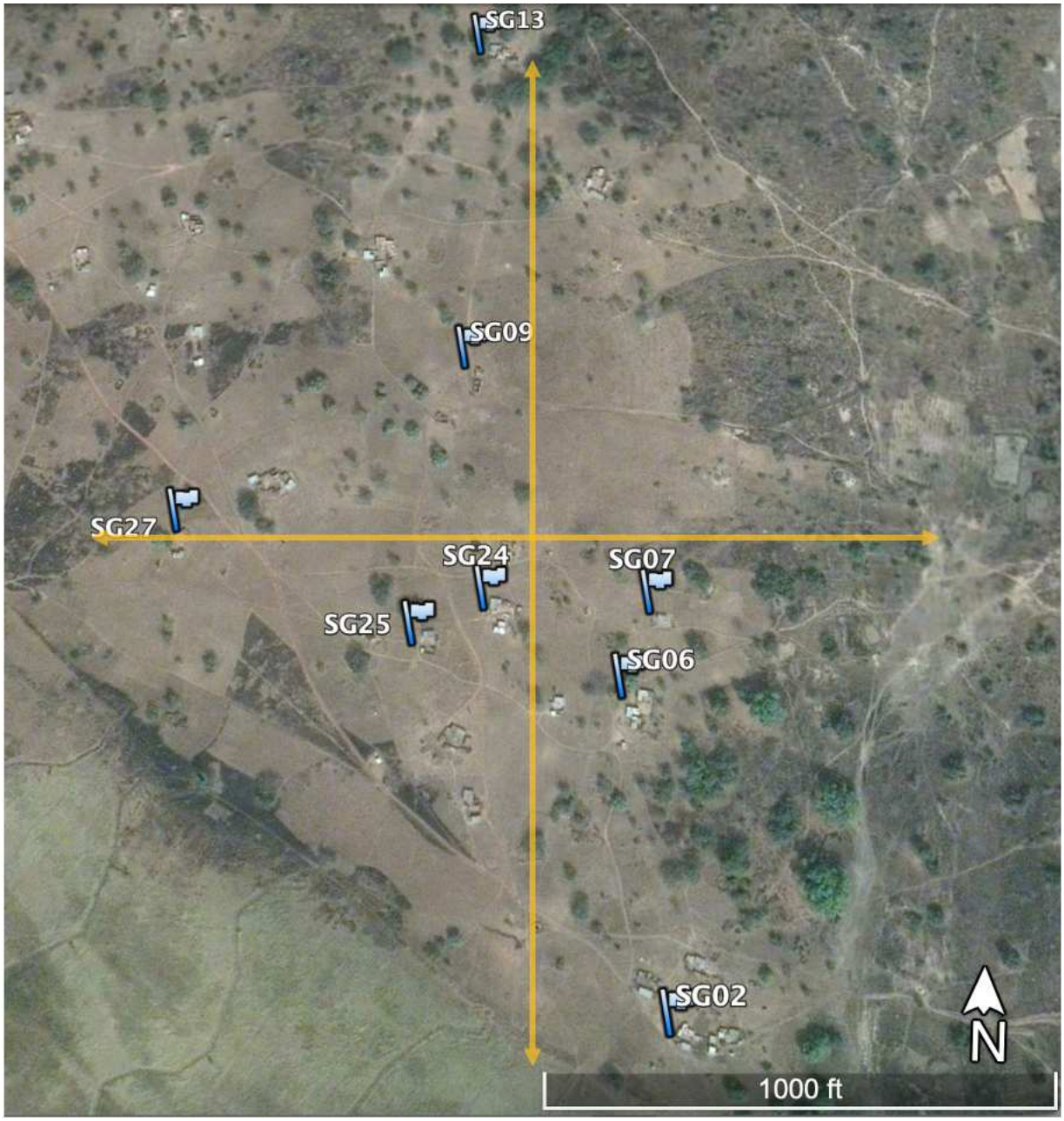

Figure S2.2. Example of a RIMDAMAL II village transect. Eight household were selected in each village for weekly mosquito sampling. These households were chosen by making one east-west and one north-south transect across the village. The four innermost (SG07, SG06, SG25, and SG24) and the four outermost households (SG02, SG27, SG09, SG13) lying on or closest to these transects were selected for entomological sampling.

S3. Chapter 4 Supplemental Material

Table S3.1. Summary of all anophelines collected from the field during the 2019 RIMDAMAL II field season, by sampling village and trap method

Village	Trap type	MDA1 + 1	MDA1 + 3	MDA2 + 1	MDA2 + 3	MDA3 + 1	MDA3 + 3	MDA4 + 1	MDA4 + 3	Village total by trap
DB	ASP	25	25	34	30	25	33	35	22	229
	LTC Indoors	1	44	32	40	8	10	7	4	146
	LTC Outdoors	0	0	0	1	3	1	0	0	5
DL	ASP	25	38	34	34	30	34	34	30	259
	LTC indoors	15	3	8	0	12	14	2	3	57
	LTC Outdoors	5	0	10	27	5	5	2	24	78
KP	ASP	35	19	31	24	19	28	27	20	203
	LTC Indoors	0	2	0	19	0	1	3	2	27
	LTC Outdoors	1	0	0	1	0	0	2	0	4
KS	ASP	14	21	27	16	25	21	21	20	165
	LTC Indoors	0	3	27	11	10	4	9	3	67
	LTC Outdoors	20	2	13	14	9	2	11	2	73
SG	ASP	11	26	24	28	21	35	29	32	206
	LTC Indoors	7	6	5	0	2	21	14	0	55
	LTC Outdoors	1	4	13	14	11	7	11	0	61
TG	ASP	18	18	35	28	34	30	31	20	214
	LTC Indoors	4	6	0	2	2	0	6	1	21
	LTC Outdoors	2	1	3	5	11	2	0	3	27
2019 RIMDAMAL II total:		184	218	296	294	227	248	244	186	1897

Table S3.2. Summary of all anophelines collected from the field during the 2020 RIMDAMAL II field season, by sampling village and trap method

Village	Trap type	MDA5 + 1	MDA5 + 3	MDA6 + 1	MDA6 + 3	MDA7 + 1	MDA7 + 3	MDA8 + 1	MDA8 + 3	Village total by trap
DB	ASP	19	23	25	30	30	23	20	6	176
	LTC Indoors	7	0	0	0	4	16	1	0	28
	LTC Outdoors	5	0	0	0	4	12	3	0	24
DL	ASP	21	9	26	35	33	31	27	9	191
	LTC indoors	0	0	0	0	2	0	2	0	4
	LTC Outdoors	0	0	0	0	0	0	1	0	1
KP	ASP	11	15	6	24	15	16	10	24	121
	LTC Indoors	0	0	0	0	11	2	0	0	13
	LTC Outdoors	0	0	0	0	6	6	0	0	12
KS	ASP	15	16	18	30	23	21	13	2	138
	LTC Indoors	1	0	0	0	21	0	4	0	26
	LTC Outdoors	1	0	0	0	0	0	0	0	1
SG	ASP	16	8	12	25	24	25	15	3	128
	LTC Indoors	0	0	0	0	5	2	2	0	9
	LTC Outdoors	0	0	0	0	6	0	4	0	10
TG	ASP	13	14	19	25	22	24	14	14	145
	LTC Indoors	0	0	0	0	1	0	1	0	2
	LTC Outdoors	0	0	0	0	0	0	2	0	2
2020 RIMDAMAL II total:		109	85	106	169	207	178	119	58	1031

Table S3.3. Quantification results and demographic information for mosquito head+thorax samples that tested positive for *P. falciparum* over the course of RIMDAMAL II

Sample number	Study year	Village	Trap type	Trap location	MDA time	Mosquito clade	*An. gambiae* species	Genomes per sample
363	2019	DL	ASP	Indoors	MDA1+1	*An. gambiae* s.l	*An. coluzzii*	23,930.30
519	2019	KP	ASP	Indoors	MDA1+1	*An. gambiae* s.l	*An. gambiae* s.s	33,851.17
943	2019	SG	ASP	Indoors	MDA1+3	*An. gambiae* s.l	*An. coluzzii*	23,314.65
979	2019	KP	ASP	Indoors	MDA1+3	*An. gambiae* s.l	*An. coluzzii*	153.04
1196	2019	DL	LT	Indoors	MDA2+1	*An. gambiae* s.l	*An. gambiae* s.s	517.43
1553	2019	TG	ASP	Indoors	MDA2+1	*An. funestus*	na	2,935.70
1876	2019	TG	ASP	Indoors	MDA2+3	*An. gambiae* s.l	*An. gambiae* s.s	842.12
1975	2019	KS	ASP	Indoors	MDA2+3	*An. gambiae* s.l	*An. coluzzii*	4,006.39
1977	2019	KS	ASP	Indoors	MDA2+3	*An. funestus*	na	26,487.05
3193	2019	TG	ASP	Indoors	MDA3+1	*An. funestus*	na	3,651.75
3297	2019	KP	ASP	Indoors	MDA3+1	*An. funestus*	na	7,290.88
3590	2019	TG	ASP	Indoors	MDA3+3	*An. gambiae* s.l	*An. gambiae* s.s	802.17
3606	2019	TG	ASP	Indoors	MDA3+3	*An. gambiae* s.l	*An. gambiae* s.s	1,527.67
3702	2019	DB	ASP	Indoors	MDA3+3	*An. funestus*	na	11,592.94
3840	2019	DL	ASP	Indoors	MDA3+3	*An. gambiae* s.l	*An. gambiae* s.s	532.36
3857	2019	DL	LT	Indoors	MDA3+3	*An. gambiae* s.l	*An. gambiae* s.s	817.37
3904	2019	SG	ASP	Indoors	MDA3+3	*An. gambiae* s.l	*An. coluzzii*	1,621.16
4321	2019	DB	ASP	Indoors	MDA4+1	*An. gambiae* s.l	*An. gambiae* s.s	4,523.72
4331	2019	DB	ASP	Indoors	MDA4+1	*An. gambiae* s.l	*An. coluzzii*	80,968.23
4355	2019	DB	ASP	Indoors	MDA4+1	*An. gambiae* s.l	*An. gambiae* s.s	244.89
4373	2019	DB	ASP	Indoors	MDA4+1	*An. gambiae* s.l	*An. coluzzii*	4,827.04
4751	2019	TG	ASP	Indoors	MDA4+1	*An. gambiae* s.l	*An. gambiae* s.s	2,567.62
4789	2019	KP	ASP	Indoors	MDA4+1	*An. funestus*	na	1,452.95
4929	2019	KS	ASP	Indoors	MDA4+3	*An. gambiae* s.l	*An. gambiae* s.s	2,223.65

4933	2019	KS	ASP	Indoors	MDA4+3	*An. gambiae* s.l	*An. gambiae* s.s	601.59
4989	2019	TG	ASP	Indoors	MDA4+3	*An. gambiae* s.l	An. arabiensis	354.73
5007	2019	KP	ASP	Indoors	MDA4+3	*An. gambiae* s.l	*An. gambiae* s.s	251.26
5073	2019	DB	ASP	Indoors	MDA4+3	*An. funestus*	na	7,719.46
5089	2019	DB	ASP	Indoors	MDA4+3	*An. funestus*	na	8,064.18
5095	2019	DB	ASP	Indoors	MDA4+3	*An. gambiae* s.l	*An. gambiae* s.s	5,949.56
5595	2020	TG	ASP	Indoors	MDA5+1	*An. gambiae* s.l	*An. gambiae* s.s	767.30
5606	2020	KS	ASP	Indoors	MDA5+1	*An. funestus*	na	11,402.40
5669	2020	DB	ASP	Indoors	MDA5+1	*An. gambiae* s.l	*An. gambiae* s.s	590.46
5712	2020	DB	LT	Indoors	MDA5+1	*An. gambiae* s.l	*An. gambiae* s.s	1,692.70
5776	2020	SG	ASP	Indoors	MDA5+1	*An. gambiae* s.l	*An. coluzzii*	3,512.16
5842	2020	DB	ASP	Indoors	MDA5+3	*An. gambiae* s.l	*An. gambiae* s.s	47,187.90
5852	2020	DB	ASP	Indoors	MDA5+3	*An. gambiae* s.l	*An. coluzzii*	1,097.26
5868	2020	DB	ASP	Indoors	MDA5+3	*An. gambiae* s.l	*An. gambiae* s.s	62,272.69
5870	2020	DB	ASP	Indoors	MDA5+3	*An. gambiae* s.l	*An. gambiae* s.s	61,286.76
5917	2020	SG	ASP	Indoors	MDA5+3	*An. gambiae* s.l	*An. gambiae* s.s	1,025.16
5943	2020	KS	ASP	Indoors	MDA5+3	*An. gambiae* s.l	*An. gambiae* s.s	458.08
5945	2020	KS	ASP	Indoors	MDA5+3	*An. gambiae* s.l	An. arabiensis	40,619.15
5947	2020	KS	ASP	Indoors	MDA5+3	*An. gambiae* s.l	*An. gambiae* s.s	90,774.23
6076	2020	SG	ASP	Indoors	MDA6+1	*An. gambiae* s.l	*An. gambiae* s.s	703.85
6162	2020	DB	ASP	Indoors	MDA6+1	*An. gambiae* s.l	*An. gambiae* s.s	22,016.35
6164	2020	DB	ASP	Indoors	MDA6+1	*An. gambiae* s.l	*An. gambiae* s.s	19,051.51
6166	2020	DB	ASP	Indoors	MDA6+1	*An. gambiae* s.l	*An. gambiae* s.s	539.32
6188	2020	DB	ASP	Indoors	MDA6+1	*An. gambiae* s.l	*An. gambiae* s.s	25,233.84
6200	2020	DB	ASP	Indoors	MDA6+1	*An. gambiae* s.l	*An. gambiae* s.s	425.65
6212	2020	DB	ASP	Indoors	MDA6+1	*An. gambiae* s.l	*An. gambiae* s.s	7,073.74
6214	2020	DB	ASP	Indoors	MDA6+1	*An. gambiae* s.l	*An. gambiae* s.s	1,232.85
6224	2020	TG	ASP	Indoors	MDA6+1	*An. gambiae* s.l	*An. gambiae* s.s	2,915.03
6246	2020	TG	ASP	Indoors	MDA6+1	*An. gambiae* s.l	*An. gambiae* s.s	4,088.49

6286	2020	KS	ASP	Indoors	MDA6+1	*An. gambiae* s.l	*An. gambiae* s.s	8,528.35
6290	2020	KS	ASP	Indoors	MDA6+1	*An. gambiae* s.l	*An. gambiae* s.s	7,871.56
6315	2020	DL	ASP	Indoors	MDA6+1	*An. gambiae* s.l	*An. gambiae* s.s	289.21
6371	2020	DL	ASP	Indoors	MDA6+3	*An. gambiae* s.l	*An. gambiae* s.s	585.95
6397	2020	DL	ASP	Indoors	MDA6+3	*An. gambiae* s.l	*An. gambiae* s.s	47,520.16
6399	2020	DL	ASP	Indoors	MDA6+3	*An. gambiae* s.l	*An. gambiae* s.s	32,037.06
6405	2020	DL	ASP	Indoors	MDA6+3	*An. gambiae* s.l	*An. gambiae* s.s	1,375.73
6427	2020	DL	ASP	Indoors	MDA6+3	*An. gambiae* s.l	*An. coluzzii*	15,588.66
6487	2020	KS	ASP	Indoors	MDA6+3	*An. gambiae* s.l	*An. gambiae* s.s	19,579.28
6537	2020	TG	ASP	Indoors	MDA6+3	*An. gambiae* s.l	*An. gambiae* s.s	14,104.80
6571	2020	DB	ASP	Indoors	MDA6+3	*An. gambiae* s.l	*An. coluzzii*	36,717.33
7237	2020	TG	ASP	Indoors	MDA7+1	*An. gambiae* s.l	*An. gambiae* s.s	912.97
7501	2020	DB	ASP	Indoors	MDA7+1	*An. gambiae* s.l	*An. gambiae* s.s	1,617.90
7509	2020	DB	ASP	Indoors	MDA7+1	*An. gambiae* s.l	*An. gambiae* s.s	8,169.21
7565	2020	DB	ASP	Indoors	MDA7+1	*An. gambiae* s.l	*An. gambiae* s.s	6,252.58
7878	2020	SG	ASP	Indoors	MDA7+3	*An. gambiae* s.l	*An. gambiae* s.s	4,533.60
8040	2020	DL	ASP	Indoors	MDA7+3	*An. gambiae* s.l	*An. gambiae* s.s	907.72
8119	2020	DB	LT	Outdoors	MDA7+3	*An. gambiae* s.l	*An. gambiae* s.s	1,751.51
8216	2020	KS	ASP	Indoors	MDA7+3	*An. gambiae* s.l	*An. gambiae* s.s	14,255.29
8388	2020	SG	ASP	Indoors	MDA8+1	*An. gambiae* s.l	*An. gambiae* s.s	3,138.36
8408	2020	DB	ASP	Indoors	MDA8+1	*An. gambiae* s.l	*An. coluzzii*	9,537.47
8452	2020	SG	LT	Indoors	MDA8+1	*An. gambiae* s.l	*An. gambiae* s.s	53,740.01
8453	2020	SG	LT	Outdoors	MDA8+1	*An. gambiae* s.l	*An. coluzzii*	9,000.70
8619	2020	KP	ASP	Indoors	MDA8+3	*An. gambiae* s.l	*An. gambiae* s.s	1,997.09
8691	2020	DB	ASP	Indoors	MDA8+3	*An. gambiae* s.l	*An. gambiae* s.s	590.10

Table S3.4. Quantification results and demographic information for mosquito head+thorax samples that tested positive for *P. ovale* over the course of RIMDAMAL II

Sample number	Study year	Village	Trap type	Trap location	MDA time	Mosquito clade	*An. gambiae* species	Genomes per sample
717	2019	KS	ASP	Indoors	MDA1+3	*An. funestus*	na	125.23
719	2019	KS	ASP	Indoors	MDA1+3	*An. funestus*	na	859.70
739	2019	TG	ASP	Indoors	MDA1+3	*An. gambiae* s.l	*An. gambiae* s.s	696.78
799	2019	DL	ASP	Indoors	MDA1+3	*An. funestus*	na	98.59
955	2019	SG	ASP	Indoors	MDA1+3	*An. funestus*	na	1,697.88
963	2019	SG	ASP	Indoors	MDA1+3	*An. gambiae* s.l	*An. gambiae* s.s	1,258.20
1182	2019	DL	ASP	Indoors	MDA2+1	*An. gambiae* s.l	*An. gambiae* s.s	1,588.32
1235	2019	SG	LT	Outdoors	MDA2+1	*An. gambiae* s.l	*An. gambiae* s.s	1,317.78
1295	2019	DB	ASP	Indoors	MDA2+1	*An. gambiae* s.l	*An. gambiae* s.s	1,172.95
1406	2019	KP	ASP	Indoors	MDA2+1	*An. gambiae* s.l	*An. gambiae* s.s	1,502.61
1971	2019	KS	ASP	Indoors	MDA2+3	*An. funestus*	na	705.28
3034	2019	DL	ASP	Indoors	MDA3+1	*An. gambiae* s.l	*An. gambiae* s.s	920.55
3047	2019	DB	LT	Outdoors	MDA3+1	*An. funestus*	na	737.94
3313	2019	SG	ASP	Indoors	MDA3+1	*An. gambiae* s.l	*An. gambiae* s.s	178.20
3337	2019	SG	ASP	Indoors	MDA3+1	*An. funestus*	na	1,895.30
3359	2019	SG	LT	Outdoors	MDA3+1	*An. gambiae* s.l	*An. gambiae* s.s	934.91
3546	2019	KS	ASP	Indoors	MDA3+3	*An. gambiae* s.l	*An. gambiae* s.s	1,429.63
3676	2019	KP	ASP	Indoors	MDA3+3	*An. gambiae* s.l	*An. gambiae* s.s	1,117.51
3686	2019	KP	ASP	Indoors	MDA3+3	*An. gambiae* s.l	*An. gambiae* s.s	2,061.21
3834	2019	DL	ASP	Indoors	MDA3+3	*An. gambiae* s.l	*An. gambiae* s.s	1,306.32
3934	2019	SG	ASP	Indoors	MDA3+3	*An. gambiae* s.l	*An. gambiae* s.s	2,233.99
4355	2019	DB	ASP	Indoors	MDA4+1	*An. gambiae* s.l	*An. gambiae* s.s	3,020.10
4391	2019	DB	LT	Indoors	MDA4+1	*An. gambiae* s.l	*An. gambiae* s.s	1,936.82
4582	2019	SG	LT	Indoors	MDA4+1	*An. gambiae* s.l	*An. gambiae* s.s	1,640.17

4731	2019	TG	ASP	Indoors	MDA4+1	*An. gambiae* s.l	*An. gambiae* s.s	2,105.70
4923	2019	KS	ASP	Indoors	MDA4+3	*An. funestus*	na	992.78
4955	2019	KS	LT	Outdoors	MDA4+3	*An. funestus*	na	702.21
4956	2019	KS	LT	Indoors	MDA4+3	*An. funestus*	na	1,342.93
4969	2019	TG	ASP	Indoors	MDA4+3	*An. funestus*	na	2,189.93
4993	2019	TG	ASP	Indoors	MDA4+3	*An. funestus*	na	920.36
5006	2019	TG	LT	Outdoors	MDA4+3	*An. funestus*	na	2,655.05
5027	2019	KP	ASP	Indoors	MDA4+3	*An. funestus*	na	1,642.65
5047	2019	KP	LT	Indoors	MDA4+3	*An. funestus*	na	3,739.43
5077	2019	DB	ASP	Indoors	MDA4+3	*An. gambiae* s.l	*An. gambiae* s.s	877.99
5089	2019	DB	ASP	Indoors	MDA4+3	*An. funestus*	na	775.67
5099	2019	DB	LT	Indoors	MDA4+3	*An. funestus*	na	25.82
5124	2019	DL	ASP	Indoors	MDA4+3	*An. funestus*	na	38.12
5130	2019	DL	ASP	Indoors	MDA4+3	*An. funestus*	na	3,102.14
5154	2019	DL	ASP	Indoors	MDA4+3	*An. funestus*	na	1,097.93
5204	2019	SG	ASP	Indoors	MDA4+3	*An. funestus*	na	1,618.88
8186	2019	KS	ASP	Indoors	MDA7+3	*An. gambiae* s.l	*An. gambiae* s.s	23,386.15
8218	2020	KS	ASP	Indoors	MDA7+3	*An. gambiae* s.l	*An. gambiae* s.s	1,619.05

Table S3.5. Quantification results and demographic information for mosquito head+thorax samples that tested positive for *P. malariae* over the course of RIMDAMAL II

Sample number	Study year	Village	Trap type	Trap location	MDA time	Mosquito clade	*An. gambiae* species	Genomes per sample
555	2019	SG	LT	Indoors	MDA1+1	*An. funestus*	na	5,216.57
1166	2019	DL	ASP	Indoors	MDA2+1	*An. gambiae* s.l	*An. gambiae* s.s	1,267.25
1364	2019	SG	ASP	Indoors	MDA2+1	*An. funestus*	na	748.82
1380	2019	KP	ASP	Indoors	MDA2+1	*An. gambiae* s.l	*An. gambiae* s.s	1,180.93
1844	2019	TG	ASP	Indoors	MDA2+3	*An. funestus*	na	983.49
3059	2019	DL	LT	Indoors	MDA3+1	*An. funestus*	na	834.24
3366	2019	KP	LT	Outdoors	MDA3+1	*An. gambiae* s.l	*An. gambiae* s.s	1,378.16
3985	2019	SG	LT	Outdoors	MDA3+3	*An. gambiae* s.l	*An. gambiae* s.s	1,532.74
4337	2019	DB	ASP	Indoors	MDA4+1	*An. gambiae* s.l	*An. gambiae* s.s	1,335.71
4800	2019	KP	ASP	Indoors	MDA4+1	*An. gambiae* s.l	*An. gambiae* s.s	917.80
4967	2019	TG	ASP	Indoors	MDA4+3	*An. funestus*	na	2,463.97
4971	2019	TG	ASP	Indoors	MDA4+3	*An. funestus*	na	2,316.84
4983	2019	TG	ASP	Indoors	MDA4+3	*An. funestus*	na	1,456.22
5081	2019	DB	ASP	Indoors	MDA4+3	*An. gambiae* s.l	*An. gambiae* s.s	3,532.56
5124	2019	DL	ASP	Indoors	MDA4+3	*An. funestus*	na	49,192.24
5206	2019	SG	ASP	Indoors	MDA4+3	*An. funestus*	na	3,887.07
8058	2020	DB	ASP	Indoors	MDA7+3	*An. gambiae* s.l	*An. gambiae* s.s	66,246.63
8066	2020	DB	ASP	Indoors	MDA7+3	*An. gambiae* s.l	*An. gambiae* s.s	41,727.35
8116	2020	DB	LT	Outdoors	MDA7+3	*An. gambiae* s.l	*An. gambiae* s.s	43,755.80

Table S3.6. Parity rates calculated from *An. funestus* and *An. gambiae* s.l sampled across six villages during RIMDAMAL II

Year	MDA time	Village	Species	Parity rate by village (N parous/N dissected)	Parity rate by MDA time (N parous/N dissected)	Survival rate	P_d
2019	MDA1+1	DL	*An. gambiae* s.l	83.3% (10/12)	77.6% (45/58)	0.41	1.39E-4
		KP	*An. gambiae* s.l	78.6% (11/14)			
		KS	*An. gambiae* s.l	72.7% (16/22)			
		SG	*An. gambiae* s.l	100% (4/4)			
		TG	*An. gambiae* s.l	50% (3/6)			
	MDA2+1	DL	*An. gambiae* s.l	69.2% (9/13)	52.8% (28/53)	0.11	2.00E-10
		KP	*An. gambiae* s.l	45.0% (9/20)			
		SG	*An. gambiae* s.l	58.8%(10/17)			
		TG	*An. gambiae* s.l	0.0% (0/3)			
	MDA2+3	DB	*An. gambiae* s.l	43.0% (6/14)	49.3% (36/73)	0.08	1.80E-11
		DL	*An. gambiae* s.l	37.5% (6/16)			
		KP	*An. gambiae* s.l	64.3% (9/14)			
		KS	*An. gambiae* s.l	66.7%(10/15)			
		SG	*An. gambiae* s.l	40.0% (4/10)			
		TG	*An. gambiae* s.l	25% (1/4)			
	MDA3+1	DB	*An. gambiae* s.l	58.3% (7/12)	43.5% (16/46)	0.02	8.86E-17
		DL	*An. gambiae* s.l	11.1% (1/9)			
		KP	*An. gambiae* s.l	62.5% (5/8)			
		SG	*An. gambiae* s.l	20.0% (2/10)			
		TG	*An. gambiae* s.l	14.3% (1/7)			
	MDA3+3	DB	*An. gambiae* s.l	66.7% (4/6)	47.1% (16/34)	0.07	3.49E-12
		DL	*An. gambiae* s.l	33.3% (3/9)			
		KP	*An. gambiae* s.l	50.0% (1/2)			
		SG	*An. gambiae* s.l	47.1% (8/17)			

	MDA4+1	DB	*An. gambiae* s.l	37.5% (3/8)	50.7% (34/67)	0.09	4.89E-11
		DL	*An. gambiae* s.l	40.0% (8/20)			
		KP	*An. gambiae* s.l	62.5% (10/16)			
		KS	*An. gambiae* s.l	0.0% (0/1)			
		SG	*An. gambiae* s.l	52.9% (9/17)			
		TG	*An. gambiae* s.l	80.0% (4/5)			
	MDA4+3	DB	*An. gambiae* s.l	83.3% (5/6)	80.0% (8/10)	0.46	4.06E-4
		DL	*An. gambiae* s.l	100% (1/1)			
		KP	*An. gambiae* s.l	100% (2/2)			
		TG	*An. gambiae* s.l	0.0% (0/1)			
2020	MDA5+1	DB	*An. gambiae* s.l	100% (12/12)	82.4% (14/17)	0.51	1.11E-3
		KS	*An. gambiae* s.l	0.0% (0/3)			
		SG	*An. gambiae* s.l	100% (2/2)			
	MDA7+1	DB	*An. gambiae* s.l	50% (2/4)	69.1% (38/55)	0.27	2.40E-6
		KP	*An. gambiae* s.l	100% (5/5)			
		KS	*An. gambiae* s.l	68.8% (11/16)			
		SG	*An. gambiae* s.l	69.0% (20/29			
		TG	*An. gambiae* s.l	0.0% (0/1)			
	MDA7+3	DB	*An. gambiae* s.l	61.1% (11/18)	61.1% (11/18)	0.18	3.27E-8
	MDA8+1	DB	*An. gambiae* s.l	0.0% (0/2)	86.7% (13/15)	0.61	6.68E-3
		DL	*An. gambiae* s.l	100% (3/3)			
		KP	*An. gambiae* s.l	100% (1/1)			
		KS	*An. gambiae* s.l	100% (3/3)			
		SG	*An. gambiae* s.l	100% (6/6)			

Villages: DB = Dangbara; DL = Dialanpozu; KP = Kolepar, KS = Konsabla; SG = Segri; TG = Tampé-Gougougré. P_d = proportion of the mosquito population that reaches an epidemiologically dangerous age for malaria transmission.

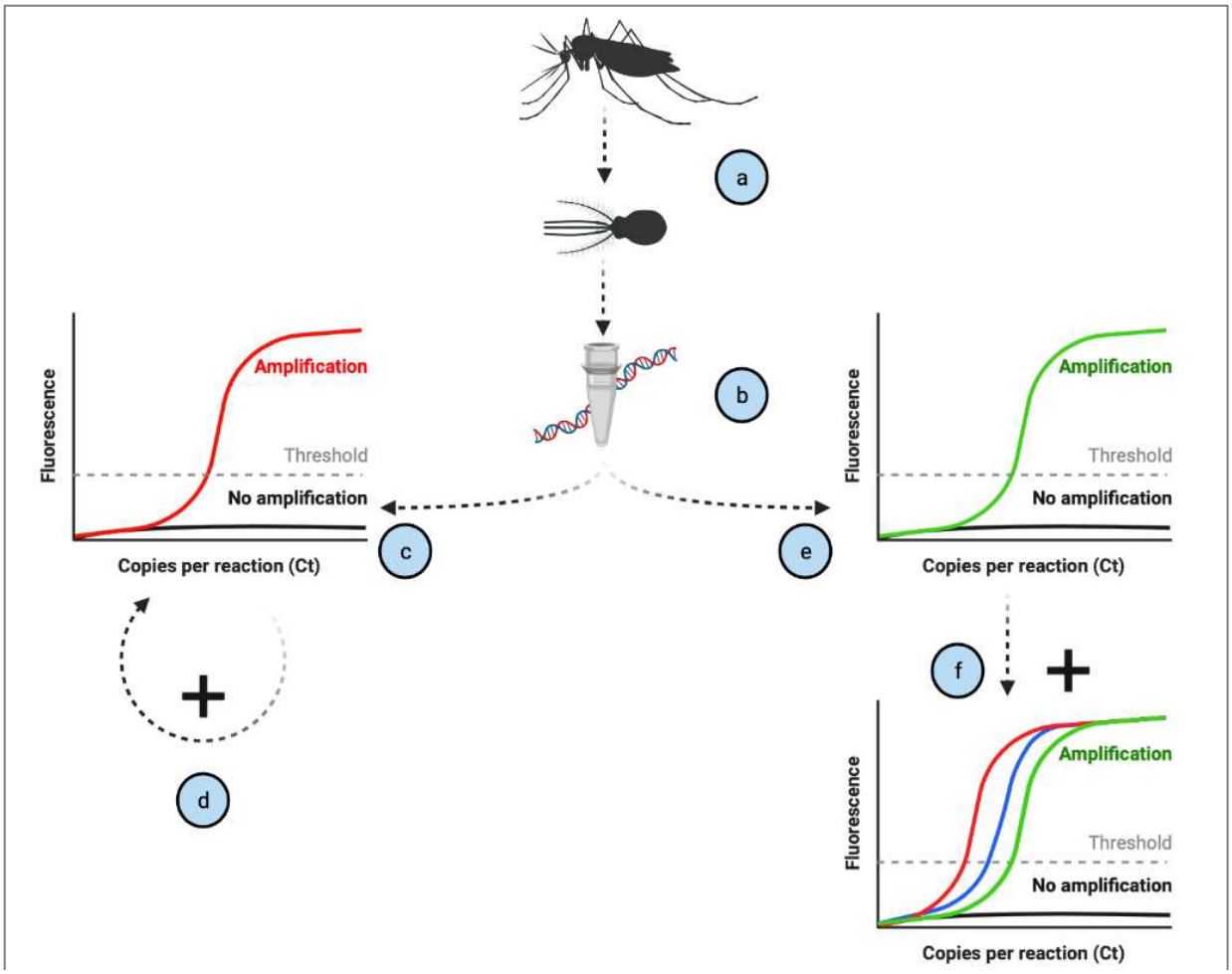

Figure S3.1. qPCR pipeline for *Plasmodium* detection in female *An. gambiae s.l* and *An. funestus* collected from RIMDAMAL II. Head+thoraces were separated from abdomens and stored in RNALater® before being shipped to Colorado State University (a). Samples were then removed and DNA extracted and cleaned (b). An aliquot of mosquito head+thorax DNA was then tested for *P. falciparum* absence/presence via the Hofmann et al protocol (c). If the result was negative, no further analysis was conducted. However, positive samples were run through the Hofmann et al protocol a second time to reconfirm positivity and quantify *Plasmodium* genomes per sample (d). A second aliquot of mosquito head+thorax DNA was then tested for *P. ovale*, *P. malariae,* and *P. vivax* absence/presence via the Bass et al protocol (e). If the result was negative, no further analysis was conducted. Positive samples were run through the Phuong et al protocol confirm positivity, distinguish the *Plasmodium* species, and quantify *Plasmodium* genomes per sample (f). All true positives detected in steps (d) and (f) also underwent mosquito species identification via the Wilkins et al protocol.

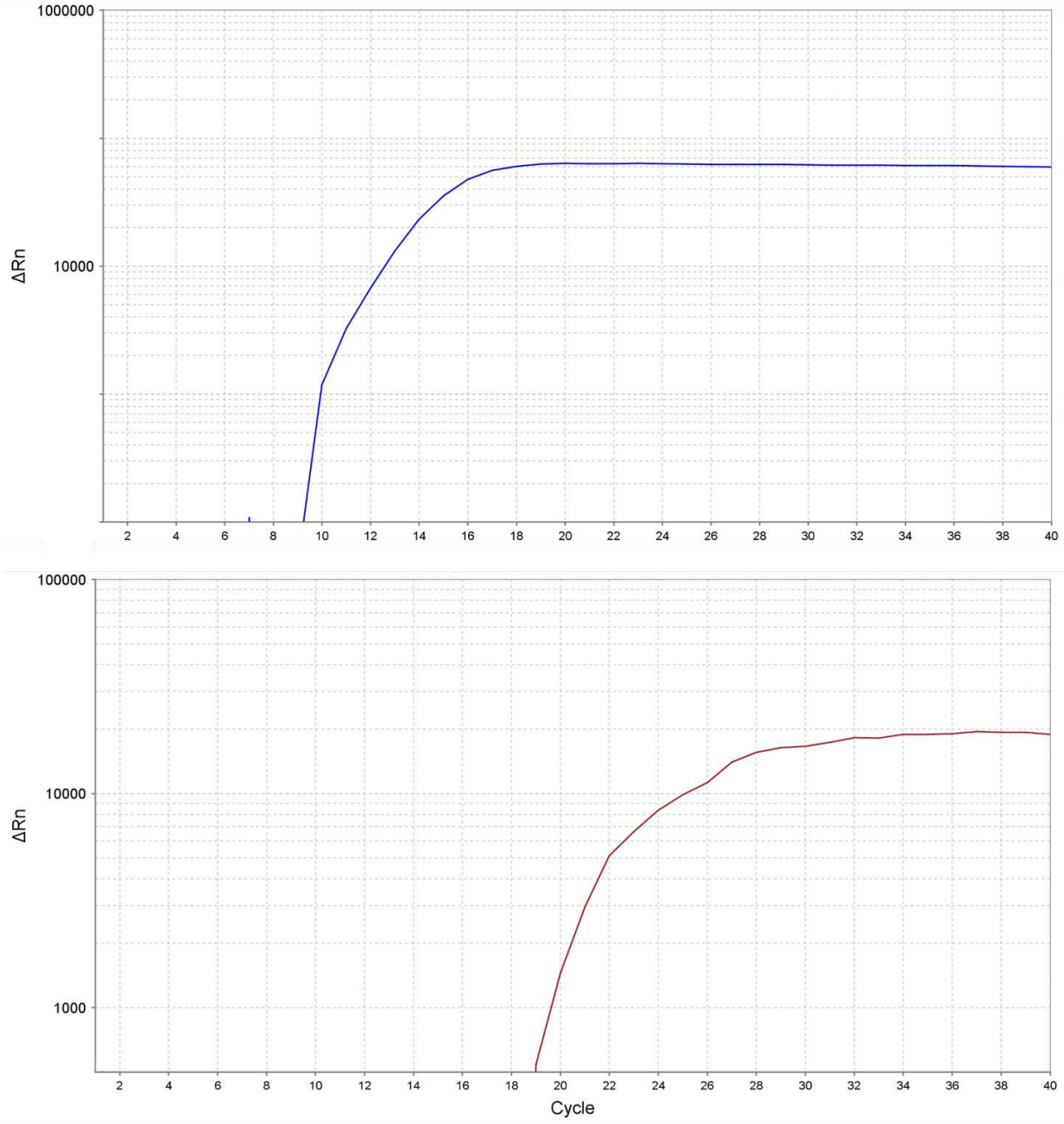

Figure S3.2. Examples of positive qPCR results for the Bass et al protocol. In this protocol, samples either tested positive for non-specific *P. ovale, P. vivax,* and *P. malariae* (blue, top image) or *P. falciparum* (red, bottom image). Depicted results were derived from DNA extracts of *Anopheles* head+thorax collected during the 2019 field season of RIMDAMAL II.

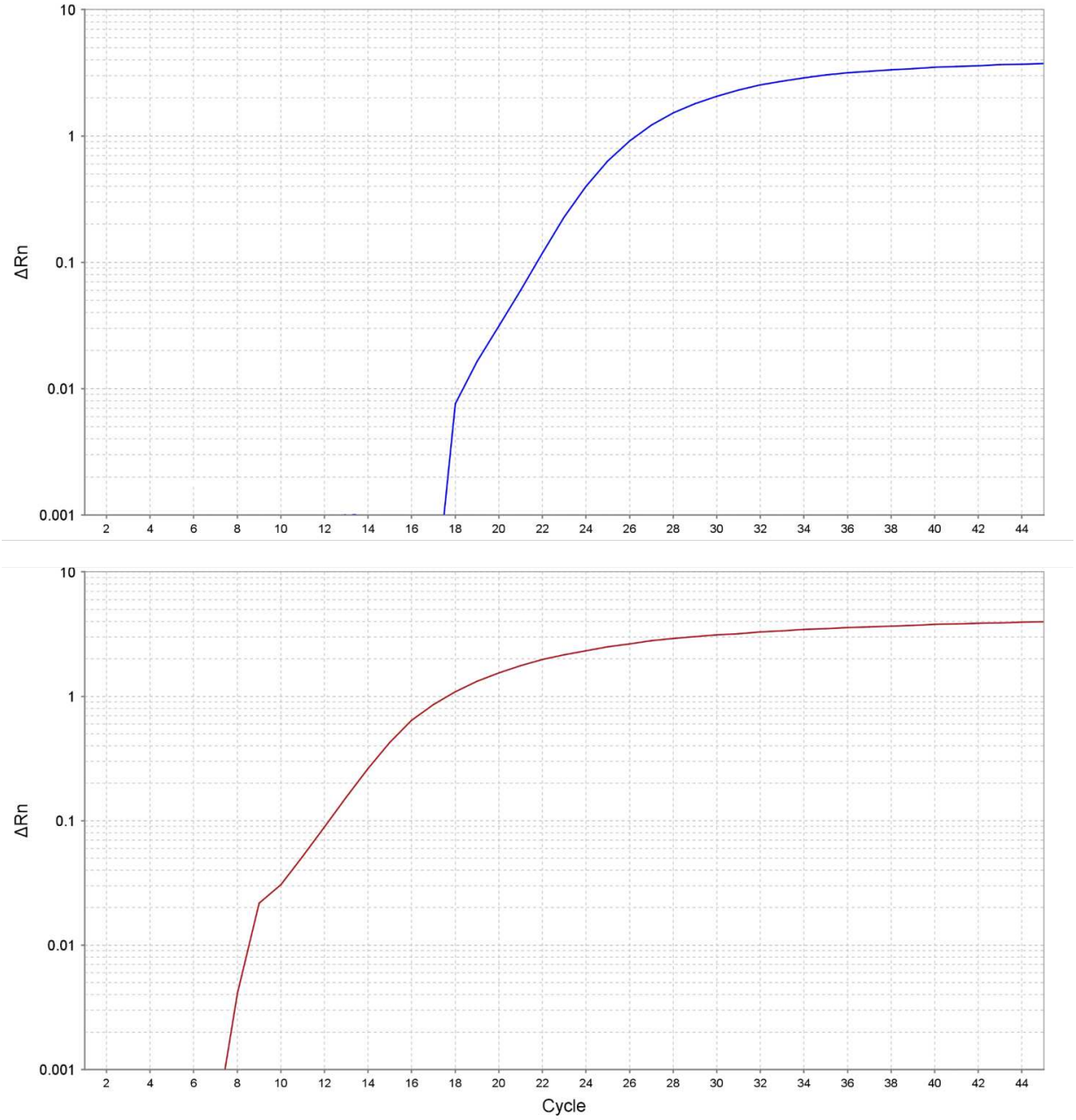

Figure S3.3. Examples of positive qPCR results for the Phuong et al protocol. In this assay, positive results were specific for *P. ovale* (blue, top image), *P. vivax,* and *P. malariae* (red, bottom image). Depicted results were derived from DNA extracts of *Anopheles* head+thorax collected during RIMDAMAL II 2020 field season. Because no mosquito tested positive for *P. vivax,* no sample-derived amplification curve is shown.

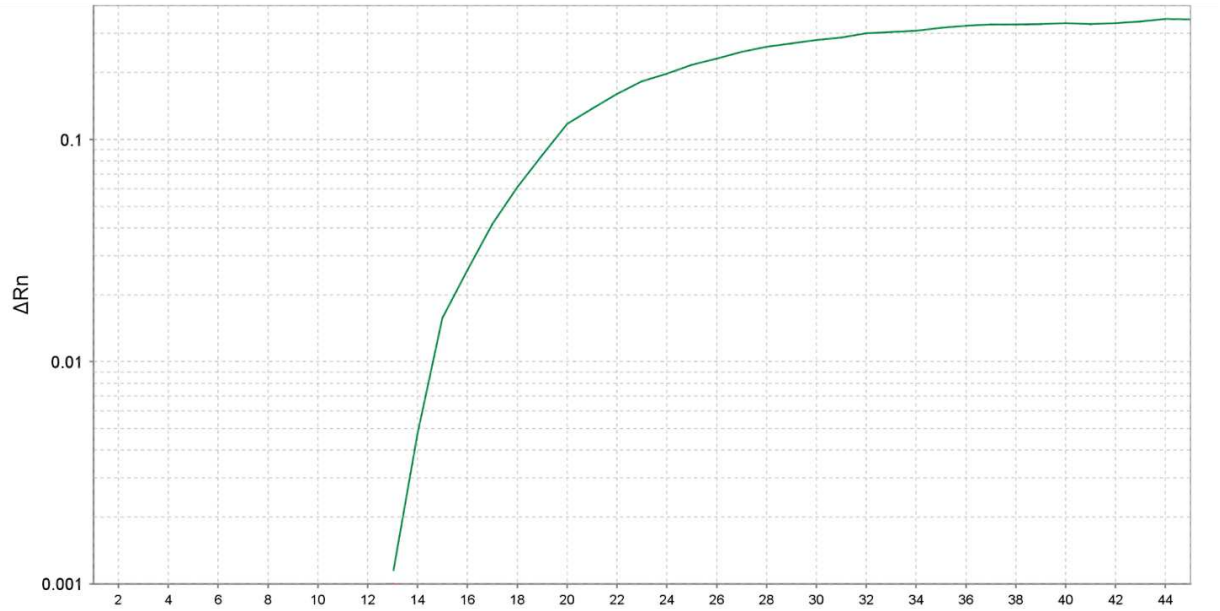

Figure S3.4. An example of a positive *P. vivax* qPCR result for the Phuong et al protocol. The example depicted was derived from a standard curve since no sample tested positive for *P. vivax*.

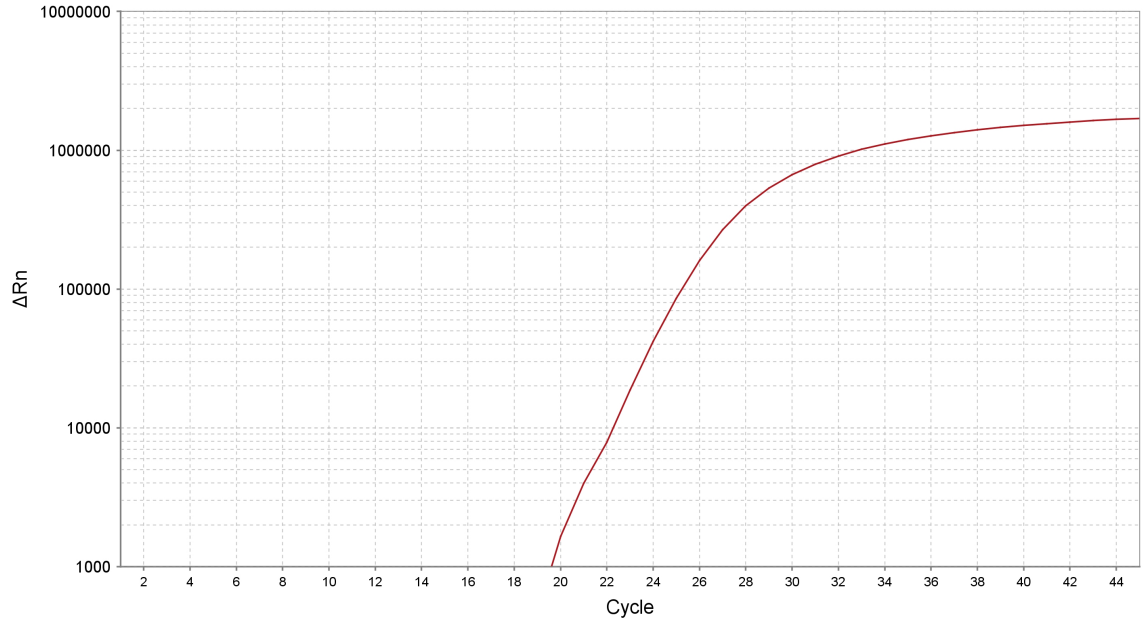

Figure S3.5. An example of a positive qPCR result for the Hoffman et al protocol. In this assay, samples only tested positive for *P. falciparum* (red). Depicted results were derived from DNA extracts of *Anopheles* head+thorax collected during the RIMDAMAL II 2020 field season.